ELSEVIER

Tetrahedron

Tetrahedron Vol. 60, No. 33, 2004

Tetrahedron Symposium-in-Print Number 104

Chemistry of biologically and physiologically intriguing phenomena

Guest editor: Daisuke Uemura

Department of Chemistry, Graduate School of Science, Nagoya University, Chikusa-ku, Nagoya 464-8602, Japan

Contents

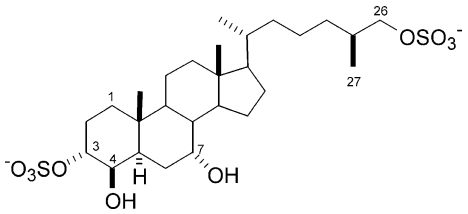

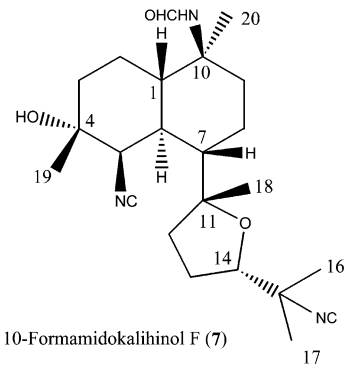

10-Formamidokalihinol F (**7**)

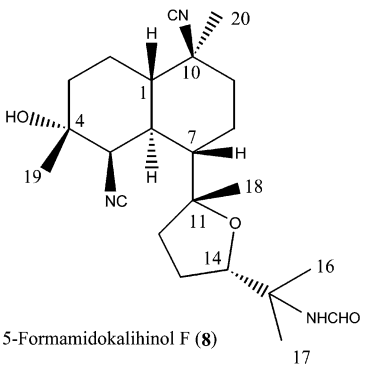

15-Formamidokalihinol F (**8**)

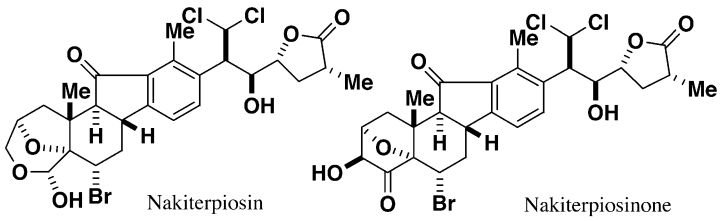

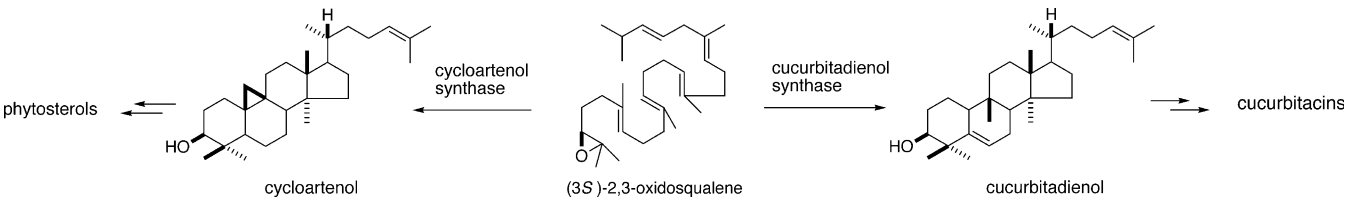

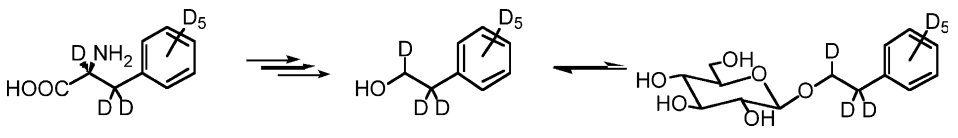

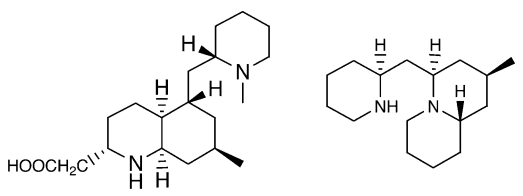

1 **6**

Six new alkaloids, cermizines A (**1**), B (**2**), C (**3**), and D (**6**), and senepodines G (**4**) and H (**5**) as well as two new cernuine *N*-oxide (**7**) and lycocernuine *N*-oxide (**8**), have been isolated from the club moss *Lycopodium cernuum* and *L. chinense*.

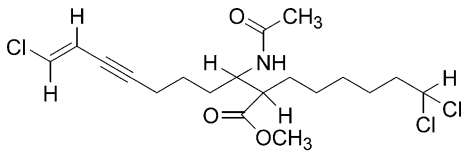

Taveuniamide A (**1**)

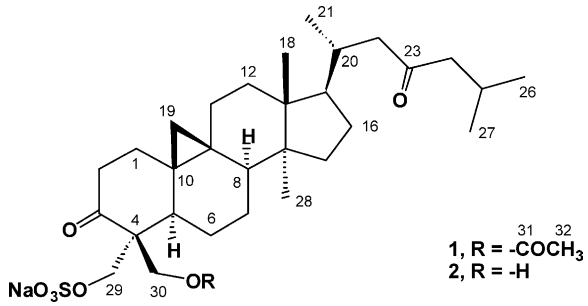

1, R = -COCH$_3$
2, R = -H

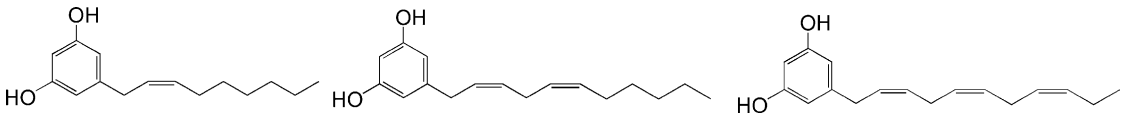

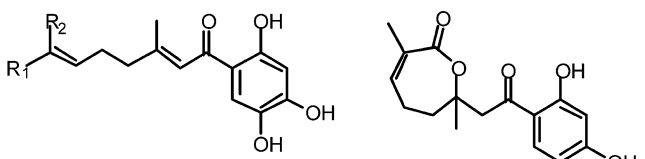

orirubenone A $R_1 = CH_3$, $R_2 = COOH$
orirubenone B $R_1 = COOH$, $R_2 = CH_3$

orirubenone C

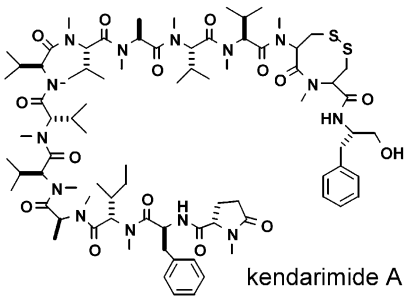

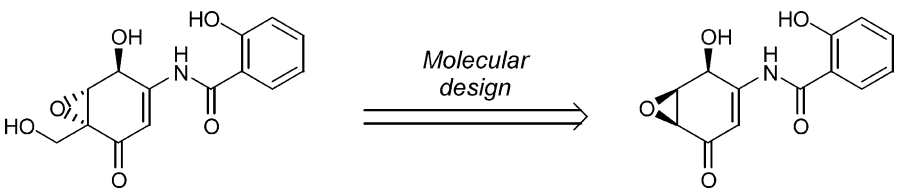

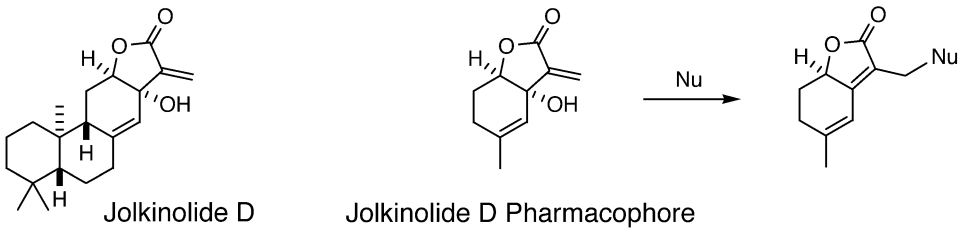

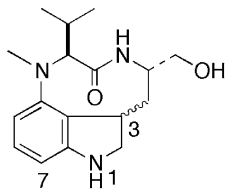

(3*R*)-Indolinelactam-V (**8**)
(3*S*)-Indolinelactam-V (**11**)

Two diastereomers of indolinelactam-Vs (**8**, **11**) and their 1-and 7-hexyl analogues were synthesized. Their conformation and binding affinities for synthetic C1 peptides of all PKC isozymes were examined.

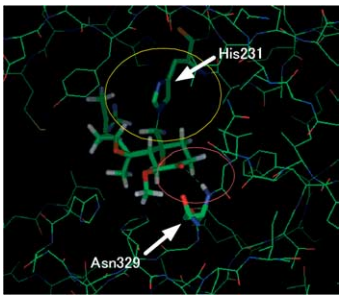

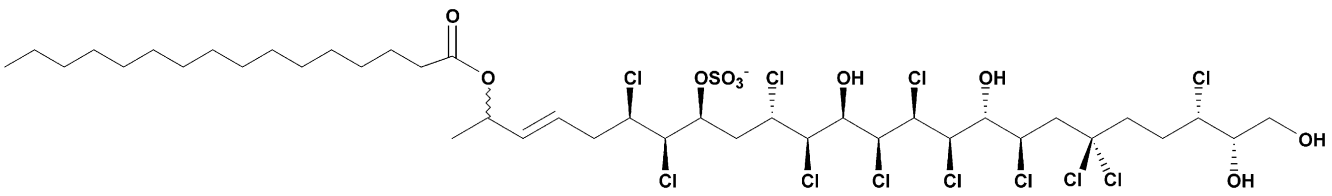

OTHER CONTENTS

*Corresponding author

COVER

Nature has an enormous, almost incomprehensive, capacity for diversity and adaptation.

Indexed/Abstracted in: AGRICOLA, Beilstein, BIOSIS Previews, CAB Abstracts, Chemical Abstracts. Current Contents: Life Sciences, Current Contents: Physical, Chemical and Earth Sciences, Current Contents Search, Derwent Drug File, Ei Compendex, EMBASE/Excerpta Medica, Medline, PASCAL, Research Alert, Science Citation Index, SciSearch

ELSEVIER

ISSN 0040-4020

Tetrahedron Symposia-in-Print

Series Editor
Professor H. H. Wasserman, Department of Chemistry, Yale University, P.O. Box 208107, New Haven, CT 06520-8107, U.S.A.

Tetrahedron Symposia-in-Print comprise collections of original research papers covering timely areas of organic chemistry.

Each symposium is organized by a Symposium Editor who will invite authors, active in the selected field, to submit original articles covering current research, complete with experimental sections. These papers will be rapidly reviewed and processed for publication by the Symposium Editor under the usual refereeing system.

Authors who have not already been invited, and who may have obtained recent significant results in the area of the announced symposium, may also submit contributions for Editorial consideration and possible inclusion. Before submitting such papers authors should send an abstract to the Symposium Editor for preliminary evaluation. Firm deadlines for receipt of papers will allow sufficient time for completion and presentation of ongoing work without loss of the freshness and timeliness of the research results.

Symposia-in-Print—already published

1. Recent trends in organic photochemistry, Albert Padwa, Ed. *Tetrahedron* **1981**, *37*, 3227–3420.
2. New general synthetic methods, E. J. Corey, Ed. *Tetrahedron* **1981**, *37*, 3871–4119.
3. Recent developments in polycyclopentanoid chemistry, Leo A. Paquette, Ed. *Tetrahedron* **1981**, *37*, 4357–4559.
4. Biradicals, Josef Michl, Ed. *Tetrahedron* **1982**, *38*, 733–867.
5. Electron-transfer initiated reactions, Gary B. Schuster, Ed. *Tetrahedron* **1982**, *38*, 1025–1122.
6. The organic chemistry of animal defense mechanisms, Jerrold Meinwald, Ed. *Tetrahedron* **1982**, *38*, 1853–1970.
7. Recent developments in the use of silicon in organic synthesis, Hans Reich, Ed. *Tetrahedron* **1983**, *39*, 839–1009.
8. Linear tetrapyrroles, Ray Bonnett, Ed. *Tetrahedron* **1983**, *39*, 1837–1954.
9. Heteroatom-directed metallations in heterocyclic synthesis, George R. Newkome, Ed. *Tetrahedron* **1983**, *39*, 1955–2091.
10. Recent aspects of the chemistry of β-lactams, J. E. Baldwin, Ed. *Tetrahedron* **1983**, *39*, 2445–2608.
11. New spectroscopic techniques for studying metabolic processes, A. I. Scott, Ed. *Tetrahedron* **1983**, *39*, 3441–3626.
12. New developments in indole alkaloids, Martin E. Kuehne, Ed. *Tetrahedron* **1983**, *39*, 3627–3780.
13. Recent aspects of the chemistry of nucleosides, nucleotides and nucleic acids, Colin B. Reese, Ed. *Tetrahedron* **1984**, *40*, 1–164.
14. Bioorganic studies on receptor sites, Koji Nakanishi, Ed. *Tetrahedron* **1984**, *40*, 455–592.
15. Synthesis of chiral non-racemic compounds, A. I. Meyers, Ed. *Tetrahedron* **1984**, *40*, 1213–1418.
16. Control of acyclic stereochemistry, Teruaki Mukaiyama, Ed. *Tetrahedron* **1984**, *40*, 2197–2344.
17. Recent aspects of anthracyclinone chemistry, T. Ross Kelly, Ed. *Tetrahedron* **1984**, *40*, 4537–4794.
18. The organic chemistry of marine products, Paul J. Scheuer, Ed. *Tetrahedron* **1985**, *41*, 979–1108.
19. Recent aspects of carbene chemistry, Matthew Platz, Ed. *Tetrahedron* **1985**, *41*, 1423–1612.
20. Recent aspects of singlet oxygen chemistry of photooxidation, Isao Saito and Teruo Matsuura, Eds. *Tetrahedron* **1985**, *41*, 2037–2236.
21. Synthetic applications of dipolar cycloaddition reactions. Wolfgang Oppolzer, Ed. *Tetrahedron* **1985**, *41*, 3447–3568.
22. Selectivity and synthetic applications of radical reactions, Bernd Giese, Ed. *Tetrahedron* **1985**, *41*, 3887–4302.
23. Recent aspects of organoselenium chemistry, Dennis Liotta, Ed. *Tetrahedron* **1985**, *41*, 4727–4890.
24. Application of newer organometallic reagents to the total synthesis of natural products, Martin Semmelhack, Ed. *Tetrahedron* **1985**, *41*, 5741–5900.
25. Formal transfers of hydride from carbon–hydrogen bonds, James D. Wuest, Ed. *Tetrahedron* **1986**, *42*, 941–1208.
26. Synthesis of non-natural products: challenge and reward, Philip E. Eaton, Ed. *Tetrahedron* **1986**, *42*, 1549–1916.
27. New synthetic methods—II, F. E. Ziegler, Ed. *Tetrahedron* **1986**, *42*, 2777–3028.
28. Structure and reactivity of organic radical ions, Heinz D. Roth, Ed. *Tetrahedron* **1986**, *42*, 6097–6350.
29. Organic chemistry in anisotropic media, V. Ramamurthy, J. R. Scheffer and N. J. Turro, Eds. *Tetrahedron* **1987**, *43*, 1197–1746.
30. Current topics in sesquiterpene synthesis, John W. Huffman, Ed. *Tetrahedron* **1987**, *43*, 5467–5722.
31. Peptide chemistry: design and synthesis of peptides, conformational analysis and biological functions, Victor J. Hruby and Robert Schwyzer, Eds. *Tetrahedron* **1988**, *44*, 661–1006.
32. Organosilicon chemistry in organic synthesis, Ian Fleming, Ed. *Tetrahedron* **1988**, *44*, 3761–4292.
33. α-Amino acid synthesis, Martin J. O'Donnell, Ed. *Tetrahedron* **1988**, *44*, 5253–5614.
34. Physical-organic/theoretical chemistry: the Dewar interface, Nathan L. Bauld, Ed. *Tetrahedron* **1988**, *44*, 7335–7626.
35. Recent developments in organocopper chemistry, Bruce H. Lipshutz, Ed. *Tetrahedron* **1989**, *45*, 349–578.
36. Organotin compounds in organic synthesis, Yoshinori Yamamoto, Ed. *Tetrahedron* **1989**, *45*, 909–1230.

37. Mycotoxins, Pieter S. Steyn, Ed. *Tetrahedron* **1989**, *45*, 2237–2464.
38. Strain-assisted syntheses, Léon Ghosez, Ed. *Tetrahedron* **1989**, *45*, 2875–3232.
39. Covalently linked donor–acceptor species for mimicry of photosynthetic electron and energy transfer, Devens Gust and Thomas A. Moore, Eds. *Tetrahedron* **1989**, *45*, 4669–4912.
40. Aspects of modern carbohydrate chemistry, S. Hanessian, Ed. *Tetrahedron* **1990**, *46*, 1–290.
41. Nitroalkanes and nitroalkenes in synthesis, Anthony G. M. Barrett, Ed. *Tetrahedron* **1990**, *46*, 7313–7598.
42. Synthetic applications of anodic oxidations, John S. Swenton and Gary W. Morrow, Eds. *Tetrahedron* **1991**, *47*, 531–906.
43. Recent advances in bioorganic chemistry, Dale L. Boger, Ed. *Tetrahedron* **1991**, *47*, 2351–2682.
44. Natural product structure determination, R. B. Bates, Ed. *Tetrahedron* **1991**, *47*, 3511–3664.
45. Frontiers in natural products biosynthesis. Enzymological and molecular genetic advances, D. E. Cane, Ed. *Tetrahedron* **1991**, *47*, 5919–6078.
46. New synthetic methods—III, S. E. Denmark, Ed. *Tetrahedron* **1992**, *48*, 1959–2222.
47. Organotitanium reagents in organic chemistry, M. T. Reetz, Ed. *Tetrahedron* **1992**, *48*, 5557–5754.
48. Total and semi-synthetic approaches to taxol, J. D. Winkler, Ed. *Tetrahedron* **1992**, *48*, 6953–7056.
49. Synthesis of optically active compounds—prospects for the 21st century, Kenji Koga and Takayuki Shioiri, Eds. *Tetrahedron* **1993**, *49*, 1711–1924.
50. Peptide secondary structure mimetics, Michael Kahn, Ed. *Tetrahedron* **1993**, *49*, 3433–3689.
51. Transition metal organometallics in organic synthesis, Anthony J. Pearson, Ed. *Tetrahedron* **1993**, *49*, 5415–5682.
52. Palladium in organic synthesis, Jan-E. Bäckvall, Ed. *Tetrahedron* **1994**, *50*, 285–572.
53. Recent progress in the chemistry of enediyne antibiotics, Terrence W. Doyle and John F. Kadow, Eds. *Tetrahedron* **1994**, *50*, 1311–1538.
54. Catalytic asymmetric addition reactions, Stephen F. Martin, Ed. *Tetrahedron* **1994**, *50*, 4235–4574.
55. Mechanistic aspects of polar organometallic chemistry, Manfred Schlosser, Ed. *Tetrahedron* **1994**, *50*, 5845–6128.
56. Molecular recognition, Andrew D. Hamilton, Ed. *Tetrahedron* **1995**, *51*, 343–648.
57. Recent advances in the chemistry of zirconocene and related compounds, Ei-ichi Negishi, Ed. *Tetrahedron* **1995**, *51*, 4255–4570.
58. Fluoroorganic chemistry: synthetic challenges and biomedicinal rewards, Giuseppe Resnati and Vadim A. Soloshonok, Eds. *Tetrahedron* **1996**, *52*, 1–330.
59. Novel applications of heterocycles in synthesis, A. R. Katritzky, Ed. *Tetrahedron* **1996**, *52*, 3057–3374.
60. Fullerene chemistry, Amos B. Smith III, Ed. *Tetrahedron* **1996**, *52*, 4925–5262.
61. New synthetic methods—IV. Organometallics in organic chemistry, István E. Markó, Ed. *Tetrahedron* **1996**, *52*, 7201–7598.
62. Cascade reactions, Ron Grigg, Ed. *Tetrahedron* **1996**, *52*, 11385–11664.
63. Applications of solid-supported organic synthesis in combinatorial chemistry, James A. Bristol, Ed. *Tetrahedron* **1997**, *53*, 6573–6706.
64. Recent applications of synthetic organic chemistry, Stephen F. Martin, Ed. *Tetrahedron* **1997**, *53*, 8689–9006.
65. Chemical biology, Gregory L. Verdine and Julian Simon, Eds. *Tetrahedron* **1997**, *53*, 11937–12066.
66. Recent aspects of S, Se, and Te chemistry, Richard S. Glass and Renji Okazaki, Eds. *Tetrahedron* **1997**, *53*, 12067–12318.
67. Modern organic chemistry of polymerization, H. K. Hall Jr., Ed. *Tetrahedron* **1997**, *53*, 15157–15616.
68. New synthetic methods—V, John L. Wood, Ed. *Tetrahedron* **1997**, *53*, 16213–16606.
69. New developments in organonickel chemistry, Bruce H. Lipshutz and Tien-Yau Luh, Eds. *Tetrahedron* **1998**, *54*, 1021–1316.
70. Solution phase combinatorial chemistry, David L. Coffen, Ed. *Tetrahedron* **1998**, *54*, 3955–4150.
71. Heterocycles in asymmetric synthesis, Alexandre Alexakis, Ed. *Tetrahedron* **1998**, *54*, 10239–10554.
72. Recent advances of phase-transfer catalysis, Takayuki Shioiri, Ed. *Tetrahedron* **1999**, *55*, 6261–6402.
73. Olefin metathesis in organic synthesis, Marc L. Snapper and Amir H. Hoveyda, Eds. *Tetrahedron* **1999**, *55*, 8141–8262.
74. Stereoselective carbon–carbon bond forming reactions, Harry H. Wasserman, Stephen F. Martin and Yoshinori Yamamoto, Eds. *Tetrahedron* **1999**, *55*, 8589–9006.
75. Applications of combinatorial chemistry, Miles G. Siegel and Stephen W. Kaldor, Eds. *Tetrahedron* **1999**, *55*, 11609–11710.
76. Advances in carbon–phosphorus heterocyclic chemistry, François Mathey, Ed. *Tetrahedron* **2000**, *56*, 1–164.
77. Transition metal organometallics in organic synthesis, Kenneth M. Nicholas, Ed. *Tetrahedron* **2000**, *56*, 2103–2338.
78. Organocopper chemistry II, Norbert Krause, Ed. *Tetrahedron* **2000**, *56*, 2727–2904.
79. Carbene complexes in organic chemistry, James W. Herndon, Ed. *Tetrahedron* **2000**, *56*, 4847–5044.
80. Recent aspects of the chemistry of β-lactams—II, Marvin J. Miller, Ed. *Tetrahedron* **2000**, *56*, 5553–5742.
81. Molecular assembly and reactivity of organic crystals and related structures, Miguel A. Garcia-Garibay, Vaidhyanathan Ramamurthy and John R. Scheffer, Eds. *Tetrahedron* **2000**, *56*, 6595–7050.
82. Protein engineering, Richard Chamberlin, Ed. *Tetrahedron* **2000**, *56*, 9401–9526.
83. Recent advances in peptidomimetics, Jeffrey Aubé, Ed. *Tetrahedron* **2000**, *56*, 9725–9842.
84. New synthetic methods—VI, George A. Kraus, Ed. *Tetrahedron* **2000**, *56*, 10101–10282.
85. Oxidative activation of aromatic rings: an efficient strategy for arene functionalization, Stéphane Quideau and Ken S. Feldman, Eds. *Tetrahedron* **2001**, *57*, 265–424.
86. Lewis acid control of asymmetric synthesis, Keiji Maruoka, Ed. *Tetrahedron* **2001**, *57*, 805–914.
87. Novel aromatic compounds, Lawrence T. Scott and Jay S. Siegel, Eds. *Tetrahedron* **2001**, *57*, 3507–3808.
88. Asymmetric synthesis of novel sterically constrained amino acids, Victor J. Hruby and Vadim A. Soloshonok, Eds. *Tetrahedron* **2001**, *57*, 6329–6650.
89. Recognition-mediated self-assembly of organic systems, Vincent M. Rotello, Ed. *Tetrahedron* **2002**, *58*, 621–844.
90. Synthesis of marine natural products containing polycyclic ethers, Masahiro Hirama and Jon D. Rainier, Eds. *Tetrahedron* **2002**, *58*, 1779–2040.

91. Fluorous chemistry, John A. Gladysz and Dennis P. Curran, Eds. *Tetrahedron* **2002**, *58*, 3823–4132.
92. Recent developments in chiral lithium amide base chemistry, Peter O'Brien, Ed. *Tetrahedron* **2002**, *58*, 4567–4734.
93. Beyond natural product synthesis (Tetrahedron Prize for Creativity in Organic Chemistry 2001 - Yoshito Kishi), Harry H. Wasserman and Stephen F. Martin, Eds. *Tetrahedron* **2002**, *58*, 6223–6602.
94. Strained heterocycles as intermediates in organic synthesis, Amy R. Howell, Ed. *Tetrahedron* **2002**, *58*, 6979–7194.
95. Molecular design of Lewis and Brønsted acid catalysts—the key to environmentally benign reagents (Tetrahedron Chair 2002), Hisashi Yamamoto, Ed. *Tetrahedron* **2002**, *58*, 8153–8364.
96. Recent developments in dendrimer chemistry, David K. Smith, Ed. *Tetrahedron* **2003**, *59*, 3787–4024.
97. Art, science and technology in total synthesis (Tetrahedron Prize for Creativity in Organic Chemistry 2002 - K. C. Nicolaou), Stephen F. Martin and Harry H. Wasserman, Eds. *Tetrahedron* **2003**, *59*, 6667–7070.
98. New synthetic methods—VII, Brian M. Stoltz, Ed. *Tetrahedron* **2003**, *59*, 8843–9030.
99. Oxiranyl and aziridinyl anions as reactive intermediates in synthetic organic chemistry, S. Florio, Ed. *Tetrahedron* **2003**, *59*, 9683–9864.
100. Recent advances in rare earth chemistry, Shū Kobayashi, Ed. *Tetrahedron* **2003**, *59*, 10339–10598.
101. Biocatalysts in synthetic organic chemistry, S. M. Roberts, Ed. *Tetrahedron* **2004**, *60*, 483–806.
102. Recent advances in the chemistry of zirconocenes, Keisuke Suzuki and Peter Wipf, Eds. *Tetrahedron* **2004**, *60*, 1257–1424.
103. Atropisomerism, Jonathan Clayden, Ed. *Tetrahedron* **2004**, *60*, 4325–4558.
104. Chemistry of biologically and physiologically intriguing phenomena, Daisuke Uemura, Ed. *Tetrahedron* **2004**, *60*, 6959–7098.

Available online at www.sciencedirect.com
SCIENCE DIRECT®
Tetrahedron 60 (2004) 6969
Tetrahedron

Preface

Chemistry of biologically and physiologically intriguing phenomena

The discovery of a new chemical substance frequently triggers a breakthrough in basic sciences. This Symposium-in-Print focuses on the identification of key natural compounds that control biologically and physiologically intriguing phenomena. Although such phenomena continue to attract considerable attention in a wide range of scientific fields, biological/biochemical studies of these phenomena are hampered mainly due to the instability and rarity of the relevant chemicals. To overcome difficulties in their isolation and characterization, research on this issue is aimed at the development of new methods in structural elucidation and mode-of-action studies, including bio-assays, based on the newest technologies in natural product chemistry, molecular biology, spectroscopic science and organic synthesis.

This Symposium-in-Print contains 16 papers classified into four groups: (1) bioactive molecules in transient or unstable states, (2) extremely effective key bioactive molecules, (3) unknown molecules implicated in important biological phenomena, and (4) determination of the structure of key molecules by innovative methods.

This special issue highlights the fact that careful observation in the field is extremely important in the pursuit of these key compounds.

New natural products continue to fascinate us because of the extremely unexpected structures of the molecules, their biologically intriguing mode of action, and their sacred and inviolable roles in the eco-system. Chemists are not yet adept at easily creating molecules with high potency for use as medicines. In contrast, Nature has an enormous, almost incomprehensible, capacity for diversity and adaptation.

Daisuke Uemura
Department of Chemistry, Graduate School of Science, Nagoya University, Chikusa-ku, Nagoya 464-8602, Japan
E-mail address: uemura@chem3.chem.nagoya-u.ac.jp

doi:10.1016/j.tet.2004.06.002

Available online at www.sciencedirect.com
SCIENCE DIRECT
Tetrahedron 60 (2004) 6971–6980
Tetrahedron

Synthesis and identification of an endogenous sperm activating and attracting factor isolated from eggs of the ascidian *Ciona intestinalis*; an example of nanomolar-level structure elucidation of novel natural compound

Tohru Oishi,[a] Hiroshi Tsuchikawa,[a] Michio Murata,[a,*] Manabu Yoshida[b] and Masaaki Morisawa[b]

[a]*Department of Chemistry, Graduate School of Science, Osaka University, Toyonaka, Osaka 560-0043, Japan*
[b]*Misaki Marine Biological Station, Graduate School of Science, University of Tokyo, Miura, Kanagawa 238-0225, Japan*

Received 27 June 2003; revised 22 February 2004; accepted 22 February 2004

Available online 19 June 2004

Abstract—A sperm-activating and attracting factor (SAAF) was isolated from the eggs of the ascidian *Ciona intestinalis*, and its structure was deduced with only approximately 4 μg of the specimen. Based upon the proposed structure, two epimers were synthesized from chenodeoxycholic acid in 16 steps. Comparison between synthetic and natural compounds led to the unambiguous structure determination of SAAF to be (3*R*,4*R*,7*R*,25*S*)-3,4,7,26-tetrahydroxycholestane-3,26-disulfate. The synthetic pure specimen was also utilized to confirm that both sperm-activation and attraction were elicited by a single compound.

1. Introduction

Sperm chemotractants, ubiquitously found in the animal kingdom, play an essential role in fertilization.[1,2] Chemotaxis of sperm toward an egg is a crucial event particularly in aquatic environment, where sperm frequently travels long distance to run into an egg. The relevant factors may control the chance of intra- or inter-species mating, which may take part in securing biodiversity, and thus have been a target of biological research for a long time. To investigate the molecular basis of fertilization, the pure specimen of a sperm attractant is indispensable, particularly for tracking signal transduction from chemoreception to flagellar movement. Although numerous peptides and small organic compounds have been so far proposed as a candidate of chemoattractant,[3,4] only a few of them have been unambiguously identified as an endogenous factor,[5] such as those for the sea urchin *Arbacia punctulata*,[6] the coral *Montipora digitata*,[7] and the frog *Xenopus laevis*. The difficulty in these studies lies in the quantification of chemotactic activity of sperm. Two of the authors at Misaki Marine Biological Station have extensively examined the chemotaxis in ascidian and clearly demonstrated that sperm activation and attractant are caused by different mechanism.[8,9] In the present study, we report the structural elucidation and synthesis of the sperm-activating and attracting factor (SAAF) from a species of acidean.[10,11]

2. Results and discussion

2.1. Structure determination

SAAF was extracted and purified from the eggs of the ascidian *Ciona intestinalis* as previously described.[12,13] During the purification procedure, the sperm-activating and attracting activities were always found in same fractions, indicating that both activities were elicited by a single compound. The chemical structure of SAAF was deduced based on NMR and mass spectrometry. The molecular-related ions were observed in negative ion FAB MS at *m/z* 617 and 595, which corresponded to $(X-H)^-$ and $(X-Na)^-$, respectively. In addition, a prominent ion peak at *m/z* 515 corresponded to a fragment lost typical for a sulfate ester ($-SO_3Na+H$). These data indicate that SAAF has two sulfate ester groups and, after one of them is lost, it still possesses a negatively charged group (=sulfate) to give rise to a prominent ion at *m/z* 515. High-resolution ESI-TOF MS further supported the presence of two sulfate esters by giving rise to the exact mass of *m/z* 297.1273 for a divalent anion, corresponding to $C_{27}H_{48}O_{18}S_2$ (calculated mass, *m/z* 297.1266). Two-dimensional ^1H NMR (2D TOCSY) spectrum in Figure 3 was successfully determined with

Keywords: Sperm-activating and attracting factor; Sterol disulfate; Structure determination; Synthesis.
* Corresponding author. Tel./fax: +81-6-6850-5774;
e-mail address: murata@ch.wani.osaka-u.ac.jp

0040–4020/$ - see front matter © 2004 Elsevier Ltd. All rights reserved.
doi:10.1016/j.tet.2004.02.075

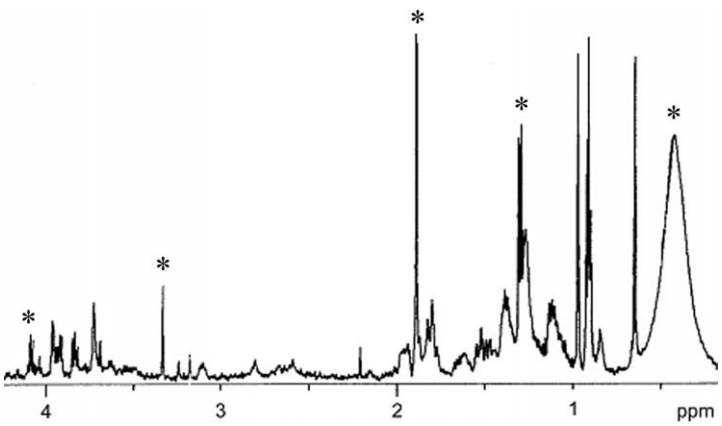

Figure 1. ^{1}H NMR spectrum of SAAF (**1**, ca. 4 μg); D_2O, 500 MHz. The spectrum was measured with using a special probe (Nanolac, Z-Spec-SMIDG500) for 1.7-mm diameter sample tube on a JEOL L-500 spectrometer. *Signals due to impurities. The broad peak at δ 0.4 is due to silicon grease outside of the tube used for sliding the tube into a spinner.

approximately 4 μg based upon an NMR spectrum in comparison with that of a synthetic specimen. The spectra revealed two singlet methyl signals at δ 0.65 and 0.97 characteristic of steroid skeletons. Additional two methyl doublets at δ 0.90 and 0.92 and complex signals at 0.8–2.0 ppm further support the presence of a steroid backbone. The down-field signals at δ 4.41, 3.96, 3.92, 3.83, and 3.72 correspond to five protons on four oxygen-bearing carbon atoms (those at δ 3.92/3.83 were apparently derived from a methylene group). Among these, the connectivity of signals at δ 4.41, 3.92, and 3.72 was elucidated by 2D TOCSY (Fig. 3). This structural moiety fits the C3–C7 part of a steroid skeleton. Signals at δ 3.92 and 3.83, which revealed geminal coupling, were assigned to a methylene group of C26 on the basis of relayed coupling to one of the methyl doublets. The location of sulfate groups was deduced from low-field chemical shifts of signals at δ 4.41 and 3.92/3.83 in comparison with those of hydroxyl-bearing methine and methylene groups. Moreover, their chemical shifts agreed well with reported values for starfish sterol sulfates.[12] Those spectral data indicated that SAAF was a novel sulfated steroid, 3,4,7,26-tetrahydroxy-cholestane-3,26-disulfate (Fig. 1).

High-energy collision-induced dissociation (CID) MS/MS is a versatile tool for structural elucidation of ionic compounds.[13] We adopted the tandem MS instrument of EB–EB geometry with the negative-ion fast atom bombardment (FAB) ionization method. The product ion spectrum was recorded for precursor ions at *m*/*z* 515, which corresponds to a desulfated product of SAAF presumably generated through the first MS section. The structural basis of the assignment for major product ions is shown in Figure 2. These fragmentations are reasonably explained by the

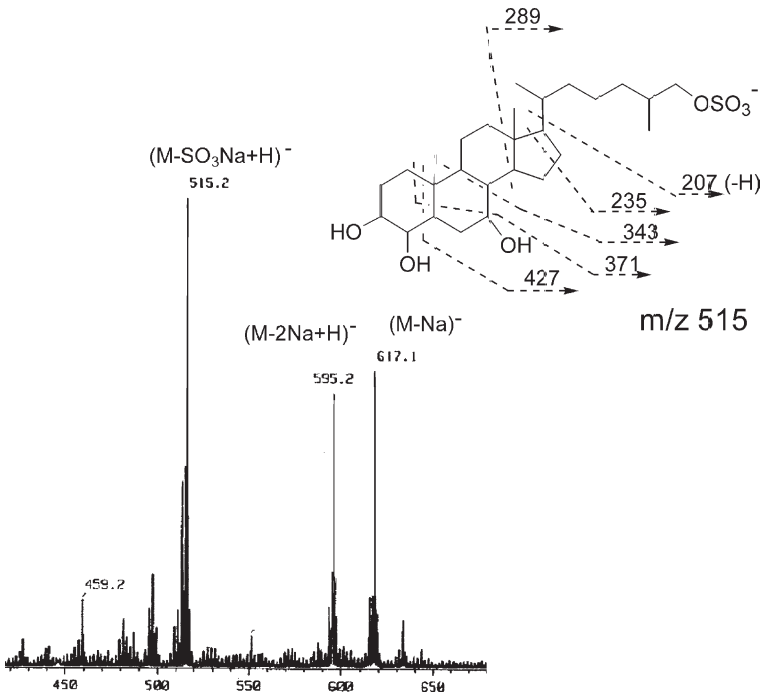

Figure 2. Normal FAB spectrum of SAAF (1) and fragment patterns for 3-*O*-defulfated ion of SAAF. Product ion spectra were obtained by CID MS/MS experiments. See text for details.[10]

proposed structure, particularly for the part of three oxygen functionalities, hence confirming the planner structure of SAAF.

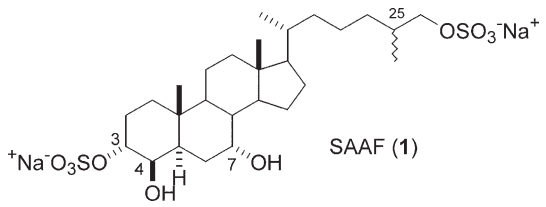

This working structure of SAAF was derived from limited NMR and MS data, hence leaving some ambiguities to be addressed. For the sterol skeleton, where ^{1}H NMR signals heavily overlap, no clear evidence was obtained regarding stereochemistry. Chemical synthesis was thus necessary for the complete structure identification. For this purpose, we had to deduce the configuration of SAAF. First, the skeletal stereostructure was deduced to be cholestan by the following two reasons; most of sterols isolated from tunicates possess a cholestan skeleton and a large coupling constant between H-5 and H-6 suggested the *trans* fusion of rings A and B. The stereochemistry of oxygenated carbon atoms was deduced from the small coupling constants for the signals at δ 4.41, 3.96, and 3.72 as one can observe in the attached 1D spectrum of Figure 3. The data clearly reveal that no diaxial coupling is involved in these spin systems, which indicates that all the three oxygen atoms were axially oriented. The stereochemistry at C25, which could not be assigned by NMR, remained to be elucidated by synthesizing both epimers at this positions.

2.2. Synthesis of SAAF and 25-*epi*-SAAF

Synthesis plan of SAAF and its C-25 epimer is shown in Scheme 1. We planed a versatile route that could provide both diastereomers by introducing the side chain using **4** and **5** at the latest steps via a common intermediate **6**, which would be synthesized from chenodeoxycholic acid **7**.

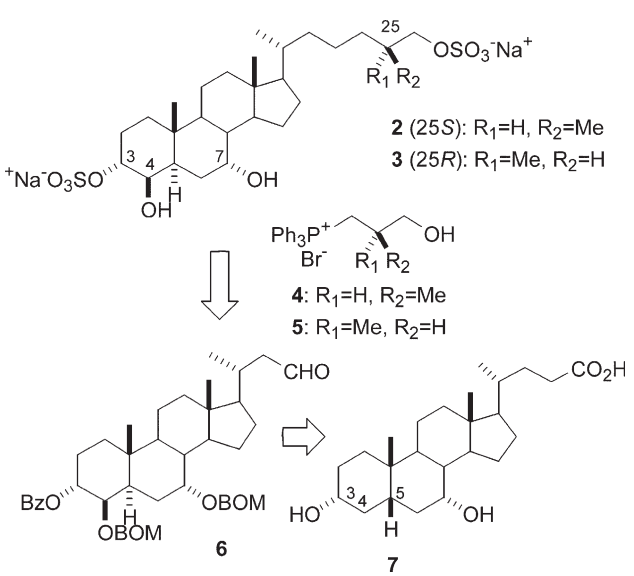

Scheme 1. Synthesis plan of SAAF and 25-*epi*-SAAF.

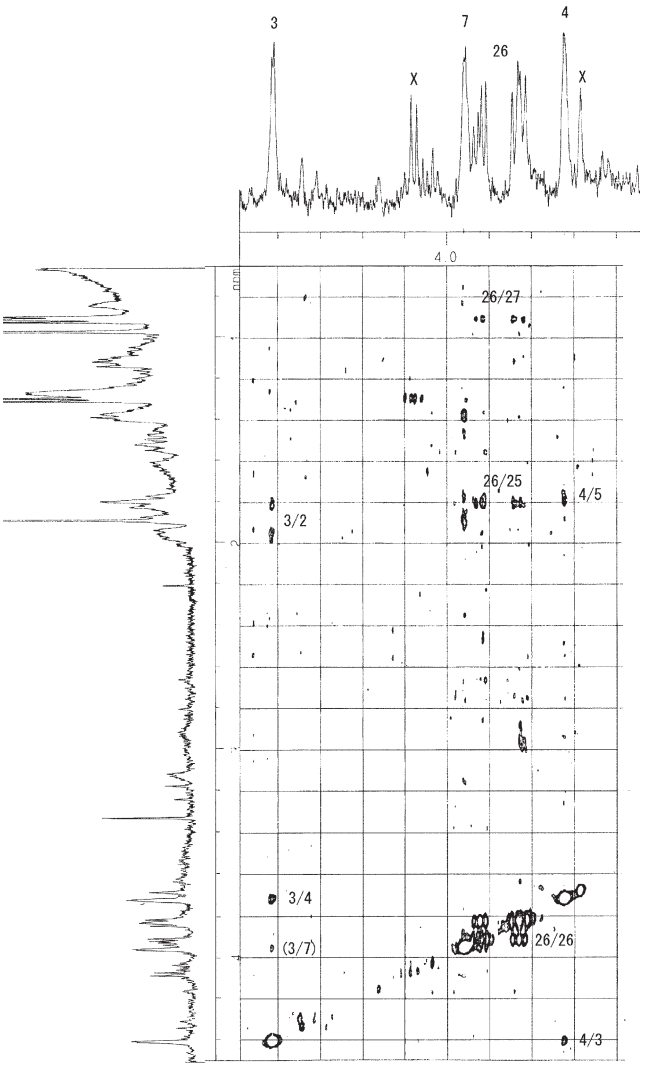

Figure 3. TOCSY spectrum of SAAF (**1**) of an extremely limited amound (ca. 4 μg). The spectrum was measured as the same conditions as those in Figure 1.

Synthesis of SAAF commenced with 7α-hydroxy-3-oxo-5β-cholan-24-oate (**8**), prepared from **7** in two steps (Scheme 2).[14] Oxidation of **8** with molecular oxygen in the presence of *t*-BuOK proceeded regioselectively via the C-4 enolate, and following esterification of the concomitantly hydrolyzed product afforded 3-keto-4-enol **9**. Selective protection of the C-7 alcohol of **9** as its benzyloxymethyl (BOM) ether in the presence of C-4 enol yielded **10**. Reduction of **10** with $NaBH_4$ proceeded stereoselectively at C-3 to give cyclic enol borate **11**, and hydrolysis of **11** with 1 M HCl yielded 4-keto-3-ol **12a** concomitant with its C-5 epimer **12b** as an inseparable mixture in a 1:1.8 ratio. Treatment of the mixture with $NaBH_4$ gave the desired diol **13a** from **12a** and diastereomer **13b** from **12b** in 20 and 36%, respectively. The stereochemistry of **12a** was unambiguously determined by ^{1}H NMR analysis. Isomerization of **12b** to **12a** under the basic conditions failed to give 3-keto-4-ol **12c** as a single isomer. Attempts to reduce **9** using other conventional methods were unsuccessful due to the formation of undesired diastereomers preferentially with low reproducibility. Finally, a solid-phase reduction of **10** with $NaBH_3CN$ on

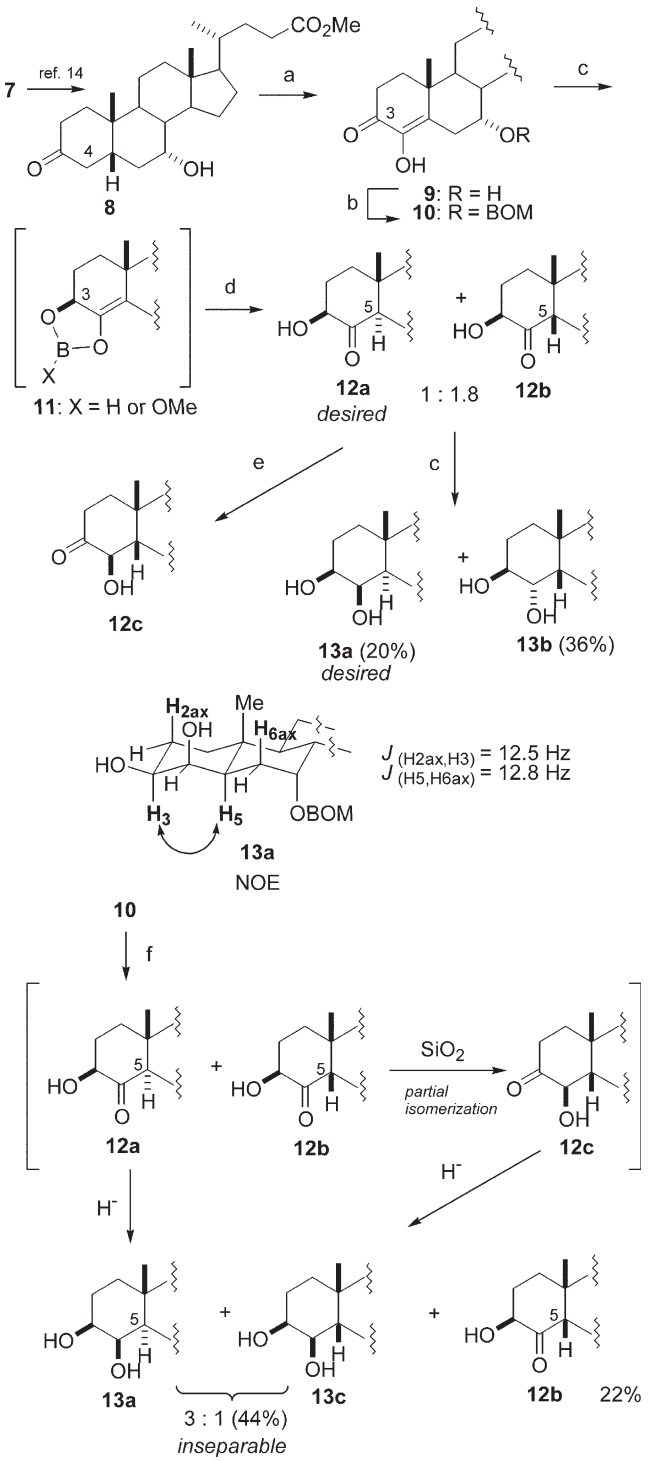

Scheme 2. Reagents and conditions: (a) *t*-BuOK, O_2, *t*-BuOH, then CH_2N_2, Et_2O, MeOH, $CHCl_3$ (71%); (b) BOMCl, *i*-Pr_2NEt, CH_2Cl_2 (60%); (c) $NaBH_4$; $CHCl_3$, MeOH, 0 °C; (d) 1 M HCl; (e) DBU, THF, 60 °C; (f) $NaBH_3CN$, SiO_2, $CHCl_3$, MeOH, then evaporated.

silica gel was found to afford desired diol **13a** in moderate yield. A solution of **10** in chloroform and methanol was added $NaBH_3CN$ (5 equiv.) and silica gel (**10**–silica gel=1:3, w/w). After stirring for 10 min the solvent was removed under reduced pressure, and the residue was stirred without solvent. Under the reaction conditions, hydrolysis of the borate **11** proceeded smoothly to give a mixture of **12a** and **12b**. Further reduction of **12a** proceeded smoothly to give **13a**, whereas **12b** remained intact and easily separated from **13a**. However, partial isomerization of **12b** occurred to give **12c**, which was further reduced to **13c** resulting in the formation of inseparable mixture of **13a** and **13c** in a ratio of 3:1 (44%). Even though the yield of **13a** should be improved, the contiguous stereogenic centers at C-3, C-4, and C-5 on the steroid framework were properly installed for the next operations.

Treatment of the mixture of diols **13a** and **13c** with thionyl chloride followed by oxidation with RuO_2–$NaIO_4$ gave cyclic sulfate **14a** in 65% yield for two steps,[15] which was easily separated from 5β-isomer **14b** (11%) by silica gel chromatography (Scheme 3). Regioselective opening of the cyclic sulfate at C-3 position was successfully achieved by treating with benzoic acid in the presence of Cs_2CO_3 in DMF (75%) followed by hydrolysis of the resulting sulfate.[16] Protection of the resulting C-4 alcohol (**15**) as BOM ether afforded benzoate **16** as a single isomer (71%). Exposure of **16** to *t*-BuOK in *t*-BuOH resulted in the selective hydrolysis of the methyl ester in the presence of benzoate ester to yield carboxylic acid **17** (95%), which was further converted to iodide **18** through the decarboxylation by treating with $Pb(OAc)_4$ in the presence of iodine under irradiation using a tungsten lamp (84%).[17]Oxidation of **18** with DMSO in the presence of 2,4,6-collidine gave an aldehyde **6** (94%), a common precursor of the two diastereomers at C-25. Elongation of the side chain was achieved through a Wittig reaction between the aldehyde **6**, and an ylide generated from (*R*)-phosphonium salt **4**[18] and *n*-BuLi–TMSCl[19] to give olefin **19** (*E*/*Z*=1:8) in 69% yield. Reductive removal of the benzoyl group of **19** with $LiAlH_4$ gave diol **20**, which was converted to the corresponding sodium bis-sulfate through the successive treatment with SO_3·Py and ion-exchange resin (IR-120B, Na^+ form). Hydrogenation of the double bond and concomitant removal of the BOM groups afforded 25*S*-isomer (**2**), and the resulting polar material was purified by reverse-phase HPLC. The C-25 epimer **3** was synthesized by the identical procedure as **2** except for the use of (*S*)-phosphonium salt **5** in place of **4**.

2.3. Comparison with the natural product

The ^1H NMR spectrum of the natural product was compared with those of the synthetic samples, **2** (25*S*) and **3** (25*R*), as shown in Figure 4.[10] The areas other than those in Figure 4 were indistinguishable among the natural SAAF and the synthetic pair. While the chemical shifts of the 25-methyl group and H-26a in **3** do not match those of the natural product ($\Delta\delta$ values for H-26a and 25-methyl are −0.014 and −0.007 ppm, respectively), those of **2** are identical with SAAF as are other resonances of the steroid framework.[4] Thus, the configuration of the side chain was confirmed as 25*S*, resulting in the first synthesis of SAAF. When the bioactivity and biosynthetic rationality are taken into account, the absolute stereochemistry is assigned to be 3*R*, 4*R*, 7*R*, and 25*S*.

Both the sperm-activating and attracting activity of synthetic SAAF were bioassayed using methods previously reported.[4] Synthetic SAAF (**2**) activated sperm of the ascidian *C. intestinalis* at 3.7 nM and concurrently exhibited

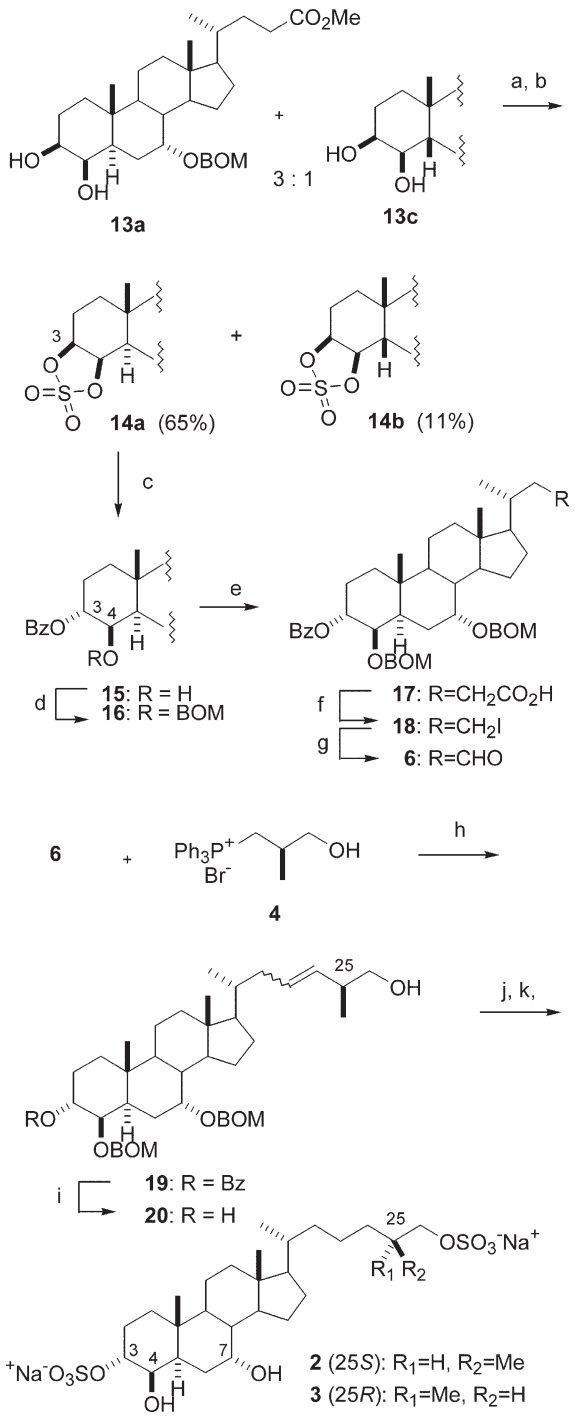

Scheme 3. Reagents and conditions: (a) $SOCl_2$, Et_3N, THF, 94%; (b) $RuCl_3{\cdot}nH_2O$, $NaIO_4$, **14a** (65%), **14b** (11%); (c) $PhCO_2H$, Cs_2CO_3, DMF; then conc. H_2SO_4, THF, 75%; (d) BOMCl, *i*-Pr_2NEt, CH_2Cl_2 (84%); (e) *t*-BuOK, *t*-BuOH, 95%; (f) $Pb(OAc)_4$, I_2, hν, CCl_4, hν (300 W tungsten lamp), 84%; (g) DMSO, 2,4,6-collidine, 94%; (h) *n*-BuLi, TMSCl, THF, then 0.5 M HCl, 69%; (i) $LiAlH_4$, THF, 80%; (j) $SO_3{\cdot}Py$, Py, then Amberite IR-120B Na^+ form; (k) Pd/C, H_2, MeOH.

the attracting activity at <10 nM;[11] these quantitative evaluations were first accomplished with the synthetic specimen. The concentration of SAAF (10 nM) is for an aqueous gel in a capillary from which SAAF diffuses to a sperm-containing medium. Thus, the minimum active concentration is thought to be the subnano–pico molar range. It is noteworthy that 25-*epi*-SAAF (**3**) possesses comparative activities as those with SAAF (activated at ~3.7 nM and attracted at <10 nM).

We succeeded in elucidating the structure of SAAF with only ca. 4 μg of a specimen. This may be partly due to the sensitivity improvement of modern NMR instruments as demonstrated by the special probe for a capillary tube. We rather think that the high purity of the specimen is a key point. Usually, it is very difficult to prepare the microgram amount of an NMR sample without contaminations, which may come from both HPLC and NMR solvents or from containers. In this study, the sample was mostly treated as a aqueous solution in plastic vessels, which helped reducing the contamination with detergents or plasticizers; the only prominent contaminant seen in Figure 1 is lactic acid, one of common impurities under aqueous conditions. Another problem encountered in 2D NMR measurements is that an enormous solvent peak often results in an uneven base plane. In this study, the volume of the solution was only 20 μL, which effectively reduced the contamination and secure the flatness of the base line or base plane in NMR

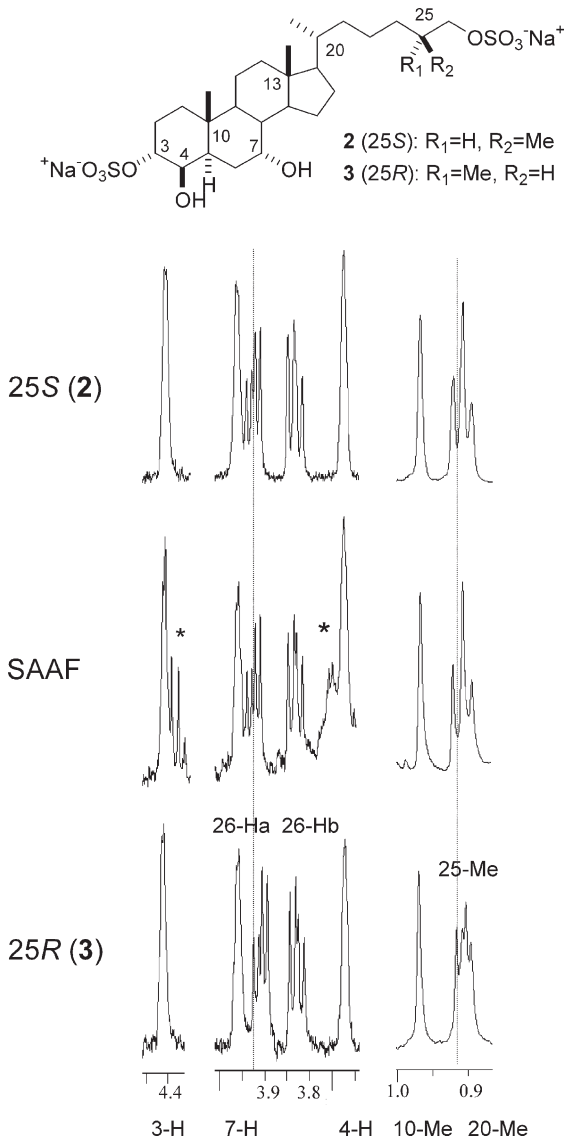

Figure 4. Partial ^1H NMR spectra of SAAF, **2**(25*S*), and **3**(25*R*). Asterisks indicate the signals attributed to contaminants.

measurements. The other methodology useful for the structure analysis in nanomolar scale is MS/MS; in particular, high energy collision experiments are helpful since C–C bond cleavages provides the information about skeletal structures. Key steps in this study was to obtain the reliable working structures and to synthesize these effectively.

3. Conclusion

In conclusion, the sperm-activating and attracting factor (SAAF) was synthesized from **7** in 17 steps, which led to the unambiguous structure determination of SAAF to be (3*R*,4*R*,7*R*,25*S*)-3,4,7,26-tetrahydroxycholestane-3,26-disulfate (**2**). The synthetic pure specimen was also used to confirm the dual sperm-activating and attracting activity. Currently, we are preparing molecular probes to be used for identification of the receptor and the relevant signal transduction pathway(s).

4. Experimental

All reactions sensitive to air or moisture were carried out under argon atmosphere in dry, freshly distilled solvents under anhydrous conditions, unless otherwise noted. THF was distilled sodium/benzophenone, diethyl ether (Et_2O) from $LiAlH_4$, diisopropylamine, diisopropylethylamine (*i*-Pr_2NEt), pyridine, from calcium hydride, and DMF, DMSO and HMPA from calcium hydride under reduced pressure. Dichloromethane (CH_2Cl_2) and toluene was dried over activated MS4A. All other reagents were used as supplied unless otherwise stated. Analytical thin-layer chromatography (TLC) was performed using E. Merck Silica gel 60 F254 pre-coated plates. Column chromatography was performed using 100–210 μm Silica Gel 60N (Kanto Chemical), and for flash column chromatography 40–63 μm Silica Gel 60N (Merck) was used. ^1H and ^{13}C NMR spectra were recorded on a JEOL EX-270 (270 MHz), a JEOL GSX-500 (500 MHz), or JEOL JMN-LA500 (500 MHz) spectrometer. Chemical shifts are reported in δ (ppm) using residual $CHCl_3$ as an internal standard of δ 7.26 and δ 77.00 for ^1H and ^{13}C NMR, respectively. Signal patterns are indicated as s, singlet; d, doublet; t, triplet; q, quartet; m, multiplet; br, broad peak. IR spectra were recorded on a Jasco FT/IR-300E spectrometer. Mass spectra (ESI) were recorded on a ThermoQuest LCQ DECA instrument. Optical rotations were recorded on a Perkin–Elmer 241 polarimeter.

4.1. Structure determination

Materials. The ascidians, *C. intestinalis* was collected at the Onagawa Bay (Miyagi prefecture), Aburatsubo Bay (Kanagawa prefecture), and Ootsuchi Bay (Iwate prefecture) in Japan. SAAF was extracted and purified as reported previously.[10]

Structure analysis of SAAF. Electrospray-ionization time-of-flight (ESI-TOF) MS was performed in the negative-ion mode with a Mariner (ABI) mass spectrometer. ^1H NMR spectra of SAAF in 20 μL of a D_2O solution were recorded at 23 °C on a JEOL L-500 spectrometer (500 MHz) with a 1.7-mm probe (Nanolac, Z-Spec-SMIDG500). 2D TOCSY spectra were measured for a spin locking time of 20 ms with data matrices of 2k×512 (a total of 82,000 acquisitions for 35 h) while a peak of solvent-derived deuterium being presaturated. Fast atom bombardment (FAB) MS/MS experiments were carried out in the negative-ion mode using a HX-110/HX-110 tandem mass spectrometer (JEOL) equipped with a variable dispersion array detector (MS-ADS11). Collision-induced dissociation (CID) was effected by introducing helium at a pressure that reduced the intensity of precursor ions to 30%.

4.2. Synthesis of SAAF and 25-*epi*-SAAF

4.2.1. Methyl 7α-hydroxy-3,4-dioxo- cholan-24-oate 9. To a stirred solution of **8** (2.57 g, 6.35 mmol) in ^{t}BuOH (15 mL) was added ^{t}BuOK (2.10 g, 19.1 mmol) and the resulting suspension was stirred for 1.5 h at rt under oxygen atmosphere (under the reaction conditions, the methyl ester was hydrolyzed to give the corresponding carboxylate). The reaction was carefully quenched with 1.87 M NH_4Cl (130 mL). The reaction mixture was extracted with ethyl acetate, and the combined organic layer was concentrated. The residue was dissolved in chloroform (10 mL) and methanol (10 mL), which was treated with a solution of diazomethane in ether at 0 °C and the mixture stirred for 1 h. Evaporation followed by silica gel column chromatography (hexane/ethyl acetate=8:1–2:1) gave **9** (1.81 g, 68% from **8**) as colorless solid.

Compound **9**. R_f 0.20 (hexane/ethyl acetate=2:1); IR (KBr) 3448, 2940, 1736, 1670, 1636, 1381, 1169 cm^{-1}; ^1H NMR (500 MHz, $CDCl_3$) δ 6.11 (1H, s, 4-OH), 3.96 (1H, s, 7-H), 3.64 (3H, s, CO_2CH_3), 3.14 (1H, dd, *J*=15.5, 3.5 Hz, 6-Ha), 2.16 (1H, dd, *J*=15.5, 3.5 Hz, 6-Hb), 1.16 (3H, s, 10-Me), 0.90 (3H, d, *J*=7.0 Hz, 20-Me), 0.68 (3H, s, 13-Me); ^{13}C NMR (500 MHz, $CDCl_3$) δ 192.9, 174.5, 143.3, 135.9, 67.8, 55.7, 51.5, 50.3, 45.6, 42.4, 39.4, 39.2, 37.6, 35.4, 34.4, 31.8, 31.6, 31.0, 31.0, 28.1, 23.6, 20.8, 18.3, 16.8, 11.9.

4.2.2. Methyl 7α-benzyloxymethoxy-3,4-dioxocholan-24-oate 10. To a solution of **9** (2.63 g, 6.29 mmol) in dichloromethane (18.9 mL) was added diisopropylethylamine (2.19 mL, 12.6 mmol) and BOMCl (1.31 mL, 9.44 mmol), and the mixture was stirred for 18 h at rt. The reaction was quenched with water and extracted with dichloromethane. The combined organic layer was washed with saturated NaCl, dried over anhydrous $MgSO_4$, and filtered. Concentration followed by purification by flash column chromatography (hexane/ethyl acetate=10:1–5:1) gave **10** (2.03 g, 60%) as colorless amorphous, and 17% of **9** (464 mg) was recovered.

Compound **10**. Colorless amorphous; R_f 0.55 (hexane/ethyl acetate=2:1); $[\alpha]_D^{22}$ −2.4° (*c* 1.58, $CHCl_3$); IR (KBr) 3456, 2960, 1740, 1664, 1636, 1380, 1172, 1052 cm^{-1}; ^1H NMR (500 MHz, $CDCl_3$) δ 7.36–7.24 (5H, m, Ph), 6.03 (1H, s, 4-OH), 4.88 (1H, d, *J*=7.0 Hz, OCH_2OBn), 4.74 (1H, d, *J*=7.0 Hz, OCH_2OBn), 4.65 (1H, d, *J*=11.5 Hz, OCH_2Ph), 4.57 (1H, d, *J*=11.5 Hz, OCH_2Ph), 3.88 (1H, s, 7-H), 3.65 (3H, s, CO_2CH_3), 3.39 (1H, dd, *J*=16.0, 3.0 Hz, 6-Ha), 2.00 (1H, dd, *J*=16.0, 3.0 Hz, 6-Hb), 1.16 (3H, s, 10-Me), 0.91

(3H, d, J=6.5 Hz, 20-Me), 0.68 (3H, s, 13-Me); ^{13}C NMR (500 MHz, $CDCl_3$) δ 193.1, 174.5, 142.8, 137.9, 136.7, 128.2, 127.6, 127.5, 93.7, 73.7, 70.0, 55.6, 51.5, 49.9, 45.9, 42.4, 39.6, 39.1, 37.6, 35.4, 34.5, 31.9, 31.1, 31.0, 28.5, 28.1, 24.0, 20.8, 18.4, 16.9, 11.8; MS (ESI) m/z 561 $(M+Na)^+$.

4.2.3. Methyl 7α-benzyloxymethoxy-3β,4β-dihydroxy-5α-cholan-24-oate 13a. To a stirred solution of **10** (1.01 g, 1.88 mmol) in chloroform (4 mL) and methanol (4 mL) was added $NaBH_3CN$ (589 mg, 9.37 mmol) and silica gel (3.00 g), and the reaction mixture was stirred for 10 min at rt. The solvent was evaporated and the residue was stirred for 1 h at rt. The residue was added chloroform (4 mL) and methanol (4 mL) again and stirred for 10 min. The solvent was removed by evaporation and the resulting residue was stirred for 3 h at rt. The same procedure was repeated again and the residue was stirred for 13 h at rt. The residue was washed with a mixed solvent of chloroform and methanol (chloroform/methanol=2:1), and the precipitates were removed by filtration. The residue was washed with the same solvent three times. The combined filtrate was concentrated, and the residue was dissolved in ethyl acetate. The organic layer was washed with saturated NaCl, dried over $MgSO_4$, and concentrated under reduced pressure. The residue was purified by flash column chromatography (hexane/ethyl acetate=8:1–2:1) to give a mixture of **13a** and **13c** (443 mg, 44% **13a/13c**=3:1), which was separated from **12b** (220 mg, 22%).

Compound **13a**: R_f 0.15 (hexane/ethyl acetate=2:1); ^{1}H NMR (500 MHz, $CDCl_3$) δ 7.35–7.24 (5H, m, Ph), 4.83 (1H, d, J=7.5 Hz, OCH_2OBn), 4.76 (1H, d, J=7.5 Hz, OCH_2OBn), 4.60 (1H, d, J=12.0 Hz, OCH_2Ph), 4.57 (1H, d, J=12.0 Hz, OCH_2Ph), 3.75 (1H, d, J=1.5 Hz, 7-H), 3.64 (3H, s, CO_2Me), 3.59 (1H, s, 4-H), 3.54 (1H, m, 3-H), 1.59 (1H, d, J=13.0 Hz, 5-H), 1.01 (3H, s, 10-Me), 0.90 (3H, d, J=7.0 Hz, 20-Me), 0.62 (3H, s, 13-Me).

Compound **13c**. ^{1}H NMR (500 MHz, $CDCl_3$) δ 7.36–7.24 (5H, m, Ph), 4.93 (1H, d, J=5.5 Hz, OCH_2OBn), 4.63 (1H, d, J=5.5 Hz, OCH_2OBn), 4.62 (1H, d, J=12.0 Hz, OCH_2Ph), 4.57 (1H, d, J=12.0 Hz, OCH_2Ph), 4.26 (1H, m, 4-H), 3.95 (1H, d, J=2.5 Hz, 3-H), 3.64 (3H, s, CO_2Me), 3.57 (1H, d, J=2.5 Hz, 7-H), 3.35 (1H, d, J=6.0 Hz, 4-OH), 0.94 (3H, s, 10-Me), 0.90 (3H, d, J=7.0 Hz, 20-Me), 0.62 (3H, s, 13-Me).

4.2.4. Methyl 7α-benzyloxymethoxy-3β,4β-cyclic sulfate-5α-cholan-24-oate 14a. To a stirred solution of **13a** and **13c** (437 mg, 0.801 mmol) and triethylamine (446 μL, 3.22 mmol) in THF (3 mL) was added a solution of thionyl chloride (94.6 μL, 1.21 mmol) in THF (1 mL) and stirred for 10 min at 0 °C. The reaction mixture was quenched with water and extracted with ethyl acetate. The combined organic layer was washed with saturated NaCl, dried over anhydrous $MgSO_4$. Concentration followed by flash column chromatography (hexane/ethyl acetate=50:1–10:1) gave a mixture of cyclic sulfites (441 mg, 94%) as colorless oil. The mixture of cyclic sulfites (552 mg, 0.938 mmol) was dissolved in a mixed solvent of acetonitrile (4.6 mL), CCl_4 (3.0 mL), and 50 mM phosphate buffer (3.0 mL). To the solution was added $RuCl_3$ (19.5 mg, 94 μmol), $NaIO_4$ (241 mg, 1.13 μmol) in a mixed solvent of acetonitrile (2.3 mL), CCl_4 (1.5 mL), and 50 mM phosphate buffer (1.5 mL). The reaction mixture was stirred for 20 min, then quenched with saturated $Na_2S_2O_3$ and extracted with ethyl acetate. The organic layers were combined, washed with saturated NaCl, dried over dried over $MgSO_4$, filtered. Concentration followed by florisil column chromatography (hexane/ethyl acetate=30:1–6:1) gave cyclic sulfate **14a** (367 mg, 65%) as colorless amorphous, and side product **14b** (62 mg, 11%).

Compound **14a**. Colorless amorphous; R_f 0.32 (hexane/ethyl acetate=5:1, 3 times development); $[\alpha]_D^{23}$ +6.4° (c 0.12, $CHCl_3$); IR (thin film) 2945, 2869, 1736, 1381, 1208, 1039 cm^{-1}; ^{1}H NMR (500 MHz, $CDCl_3$) δ 7.36–7.27 (5H, m, Ph), 4.82 (1H, d, J=7.0 Hz, OCH_2OBn), 4.74 (1H, d, J=7.0 Hz, OCH_2OBn), 4.63–4.56 (4H, m, OCH_2Ph, 3,4-H), 3.74 (1H, d, J=2.0 Hz, 7-H), 3.64 (3H, s, CO_2CH_3), 1.03 (3H, s, 10-Me), 0.90 (3H, d, J=7.0 Hz, 20-Me), 0.63 (3H, s, 13-Me); ^{13}C NMR (500 MHz, $CDCl_3$) δ 174.5, 137.7, 128.4, 127.8, 127.3, 94.7, 85.8, 83.0, 75.2, 70.3, 55.6, 51.5, 49.9, 46.5, 42.5, 40.0, 39.6, 39.0, 35.4, 34.9, 34.1, 31.1, 31.0, 30.6, 28.0, 23.7, 20.4, 18.3, 12.9, 11.9; MS (ESI) m/z 627 $(M+Na)^+$.

Compound **14b**. Amorphous material; R_f 0.43 (hexane/EtOAc=5:1, 3 times development); $[\alpha]_D^{23}$ +32.1° (c 1.44, $CHCl_3$); IR (thin film) 2945, 2870, 1736, 1382, 1208, 1035 cm^{-1}; ^{1}H NMR (500 MHz, $CDCl_3$) δ 7.35–7.26 (5H, m, Ph), 5.76 (1H, dd, J=10.0, 4.5 Hz, 4-H), 5.12 (1H, q, J=4.5 Hz, 3-H), 4.81 (1H, d, J=6.5 Hz, OCH_2OBn), 4.74 (1H, d, J=6.5 Hz, OCH_2OBn), 4.62 (1H, d, J=12.0 Hz, OCH_2Ph), 4.59 (1H, d, J=12.0 Hz, OCH_2Ph), 3.76 (1H, d, J=2.5 Hz, 7-H), 3.64 (3H, s, CO_2CH_3), 1.03 (3H, s, 10-Me), 0.90 (3H, d, J=7.0 Hz, 20-Me), 0.63 (3H, s, 13-Me); ^{13}C NMR (500 MHz, $CDCl_3$) δ 174.4, 137.5, 128.3, 127.6, 127.5, 94.2, 86.4, 81.5, 74.7, 70.6, 55.6, 51.5, 49.7, 42.7, 42.6, 39.1, 39.0, 36.2, 35.4, 35.0, 31.1, 31.0, 29.3, 28.1, 25.6, 23.9, 23.0, 21.6, 20.7, 18.4, 11.8; MS (ESI) m/z 627 $(M+Na)^+$.

4.2.5. Methyl 3α-benzoyloxy-4β,7α-dibenzyloxy- methoxy-5α- cholan-24-oate 15. A mixture of **13a** (109 mg, 0.180 mmol), benzoic acid (55 mg, 0.450 mmol), and Cs_2CO_3 (147 mg, 0.450 mmol) in a 10 mL flask was dried under the reduced pressure. To the mixture was added DMF (2 mL) and stirred for 6 h at rt. The solvent was removed under reduced pressure, and the residue was purified by silica gel column chromatography (hexane/ethyl acetate=5:1–2:1, then chloroform/methanol=1:0–1:2) to give 3-O-benzoyl-4-O-sulfate (R_f 0.30, 5:1—chloroform/methanol) (110 mg) as a mixture of benzoic acid, and 21 mg (19%) of **14a** was recovered. To the solution of 3-O-benzoyl-4-O-sulfate (110 mg) in THF (2.4 mL) was added a solution of conc. sulfuric acid (54 μL) in THF (0.1 mL). The mixture was stirred for 15 min at rt, then quenched with saturated $NaHCO_3$ and extracted with ethyl acetate. The combined organic layer was washed with saturated $NaHCO_3$, dried over $MgSO_4$, filtered, and concentrated under reduced pressure to give **15** (71 mg, 75% from **14a**).

Compound **15**. Amorphous material; R_f 0.43 (hexane/ethyl acetate=2:1); IR (thin film) 3487, 2940, 1734, 1717, 1270,

1111, 1041 cm^{-1}; ^1H NMR (500 MHz, $CDCl_3$) δ 8.01 (2H, d, J=8.0 Hz, $PhCO_2$), 7.53–7.06 (8H, m, $PhCO_2$, Ph), 5.13 (1H, d, J=2.5 Hz 3-H), 4.81 (1H, d, J=7.0 Hz, OCH_2OBn), 4.72 (1H, d, J=7.0 Hz, OCH_2OBn), 4.47 (1H, d, J=12.0 Hz, OCH_2Ph), 4.43 (1H, d, J=12.0 Hz, OCH_2Ph), 3.74 (1H, s, 7-H), 3.67 (1H, s, 4-H), 3.64 (3H, s, CO_2CH_3), 2.08 (1H, dt, J=13.5, 3.0 Hz, 5-H), 1.08 (3H, s, 10-Me), 0.91 (3H, d, J=7.0 Hz, 20-Me), 0.64 (3H, s, 13-Me); ^{13}C NMR (500 MHz, $CDCl_3$) δ 174.6, 165.5, 137.6, 132.9, 130.3, 129.5, 128.3, 128.2, 127.4, 127.1, 95.0, 73.2, 73.2, 69.5, 55.7, 51.5, 50.2, 47.3, 42.6, 39.8, 39.2, 38.2, 35.9, 35.4, 32.9, 31.1, 31.1, 30.8, 28.1, 23.8, 22.1, 20.1, 18.4, 13.5, 11.9; MS (ESI) m/z 669 $(M+Na)^+$.

4.2.6. Methyl 3α-benzoyloxy-4β,7α-dibenzyloxy-methoxy-5α-cholan-24-oate 16. To a solution of **15** (71 mg, 0.110 mmol) in dichloromethane (1 mL) was added diisopropylethylamine (345 μL, 1.98 mmol) and BOMCl (122 μL, 0.880 mmol) and the mixture was stirred for 22 h at rt. The reaction mixture was quenched with water and extracted with dichloromethane. The combined organic layer was washed with saturated NaCl, dried over $MgSO_4$, and concentrated under reduced pressure. The residue was purified by silica gel column chromatography (hexane/ethyl acetate=15:1–4:1) to give **16** (56 mg, 67%) as colorless oil and 11 mg (15%) of **15** was recovered.

Compound **16**. Colorless oil; R_f 0.63 (hexane/ethyl acetate=2:1); $[\alpha]_D^{22}$ −6.4° (*c* 0.64, $CHCl_3$); IR (thin film) 2943, 1734, 1717, 1270, 1099, 1038, 1026 cm^{-1}; ^1H NMR (500 MHz, $CDCl_3$) δ 8.00 (2H, d, J=8.0 Hz, $PhCO_2$), 7.52–7.09 (13H, m, $PhCO_2$, Ph), 5.28 (1H, d, J=3.0 Hz 3-H), 4.82, 4.80, 4.71 and 4.70 (4H, d×4, J=7.0 Hz, OCH_2O), 4.64, 4.60, 4.49 and 4.47 (4H, d×4, J=12.0 Hz, OCH_2Ph), 3.74 (1H, s, 7-H), 3.65 (3H, s, CO_2CH_3), 3.57 (1H, s, 4-H), 1.07 (3H, s, 10-Me), 0.91 (3H, d, J=7.0 Hz, 20-Me), 0.65 (3H, s, 13-Me); ^{13}C NMR (500 MHz, $CDCl_3$) δ 174.6, 165.4, 137.7, 137.6, 132.8, 130.4, 129.4, 128.3, 128.2, 127.7, 127.5, 127.4, 127.2, 94.7, 94.5, 79.2, 76.4, 70.5, 69.7, 69.5, 55.7, 51.5, 50.1, 47.2, 42.6, 39.8, 39.2, 38.1, 35.9, 35.4, 32.9, 31.1, 28.1, 23.8, 22.4, 20.3, 18.4, 13.3, 11.9; MS (ESI) m/z 789 $(M+Na)^+$.

4.2.7. 3α-Benzoyloxy-4β,7α-dibenzyloxymethoxy-5α-cholan-24-oic acid 17. To a solution of **16** (4.9 mg, 6.39 μmol) in ^{t}BuOH (0.1 mL) was added ^{t}BuOK (2.2 mg, 19.2 μmol), and the mixture was stirred for 2 h at rt. The reaction mixture was quenched with saturated NH_4Cl, and extracted with ethyl acetate. The combined organic layer was washed with saturated NaCl. Concentration followed by silica gel column chromatography (hexane/ethyl acetate=8:1–4:1) gave **17** (4.6 mg, 95%) as colorless amorphous.

Compound **17**. Amorphous material; R_f 0.27 (hexane/ethylacetate=2:1); IR (thin film) 1714, 1451, 1270, 1101, 1038 cm^{-1}; ^1H NMR (500 MHz, $CDCl_3$) δ 8.00 (2H, d, J=8.0 Hz, $PhCO_2$), 7.53–7.09 (13H, m, $PhCO_2$, Ph), 5.27 (1H, d, J=3.0 Hz 3-H), 4.82, 4.79, 4.71 and 4.70 (4H, d×4, J=7.0 Hz, OCH_2O), 4.64, 4.60, 4.49 and 4.47 (4H, d×4, J=12.0 Hz, OCH_2Ph), 3.73 (1H, s, 7-H), 3.56 (1H, s, 4-H), 1.06 (3H, s, 10-Me), 0.92 (3H, d, J=6.5 Hz, 20-Me), 0.65 (3H, s, 13-Me); ^{13}C NMR (500 MHz, $CDCl_3$) δ 179.9, 165.4, 137.7, 137.6, 132.8, 130.4, 129.4, 128.3, 128.2, 127.7, 127.5, 127.4, 127.2, 94.6, 94.5, 79.2, 76.4, 70.5, 69.7, 69.5, 55.7, 50.2, 47.2, 42.6, 39.8, 39.2, 38.1, 35.9, 35.4, 32.8, 31.0, 30.8, 28.1, 23.8, 22.4, 20.3, 18.3, 13.3, 11.9; MS (ESI) m/z 776 $(M+Na)^+$.

4.2.8. 24-Nor-5α-cholane-4β,7α-dibenzyloxymethoxy-23-iodo-3α-ol, benzoate 18. A solution of **17** (43 mg, 57.1 μmol), $Pb(OAc)_4$ (38 mg, 86 μmol), and iodine (43 mg, 171 μmol) in CCl_4 (2 mL) was refluxed for 20 min under irradiation of tungsten lamp (300 W). The reaction mixture was quenched with saturated $Na_2S_2O_3$, and extracted with dichloromethane. The combined organic layer was washed with saturated NaCl, and dried over $MgSO_4$. Concentration followed by silica gel column chromatography (hexane/ethyl acetate=20:1–2:1) gave **18** (40 mg, 84%) as colorless oil.

Compound **18**. Colorless oil; R_f 0.43 (hexane/ethyl acetate=5:1); IR (thin film) 3424, 1715, 1452, 1270, 1109, 1039 cm^{-1}; ^1H NMR (500 MHz, $CDCl_3$) δ 8.00 (2H, d, J=7.5 Hz, $PhCO_2$), 7.53–7.09 (13H, m, $PhCO_2$, Ph), 5.27 (1H, q, J=2.5 Hz 3-H), 4.82, 4.79 and 4.70×2 (4H, d×4, J=7.0 Hz, OCH_2OBn), 4.64, 4.60, 4.49 and 4.47 (4H, d×4, J=12.0 Hz, OCH_2Ph), 3.73 (1H, d, J=1.5 Hz 7-H), 3.57 (1H, s, 4-H), 3.29 (1H, td, J=9.0, 5.5 Hz, 23-Ha), 3.08 (1H, q, J=9.0 Hz, 23-Hb), 1.07 (3H, s, 10-Me), 0.91 (3H, d, J=6.5 Hz, 20-Me), 0.66 (3H, s, 13-Me); ^{13}C NMR (500 MHz, $CDCl_3$) δ 165.4, 137.7, 137.6, 132.8, 130.4, 129.4, 128.3, 128.2, 127.7, 127.5, 127.4, 127.2, 94.6, 94.5, 79.2, 76.4, 70.5, 69.7, 69.5, 55.6, 50.2, 47.2, 42.7, 39.7, 39.2, 38.1, 37.3, 35.9, 32.8, 31.0, 28.1, 23.8, 22.4, 20.2, 17.9, 13.3, 11.9, 5.4; MS (ESI) m/z 857 $(M+Na)^+$.

4.2.9. 3α-Benzoyloxy-4β,7α-dibenzyloxymethoxy-24-nor-5α-cholan-23-al 6. To a solution of iodide **18** (14 mg, 17 μmol) in DMSO (0.5 mL) was added 2,4,6-collidine (11 μL, 81 μmol). After stirring for 10 min at 150 °C, the reaction mixture was cooled to rt, then quenched with water, and extracted with dichloromethane. The combined organic layer was washed with 0.5 M HCl and saturated NaCl, dried over $MgSO_4$, filtered, and concentrated under reduced pressure. The residue was purified by silica gel column chromatography (hexane/ethyl acetate=15:1–8:1) to give **6** (11 mg, 94%) as colorless oil.

Compound **6**. Colorless oil; R_f 0.25 (hexane: ethyl acetate=5:1); $[\alpha]_D^{23}$ −11.3° (*c* 0.23, $CHCl_3$); IR (thin film) 2933, 2719, 1718, 1270, 1108, 1038, 1026 cm^{-1}; ^1H NMR (500 MHz, $CDCl_3$) δ 9.73 (1H, dd, J=3.5, 1.0 Hz, CHO), 8.00 (2H, d, J=8.5 Hz, $PhCO_2$), 7.56–7.09 (13H, m, $PhCO_2$, Ph), 5.27 (1H, q, J=3.5 Hz 3-H), 4.82, 4.78, 4.70 and 4.69 (4H, d×4, J=7.0 Hz, OCH_2O), 4.64, 4.60, 4.49 and 4.46 (4H, d×4, J=12.0 Hz, OCH_2Ph), 3.72 (1H, s, 7-H), 3.57 (1H, s, 4-H), 1.07 (3H, s, 10-Me), 1.01 (3H, d, J=6.0 Hz, 20-Me), 0.70 (3H, s, 13-Me); ^{13}C NMR (500 MHz, $CDCl_3$) δ 203.3, 165.4, 160.7, 137.7, 137.6, 132.8, 130.4, 129.4, 128.3, 128.2, 127.7, 127.5, 127.4, 127.2, 94.6, 94.6, 79.2, 76.4, 70.5, 69.8, 69.5, 55.8, 50.9, 50.2, 47.2, 42.7, 39.8, 39.1, 38.1, 35.9, 32.9, 31.7, 31.0, 28.4, 23.8, 22.4, 20.2, 20.1, 13.3, 11.9; MS (ESI) m/z 777 $(M+MeOH+Na)^+$.

4.2.10. 104β,7α-Dibenzyloxymethoxy-5α-cholest-23-ene-3α,26-diol,3α-benzoate, (25*S*) 19. To a stirred suspension of phosphonium salt **4** (101 mg, 0.243 mmol) in (1 mL) was added in dropwise a solution of 1.6 M *n*-BuLi in hexane (304 μl, 0.486 mmol) at −78 °C, then stirred for 10 min at 0 °C. TMSCl (31 μl, 0.243 mmol) was added to the reaction mixture at 0 °C, and stirred for 30 min at rt. A portion of the resulting solution of the ylide (324 μL, 60.9 μmol) was added to the solution of **6** (11.0 mg, 15.2 μmol) in THF (0.54 mL) at −78 °C, and stirred for 15 min, then stirred at 0 °C for 1 h, and stirred for 2 h at rt. The reaction mixture was quenched with 0.5 M HCl (0.2 mL) and stirred for 10 min at rt, and extracted with ether. Combined organic layer was washed with saturated NaCl. Concentration followed by silica gel column chromatography (hexane/ethylacetate=10:1–5:1) gave **19** (8.2 mg, *E*/*Z*=1:8, 69%) as colorless oil.

Compound **19**. Colorless oil; R_f 0.45 (1:2—ethyl acetate/hexane); ^{1}H NMR (500 MHz, $CDCl_3$) δ 8.00 (2H, d, *J*=7.5 Hz, $PhCO_2$), 7.52–7.09 (13H, m, $PhCO_2$, Ph), 5.53–5.44 (1H, m, 23-H), 5.27 (1H, d, *J*=2.5 Hz 3-H), 5.22 (1H, dd, *J*=15.5, 8.0 Hz, 24-H,E), 5.15 (1H, t, *J*=10.5 Hz, 24-H,Z), 4.82, 4.80, 4.71 and 4.70 (4H, d×4, *J*=6.5 Hz, OCH_2O), 4.64, 4.60, 4.49 and 4.47 (4H, d×4, *J*=12.0 Hz, OCH_2Ph), 3.73 (1H, s, 7-H), 3.57 (1H, s, 4-H), 3.46 (1H, dd, *J*=10.0, 6.0 Hz 26-Ha), 3.36–3.31 (1H, m, 26-Hb), 1.07 (3H, s, 10-Me), 0.93 (3H, d, *J*=6.0 Hz, 20-Me or 25-Me), 0.92 (3H, d, *J*=6.0 Hz, 20-Me or 25-Me), 0.66 (3H, s, 13-Me).

4.2.11. 4β,7α-Dibenzyloxymethoxy-5α-cholest-23-ene-3α,26-diol, (25*S*) 20. To a solution of **19** (8.2 mg, 10.5 μmol) in THF (0.6 mL) was added $LiAlH_4$ (4.0 mg, 105 μmol) at 0 °C. After stirring for 15 min, the reaction was quenched with water and diluted with ether, and the resulting precipitates were removed by filtration through the Celite pad. The filtrate was concentrated and purified by silica gel column chromatography (hexane/ethyl acetate=5:1–2:1) to give **20** (6.2 mg, 87%) as colorless oil.

Compound **20**. Colorless oil; R_f 0.20 (1:2—hexane/ethyl acetate=2:1); ^{1}H NMR (500 MHz, $CDCl_3$) δ 7.35–7.24 (10H, m, Ph), 5.53–5.44 (1H, m, 23-H), 5.21 (1H, dd, *J*=15.5, 8.0 Hz, 24-H,*E*), 5.16 (1H, t, *J*=10.5 Hz, 24-H,*Z*), 4.83, 4.75 and 4.72 (3H, d×3, *J*=7.5 Hz, OCH_2O), 4.65–4.55 (5H, m, OCH_2O×1 and OCH_2Ph×4), 3.93 (1H, d, *J*=2.5 Hz, 3-H), 3.74 (1H, s, 7-H), 3.48–3.43 (1H, m, 26-Ha), 3.36–3.31 (2H, m, 26-Hb and 4-H), 0.99 (3H, s, 10-Me), 0.92 (3H, d, *J*=7.0 Hz, 20-Me or 25-Me), 0.91 (3H, d, *J*=5.0 Hz, 20-Me or 25-Me), 0.64 (3H, s, 13-Me).

4.2.12. (3α,4β,7α,25*S*)-3,4,7,26-Tetrahydroxy-5α-cholestane-3,26-disulfate 2. A mixture of **20** (4.1 mg, 6.07 μmol) and SO_3·Py (19.3 mg, 0.121 mmol) in a 10 mL flask was dried under the reduced pressure. To the mixture was added pyridine (0.6 mL) and the resulting mixture was stirred for 50 min at 60 °C. The pyridine was removed and dried in vacuo for 5 h. To the residue was added ether, and decanted to remove excess SO_3·Py. The precipitates were dissolved in chloroform, and insoluble impurities were removed by decantation. The solvent was removed under the reduced pressure to give the pyridinium salt. To the solution of the residue in methanol (2.0 mL) was added Amberite IR-120B (1.7 g), and stirred for 3 h at rt. The resin was removed by filtration, and the filtrate was concentrated. The residue was dissolved in methanol (2.0 mL) again, and the solution was added Amberite IR-120B (1.7 g), and stirred for 4.5 h at rt. The resin was removed by filtration, and the filtrate was concentrated. The residue was dissolved in methanol (2.0 mL) and added 10% Pd on charcoal (52 mg, 61 μmol). The mixture was stirred under the hydrogen atmosphere for 2.5 h at rt. The catalyst was removed by filtration through Celite pad, and the filtrate was concentrated in vacuo. The residue was purified by HPLC to give **2** as colorless solid.

Compound **2**. Colorless solid; R_f 0.13 (chloroform/methanol=2:1); HPLC RT 5.2 min; HPLC conditions {column, TSK-GEL ODS-120T (φ 4.6×250 mm); flow rate, 1.0 mL/min; solvent A, H_2O; solvent B, CH_3CN; gradient, solvent B 21% (0–20 min)}; ^{1}H NMR (500 MHz, D_2O) δ 4.41 (1H, d, *J*=2.5 Hz, 3-H), 3.96 (1H, d, *J*=2.0 Hz 7-H), 3.92 (1H, dd, *J*=9.0, 5.5 Hz, 26-Ha), 3.83 (1H, dd, *J*=9.0, 7.0 Hz, 26-Hb), 3.72 (1H, s, 4-H), 1.81 (1H, d, *J*=15.0 Hz, 5-H), 0.97 (3H, s, 10-Me), 0.92 (3H, d, *J*=6.5 Hz, 25-Me), 0.90 (3H, d, *J*=6.5 Hz, 20-Me), 0.65 (3H, s, 13-Me); MS (ESI) *m*/*z* 297 $(M-2Na)^{-2}$.

4.2.13. (3α,4β,7α,25*R*)-3,4,7,26-Tetrahydroxy-5α-cholestane-3,26-disulfate 3. *Compound* **3**. Colorless solid; R_f 0.13 (chloroform/methanol=2:1); HPLC conditions {column, TSK-GEL ODS-120T (φ 4.6×250 mm); flow rate, 1.0 mL/min; solvent A, H_2O; solvent B, CH_3CN; gradient, solvent B 21% (0–20 min)}; ^{1}H NMR (500 MHz, D_2O) δ 4.41 (1H, d, *J*=2.5 Hz, 3-H), 3.96 (1H, d, *J*=2.5 Hz 7-H), 3.91 (1H, dd, *J*=9.0, 5.5 Hz, 26-Ha), 3.83 (1H, dd, *J*=9.0, 7.0 Hz, 26-Hb), 3.72 (1H, s, 4-H), 1.81 (1H, d, *J*=15.0 Hz, 5-H), 0.97 (3H, s, 10-Me), 0.91 (3H, d, *J*=7.0 Hz, 25-Me), 0.90 (3H, d, *J*=6.0 Hz, 20-Me), 0.65 (3H, s, 13-Me); MS (ESI) *m*/*z* 297 $(M-2Na)^{-2}$.

4.3. Estimation of the amount of natural SAAF

A standard solution of synthetic SAAF in D_2O was prepared and its concentration was estimated by ^{1}H NMR using DMF as internal standard (1.26 mM). ^{1}H NMR spectra of natural SAAF (x μg) and synthetic SAAF (4 μg and 40 μg) in 40 μL of D_2O solution were recorded on a JEOL L-500 spectrometer (500 MHz) with a 1.7-mm probe (Nanolac, Z-Spec-SMIDG500) under the same conditions (receiver gain: 28, acquisition times: 6176, temperature, 29.9 °C). The signal intensity of the natural SAAF was identical with that of the synthetic SAAF containing 4 μg of sample, and approximately tenth part of 40 μg of sample.

4.4. Biological activities

A sample in an aqueous solution was mixed with the same volume of 2% agar, and the mixture was enclosed in the tip of glass capillary with a diameter of ca. 50 μm. The capillary was inserted in sea water including an appropriate number of sperm, and images of sperm around the capillary tip were recorded onto a personal computer every 20 msec

using a high-speed CCD camera (HAS-200, Ditect) and a video card (HAS-PCI, Ditect). The position of each sperm was analyzed using the image analyzing program (Dip-motion 2D, Ditect), and parameters (the chemotaxis index, D, dD/dt, velocity, θ) were calculated from the position of the data. See a previous report for details of the bioassay.[10]

Acknowledgements

We thank Drs. M. Ikeda and H. Ohtake (Dokkyo University School of Medicine) for their help in the measurement of ESI/TOF-MS; Dr. H. Naoki (Suntory Institute for Bio-organic Research) for measurement of MS/MS; to Mr. S. Adachi (Osaka University) for NMR measurements; Dr. Tsutsui (Univ. of Tokyo) for his advice; and to Ms M. Ishikawa, Mr. H. Iryu, and Mr. M. Sekifuji (Univ. of Tokyo) for their technical work. We also thank the directors and staff of the Education and Research Center of Marine Bioresources (Tohoku University) and Otsuchi Marine Research Center (University of Tokyo) for supplying materials. This work was supported in part by a Grant-In-Aid for Scientific Research on Priority Area (A) (No. 12045235) from MEXT, Japan to M. Yoshida, M. Murata, and by Grant-In-Aids from the Ministry of Education, Culture, Sports, Science and Technology, Japan to M. Morisawa.

References and notes

1. Miller, R. L. In *Biology of Fertilization*; Metz, C. B., Monroy, A., Eds.; Academic: New York, 1985; p 275.
2. Cosson, M. P. In *Controls of Sperm Motility: Biological and Clinical Aspects*; Gagnon, C., Ed.; CRC: Boca Raton, FL, 1990; p 104.
3. Cosson, J.; Carré, D.; Cosson, M. P. *Cell Motil. Cytoskeleton* **1986**, *6*, 225.
4. Punnett, T.; Miller, R. L.; Yoo, B.-H. *J. Exp. Zool.* **1992**, *262*, 87.
5. Ward, G. E.; Brokaw, C. J.; Garbers, D. L.; Vacquier, V. D. *J. Cell Biol.* **1985**, *101*, 2324.
6. Coll, J. C.; et al. *Mar. Biol.* **1994**, *118*, 177.
7. Olson, J. H.; Xiang, X.; Ziegert, T.; Kittelson, A.; Rawls, A.; Bieber, A. L.; Chandler, D. E. *Proc. Natl. Acad. Sci. U. S. A.* **2001**, *98*, 11205.
8. Yoshida, M.; Inaba, K.; Morisawa, M. *Dev. Biol.* **1993**, *157*, 497.
9. Yoshida, M.; Inaba, K.; Ishida, K.; Morisawa, M. *Dev. Growth Differ.* **1994**, *36*, 589.
10. Yoshida, M.; Murata, M.; Inaba, K.; Morisawa, M. *Proc. Natl. Acad. Sci. U. S. A.* **2002**, *99*, 14831.
11. Oishi, T.; Tsuchikawa, H.; Murata, M.; Yoshida, M.; Morisawa, M. *Tetrahedron Lett.* **2003**, *44*, 6387.
12. Iorizzi, M.; Bryan, P.; McClintock, J.; Minale, L.; Palagiano, E.; Maurelli, S.; Ricchio, R.; Zollo, F. *J. Nat. Prod.* **1995**, *58*, 653.
13. Naoki, H.; Murata, M.; Yasumoto, T. *Rapid Commun. Mass Spectrom.* **1993**, *7*, 179.
14. Tserng, K.-Y. *J. Lipid Res.* **1978**, *19*, 501.
15. (a) Gao, Y.; Sharpless, K. B. *J. Am. Chem. Soc.* **1988**, *110*, 7538. (b) Kim, B. M.; Sharpless, K. B. *Tetrahedron Lett.* **1989**, *30*, 655.
16. (a) Trost, B. M.; Pulley, S. R. *J. Am. Chem. Soc.* **1995**, *117*, 10143. (b) Pettit, G. R.; Melody, N.; Herald, D. L. *J. Org. Chem.* **2001**, *66*, 2583.
17. Sheldon, R. A.; Kochi, J. K. *Org. React.* **1972**, *19*, 279.
18. (a) Kozikowski, A. P.; Chen, Y. Y. *J. Org. Chem.* **1981**, *46*, 5248. (b) Bergmann, J.; Löfstedt, C.; Ivanov, V. D.; Francke, W. *Eur. J. Org. Chem.* **2001**, *16*, 3175.
19. (a) White, J. D.; Jeffrey, S. C. *J. Org. Chem.* **1996**, *61*, 2600. (b) Wang, X.; Erickson, S. D.; Iimori, T.; Still, W. C. *J. Am. Chem. Soc.* **1992**, *114*, 4128.

Available online at www.sciencedirect.com
SCIENCE DIRECT®
Tetrahedron
Tetrahedron 60 (2004) 6981–6988

Kalihinols from two *Acanthella cavernosa* sponges: inhibitors of bacterial folate biosynthesis

Tim S. Bugni,[a] Maya P. Singh,[b] Lei Chen,[b] Daniel A. Arias,[b] Mary Kay Harper,[a] Michael Greenstein,[b] William M. Maiese,[b] Gisela P. Concepción,[c] Gina C. Mangalindan[c] and Chris M. Ireland[a,*]

[a]*Department of Medicinal Chemistry, University of Utah, 30 South 2000 East, Room 307, Salt Lake City, UT 84112, USA*
[b]*Wyeth Research, Pearl River, New York, NY 10965, USA*
[c]*Marine Science Institute, University of the Philippines, Diliman, Quezon City 1101, Philippines*

Received 31 May 2003; revised 27 August 2003; accepted 27 August 2003

Available online 25 June 2004

Abstract—*Acanthella* spp. sponges have been prolific sources of highly functionalized diterpene antibiotics. Two *Acanthella cavernosa* sponges were investigated based on the activity of their extracts in a screen designed to detect bacterial folate biosynthesis inhibitors. *Bacillus subtilis* PY79 strain harboring a *lacZ* reporter gene fusion to a trimethoprim-responsive promoter (P*panB*) was used for the screen. The ability of kalihinols to inhibit bacterial folate biosynthesis was investigated resulting in preliminary structure activity relationships. Eight kalihinol type diterpenes were isolated from two Philippine *Acanthella cavernosa* specimens including two new 10- and 15-formamido-kalihinol F analogs.

1. Introduction

Resistance of pathogenic microorganisms to our current arsenal of antibiotics is an ever-growing concern. The World Health Organization estimates that in the industrialized world, 60% of all hospital acquired infections are caused by drug resistant microbes.[1] The increase in resistance of infectious microorganisms provides strong evidence for the need to identify new antibiotic therapeutics. For these reasons we have been investigating marine macro- and microorganisms for antibiotic activity. Recently, we investigated sponge extracts that showed potent antimicrobial activity by inhibiting bacterial folate biosynthesis.

Folate is an essential cofactor for metabolic processes such as purine, pyrimidine, amino acid, and pantothenic acid biosynthesis. In contrast to mammalian cells, bacteria are unable to utilize exogenous folate derivatives and must therefore synthesize folate de novo. Many proteins that catalyze steps in this pathway are well conserved across most bacterial species, and some have no direct mammalian homologs. Inhibitors of dihydrofolate reductase (trimethoprim and other diaminopyrimidines) and dihydropteroate synthase (sulfonamides) are well known antibacterial agents; however, other enzymes in the folate biosynthesis pathway are relatively untapped. An alliance between Wyeth Research and Millennium Pharmaceuticals, Inc. was established to focus on developing a screen for the detection of novel inhibitors of the enzymes in the bacterial folate pathway. Transcriptional profiling of trimethoprim- and sulfamethoxazole-treated *Bacillus subtilis* PY79 cultures resulted in identification of strong up-regulation of the *panBCD* gene cluster. Therefore, the *panB* promoter was fused to the *Escherichia coli* β-galactosidase gene and integrated into the *B. subtilis* genome. Cultures of this reporter fusion strain showed greatly increased β-galactosidase activity upon inhibition of the folate pathway with trimethoprim or sulfamethoxazole. This strain provided a simple, high throughput screen for inhibitors of folate biosynthesis.[2]

During the screening process, we identified extracts from two Philippine *Acanthella cavernosa* specimens that showed potent inhibition of bacterial folate biosynthesis. *Acanthella* spp. sponges have been prolific sources of isonitrile-, isothiocyanate-, isocyanate-, and formamide-containing diterpenes.[3–7] Many of these diterpenes have been reported to exhibit potent antibacterial activity, but no data describing their mechanism of action or bacterial target has been presented. In this report, we present the structures of two new formamide-containing diterpene antibiotics,

Keywords: *Acanthella cavernosa*; Sponge; Kalihinol; Folate biosynthesis; Antibacterial; Philippines.
* Corresponding author. Tel.: +1-801-581-8305; fax: +1-801-585-6208; e-mail address: cireland@pharm.utah.edu

0040–4020/$ - see front matter © 2004 Elsevier Ltd. All rights reserved.
doi:10.1016/j.tet.2003.08.082

show that these antibiotics inhibit bacterial folate biosynthesis, and present the activity of nine kalihinol-type diterpenes.

2. Results and discussion

2.1. Isolation and elucidation

Each of the two *A. cavernosa* sponges was extracted with MeOH and fractionated using activity against *B. subtilis* (ATCC #6633) as a guide. By the use of solvent partitioning, LH-20 size-exclusion chromatography, and C_8 reversed-phase chromatography, eight kalihinol analogs were isolated and subsequently investigated for their ability to inhibit bacterial folate biosynthesis. The known kalihinols Y (**1**),[5] X (**2**),[5] and J (**3**)[3] were isolated from *A. cavernosa* (specimen PI96-3-41). From another *A. cavernosa* (specimen PDZ98-1-17), the previously reported kalihinols F (**4**)[5,7] and G (**5**)[5] were isolated along with kalihinene (**6**)[6] and two new formamido analogues, 10-formamido-kalihinol F (**7**) and 15-formamido-kalihinol F (**8**). Compounds **1**–**6** were identified by comparison with literature data while 10-formamido-kalihinol F (**7**) and 15-formamido-kalihinol F (**8**) were identified and assigned using NMR. Kalihinol A (**9**) was obtained from Professor Paul J. Scheuer for additional structure activity data.

10-Formamido-kalihinol F (**7**) was isolated as a colorless film and the ^{1}H and ^{13}C NMR spectra (see Table 1) indicated that compound **7** was a kalihinol F (**4**) analog. HRCIMS data showed that compound **7** had a molecular formula of $C_{23}H_{35}N_3O_3$. The formamide was identified from the characteristic signals at δ 8.25 (s-*trans*, H-21) and δ 8.05 (s-*cis*, H-21) that were each coupled to an amide proton at δ 5.70 (NH) and δ 5.21 (NH), respectively. 10-Formamido-kalihinol F (**7**) was found to exist with the formamide presenting a 2:3 *cis*/*trans* ratio in $CDCl_3$ and the mixture resulted in doubled carbon signals in the ^{13}C NMR spectrum.

Distinction between the isonitrile-bonded carbons and the formamide-bonded carbons was based both on chemical shift and on the nature of the ^{13}C signal. The ^{13}C signals for carbons bonded to an isonitrile are either triplets (J=5.5 Hz) or are very broad due to ^{13}C–^{14}N coupling while the formamide bonded ^{13}C signals do not exhibit this coupling. Additionally, chemical shifts for isonitrile-bonded carbons tend to be between 59 and 65 ppm, while formamide-bonded carbons tend to resonate between 55 and 59 ppm. Therefore, the formamide was at C-10 based on the ^{13}C chemical shift of C-10 (δ 55.12, s-*trans*).

15-Formamido-kalihinol F (**8**) was isolated as a colorless film with a molecular formula of $C_{23}H_{35}N_3O_3$, established by HRCIMS. Although the MS data were nearly identical for **7** and **8** indicating that compound **8** was a regio-isomer of **7**, many of the ^{1}H signals (see Table 2) were more strongly affected by the formamide geometry as compared to **7**. H-14 was observed at δ 3.81 and δ 4.18 for the *trans*/*cis* conformers, respectively. Key HMBC correlations between the gem-dimethyls (H-16 and H-17) and carbons at δ 56.62 (s-*cis* C-15) and δ 55.29 (s-*trans* C-15) helped establish that the formamide was attached to the C-15 carbon. Although the structure could be confirmed by spectroscopic data, the upfield ^{1}H shifts were difficult to assign. The compound existed as a 1:1 mixture and the equilibrium between the *trans*/*cis* isomers could not be effected easily. Several different NMR solvents were used along with variable temperatures, but the ratio did not change significantly.

Table 1. NMR data for 10-formamido-kalihinol F (**7**) in $CDCl_3$

Position	s-*trans*		s-*cis*	
	δ ^{13}C	δ ^{1}H	δ ^{13}C	δ ^{1}H
1	42.2	1.46[a]	41.2	1.46
2	21.2	1.40–1.62	21.2	1.40–1.62
3	32.7	1.78	32.8	1.78
		1.54		1.54
4	70.3		70.3	
5	63.5	4.37 (bs)	63.5	4.37 (bs)
6	36.6	2.16	36.3	2.1
7	46.5	1.74	46.6	1.74
8	20.8	1.40–1.62	20.8	1.40–1.62
9	40.9	1.81	38.2	1.74
		1.66		1.58
10	55.1		56.4	
11	87.5		87.7	
12	37.2	1.61	37.2	1.61
13	25.0	2.05	24.8	2.05
		1.85		1.65
14	82.8	3.93 (dd, J=9.0, 3.8 Hz)	82.8	3.93 (dd, J=9.0, 3.8 Hz)
15	60.1		60.1	
16	23.9	1.37	23.7	1.37
17	28.7	1.38	28.6	1.38
18	17.8	1.05	17.7	1.04
19	25.9	1.38	25.9	1.38
20	19.5	1.23	19.1	1.34
21	162.6	8.25 (d, J=12.4 Hz)	160.6	8.05 (d, J=1.8 Hz)
NH		5.70 (d, J=12.4 Hz)		5.21 (bs)

[a] Unless the multiplicity is indicated, the ^{1}H shift was estimated from gHSQC spectra.

Table 2. NMR data for 15-formamido-kalihinol F (**8**) in $CDCl_3$

Position	s-*trans*		s-*cis*	
	δ ^{13}C	δ ^{1}H	δ ^{13}C	δ ^{1}H
1	42.4[a]	1.77[b]	42.2[a]	1.74
2	21.4		21.4	
3	32.5	1.81	32.5	1.81
		1.60		1.60
4	70.3[a]		70.1[a]	
5	63.5	4.39 (bs)	63.5	4.30 (bs)
6	35.9	1.99	35.9	1.99
7	47.1[a]	1.60	46.4[a]	1.61
8	24.2[a]		24.1[a]	
9	40.1[a]	1.76	39.9[a]	1.72
10	59.9		59.9	
11	86.6		86.2	
12	38.7	1.52	38.3	1.52
13	24.5[a]		24.3[a]	
14	84.1	3.81 (dd, *J*=9.1, 5.1 Hz)	82.4	4.18 (dd, *J*=9.1, 5.1 Hz)
15	55.3		56.7	
16	22.7	1.27	23.1	1.35
17	25.8	1.29	24.7	1.34
18	17.8	1.01	17.5	1.01
19	28.6	1.41	28.6	1.38
20	20.8	1.31	20.7	1.31
21	163.1	8.27 (d, *J*=12.5 Hz)	161.2	8.05 (d, *J*=1.8 Hz)
NH		5.98 (d, *J*=12.5 Hz)		5.59 (bs)

[a] For each position the assignment for *cis* and *trans* may be interchanged.
[b] Unless the multiplicity is indicated, the ^{1}H shift was estimated from gHSQC spectra.

Therefore, the assignments were made almost entirely from HSQC spectra and most of the upfield protons appeared to be the same for both the *cis* and *trans* isomers since small differences could not be observed if present. The overlap precluded absolute assignment of all ^{13}C shifts for both the *cis* and *trans* isomers (see Table 2). The relative stereochemistry for both **7** and **8** was determined by comparing the ^{13}C shifts and optical rotation to kalihinol F (**4**). Aside from the differences due to the formamide moieties, both **7** and **8** had ^{13}C shifts that were nearly identical to those reported for kalihinol F (**4**).

The use of a higher field instrument (500 MHz vs 300 MHz) and the use of 2D experiments have allowed us to make minor changes to the NMR assignments for kalihinols Y (**1**) and J (**3**). For kalihinol Y (**1**) the assignments of the bridge head carbons have been reversed as compared to the original report. These assignments were based on HMBC correlations between olefinic methylene protons (H-20) and a carbon at δ 37.8 ppm, which we have assigned as C-1. The chemical shifts of C-1 and C-6 (δ 42.0) in kalihinol Y (**1**) differ from other kalihinols in that C-1 is usually near 42 ppm and C-6 is typically around 38 ppm. Although the new assignments were fully supported by the HMBC spectrum, the switch in chemical shifts for kalihinol Y (**1**) seemed unusual and was further investigated using Upsol[8]

Table 3. Activity of kalihinols and some reference antibiotics in the folate induction assay[a]

Compound	Induction ratio for different drug concentrations									
	8 μg/mL	4	2	1	0.5	0.25	0.125	0.06	0.03	0.015
Kalihinol Y (**1**)	**3.1**[b]	**5.6**	**7.9**	**5.6**	**5.9**	**4.2**	**3.3**	2.6	1	0.8
Kalihinol X (**2**)	**9.7**	**11.6**	**12.1**	**11.3**	**8.1**	**6.3**	**4.4**	2.6	1.3	1.2
Kalihinol J (**3**)	0.6	0.9	1	1.5	1.4	1.4	0.9	1.4	1.1	1.3
Kalihinol F (**4**)	**9.5**	**8.2**	**7.1**	**3.9**	1.3	0.2	1.1	1.6	1.5	1.4
Kalihinol G (**5**)	**6.8**	**6.3**	**5.5**	**3.8**	0.9	0.8	1.5	1.5	1.4	1.2
Kalihinene (**6**)	**25.0**	**14.7**	**7.0**	1.6	1.3	**3.5**	2.2	2.2	1.7	1.7
10-Formamido-kalihinol F (**7**)	1.9	0.9	0.4	0.3	0.7	0.9	1.1	1	0.9	1.2
15-Formamido-kalihinol F (**8**)	**6.1**	**4.7**	**2.5**	0.5	1	1.4	1.6	1.5	1.4	1.2
Kalihinol A (**9**)	**3.4**	1.1	1.5	1.6	1.5	1.4	1.2	1.4	1.3	1.2
Trimethoprim	**14.7**	**15.9**	**15**	**12.4**	**10.7**	**7.4**	**5.1**	2.3	1.5	1.3
Sulfamethoxazole	**5.3**	**5.3**	**5.6**	**4.4**	**3.7**	2.6	2.4	2.0	1.2	1.2
Rifampin	NT[c]	NT	2.1	2.1	2.1	1.9	2.9	**3.1**	2.9	2.6
Chloramphenicol	2.9	1.9	1.4	1.9	1.7	2.1	2.2	1.9	1.2	1
Ciprofloxacin	NT	NT	**3.8**	**5.5**	**8.3**	**10.2**	**12.7**	**9.7**	**4.0**	2.2
Polymyxin B	1.1	1.5	2	2	NT	NT	NT	NT	NT	NT
Penicillin G	NT	NT	NT	1.3	1.2	1.2	1.2	1.3	1.1	1.1

[a] Log-phase culture of *B. subtilis* PY79 (100 μL, OD_{600} of 0.16) treated with drug or DMSO (1 μL) for 5 h and luminescence read after 2 h of lysis buffer addition.
[b] Bold is used to indicate that the induction ratio is above 3 and considered active.
[c] Indicates not tested.

for chemical shift predictions. For similarly substituted decalin systems, the program predicted that C-1 shifts would be downfield of C-6 if C-10 were substituted with an isonitrile and a methyl. However, when C-10 was an olefin the predicted shift for C-1 was upfield of C-6 again consistent with our assignments.

For kalihinol J (**3**), our assignments differed from the original assignments at C-10 and C-15. Originally, C-10 was reported to have a chemical shift at δ 76.5, which is inconsistent with our data. We observed C-10 at δ 63.6 and the shift was confirmed by an HMBC correlation to the adjacent methyl protons (H-20). We observed a shift at δ 76.6 and assigned that to C-15 based on HMBC correlations to each of the gem-dimethyls, which show HMBC correlations to each other. Originally, C-15 was assigned the same chemical shift as C-4 and was reported at δ 71.1. The original report only reported one ^{13}C signal in the 63–64 ppm range and it is likely that the broad nature of isonitrile- and isothiocyanate-bonded ^{13}C signals combined with a lower field NMR did not allow both resonances to be observed.

2.2. Biological activities

Activity of the crude extracts in the primary folate screen (β-galactosidase induction assay) was used to prioritize selected leads for fractionation and structure elucidation. Antibacterial activity against *B. subtilis* and activity in the primary induction assay were used for activity-guided fractionation. The active fractions were then tested in the rescue assay to determine their specific effects on bacterial folate biosynthesis and to ensure selectivity. The rescue assay was based on the known fact that the presence of essential folate-cofactor-derived metabolites (pantothenate, glycine, methionine, thymidine and adenine) in the growth medium rescues bacteria from the negative effects of folate biosynthesis inhibition.

Activities of the kalihinols and known antibiotics in the primary folate screen are given in Table 3. Trimethoprim and sulfamethoxazole were used as control folate biosynthesis inhibitors. Kalihinols Y (**1**), X (**2**), F (**4**), G (**5**), kalihinene (**6**) and 15-formamido-kalihinol F (**8**) were found to be active in the primary induction assay while kalihinol A

Table 4. Antibacterial activity of kalihinols in different media and rescue of *B. subtilis* PY79 in the supplemented TSS medium

Compound	Conc. (μg/spot)	Zone of growth inhibition (mm)[a]		
		BS-PY79 on TSS	BS-PY79 on TSS+	SA375 on NBA
Kalihinol Y (**1**)	25	**15**[b]	**10**:**13H**[c]	20
	12.5	**14**	**14H**	20
	6.25	**13**	**14H**	20
	3.125	**13**	**13H**	20
	1.56 (MIC[d])	**13**	**13H**	19
Kalihinol X (**2**)	6.25	11	10	19
	3.125	12	11	19
	1.56 (MIC)	12	11	19
Kalihinol J (**3**)	50 (MIC)	7H	7H	10H
	25	7H	7H	10H
Kalihinol F (**4**)	25	**19**	**16**	22
	12.5 (MIC)	**15**	**14H**	19
	6.25	**8**	**8VH**[e]	14
	1.56	**10H**	**0**	0
Kalihinol G (**5**)	25	**17**	**14**	20
	12.5	**16**	**14**	21
	6.25	**15**	**13H**	21
	3.12 (MIC)	**14H**	**11H**	20
Kalihinene (**6**)	25	**11**	**8**	11
	12.5	**11**	**7**	10
	6.25 (MIC)	**9**	**7**	9
10-Formamido-kalihinol F (**7**)	50 (MIC)	11H	12H	16
15-Formamido-kalihinol F (**8**)	50 (MIC)	**11**	**8H**	16
Kalihinol A (**9**)	50 (MIC)	17H	17H	24
	25	15H	16H	22
Trimethoprim	2	**28**	**0**	14H
	1 (MIC)	**24**	**0**	10H
	0.5	**19**	**0**	0
Sulfamethoxazole	4 (MIC)	**27H**	**0**	27H
	2	**26H**	**0**	26H
Chloramphenicol	16 (MIC)	14	12	0
Ciprofloxacin	1 (4×MIC)	19	18	20
Rifampin	1 (30×MIC)	18	17	26
Polymyxin B	16	11	9	0
DMSO	10 μL	0	0	0

[a] Rescue of *B. subtilis* PY79 (loss or decrease in the zone of inhibition on TSS+agar compared to those on TSS agar, indicated in bold type) and activity against *S. aureus* (SA375) was determined by the agar diffusion assay.
[b] Bold is used to indicate values that show significant differential.
[c] Indicates a hazy zone.
[d] MICs (minimum inhibitory concentrations, μg/mL) were determined by the microbroth dilution method in low-salt LB medium using a log-phase culture of *B. subtilis* PY79 (OD_{600}=0.01) as inoculum and incubation at 30 °C for 16 h.
[e] Indicates a very hazy zone. Kalihinols were inactive against *C. albicans*.

(**9**) was borderline with an induction ratio of 3.4 at the highest concentration tested (Table 3). The weak activity of kalihinol A (**9**) as compared to X (**2**) and Y (**1**) indicates that substitutions at C-10 effect overall potency. Although 15-formamido-kalihinol F (**8**) showed moderate induction in the luminescence assay, the other formamido-containing kalihinols showed no induction. Additionally, the formamido analogs were the least active with MICs of 50 μg/mL. Since the position of the formamido did not significantly change the activity (identical MICs), the moiety might effect cellular uptake or specificity. The pyranyl-type kalihinols Y (**1**) and X (**2**) are the most potent antibacterials based on the MIC values for each (1.56 μg/mL), but they showed little differential in the rescue assay as compared to trimethoprim and sulfamethaoxazole which could indicate a secondary mechanism of action. Among the kalihinols, the furanyl type kalihinols (F (**4**), G (**5**), kalihinene (**6**)) showed the largest differential and perhaps the furanyl moiety could be important for specificity toward the folate pathway. Although rifampin and ciprofloxacin with very different modes-of-action also appeared to be active in the primary assay with low levels of induction, only the sulfa drugs and some of the kalihinols exhibited differential activity in the rescue assay (Table 4) indicating inhibition of bacterial folate biosynthesis.

3. Conclusion

The kalihinols display potent antibiotic activity and data presented here show that the furanyl type kalihinols are more selective inhibitors of bacterial folate biosynthesis than the pyranyl series. Since the rescue data for the kalihinols was not as distinct as for the controls, the kalihinols might have a secondary mechanism. Additionally, these data show that the C-10 position appears to be important for potency while formamide substituents markedly decrease activity. Further studies will be necessary to determine the specific target within the folate pathway. Compounds **7** and **8** are the first formamido containing analogs of kalihinol F (**4**) and could be derived from an isocyanato functionality.[9] The assay system employed for these studies can be used to identify antibacterial agents that are selective inhibitors of bacterial folate biosynthesis and will be useful for future antibiotic drug discovery. The overall results elaborate a major bacterial target for some of the kalihinol family of diterpenes.

4. Experimental

4.1. General procedures

The ^{1}H and ^{13}C spectra were obtained at 500 and 125 MHz, respectively, on a Varian Unity 500 spectrometer equipped with a Nalorac 3 mm probe at 26 °C. Proton shifts are reported in parts per million relative to the reference solvent signals at δ 7.24 for ^{1}H and δ 77.0 for ^{13}C for $CDCl_3$. UV spectra were obtained in MeOH on a Hewlett Packard 8452A diode array spectrophotometer. High- and low-resolution mass spectral measurements were made on a Finnegan MAT 95 high-resolution spectrometer. IR spectra were recorded on a Jasco FTIR-420 spectrophotometer and optical rotations were measured using a Jasco DIP-370 polarimeter in a 5 cm cell. Size-exclusion chromatography was performed using a glass column (4.5×46 cm) packed with Lipophilic Sephadex LH-20 (Sigma) in conjunction with a SpectraChrom CF-1 fraction collector. An Agilent 1100 equipped with a Rheodyne manual injector, a PDA detector, and a quaternary pump system was used for HPLC separations. An Agilent XDB C_8 column (9.4×250 mm) was used for semi-preparative HPLC separations. All solvents used for HPLC, UV, OR, and IR were Fisher HPLC grade and the H_2O was Barnstead E-pure 0.2 μm filtered. All reference antimicrobial agents and other media components were purchased from either Difco or Sigma Chemical Co., St Louis, MO. The chemiluminescent substrate Galacton-Star (GS040) and Sapphire-II enhancer (LAX250) used in the folate assay was purchased from PE Applied Biosystems, Bedford, MA.

4.2. Animal material

Sponge sample PI96-3-41 was obtained in March of 1996 by SCUBA at Dibud, Philippines (15° 40.21′, 121° 35.46′). Sponge sample PDZ98-1-17 was obtained in Davao Gulf, Mindanao, Philippines in 1998 by SCUBA. Both sponge specimens were stored at −20 °C in MeOH and each of the two sponges was identified as *Acanthella cavernosa*. Voucher samples are held at the University of Utah.

4.3. Microbiological media

Low-salt Luria-Bertani (LB) broth (per liter) contained: 10 g Bacto tryptone, 5 g Bacto yeast extract and 5 g NaCl in deionized water, adjusted to pH 7.0 with 5 N NaOH, and autoclaved at 15 psi for 25 min. TSS minimal agar medium (per liter) contained: 2 g NH_4Cl, 0.35 g $K_2HPO_4{\cdot}3H_2O$, 6 g tris base, 2 g sodium glutamate, 1 mM $CaCl_2$, 1 mM $MgSO_4$, 5 g glucose, 15 g Bacto agar and 10 mL of filter-sterilized 100× trace elements mix (125 mg $MgCl_2{\cdot}6H_2O$, 5.5 mg $CaCl_2$, 13.5 mg $FeCl_2{\cdot}4H_2O$, 1 mg $MnCl_2{\cdot}4H_2O$, 1.7 mg $ZnCl_2$, 0.43 mg $CuCl_2{\cdot}2H_2O$, 0.6 mg $CoCl_2{\cdot}6H_2O$, 0.6 mg $Na_2MoO_4{\cdot}2H_2O$ and two drops of conc. HCl in 1 L deionized water). Sodium glutamate and glucose solutions were made at 5 and 50% w/v, respectively, and filter sterilized before their additions to the final medium. For the supplemented TSS media (TSS+), a filter-sterilized mix of supplements was added to the minimal TSS medium to yield final concentrations of 0.04 mg/mL adenine, 0.4 mg/mL thymidine, 0.1 mg/mL glycine, 0.2 mg/mL methionine, and 0.002 mg/mL calcium pantothenate. Difco nutrient agar (NA) media was used for making *Staphylococcus aureus* assay plates.

4.4. In vitro antimicrobial activity

The in vitro antibacterial activities were determined by the agar diffusion or microbroth dilution method as previously described.[10] For the agar diffusion, assay plates (12″×12″ Sumilon) were prepared by pouring 125 mL of agar medium (tempered at 50 °C) inoculated with an overnight broth culture of the test organisms (adjusted to a final inoculum density of approximately 10^6 cells per mL). The medium was allowed to solidify and 10 μL volumes of antibiotic solutions diluted in DMSO or water were dispensed onto the

agar surface, and the plates were incubated at 37 °C for 18 h. The zones of growth inhibition were measured in millimeters (mm) using a hand-held digital caliper.

4.5. Induction assay for inhibitors of folate biosynthesis

The assay organism *B. subtilis* PY79 (*amy*::P*panB-lacZ*, CAT) was grown at 30 °C and 200 RPM) in the low-salt LB to an exponential phase (OD_{600}=0.6–0.8). The culture was diluted 1:6 in fresh LB broth and 100 μL volumes were used to inoculate the wells of a 96-well white Optiplate containing 1 μL of the test drug at 100× concentration or water (or DMSO) for untreated control. The plate was incubated at 30 °C for 5 h with shaking. At the end of the incubation period the plate was either frozen at −80 °C or processed immediately. For immediate processing, 100 μL of the freshly prepared mixture of the substrate Galacton-Star (0.4 parts), Sapphire-II Enhancer (2 parts) in 7.6 parts of the lysis buffer (0.026% sodium deoxycholic acid, 0.053% hexadecyltrimethyl-ammonium bromide, 265 mM NaCl, 395 mM HEPES, pH 7.5) was added to each well. The plate was incubated at room temperature for 2 h and luminescence for each well was read using a Luminometer (Victor[2] V, Perkin Elmer, USA). The induction ratio (luminescence count for drug treated/untreated) for each well was calculated and induction ratios of >3.0 were recorded as active.

4.6. Rescue assay for true inhibitors of folate biosynthesis

Antibacterial activities of the compounds were tested by the agar diffusion method (as described in the in vitro antimicrobial testing) in TSS and TSS+media. Test organism *B. subtilis* PY79 was grown overnight in low-salt LB at 37 °C and 200 RPM to a final OD_{600}>4.5. The overnight culture (625 μL) was added to 125 mL of TSS or TSS+agar medium tempered at 50 °C and poured into a Nunc square plate (12×12 in, Nalgene). After the agar solidified, 10 μL volumes of the drug solutions were spotted directly onto the surface and the plates were incubated at 37 °C for 18 h. Zones of growth inhibition were measured as described earlier.

4.7. Extraction and isolation

Biological activity against *B. subtilis* (ATCC 6633, disk diffusion method) was used as a guide for purification. Additionally, activity was confirmed by screening fractions for their ability to inhibit bacterial folate biosynthesis.

Sponge sample PI96-3-41 (49.28 g, wet weight) was extracted with MeOH (3×400 mL) and concentrated under vacuum to yield 3.66 g of crude extract. The crude extract was dissolved in 90% MeOH/H_2O (100 mL) and extracted with hexanes (3×100 mL). To the aqueous MeOH was added 40 mL of H_2O and extracted with $CHCl_3$ (3×100 mL). The hexanes, $CHCl_3$, and aqueous MeOH fractions were evaporated to dryness using a combination of rotary evaporation and vacuum to yield 440 mg, 300 mg, and 2.97 g, respectively. Activity was concentrated in the $CHCl_3$ fraction, which was subsequently separated on LH-20 using 1:1 $CHCl_3$/MeOH as eluant. After 100 mL had eluted, a fraction collector was used to collect 44 fractions (8 mL). The most active fractions (29–36) were combined and subsequently separated by C_8 semi-preparative HPLC using a linear gradient from 60% H_2O/40% CH_3CN to 100% CH_3CN over 20 min at a flow rate of 3.5 mL/min. Kalihinol Y (**1**) eluted at 19.7 min, and kalihinol X (**2**) eluted at 20.3 min. A peak eluting at 15.0 min was further purified by C_8 HPLC using isocratic conditions (3.5 mL/min, 75% MeOH/25% H_2O) and yielded kalihinol J (**3**) (R_t 15.4 min). Solvents were removed under reduced pressure.

Sponge sample PDZ98-1-17 (74.63 g, wet weight) was extracted with MeOH (3×600 mL) and concentrated under vacuum to yield 7.63 g of crude extract. The crude extract was dissolved in 90% MeOH/H_2O (150 mL) and extracted with hexanes (3×100 mL). To the aqueous MeOH was added 60 mL of H_2O and extracted with $CHCl_3$ (3×150 mL). The hexanes, $CHCl_3$, and aqueous MeOH fractions were evaporated to dryness using a combination of rotary evaporation and vacuum to yield 530 mg, 620 mg, and 6.18 g, respectively. The active $CHCl_3$ fraction was separated on LH-20 using 1:1 $CHCl_3$/MeOH. 125 mL were collected in a flask prior to using a fraction collector to collect 48 (8 mL) fractions. Based on the activity against *B. subtilis*, fractions 27–33 were combined to yield 156.0 mg of active material that was further purified using C_8 HPLC. Isocratic conditions (60% H_2O/40% CH_3CN) were used for the first 10 min followed by a gradient from 40% CH_3CN to 100% CH_3CN over 50 min. 10-Formamido-kalihinol F (**7**, 1.6 mg) eluted at 10.9 min; 15-formamido-kalihinol F (**8**, 2.9 mg) eluted at 13.5 min; kalihinol F (**4**, 16.5 mg) eluted at 24.7 min; kalihinol G (**5**, 1.2 mg) eluted at 32.1 min; and kalihinene (**6**, 0.6 mg) eluted at 40.1 min. All solvents were removed under reduced pressure.

4.7.1. Kalihinol Y (1). $[\alpha]_D^{25}=-23°$ (*c* 0.09, $CHCl_3$); UV (MeOH) λ_{max} (log ε) 204 (4.47), 238 (sh. 3.64); IR ν_{max} ($CHCl_3$) 3604, 2990, 2939, 2148, 1380 cm^{-1}; ^1H NMR (500 MHz, $CDCl_3$) δ 1.62 (1H, m, H-1), 1.71 (1H, m, H-2a), 1.69 (1H, m, H-2b), 1.88 (2H, m, H-3), 4.47 (1H, bm, H-5), 1.82 (1H, m, H-6), 1.78 (1H, m, H-7), 2.03 (1H, m, H-8), 2.29 (1H, dt, *J*=13.0, 3.5 Hz, H-9a), 1.60 (1H, m, H-9b), 1.60 (1H, m, H-12a), 1.51 (1H, m, H-12b), 2.01 (1H, m, H-13), 3.74 (1H, dd, *J*=12.2, 4.5 Hz), 1.32 (3H, s, H-16), 1.34 (3H, s, H-17), 1.13 (3H, s, H-18), 1.39 (3H, s, H-19), 4.68 (1H, d, *J*=1.6 Hz, H-20a), 4.58 (1H, d, *J*=1.6 Hz, H-20b); ^{13}C NMR (500 MHz, $CDCl_3$) δ 37.8 (C-1), 24.1 (C-2), 32.6 (C-3), 70.7 (C-4), 64.0 (C-5), 42.0 (C-6), 49.6 (C-7), 28.8 (C-8), 35.7 (C-9), 151.0 (C-10), 77.0 (C-11), 38.3 (C-12), 28.8 (C-13), 64.5 (C-14), 76.5 (C-15), 22.8 (C-16), 30.6 (C-17), 19.1 (C-18), 27.5 (C-19), 105.3 (C-20), 156.3 (NC); HRCIMS *m/z* 366.2193 ($[M+H]^+$ calcd for $C_{21}H_{33}ClNO_2$, 366.2200).

4.7.2. Kalihinol X (2). $[\alpha]_D^{25}=-30°$ (*c* 0.09, $CHCl_3$); UV (MeOH) λ_{max} (log ε) 204 (4.41), 244 (4.12); IR ν_{max} ($CHCl_3$) 3611, 2990, 2941, 2144, 2103, 1454, 1382 cm^{-1}; ^1H NMR (500 MHz, $CDCl_3$) δ 1.43 (1H, m, H-1), 1.73 (1H, m, H-2a), 1.58 (1H, m, H-2b), 1.82 (1H, m, H-3a), 1.56 (1H, m, H-3b), 4.56 (1H, bs, H-5), 2.16 (1H, m, H-6), 1.62 (1H, m, H-7), 1.62 (1H, m, H-8a), 1.26 (1H, m, H-8b), 1.64 (1H, m, H-9a), 1.50 (1H, m, H-9b), 1.93 (1H, m, H-12a), 1.46 (1H, m, H-12b), 2.00 (1H, m, H-13a), 2.08 (1H, m, H-13b),

3.72 (1H, dd, *J*=12.7, 4.4 Hz, H-14), 1.35 (3H, s, H-16), 1.33 (3H, s, H-17), 1.23 (3H, s, H-18), 1.39 (3H, s, H-19), 1.38 (3H, s, H-20); ^{13}C NMR (500 MHz, $CDCl_3$) δ 43.2 (C-1), 21.8 (C-2), 32.4 (C-3), 70.1 (C-4), 63.6 (C-5), 36.4 (C-6), 48.6 (C-7), 22.2 (C-8), 38.0 (C-9), 64.3 (C-10), 77.2 (C-11), 39.3 (C-12), 27.4 (C-13), 64.3 (C-14), 75.9 (C-15), 22.8 (C-16), 30.6 (C-17), 19.1 (C-18), 28.7 (C-19), 27.5 (C-20), 132.1 (NCS), 156.7 (NC); HRCIMS *m/z* 425.2031 ([M+H]$^+$ calcd for $C_{22}H_{34}ClN_2O_2S$, 425.2029).

4.7.3. Kalihinol J (3). $[\alpha]_D^{25}$=+24° (*c* 0.03, $CHCl_3$); UV (MeOH) λ_{max} (log ε) 204 (4.36), 242 (3.47); IR ν_{max} ($CHCl_3$) 3407, 2988, 2955, 2108 (br), 1684, 1456, 1386 cm^{-1}; ^{1}H NMR (500 MHz, $CDCl_3$) δ 1.43 (1H, dt, *J*=11.7, 3.3 Hz, H-1), 1.62 (2H, m, H-2), 1.58 (1H, m, H-3a), 1.42 (1H, m, H-3b), 4.28 (1H, bd, *J*=11.0 Hz, H-5), 2.42 (1H, dt, *J*=11.7, 2.4 Hz, H-6), 1.53 (1H, m, H-7), 1.57 (1H, m, H-8a), 1.38 (1H, m, H-8b), 1.87 (1H, dt, *J*=13.5, 3.2 Hz, H-9a), 1.58 (1H, m, H-9b), 1.62 (1H, m, H-12a), 1.42 (1H, m, H-12b), 2.08 (1H, dt, *J*=12.8, 4.3 Hz, H-13a), 1.99 (1H, m, H-13b), 3.67 (1H, dd, *J*=12.5, 4.3 Hz, H-14), 1.38 (3H, s, H-16), 1.31 (3H, s, H-17), 1.34 (3H, s, H-18), 1.20 (3H, s, H-19), 1.36 (3H, s, H-20), 8.14 (1H, d, *J*=11.7 Hz, CHO), 5.70 (1H, bt, *J*=11.7 Hz, NH); ^{13}C NMR (500 MHz, $CDCl_3$) δ 43.2 (C-1), 22.31 (C-2), 33.2 (C-3), 71.0 (C-4), 58.7 (C-5), 36.2 (C-6), 45.8 (C-7), 22.3 (C-8), 38.7 (C-9), 63.6 (C-10), 79.1 (C-11), 37.9 (C-12), 27.5 (C-13), 64.3 (C-14), 76.6 (C-15), 23.4 (C-16), 31.3 (C-17), 19.6 (C-18), 27.6 (C-19), 166.6 (CHO), 131.9 (NCS); HRCIMS *m/z* 443.2128 ([M+H]$^+$ calcd for $C_{22}H_{36}ClN_2O_3S$, 443.2136).

4.7.4. Kalihinol F (4). $[\alpha]_D^{25}$=+6° (*c* 0.22, $CHCl_3$); UV (MeOH) λ_{max} (log ε) 204 (4.30), 236 (sh, 3.56); IR ν_{max} ($CHCl_3$) 3416, 3005, 2952, 2140, 1455, 1386 cm^{-1}; ^{1}H NMR (500 MHz, $CDCl_3$) δ 1.77 (1H, m, H-1), 1.84 (1H, m, H-2a), 1.52 (1H, m, H-2b), 1.83 (1H, m, H-3a), 1.59 (1H, m, H-3b), 4.34 (1H, bs, H-5), 1.99 (1H, m, H-6), 1.75 (1H, m, H-7), 1.63 (1H, m, H-8a), 1.15 (1H, m, H-8b), 2.00 (1H, m, H-9a), 1.88 (1H, m, H-9b), 1.74 (1H, m, H-12a), 1.62 (1H, m, H-12b), 2.04 (1H, m, H-13a), 1.84 (1H, m, H-13b), 3.93 (1H, dd, *J*=9.3, 4.0 Hz, H-14), 1.37 (3H, bs, H-16), 1.38 (3H, bs, H-17), 1.02 (3H, s, H-18), 1.39 (3H, s, H-19), 1.30 (3H, bs, H-20); ^{13}C NMR (500 MHz, $CDCl_3$) δ 42.1 (C-1), 21.5 (C-2), 32.6 (C-3), 70.3 (C-4), 63.3 (t, *J*=5.5 Hz,

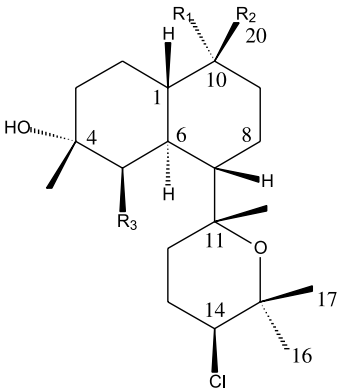

	R_1	R_2	R_3
Kalihinol Y (**1**)	═CH$_2$		NC
Kalihinol X (**2**)	NCS	CH_3	NC
Kalihinol J (**3**)	NCS	CH_3	NHCHO
Kalihinol A (**9**)	CH_3	NC	NC

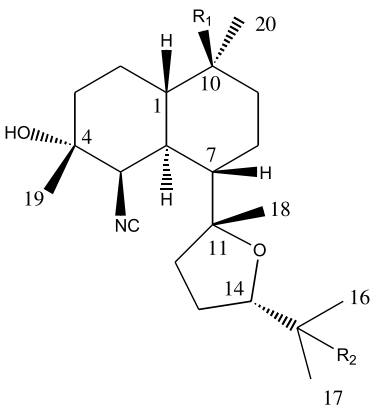

	R_1	R_2
Kalihinol F (**4**)	NC	NC
Kalihinol G (**5**)	NC	NCS
10-Formamido-kalihinol F (**7**)	NHCHO	NC
15-Formamido-kalihinol F (**8**)	NC	NHCHO

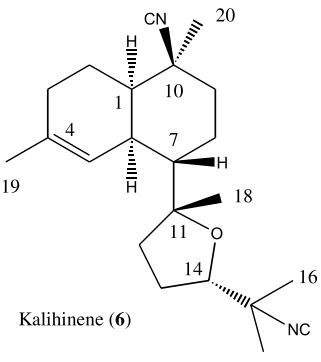

Kalihinene (**6**)

C-5), 35.9 (C-6), 46.3 (C-7), 24.2 (C-8), 39.8 (C-9), 59.8 (t, J=5.5 Hz, C-10), 87.3 (C-11), 38.2 (C-12), 25.0 (C-13), 82.8 (C-14), 60.0 (t, J=5.5 Hz, C-15), 23.9 (C-16), 25.9 (C-17), 17.8 (C-18), 28.6 (C-19), 20.7 (C-20), 153.13 (NC), 154.2 (NC), 158.1 (NC); HRCIMS m/z 384.2652 ($[M+H]^+$ calcd for $C_{23}H_{34}N_3O_2$, 384.2651).

4.7.5. Kalihinol G (5). $[\alpha]_D^{25}=-8°$ (c 0.04, $CHCl_3$); UV (MeOH) λ_{max} (log ε) 206 (4.50), 242 (4.16); IR ν_{max} ($CHCl_3$) 3410, 3004, 2951, 2139, 2104, 1457, 1386 cm^{-1}; ^1H NMR (500 MHz, $CDCl_3$) δ 1.80 (1H, m, H-1), 1.87 (2H, m, H-2), 1.85 (1H, m, H-3a), 1.59 (1H, m, H-3b), 4.34 (1H, bs, H-5), 1.96 (1H, m, H-6), 1.79 (1H, m, H-7), 1.66 (1H, m, H-8a), 1.16 (1H, m, H-8b), 1.99 (2H, m, H-9), 1.74 (1H, m, H-12a), 1.62 (1H, m, H-12b), 2.01 (1H, m, H-13a), 1.79 (1H, m, H-13b), 3.93 (1H, dd, J=9.2, 4.0 Hz), 1.34 (3H, bs, H-16), 1.37 (3H, bs, H-17), 1.02 (3H, s, H-18), 1.43 (3H, s, H-19), 1.31 (3H, s, H-20); ^{13}C NMR (500 MHz, $CDCl_3$) δ 42.1 (C-1), 21.6 (C-2), 32.6 (C-3), 70.6 (C-4), 63.2 (C-5), 36.0 (C-6), 46.3 (C-7), 24.2 (C-8), 39.8 (C-9), 59.8 (C-10), 87.3 (C-11), 38.1 (C-12), 25.1 (C-13), 83.5 (C-14), 63.7 (C-15), 25.5 (C-16), 24.3 (C-17), 17.8 (C-18), 28.8 (C-19), 20.7 (C-20); HRCIMS m/z 416.2374 ($[M+H]^+$ calcd for $C_{23}H_{34}N_3O_2S$, 416.2372).

4.7.6. Kalihinene (6). $[\alpha]_D^{25}=+16°$ (c 0.13, $CHCl_3$); UV (MeOH) λ_{max} (log ε) 208 (4.67), 238 (sh, 4.17); IR ν_{max} ($CHCl_3$) 3393, 2976, 2875, 2139, 1458, 1383 cm^{-1}; ^1H NMR (500 MHz, $CDCl_3$) δ 1.69 (1H, m, H-1), 2.00 (1H, m, H-2a), 1.29 (1H, m, H-2b), 2.01 (2H, m, H-3), 5.63 (1H, bd, J=4.4 Hz, H-5), 2.17 (1H, bm, H-6), 1.60 (1H, m, H-7), 1.13 (2H, m, H-8), 1.99 (2H, m, H-9), 1.74 (1H, m, H-12a), 1.66 (1H, m, H-12b), 1.38 (1H, m, H-13a), 1.13 (1H, m, H-13b), 3.79 (1H, bm, H-14), 1.29 (3H, bs, H-16), 1.33 (3H, bs, H-17), 1.09 (3H, s, H-18), 1.61 (3H, s, H-19), 1.51 (3H, s, H-20); ^{13}C NMR (500 MHz, $CDCl_3$) δ 43.8 (C-1), 20.4 (C-2), 30.7 (C-3), 131.1 (C-4), 126.3 (C-5), 34.7 (C-6), 48.1 (C-7), 24.7 (C-8), 33.9 (C-9), 60.9 (C-10), 86.5 (C-11), 37.2 (C-12), 25.7 (C-13), 82.9 (C-14), 60.4 (C-15), 26.4 (C-16), 25.1 (C-17), 19.7 (C-18), 23.4 (C-19), 26.8 (C-20), 153.4 (NC), 154.1 (NC); HRCIMS m/z 341.2584 ($[M+H]^+$ calcd for $C_{22}H_{33}N_2O$, 341.2593).

4.7.7. 10-Formamido-kalihinol F (7). $[\alpha]_D^{25}=+22°$ (c 0.03, $CHCl_3$); UV (MeOH) λ_{max} (log ε) 204 (4.34); IR ν_{max} ($CHCl_3$) 3600, 3425, 2940, 2141, 1681, 1458, 1381 cm^{-1}; ^1H NMR (500 MHz, $CDCl_3$) see Table 1; ^{13}C NMR (500 MHz, $CDCl_3$) see Table 1; HRCIMS m/z 402.2748 ($[M+H]^+$ calcd for $C_{23}H_{36}N_3O_3$, 402.2756).

4.7.8. 15-Formamido-kalihinol F (8). $[\alpha]_D^{25}=+9°$ (c 0.10, $CHCl_3$); UV (MeOH) λ_{max} (log ε) 206 (4.56); IR ν_{max} ($CHCl_3$) 3602, 3394, 3006, 2874, 2139, 1679, 1455, 1386 cm^{-1}; ^1H NMR (500 MHz, $CDCl_3$) see Table 2; ^{13}C NMR (500 MHz, $CDCl_3$) see Table 2; HRCIMS m/z 402.2760 ($[M+H]^+$ calcd for $C_{23}H_{36}N_3O_3$, 402.2756).

Acknowledgements

The authors gratefully acknowledge support provided by NIH grant CA36622 (C. M. I.). Funding for the Varian Unity 500-MHz NMR spectrometer was provided through NCI Grant No. 5 P30 CA 42014 and NIH Grant No. 1 S10RR 06262. Mass spectrometry was performed by Elliot M. Rachlin on a Finnigan Mat 95 funded by NSF grant CHE-9002690 and the University of Utah Institutional Funds Committee. The authors would also like to thank Drs. Leonard A. McDonald at Wyeth Research for assistance in LCMS analyses of fractions, Steven Projan at Wyeth Research for providing guidance in the screen development, Chris Murphy at Millennium Pharmaceuticals for providing guidance and the test strain PY79, and Paul J. Scheuer, Department of Chemistry, University of Hawaii at Manoa for providing Kalihinol A.

References and notes

1. World Health Organization; Infectious Disease Report 2000; http://who.int/infectious-disease-report/2000.
2. Murphy, C. *In PCT Int. Appl. US* **2002**, 31.
3. Alvi, K. A.; Tenenbaum, L.; Crews, P. *J. Nat. Prod.* **1991**, *54*, 71–78.
4. Miyaoka, H.; Shimomura, M.; Kimura, H.; Yamada, Y. *Tetrahedron* **1998**, *54*, 13467–13474. Okino, T.; Yoshimura, E.; Hirota, H.; Fusetani, N. *J. Nat. Prod.* **1996**, *59*, 1081–1083. Hirota, H.; Tomono, Y.; Fusetani, N. *Tetrahedron* **1996**, *52*, 2359–2368. Okino, T.; Yoshimura, E.; Hirota, H.; Fusetani, N. *Tetrahedron Lett.* **1995**, *36*, 8637–8640. Rodriguez, J.; Nieto, R. M.; Hunter, L. M.; Diaz, M. C.; Crews, P.; Lobkovsky, E.; Clardy, J. *Tetrahedron* **1994**, *50*, 11079–11090. Braekman, J. C.; Daloze, D.; Gregoire, F.; Popov, S.; Van Soest, R. *Bull. Soc. Chim. Belg.* **1994**, *103*, 187–191. Omar, S.; Albert, C.; Fanni, T.; Crews, P. *J. Org. Chem.* **1988**, *53*, 5971–5972. Chang, C. W. J.; Patra, A.; Roll, D. M.; Scheuer, P. J.; Matsumoto, G. K.; Clardy, J. *J. Am. Chem. Soc.* **1984**, *106*, 4644–4646.
5. Chang, C. W. J.; Patra, A.; Baker, J. A.; Scheuer, P. J. *J. Am. Chem. Soc.* **1987**, *109*, 6119–6123.
6. Fusetani, N.; Yasumuro, K.; Kawai, H.; Natori, T.; Brinen, L.; Clardy, J. *Tetrahedron Lett.* **1990**, *31*, 3599–3602.
7. Patra, A.; Chang, C. W. J.; Scheuer, P. J.; Van Duyne, G. D.; Matsumoto, G. K.; Clardy, J. *J. Am. Chem. Soc.* **1984**, *106*, 7981–7983.
8. GmbH, U. S.; 1.1 ed.; Scientific Software Engineering: Hergiswil, 1999–2000.
9. Hagadone, M. R.; Scheuer, P. J. *J. Am. Chem. Soc.* **1984**, *106*, 2447–2448.
10. Singh, M. P.; Petersen, P. J.; Weiss, W. J.; Janso, J. E.; Luckman, S. W.; Lenoy, E. B.; Bradford, P. A.; Testa, R. T.; Greenstein, M. *Antimicrob. Agents Chemother.* **2003**, *47*, 62–69.

Available online at www.sciencedirect.com
SCIENCE DIRECT®
Tetrahedron 60 (2004) 6989–6993
Tetrahedron

Nakiterpiosin and nakiterpiosinone, novel cytotoxic C-nor-D-homosteroids from the Okinawan sponge *Terpios hoshinota*

Toshiaki Teruya, Satoru Nakagawa, Tomoyuki Koyama, Hirokazu Arimoto, Masaki Kita[†] and Daisuke Uemura*

Department of Chemistry, Graduate School of Science, Nagoya University, Chikusa, Nagoya 464-8602, Japan

Received 15 July 2003; revised 6 August 2003; accepted 6 August 2003

Available online 25 June 2004

Abstract—Two new cytotoxic compounds, nakiterpiosin (**1**) and nakiterpiosinone (**2**), were isolated from the Okinawan sponge *Terpios hoshinota*. Their structures were determined by spectroscopic analysis. The absolute stereostructure of **1** was also determined by a modified Mosher's method. Nakiterpiosin (**1**) and nakiterpiosinone (**2**) showed potent cytotoxicity against mouse lymphocytic leukemia cell (P388).

1. Introduction

Coral reefs are known for their spectacular diversity and have significant aesthetic and commercial value, particularly in relation to fisheries and tourism. In addition, coral communities are good sources of medicines, including unique antimicrobial and anticancer agents.[1,2] However, many reefs around the world are increasingly threatened, principally from overfishing, pollution, typhoons, global warming and growing numbers of coral predators such as the crown-of-thorns starfish *Acanthaster planci*.[3] Recently, the overgrowth of coral communities by other organisms has been recognized as a factor that contributes to their destruction.[4] It has been reported that these organisms produce toxic compounds; for example, the steroidal alkaloids plakinamines A and B were isolated from the marine sponge *Plakina* sp. which overgrows coral heads.[5] Nakienones A-C and nakitriol were isolated from the Okinawan cyanobacteria *Synechocystis* sp. which also overgrows coral reefs.[6] Recently, we focused on the marine sponge *Terpios hoshinota*. Several large zones of the coral communities in waters off the Ryukyu Islands have been overgrown by the Okinawan sponge *T. hoshinota*.[7] We previously reported the isolation and structure determination of terpiodiene[8] from *T. hoshinota*. We report here the isolation and structure determination of nakiterpiosin[9] (**1**) and nakiterpiosinone (**2**).

2. Results and discussion

2.1. Isolation of nakiterpiosin and nakiterpiosinone

The marine sponge *T. hoshinota* (30 kg), collected at Nakijin, Okinawa Prefecture, was steeped in acetone for 7 days. The acetone extract was concentrated under reduced pressure, and the residue was extracted with ethyl acetate. The ethyl acetate-soluble portion was further partitioned between 90% aqueous methanol and hexane. The material obtained from the 90% aqueous methanol portion was successively chromatographed on silica gel and ODS silica gel, guided by cytotoxicity against P388 cells. Final purification was achieved by reversed-phase HPLC to give nakiterpiosin (**1**) [0.4 mg, IC_{50}=0.01 μg/mL] and nakiterpiosinone (**2**) [0.1 mg, IC_{50}=0.01 μg/mL].

2.2. Structure of nakiterpiosin

The molecular formula of nakiterpiosin (**1**) was determined to be $C_{27}H_{31}BrCl_2O_7$ (MNa^+, *m/z* 641.0490, Δ −1.7 mmu) by electrospray ionization mass spectrometry (ESIMS). The NMR data for **1** are summarized in Table 1. A detailed analysis of ^1H NMR, ^{13}C NMR and HMQC spectra showed that **1** contained three methyl groups, four methylenes, 12 methines, eight quaternary carbons, and two hydroxyl protons. The locations of hydroxyl groups in **1** were determined by the shifts of signals observed for H-4 (δ_H 5.28–6.20 ppm) and H-22 (δ_H 4.39–5.77 ppm) in the ^1H NMR spectrum of diacetate **3**, which was prepared by acetylation (acetic anhydride/pyridine) of **1**. Furthermore, the ^1H NMR spectrum of **1** showed the presence of a 1,2,3,4-tetrasubstituted benzene ring [δ_H 7.33 and 7.89 ppm

Keywords: C-nor-D-homosteroid; The sponge *Terpios hoshinota*; Nakiterpiosin; Nakiterpiosinone; Cytotoxicity.
* Corresponding author. Tel./fax: +81-52-789-3654;
e-mail address: uemura@chem3.chem.nagoya-u.ac.jp
[†] Research Center for Materials Science, Nagoya University.

0040–4020/$ - see front matter © 2004 Elsevier Ltd. All rights reserved.
doi:10.1016/j.tet.2003.08.083

Table 1. NMR data for nakiterpiosin in CD_3OD

Position	^1H (ppm)[a]	^{13}C (ppm)[b]	Position	^1H (ppm)[a]	^{13}C (ppm)[b]
1a	2.05 dd (12.3, 1.0)	41.7 t	14		152.3 s
1b	2.60 dd (12.3, 7.8)		15	7.33 d (8.2)	120.5 d
2	4.23 dd (7.8, 1.0)	75.1 d	16	7.89 d (8.2)	134.1 d
3a	4.09 d (11.2)	63.7 t	17		134.9 s
3b	3.11 d (11.2)		18	2.70 s	12.4 q
4	5.28 s	91.1 d	19	1.52 s	14.3 q
5		83.4 s	20	3.89 dd (10.3, 3.8)	51.5 d
6	4.70 dd (2.7, 1.4)	51.8 d	21	6.32 d (10.3)	75.2 d
7a	2.28 m	34.9 t	22	4.39 dd (8.0, 3.8)	71.2 d
7b	2.74 ddd (13.4, 2.7, 1.4)		23	3.92 ddd (8.2, 8.0, 3.7)	78.7 d
8	3.58 m	35.1 d	24a	1.71 ddd (12.8, 8.4, 8.2)	31.1 t
9	2.69 d (9.3)	63.5 d	24b	2.28 m	
10		44.8 s	25	2.69 m	33.3 d
11		204.6 s	26	1.13 d (7.3)	14.8 q
12		138.6 s	27		180.6 s
13		135.7 s			

[a] Recorded at 800 MHz. Coupling constants (Hz) are in parentheses.
[b] Recorded at 200 MHz. Multiplicity was based on the HMQC spectrum.

($^3J_{H15-H16}$=8.2 Hz)]. A detailed analysis of COSY and HOHAHA spectra of **1** allowed four partial structures, C1–C2, C6–C9, C15–16 and C20–C26.

HMBC techniques were employed to link these partial structures as shown in Figure 1 through crosspeaks due to $^2J_{CH}$, $^3J_{CH}$ long-range coupling with quaternary carbons. The HMBC crosspeaks H-26/C27 and H-25/C27 suggested the connectivity between C25 and C27. The connections around the aromatic partial structure unit were clarified by the HMBC crosspeaks H-18/C12, H-18/C13, H-18/C17, H-16/C13, H-16/C14, H-15/C17 and H-15/C12.

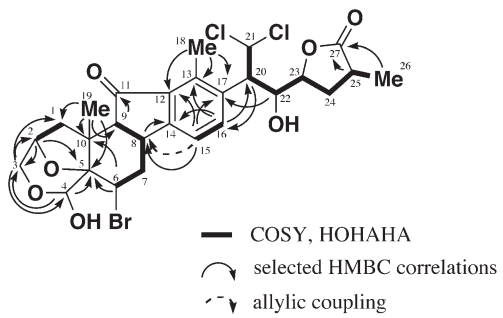

Figure 1. Structure of nakiterpiosin (**1**), based on 2D NMR correlations.

The HMBC crosspeaks H-19/C1, H-19/C5, H-19/C9, H-19/C10, H-6/C5, H-6/C10 and H-2/C5 indicated a 5,6-bicyclic ring (B,C-bicyclic ring). In addition, the B,C-bicyclic ring was linked to the A-ring to make a 6,5,6-tricyclic ring, as suggested by the HMBC crosspeaks H-2/C3, H-3/C1, H-3/C2, H-3/C4, H-4/C3 and H-4/C5. The HMBC crosspeaks H-9/C11 determined connectivity between C9 and C11. Furthermore, the HMBC crosspeaks H-16/C20, H-20/C16 and H-22/C17 suggested connectivity between C17 and C20. Allylic coupling (H-8 and H-15) and HMBC crosspeaks H-15/C8 and H-8/C14 suggested connectivity between C8 and C14. The connectivity between C11 and C12 was suggested by the chemical shift of C11, which is considered to be an α,β-unsaturated ketone. Consequently, the entire carbon chain was assembled as shown in formula **1**, and all protons and carbons were assigned as shown in Table 1.

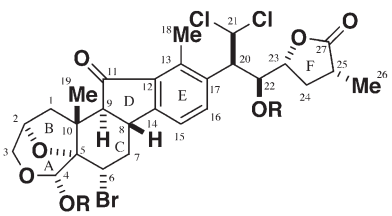

1 : **R = H** (Nakiterpiosin)
3 : **R = Ac**

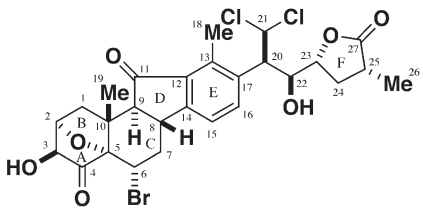

Nakiterpiosinone (**2**)

The presence of dichloromethyl group was suggested based on characteristic ^1H NMR and ^{13}C NMR signals (δ_C 75.2, δ_H 6.32).[10] Furthermore, the bromine-bearing methine carbon was considered to be C6 because of its reasonable chemical shift (δ_C 51.8, δ_H 4.70).[11,12] Thus, the gross structure of nakiterpiosin was determined to be as shown in Figure 1.

The relative stereochemistry in **1** was established by $^3J_{H-H}$ coupling constants and NOE correlations from NOESY data. The large magnitude of $^3J_{H8-H9}$=9.3 Hz and NOESY crosspeaks 19-Me/H-8 indicated that 19-Me at C10 is in an axial position. The configuration at C4 and C6 was assigned as shown in Figure 2 based on NOE crosspeaks 19-Me/H-4 and H-4/H-6. The magnitude of $^3J_{H20-H22}$=3.8 Hz and $^3J_{H22-H23}$=8.0 Hz suggested that H-20 and H-22 were located in a *gauche* arrangement while H-22 and H-23 were located in an *anti* arrangement. Therefore, based on the presumption that the alkyl chain of **1** may have a zigzag conformation, we deduced that the relative stereochemistry

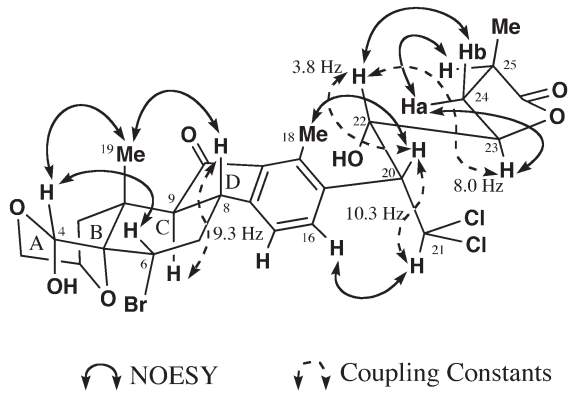

Figure 2. Relative stereochemistry of nakiterpiosin (**1**).

at C20, C22 and C23 were 20*R**, 22*S** and 23*R**. In addition, the NOE crosspeaks 18-Me/H-20, H-16/H-21, H-22/H-24b, H-23/H-24a and H-24a/H-25 suggested that the relative stereochemistries at C22, C23 and C25 were 22*S**, 23*R** and 25*R**. Eventually, all of the relative configurations of **1** were elucidated to be as shown in Figure 2.

The absolute stereostructure of **1** was determined as follows using a modified Mosher's method.[13] Treatment of **1** with (*R*)- and (*S*)-MTPACl gave (*S*)- and (*R*)-di-MTPA esters **4** and **5**, respectively. The ^{1}H NMR signals of **4** and **5** were assigned on the basis of the COSY spectra, and the $\Delta\delta$ values ($\delta_S-\delta_R$, ppm) were then calculated. The results, shown in Figure 3, established that the absolute stereochemistries of C4 and C22 were 4*R* and 22*S*, respectively. Therefore, the absolute stereostructure of nakiterpiosin (**1**) was determined as shown in formula **1**.

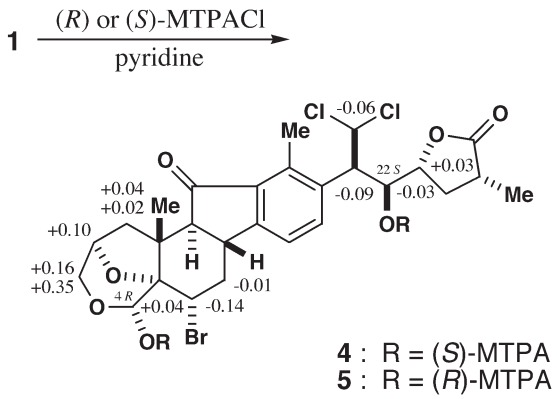

Figure 3. $\Delta\delta$ values ($\delta_S-\delta_R$) for the MTPA esters **4** and **5** in ppm.

2.3. Structure of nakiterpiosinone

The molecular formula of **2** was determined to be $C_{27}H_{29}BrCl_2O_7$ (MNa^+, *m/z* 639.0342, Δ −0.8 mmu) by ESIMS, which is 2 MS units (H_2) less than that of **1**. The ^{1}H NMR data for **2** are summarized in Table 2. A detailed analysis of COSY and HOHAHA spectra of **2** led to the four partial structures C1–C3, C6–C9, C15–C16 and C20–C26 to be constructed. The chemical shifts and the coupling constants of protons in these four parts of **2** strongly resembled those of **1**, except for H-2 (δ_H 4.58 ppm) and H-3 (δ_H 4.22 ppm). This result suggested that **2** has the similar

Table 2. NMR data for nakiterpiosinone in CD_3OD

Position	^{1}H (ppm)[a]	Position	^{1}H (ppm)[a]
1a	2.10 dd (12.8)	14	
1b	2.39 ddd (12.8, 6.0, 1.4)	15	7.36 d (8.3)
2	4.58 dd (6.0, 6.0)	16	7.92 d (8.3)
3	4.22 dd (6.0, 1.4)	17	
4		18	2.72 s
5		19	1.31 s
6	4.71 dd (2.3, 1.4)	20	3.89 dd (10.1, 3.2)
7a	2.46 ddd (13.8, 11.9, 2.3)	21	6.33 d (10.1)
7b	2.77 ddd (13.8, 2.3, 1.4)	22	4.41 dd (8.3, 3.2)
8	3.58 m	23	3.92 ddd (8.3, 8.2, 3.7)
9	2.96 d (9.2)	24a	1.73 ddd (13.3, 8.2, 8.2)
10		24b	2.30 ddd (13.3, 9.2, 3.7)
11		25	2.69 m
12		26	1.14 d (7.3)
13		27	

[a] Recorded at 800 MHz. Coupling constants (Hz) are in parentheses.

carbon skeleton as **1**, and that the A-ring in **2** is different from that of in **1**. The A-ring must contain an α-hydroxyl ketone moiety based on the molecular formula and reasonable chemical shift (H-3: δ_H 4.22 ppm). Therefore, the gross structure of nakiterpiosinone was determined to be as shown in Figure 4.

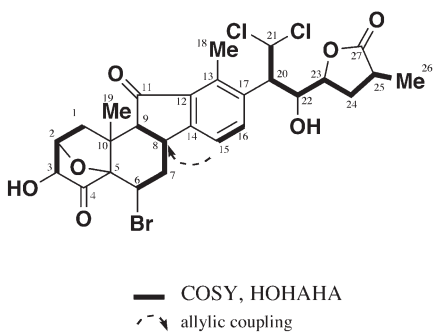

Figure 4. Structures of nakiterpiosinone (**2**) based on 2D NMR correlations.

As described in this paper, the absolute stereochemistries of nakiterpiosin (**1**) was clarified. Considering the chemical shifts and the coupling patterns in the ^{1}H NMR spectra, we can propose that the stereochemistry of nakiterpiosin (**1**) and nakiterpiosinone (**2**) may be superimposed on each other. The stereochemistry at C3 was determined by $^4J_{H-H}$ coupling constant. The equatorial orientation of H-3 was clarified by the observation of ^{1}H–^{1}H long-range coupling (W coupling, 1.4 Hz in CD_3OD) between H-1b and H-3 as shown in Figure 5. If H-3 was axial, this coupling may not be observed.

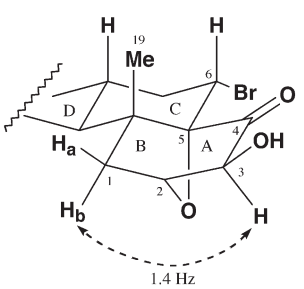

Figure 5. Relative stereochemistry of nakiterpiosinone (**2**).

3. Conclusion

In conclusion, two novel cytotoxic compounds, nakiterpiosin (**1**) and nakiterpiosinone (**2**), were isolated from the Okinawan sponge *Terpios hoshinota*. The structure of nakiterpiosin was determined based on 2D NMR spectra and a modified Mosher's method. The framework of **2** resembles veratrum alkaloids,[14] which include a C-nor-D-homosteroidal skeleton. These alkaloids are well-known metabolites of terrestrial plants, but they have not been reported previously from marine organisms. This is the first report of C-nor-D-homosteroid produced by a marine organism. **1** and **2** have similar frameworks, which implies that these compounds may be formed by similar biosynthetic processes. Nakiterpiosinone (**2**) is considered to be a biosynthetic intermediate of nakiterpiosin (**1**).

The new compounds **1** and **2** exhibited potent cytotoxicity against mouse lymphocytic leukemia cells (P388). The both IC_{50} values of **1** and **2** were 0.01 μg/mL. Since **1** and **2** exhibited same level of cytotoxicity against P388, it was presumed that the cytotoxic activities of these compounds are based on E-ring and alkyl chain. Partial structure of **1** and **2** resemble to mitotane (1,1-dichloro-2-(*o*-chlorophenyl)-2-(*p*-chlorophenyl)ethane). Mitotane inhibits mitochondrial cytochrome P450 11β/18 enzymes. In addition, mitotane causes structural damage to mitochondria in the zona reticularis and zona fasciculata. These cytotoxic effects on steroid-producing tissue lead to necrosis of vulnerable normal and tumor tissue.[15–17] Therefore, the cytotoxicity of **1** and **2** might also be derived from the dichloromethyl moiety. Cytotoxic effects of **1** and **2** against coral tissue are in progress, which would serve to understand how *T. hoshinota* kill and smother coral communities.

4. Experimental

4.1. General aspects

NMR spectra were determined on a JEOL JNM-ECP800 [800 MHz (^{1}H) and 200 MHz (^{13}C)] or a JEOL JNM-A600 [600 MHz (^{1}H) and 150 MHz (^{13}C)] spectrometer. The ^{1}H and ^{13}C chemical shifts were referenced to the solvent peaks [δ_H=3.31 ppm and δ_C=49.5 ppm in methanol-d_4]. High-resolution mass spectra (HRMS) was obtained on a PE Sciex QSTAR mass spectrometer. Column chromatography was performed on silica gel (Fuji Silysia Chemical Ltd, BW-820MH) and ODS gel (Nacalai Tesque, Cosmosil 75C_{18}-OPN). Reversed-phase high performance liquid chromatography (HPLC) was carried out on Develosil ODS-HG-5, Develosil 300C4-HG-5 (Nomura Chemical Co., Ltd). Pyridine was distilled from calcium hydride.

4.2. Isolation of nakiterpiosin (1) and nakiterpiosinone (2)

The frozen marine sponge *T. hoshinota*, which was collected at a depth of 2 m off Nakijin, Okinawa in April, 2001, was extracted twice by steeping in acetone (60 L) for 7 days. The combined extracts were concentrated and partitioned between ethyl acetate–water. The organic layer gave 15.4 g of an oil after concentration. The oil was first separated by column chromatography on silica gel (200 g) using benzene, chloroform, chloroform-methanol (40:1, 20:1, 10:1, 5:1, 2:1), and methanol. The combined residue (5.51 g) of the third and fourth fractions was further separated by chromatography on ODS (100 g) using 60% MeOH, 80% MeOH and MeOH. The fraction (533.5 mg) eluted with 80% MeOH was subjected to repeated HPLC [Develosil ODS-HG-5 (250×20 mm); flow rate 5 mL/min; detection, UV 215 nm; solvent 60% MeOH]. The fractions with retention times from 76 to 107 min were concentrated (33.8 mg) and subjected to HPLC [Develosil 300C_4-HG-5 (250×20 mm); flow rate 5 mL/min; detection, UV 215 nm; solvent 45% MeOH]. The fraction at a retention time of 129 min was concentrated (0.6 mg) and purified by HPLC [Develosil 300C_4-HG-5 (250×4.6 mm); flow rate 5 mL/min; detection UV 215 nm; solvent 40% MeOH] to give nakiterpiosin (**1**) (0.4 mg, retention time 56 min). In the same way, the fraction at a retention time of 145 min was concentrated and purified by HPLC [Develosil ODS-HG-5 (250×10 mm); flow rate 2.5 mL/min; detection UV 215 nm; solvent 60% MeOH] to give nakiterpiosinone (**2**) (0.1 mg, retention time 54 min).

4.2.1. Nakiterpiosin (1). ^{1}H and ^{13}C NMR, see Table 1; HRMS (ESI) calcd for $C_{27}H_{31}BrCl_2NaO_7$ (MNa^+) 641.0507, found 641.0490.

4.2.2. Nakiterpiosinone (2). ^{1}H NMR, see Table 2; HRMS (ESI) calcd for $C_{27}H_{29}BrCl_2NaO_7$ (MNa^+) 639.0350, found 639.0342.

4.2.3. 4,22-Diacetylnakiterpiosin (3). A solution of **1** (0.1 mg) in pyridine (0.2 mL) was treated with Ac_2O (0.1 mL). The reaction mixture was stirred at room temperature for 0.5 h and concentrated. The oily residue was purified by HPLC [Develosil ODS-HG-5 (250×10 mm); flow rate 2.5 mL/min; detection UV 215 nm; solvent 85% MeOH] to afford 4,22-diacetylnakiterpiosin (**3**): ^{1}H NMR (methanol-d_4) δ 1.16 (3H, d, J=7.3 Hz), 1.55 (3H, s), 1.60 (1H, m), 2.08 (1H, dd, J=12.3, 1.0 Hz), 2.15 (3H, s), 2.16 (3H, s), 2.35 (2H, m), 2.69 (1H, dd, J=12.3, 7.8 Hz), 2.76 (1H, m), 2.78 (3H, s), 2.79 (1H, m), 3.52 (1H, m), 3.98 (1H, d, J=11.2 Hz), 4.15 (2H, m), 4.35 (1H, m), 4.68 (1H, dd, J=2.7, 1.4 Hz), 5.77 (1H, dd, J=8.0, 3.8 Hz), 6.20 (1H, s), 6.40 (1H, d, J=10.3 Hz), 7.40 (1H, d, J=8.2 Hz), 7.83 (1H, d, J=8.2 Hz); MS (ESI) m/z 703 (MH^+).

4.2.4. (*S*)-di-MTPA ester 4. A solution of **1** (0.2 mg) in pyridine (0.2 mL) was treated with (*R*)-(+)-MTPACl (15 mg). The reaction mixture was stirred at room temperature for 11 h under N_2 atmosphere and concentrated. The oily residue was purified by HPLC [Develosil ODS-HG-5 (250×10 mm); flow rate 2.5 mL/min; detection UV 215 nm; solvent, 80% MeOH] to afford (*S*)-mono-MTPA ester. A solution of (*S*)-mono-MTPA ester in pyridine (0.2 mL) was treated with (*R*)-(+)-MTPACl (30 mg) and DMAP (10 mg). The reaction mixture was stirred at 50 °C for 4 h under N_2 atmosphere and concentrated. Toluene (2.0 mL) was added and concentrated. The oily residue was purified by HPLC [Develosil ODS-HG-5 (250×10 mm); flow rate 2.5 mL/min; detection UV 215 nm; solvent 85% MeOH] to afford (*S*)-di-MTPA ester **4**: ^{1}H NMR

(methanol-d_4) δ 2.13 (1H, m), 2.67 (1H, m), 3.33 (1H, d, J=10.6 Hz), 3.94 (1H, d, J=10.6 Hz), 3.98 (1H, m), 4.10 (1H, dd, J=9.2, 3.3 Hz), 4.29 (1H, m), 4.32 (1H, m), 5.19 (1H, d, J= 10.2 Hz), 5.86 (1H, dd, J=9.1, 3.7 Hz), 6.54 (1H, s); MS (ESI) m/z 1073 (MNa^+).

4.2.5. (*R*)-di-MTPA ester 5. A solution of **1** (0.2 mg) in pyridine (0.2 mL) was similarly treated with (*S*)-(−)-MTPACl and DMAP to afford (*R*)-di-MTPA ester **5**: ^{1}H NMR (methanol-d_4) δ 2.03 (1H, m), 2.63 (1H, m), 3.17 (1H, d, J=10.6 Hz), 3.58 (1H, d, J=10.6 Hz), 3.95 (1H, m), 4.19 (1H, dd, J=9.2, 3.3 Hz), 4.20 (1H, m), 4.46 (1H, m), 5.25 (1H, d, J=10.2 Hz), 5.89 (1H, dd, J=9.1, 3.7 Hz), 6.50 (1H, s); MS (ESI) m/z 1073 (MNa^+).

Acknowledgements

This work was supported in part by Grants-in-Aid for Scientific Research (No. 11558079) and Scientific Research on Priority Areas (A) (No. 12045235) from the Ministry of Education, Culture, Sports, Science and Technology, Japan. We are indebted to Wako Pure Chemical Industries Ltd., and Banyu Pharmaceutical Co., Ltd. for their financial support.

References and notes

1. Cragg, G. M.; Newman, D. J. *Cancer Invest.* **1999**, *17*, 153–163.
2. Long, B. H.; Carboni, J. M.; Wasserman, A. J.; Cornell, L. A.; Casazza, A. M.; Jensen, P. R.; Lindel, T.; Fenical, W.; Fairchild, C. R. *Cancer Res.* **1998**, *58*, 1111–1115.
3. Teruya, T.; Suenaga, K.; Koyama, T.; Nakano, Y.; Uemura, D. *J. Exp. Mar. Biol. Ecol.* **2001**, *266*, 123–134.
4. Hughes, T. P. *Science* **1994**, *265*, 1547–1551.
5. Rosser, R. M.; Faulkner, D. J. *J. Org. Chem.* **1984**, *84*, 5157–5160.
6. Nagle, D. G.; Gerwick, W. H. *Tetrahedron Lett.* **1995**, *6*, 849–852.
7. Yamaguchi, M. *Aquabiology* **1986**, *43*, 88–92, Abstract in English.
8. Teruya, T.; Nakagawa, S.; Koyama, T.; Suenaga, K.; Uemura, D. *Chem. Lett.* **2002**, 38–39.
9. Teruya, T.; Nakagawa, S.; Koyama, T.; Suenaga, K.; Kita, M.; Uemura, D. *Tetrahedron Lett.* **2003**, *44*, 5171–5173.
10. 1,1,2,2-Tetrachloroethane: ^{1}H NMR (800 MHz, CD_3OD) δ (ppm) 6.45 (s, 2H); ^{13}C NMR (200 MHz, CD_3OD) δ (ppm) 74.3.
11. Crews, P.; Kho-Wisemam, E.; Montana, P. *J. Org. Chem.* **1978**, *43*, 116–120.
12. Crews, P.; Naylor, S.; Hanke, F. J.; Hogue, E. R.; Kho, E.; Braslau, R. *J. Org. Chem.* **1984**, *49*, 1371–1377.
13. Ohtani, I.; Kusumi, T.; Kashiman, Y.; Kakisawa, H. *J. Am. Chem. Soc.* **1991**, *113*, 4092–4096.
14. Veratrum alkaloids are regularly reviewed in 'The Alkaloids', Specialist Periodical Reports, Royal Society of Chemistry, London, Vols. 1–13, pp 1971–1983.
15. Luton, J. P.; Mahoudeau, J. A.; Bouchard, P.; Thieblot, P.; Hautecouverture, M.; Simon, D.; Laudat, M. H.; Touitou, Y.; Bricaire, H. *N. Engl. J. Med.* **1979**, *300*, 459–464.
16. James, V. H.; Few, J. D. *Clin. Endocrinol. Metab.* **1985**, *14*, 867–892.
17. Miller, J. W.; Crapo, L. *Endocrinol. Rev.* **1993**, *12*, 443–458.

Available online at www.sciencedirect.com
SCIENCE DIRECT
Tetrahedron
Tetrahedron 60 (2004) 6995–7003

Cucurbitadienol synthase, the first committed enzyme for cucurbitacin biosynthesis, is a distinct enzyme from cycloartenol synthase for phytosterol biosynthesis

Masaaki Shibuya, Shinya Adachi and Yutaka Ebizuka*

Graduate School of Pharmaceutical Sciences, The University of Tokyo, 7-3-1 Hongo, Bunkyo-ku, Tokyo 113-0033, Japan

Received 27 August 2003; revised 23 April 2004; accepted 23 April 2004

Available online 25 June 2004

Abstract—Three oxidosqualene cyclase (OSC) cDNAs (*CPX*, *CPQ*, *CPR*) were cloned from seedlings of *Cucurbita pepo* by homology based PCR method. Their open reading frames were expressed in lanosterol synthase deficient (*erg7*) *Saccharomyces cerevisiae* strain GIL77. Analyses of in vitro enzyme activities and in vivo accumulated products in the transformants demonstrated that CPQ and CPX encode cucurbitadienol and cycloartenol synthases, respectively. These results indicated the presence of distinct OSCs for cycloartenol and cucurbitadienol synthesis in this plant.

1. Introduction

Cucurbitacins, a group of highly oxygenated tetracyclic triterpenes, occur in the restricted plant families, Cucurbitaceae, Cruciferae, Begoniaceae, Scrophulariaceae, Primulaceae and Rosaceae as bitter tasting and purgative constituents.[1,2] Their various pharmacological activities such as antitumor,[3] anti-inflammatory[4] and anti-HIV[5] activities have drawn considerable attentions. Some of them have also been recognized as ecochemicals showing interesting activities against insects.[6,7]

Structures of cucurbitacins are built up on tetracyclic cucurbitan skeleton featuring significant similarity to steroidgenic triterpenes. And thus, they were assumed to be synthesized via lanosterol, cycloartenol or parkeol,[8,9] as shown in Figure 1. Opening of the cyclopropane ring of cycloartenol in concert with hydride shift (from C5 to C10) and proton elimination (from C6) could give 10α-cucurbita-5,24-diene-3β-ol (cucurbitadienol). Alternatively, addition of proton to a double bond (Δ8,9) of lanosterol with 1,2-shifts of methyl (from C10 to C9) and hydride, and proton elimination could give cucurbitadienol. Furthermore, protonation to a double bond (Δ9,11) of parkeol with the same migrations as in lanosterol could give the same cucurbitadienol. In lower terpene biosynthesis, there are some examples of cyclases that initiate cyclization by generating carbocation from acyclic prenyl diphosphates and first produce neutral cyclic intermediates and then the same enzymes take up these intermediates and further catalyze protonation on double bond and subsequent cyclization to yield the final products.[10,11] However, no incorporation of labeled lanosterol into cucurbitacin excluded the intermediacy of lanosterol in cucurbitacin biosynthesis.[12] Balliano et al. reported the direct intermediacy of cucurbitadienol in cucurbitacin biosynthesis by demonstrating the incorporation of labeled cucurbitadienol into cucurbitacin C in *Cucumis sativus* seedlings. In the same experiments, no incorporation of cycloartenol and parkeol were observed.[13] Enzymatic conversion of oxidosqualene (OS) into cucurbitadienol was later demonstrated in the microsomal preparation from *Cucurbita maxima* seedlings.[14] From these results, it was concluded that cucurbitadienol synthase is the first pathway-specific enzyme in cucurbitacin biosynthesis, branching from sterol biosynthesis at this oxidosqualene cyclization step.

However, whether cucurbitadienol synthase and cycloartenol synthase are independent proteins, is still in question due to the following reasons. (1) Although cucurbitadienol synthase activity was demonstrated in the microsomal fraction prepared from *C. maxima* seedlings, cycloartenol synthase activity was also found in the same preparation, and the enzyme proteins were not purified.[14] (2) In recent studies on triterpene synthases in our laboratory and others', several multifunctional OSCs giving more than two cyclization products have been identified.[15–22] As shown in Figure 2, the mechanisms for cycloartenol and cucurbitadienol formation share early part in common up to

Keywords: 10α-Cucurbita-5,24-diene-3β-ol; Cucurbitadienol; Cycloartenol; Oxidosqualene; Cyclase; cDNA cloning; *Cucurbita pepo*.
* Corresponding author. Tel.: +81-3-5841-4740; fax: +81-3-5841-4744; e-mail address: yebiz@mol.f.u-tokyo.ac.jp

0040–4020/$ - see front matter © 2004 Elsevier Ltd. All rights reserved.
doi:10.1016/j.tet.2004.04.088

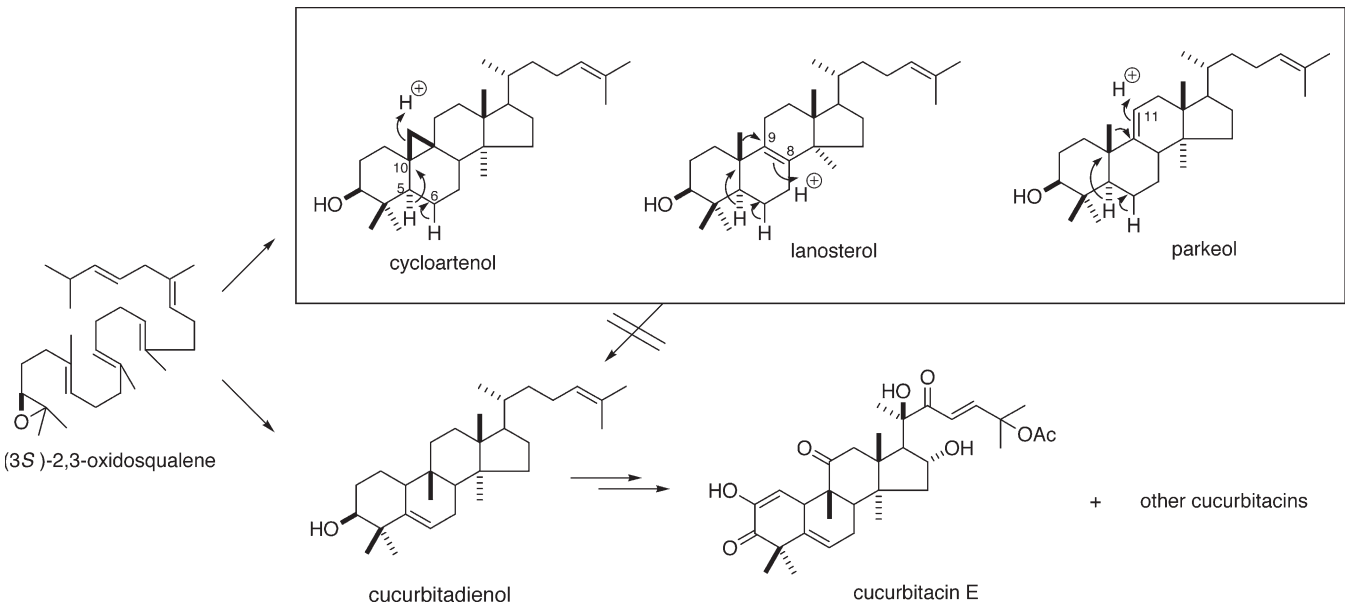

Figure 1. Biosynthesis of cucurbitacins.

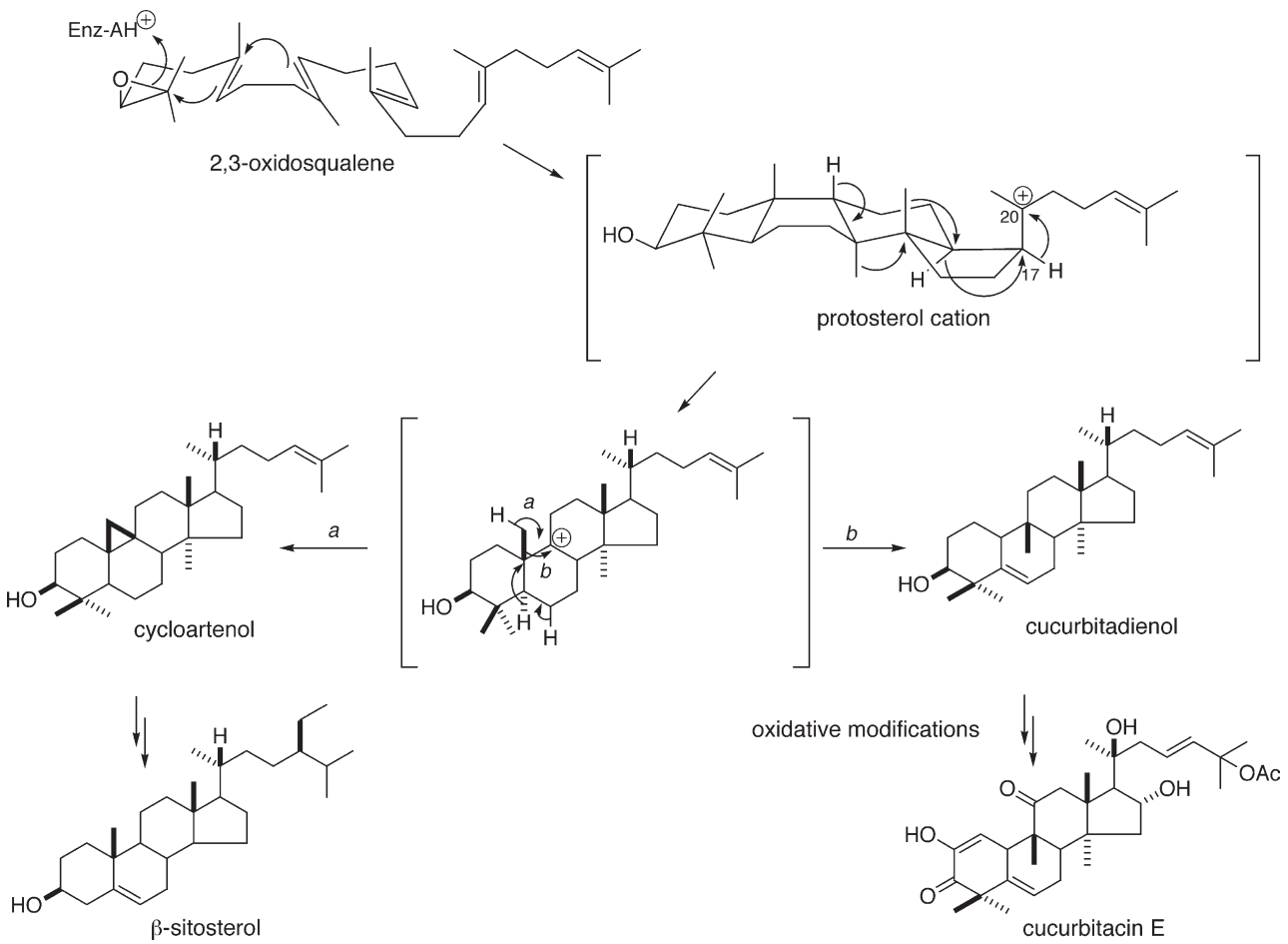

Figure 2. Formation of cycloartenol and cucurbitadienol from oxidosqualene via chair-boat-chair conformation.

lanosteryl cation stage. So, the possibility of the presence of a single enzyme giving two products, cycloartenol and cucurbitadienol, could not be excluded. (3) A single amino acid substitution of cycloartenol synthase protein resulted in generation of a mutant enzyme giving three structurally related products, cycloartenol, lanosterol and parkeol,[23,24] also supporting the possible involvement of a single enzyme for production of cycloartenol and cucurbitadienol.

In order to address this question, cDNA cloning of cucurbitadienol and cycloartenol synthases was carried out from *Cucurbita pepo* seedlings which was used in incorporation study of radio-labeled mevalonic acid into cucurbitacin B and cycloartenol.[2] By employing homology based PCRs, which were successful in our previous studies,[25] three putative OSC cDNAs were obtained and their enzyme functions were analyzed by heterologous expression in yeast. Site-directed mutagenesis on one of the OSCs, cucurbitadienol synthase (CPQ) obtained in this study, was also attempted to convert this synthase into lanosterol or cycloartenol synthases.

2. Results and discussions

2.1. cDNA cloning

The roots of 6-day-old seedlings were used for the extraction of RNA. As reported in our previous paper,[25] nested PCR was carried out with three sets of degenerate primers designed from the consensus sequences of the known OSCs. After the first PCR with the primers of 162S and 711A, the second PCRs were carried out independently with two different primer sets. The PCR with 463S and 623A primers gave a DNA fragment of expected size (396 bp), and the other with 467S and 623A gave 385 bp fragment. They were subcloned in *Escherichia coli* and 26 colonies were picked up for nucleotide sequencing. Sixteen out of 26 clones were identical to each other showing 81% sequence identity to cycloartenol synthase *GgCAS1* from *Glycyrrhiza glabra*.[26] Its full length cDNA was named as *CPX*. Another eight clones were identical with each other and showed 68% sequence identities to *CPX*, and its full-length clone was named as *CPQ*. The remaining two clones having identical sequence, showed 82% sequence identity to a putative OSC clone *LcOSC2* from *Luffa cylindrica*.[27] Its full length clone was designated as *CPR*. Based on the sequences of these fragments, the 3′- and 5′-end sequences were obtained by RACE method.[28]

2.2. Expression of cDNAs in *ERG7* deficient *Saccharomyces cerevisiae* mutant GIL77

Based on the obtained sequences, PCR primers corresponding to the sequences of 5′- and 3′-termini and incorporating appropriate restriction endonuclease sites, were synthesized to obtain the full-length clones. PCR products (2.3 kb in length) were digested with corresponding restriction enzymes, and ligated to the downstream of *GAL1* promoter of pYES2 to construct the plasmids pOSC-CPX, pOSC-CPQ and pOSC-CPR. The resulting plasmids were transferred to *S. cerevisiae* strain GIL77, a lanosterol synthase deficient mutant.[25] The transformants were cultured and *GAL1* promoter was induced by replacing the carbon source from glucose to galactose. Cells were harvested and disrupted by boiling with 20% KOH/50% ethanol aq. The resulting suspensions of disrupted cells were extracted with hexane and separated by normal phase silica gel TLC.

In the expression of CPQ, a band with slightly higher R_f value on TLC than that of triterpene monoalcohols such as cycloartenol, β-amyrin, etc., was detected by phosphomolybdic acid staining. This band was scraped off the plate, extracted with acetone and analyzed by LC-APCIMS. As shown in Figure 3, the product of CPQ and authentic cucurbitadienol eluted at the same retention time of 21 min in HPLC, and both gave the identical signals at *m*/*z* 427 as $(M+H)^+$ and *m*/*z* 409 as $(M+H-H_2O)^+$ in APCIMS. MS/MS fragmentation patterns of the signal at *m*/*z*=409 as parent ion were also identical. Further identity of the CPQ product as cucurbitadienol was obtained by NMR. The CPQ transformant was cultured in 2 l media to isolate the product (8 mg) by silica gel column chromatography. ^1H and ^{13}C NMR spectra were identical to those of authentic cucurbitadienol.[29] From these results, the product accumulated in *CPQ* transformant was identified as cucurbitadienol. In addition to cucurbitadienol, this transformant gave a trace amount of unknown compound with the same R_f value as cycloartenol on TLC. This compound was also analyzed by LC-APCIMS, which gave a single peak at retention time of 5.9 min (different from those of cycloartenol and cucurbitadienol) with the base peak at *m*/*z* 409 in APCIMS. MS/MS fragmentation of the signal at *m*/*z*=409 as parent ion was apparently different from those of cycloartenol and cucurbitadienol (data not shown). Judging from its earlier elution than tetra- and pentacyclic triterpene monoalcohols from reverse phase HPLC, this compound is assumed to possess mono- or bicyclic triterpene monoalcohol structure, but not yet identified due to its scarce availability. To exclude the possibility that this clone produces not only cucurbitadienol but also lanosterol, which might not accumulate in a detectable quantity due to its fast conversion to ergosterol by the host's enzymes, compensation for lanosterol auxotrophy of GIL77 by this clone was further examined. The GIL77 transformant with pOSC-CPQ could not grow on the media without ergosterol (data not shown), establishing CPQ does not produce lanosterol.

To examine the function of CPX, in vitro assay was carried out using [^{14}C]-labeled oxidosqualene as substrate. Supernatants obtained by centrifugation after cell lysis, served as the crude enzyme preparations. Reaction products were separated by TLC. Except for the substrate, a major radioactive band co-migrated with cycloartenol, but not with cucurbitadienol (data not shown). Further analysis of this radioactive compound was accomplished by HPLC. Radioactivity was associated dominantly in the peak corresponding to cycloartenol. These results indicated that CPX is a cycloartenol synthase of this plant for sterol biosynthesis and is not a bifunctional oxidosqualene cyclase to produce both cucurbitadienol and cycloartenol.

On the other hand, in the functional expressions of CPR under the same conditions for CPQ and CPX, no product was obtained. In our previous studies, PNZ from *Panax ginseng*,[25] TRV from *Taraxacum officinale*[30] and LcOSC2 from *L. cylindrica*,[27] also gave no cyclization product with unknown reasons.

2.3. Mutagenesis of the 488th leucine and the 489th isoleucine in cucurbitadienol synthase

Mutation of isoleucine, the 481st amino acid residue of a

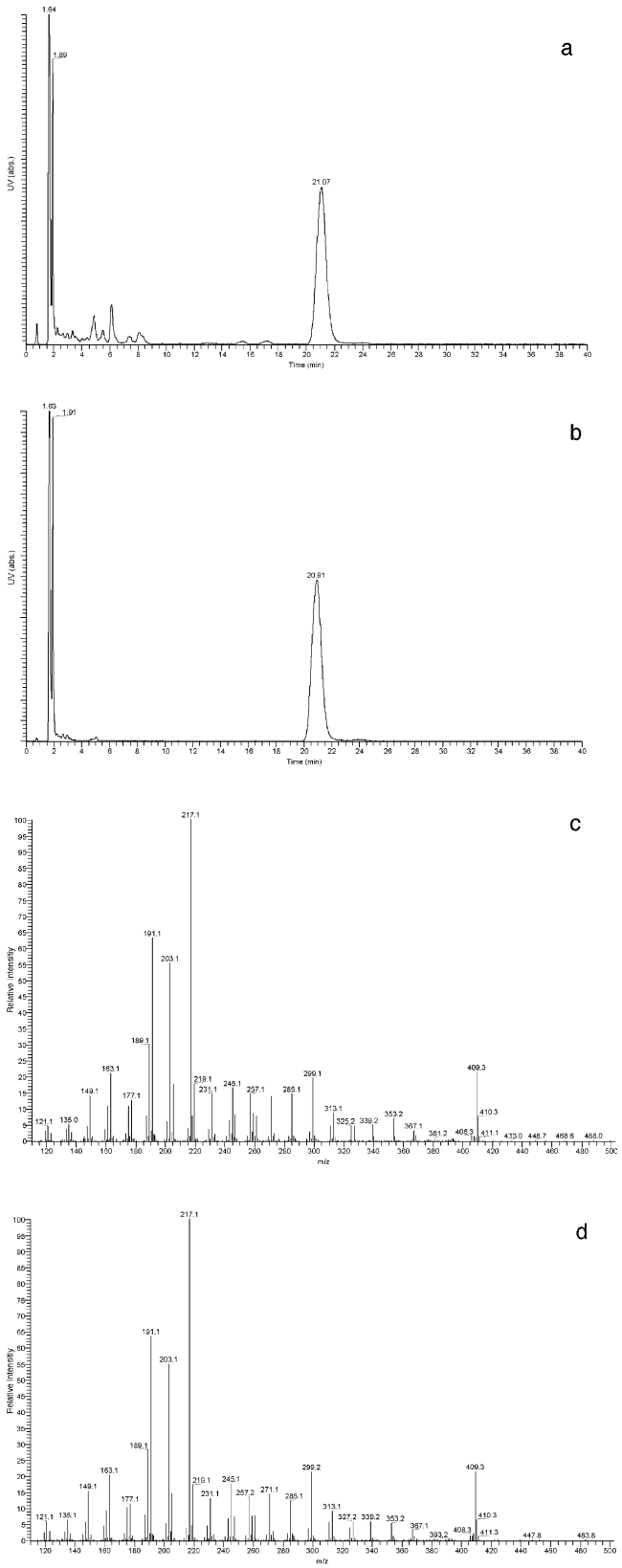

Figure 3. LC-MS analysis of the products by pOSC-CPQ. The HPCL profiles (monitored by UV absorption at 202 nm) of triterpene monoalcohol fraction obtained from yeast GIL77/pOSC-CPQ are illustrated (a), and for authentic cucurbitadienol (b), as are the MS/MS fragmentation (*m/z* 409 as parent ion) patterns for the triterpene product with retention time 21.07 min (c), and for authentic (d).

cycloartenol synthase from *Arabidopsis thaliana*, into valine led it to produce two additional cyclization products, lanosterol and parkeol. The result of this mutation was explained by slightly enlarged active site cavity due to replacement of a sec-butyl side chain with a smaller isopropyl group.[23] This steric change reduced the regiospecificity of deprotonation from C19 in cycloartenol synthase and allowed deprotonation at C8 and C11 to form lanosterol and parkeol, respectively. This isoleucine is also conserved as the 489th amino acid in CPQ, a cucurbitadienol synthase (Fig. 4). If it has the same role in cucurbitadienol synthase, the substitution of this isoleucine into valine might result in similar reduction of product specificity. And the amino acid just upstream of this isoleucine is leucine (the 488th) in cucurbitadienol synthase, but proline in all the known cycloartenol synthases, implying that this proline might contribute to locate basic amino acid residue or water molecule to the suitable position so as to remove a proton from C19 in cycloartenol synthase, while the presence of leucine in this position of cucurbitadienol synthase might be favored for a methyl group shift from C10 to C9. In order to investigate the possible role of the 488th leucine and the 489th isoleucine in cucurbitadienol synthase, three mutants of CPQ were constructed by site-directed mutagenesis. The 488th leucine was mutated to proline, and the 489th leucine to valine, to construct single mutants CPQ-L488P and CPQ-I489V, respectively. And, a double mutant CPQ-LI488-489PV in the same two positions was also constructed. The resulting plasmids were transferred into a lanosterol synthase deficient yeast mutant strain GIL77. All of the three transformants could not grow without supplement of exogenous ergosterol, indicating that these mutant proteins could not produce lanosterol. Transformant cells were extracted with hexane, and the accumulated products analyzed by LC-APCIMS. The elution profiles on LC and the fragmentations of MS were the same in all three transformants as those of the wild-type cucurbitadienol synthase, indicating that mutant proteins produced cucurbitadienol as a cyclization product (data not shown). Substitution of the 488th leucine and/or the 489th isoleucine in cucurbitadienol synthase did not result in the change of product-specificity (still giving cucurbitadienol as a product). A similar result was reported for lanosterol synthase mutant whose 454th valine was mutated to leucine causing no product change (lanosterol as a product).[23] These results indicated the role of the 481st isoleucine in cycloartenol synthase is clearly different from that of cucurbitadienol and lanosterol synthases.

2.4. Protein-sequence-based analysis among triterpene synthases

CPX, *CPQ* and *CPR* are composed of 2298, 2295 and 2280 bp nucleotide open reading frames which encode 766, 765 and 760 amino acid long proteins. They show similar degree of amino acid identities each other, 69% between *CPX* and *CPQ*, 64% between *CPX* and *CPR*, and 67% between *CPQ* and *CPR*. *CPX* a cycloartenol synthase, shows high sequence identity to the known cycloartenol synthase *LcCAS1* (94%) from *L. cylindrica* (Cucurbitaceae).[31] *CPR* whose function has not been identified

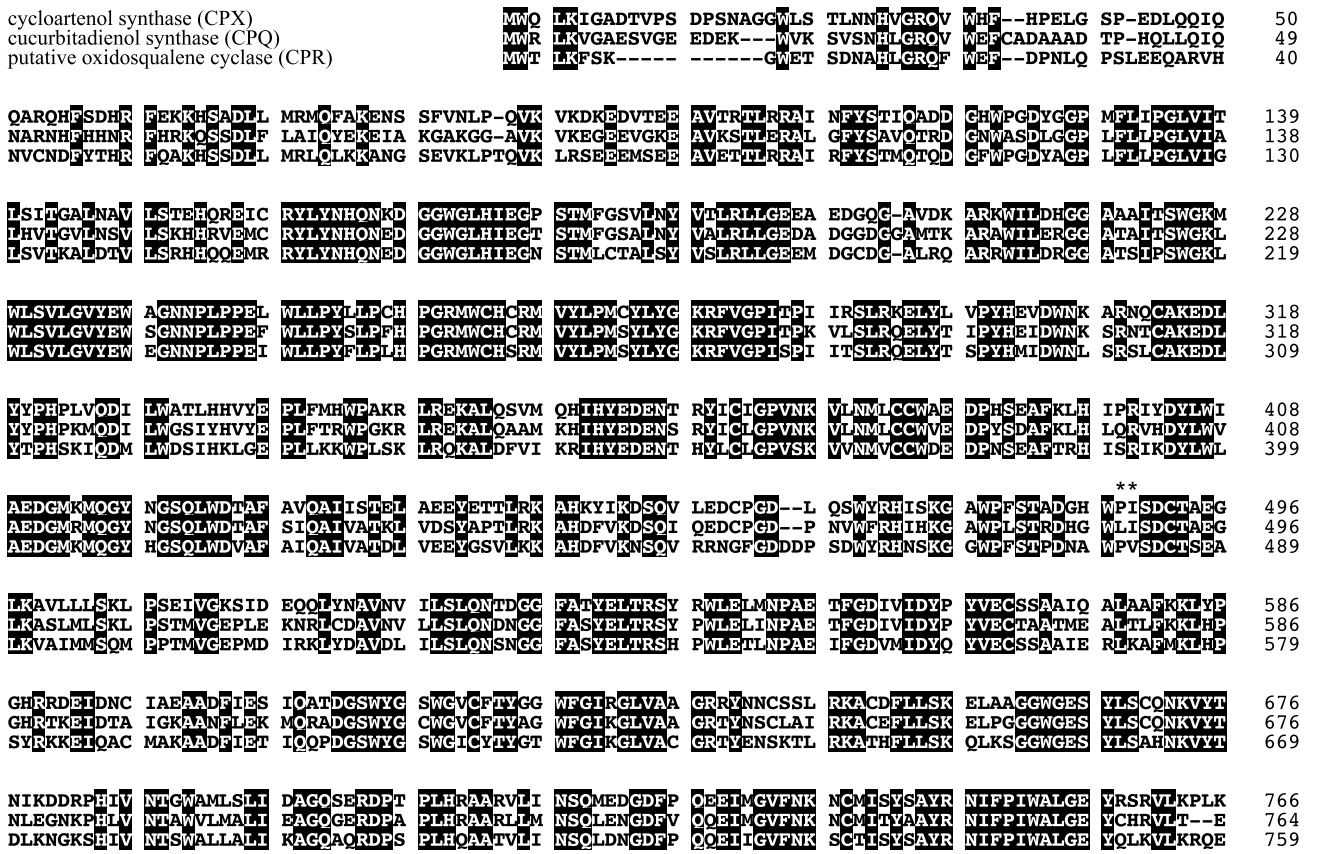

Figure 4. Multiple alignment of deduced amino acid sequences of cycloartenol synthase (CPX), cucurbitadienol synthase (CPQ) and putative oxidosqualene cyclase (CPR) from *C. pepo*. Hyphens were inserted to maximize homology. Amino acid residues identical in three protein sequences are boxed. The 488th proline and 489th isoleucine in cycloartenol synthase were marked with stars.

shows more than 85% sequence identity to a putative oxidosqualene cyclase *LcOSC2* from *L. cylindrica*.[27] Interestingly, *CPQ* shows 75% identities to cycloartenol synthase clones *PNX* and *BPX* from *P. ginseng* and *Betula platyphylla*, respectively. In our previous studies, sequence identity of more than 75% at amino acid level was good enough to assume the unknown oxidosqualene cyclase clone as cycloartenol synthase. Actually, the identities among the known cycloartenol synthases from dicotyledonous plants show more than 70% sequence identity. In the phylogenetic tree constructed from the 27 different dicotyledonous plant OSCs (Fig. 5), *CPX* situates in a cycloartenol synthase branch, and *CPR* in a branch composed of putative OSC clones, namely *PNZ* from *P. ginseng*,[25] *TRV* from *T. officinale*[30] and *LcOSC2* from *L. cylindrica*[26] while *CPQ* is out of a cycloartenol synthase branch. This tree provides some interesting insights for molecular evolution of plant OSCs. In our previous paper,[32] we proposed that pentacyclic triterpene synthases for secondary metabolism, such as lupeol synthase and β-amyrin synthase, have evolved in this order from ancestral cycloartenol synthase for sterol biosynthesis. Interestingly, cucurbitadienol synthase situates between the branches of cycloartenol and lupeol synthases, and its position in the tree is more close to the cycloartenol synthase branch. As described earlier in this paper, reaction mechanism of these two enzymes is identical up to the formation of lanosteryl cation. Oxidosqualene must be held in pre-chair-boat-chair conformation in the active site of the both enzymes to achieve the stereochemistry of the products. Opening of epoxide drives a series of electrophilic addition reactions to give protosteryl cation, and following hydride and methyl shifts give lanosteryl cation, which stands at branching point between cycloartenol and cucurbitadienol formation. Cycloartenol synthase removes a proton of methyl group at C10 to form cyclopropane ring. On the other hand, cucurbitadienol synthase further shifts methyl group from C10 to C9 and hydride from C5 to C10, and removes a proton from C6 to form double bond between C5 and C6. The reaction catalyzed by these two enzymes is fundamentally different from that of other triterpene synthases such as lupeol and β-amyrin synthases in a manner of substrate fixation. It is worthwhile to note that the similarity of reaction mechanism is well reflected in the positions of the respective oxidosqualene cyclases in the tree.

As mentioned above, *CPR* joined a branch composed of putative OSC clones, *PNZ*, *TRV* and *LcOSC2* between cycloartenol and lupeol synthase branches. Based on the correlation between reaction mechanism and location in the tree, we expected that these clones might represent tetracyclic dammarenediol synthase. Unfortunately, however, none of these clones exhibited enzyme activity in yeast expression system despite our efforts. There may be particular reasons why all of four clones in this branch showed no enzyme function, such as no conformity of these clones with yeast expression system or inherent feature of

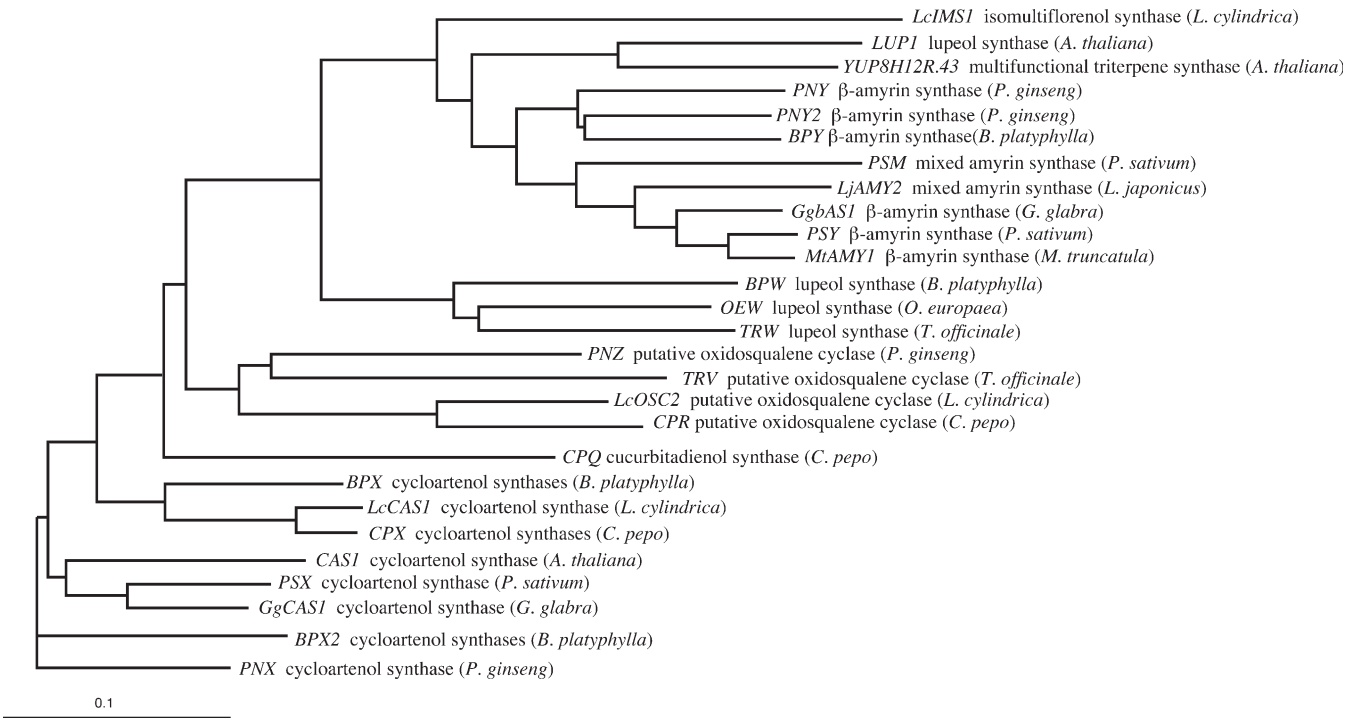

Figure 5. Phylogenetic tree of plant OSCs. Distances between each clone and group are calculated with the program CLUSTAL W. The indicated scale represents 0.1 amino acid substitution per site. The accession numbers of the sequences on EMBL, GenBank and DDBJ sequence-data banks used in this analysis are indicated in Section 3.

these clones. Further investigations are underway to resolve this question.

Cucurbitadienol synthase was successfully cloned from *P. pepo*, which catalyzes the first committed step in cucurbitacin biosynthesis, establishing that cucurbitadienol synthase is an independent enzyme from cycloartenol synthase. Cucurbitacins are bitter tasting constituents of Cucurbitaceous plants. Successful cloning of cucurbitadienol synthase has opened a way to engineer Cucurbitaceous plants to overproduce cucurbitacins of pharmaceutical importance. The cloned gene also has a good potential to be utilized for control of bitterness of crop plants like cucumber (*C. sativus* L.).

Characteristic feature of cucurbitacins is their highly oxygenated structures. In the following biosynthetic steps, cucurbitadienol is oxygenated at various positions by specific oxygenases. In higher plants, the first oxygenation step in sterol biosynthesis is the oxidation of C4α methyl group of 24-methylenecycloartenol by a non-heme iron oxygenase, and not by a cytochrome P450 type monooxygenase.[33,34] Later oxidative demethylation at C14[35] and other hydroxylations in sterol biosynthesis are catalyzed by cytochrome P450 type monooxygenases.[36,37] In contrast, except for several C9-hydroxymethyl cucurbitacins,[38] all the cucurbitacins ever isolated retain eight methyl groups of cucurbitadienol, although they are highly oxygenated. Biosynthesis of cucurbitacins seems to proceed in completely independent manner after being branched from sterol biosynthesis at cucurbitadienol synthase reaction. The next attention in cucurbitacin biosynthesis should be paid to characterize the oxygenases, which produce structural diversity of cucurbitacins.

3. Experiments

3.1. PCR and sequence analysis

Synthesis of oligo DNAs was done by Nihon Bioservice (Saitama, Japan). PCR was performed by Robo Cycler™ Gradient 40 (Stratagene). The PCR reaction products were separated by agarose gel electrophoresis, purified by a Wizard PCR Preps Kit (Promega), and ligated into pT7Blue (Novagen). Resulting plasmid was propagated in *E. coli* NovaBlue (Novagen), and isolated by GFX™ Micro Plasmid Prep Kit (Amersham Pharmacia Biotech). Sequencing was carried out by DNA Sequencer Model 4000 (Li-Cor) using Thermo Sequenase Cycle Sequencing Kit (Aloka).

3.2. cDNA cloning

Seeds of pumpkin (*C. pepo* L. cv Atlantic giant) were purchased from Takii Syubyou (Kyoto, Japan). They were immersed in water at room temperature for 6 days. RNA was extracted by phenol-SDS method from the roots. Total RNA (20 μg) was reverse transcribed to produce cDNAs using reverse transcriptase (Superscript II, GIBCO BRL) and 0.5 μg of oligo dT primer, RACE32 (5′-GACTC GAGTCGACATCGATTTTTTTTTTTTTT-3′) with dNTP (0.2 mM) in a volume of 20 μl following the manufacturer's protocol. The resulting cDNA mixture was used as the template in the following PCR.

First PCR was performed with a set of primer, 162S(5′-GAYGGIGGITGGGGIYTICA-3′) and 711A(5′-CKR TAYTCICCIARIGCCCADATIGGRAA-3′) (1 μg of primers were used in all PCR procedures for cloning),

using Ex Taq DNA polymerase (Takara Shuzo) with dNTP (0.2 mM) in a final volume of 100 μl following the manufacturer's protocol. PCR was carried out for 30 cycles with a program (94 °C, 1 min, 42 °C, 2 min, 75 °C, 3 min, and final extension at 75 °C, 10 min). To serve as the template for second PCR, primers and dNTP were removed from PCR product solution using Suprec-02 filter (Takara Shuzo) and adjusted volume to 100 μl by TE buffer (10 mM Tris–HCl, 1 mM EDTA, pH 8.0). The second PCR was carried out with two sets of primer, 463S(5′-MGI CAYATHWSIAARGGIGCITGG-3′) and 623A(5-CC CAISWICCITMCCAISWICCRTC-3′), or 467S(5′-AARG GIGCITGGCCITTYWSIAC-3′) and 623A with the first PCR product solution (3 μl) as the template under the same condition as the first PCR. The PCR product (400 or 450 bp) was subcloned to the plasmid vector (pT7-Blue). Twenty-six colonies were picked up in total, and nucleotide sequence was determined. From sequence identify, they were grouped into three, and their full length clones designated as *CPX* (16 clones),*CPQ* (8 clones) and *CPR* clones (2 clones), respectively.

According to the sequence of these three clones, specific primers for each clone were designed to obtain the 3′ and 5′ end sequences. RACE PCRs were carried out following the method described in our previous paper with some modifications.[19] Used primers were as follows. For 3′-RACE; CPX505S(5′-AGTCAATTGATGAACAACAGC-3′), CPQ443S(5′-TCAGATCCAGGAGGACTGTCC-3′), CPQ505S(5′-AGCCATTAGAAAAGAATCGCC-3′) and CPR505S(5′-AGCCAATGGACATTCGTAAAT-3′). For 5′-RACE; CPX298A(5′-TCAACTTCATGATAAGGAA CAAGA-3′), CPX355A(5′-GATATGCTGCATTACAC TCTGC-3′), CPQ201A(5′-CAAGCACGTGCTTTTGTCA TT-3′), CPQ250A(5′-CCTGGATGAAATGGTAGGCTG-3′), CPQ282A(5′-CTTGCCTTAGAGAAAGAACTT-3′), CPR201A(5′-CATCTTCTTGCTTGACGCAAG-3′), CPR282A(5′-CTTGCCTGAGGCTCGTGATTA-3′) and CPR340A(5′-TTTTGCCTTAGCTTTGAGAGT-3′).

To obtain the full-length clones, two specific primers for each clone with specific restriction enzyme sites at each end were designed. Used primers were as follows; Bam-CPX-S (5′-GCAAACGGATCCAGAATGTGGCAGCTCAAGA TT-3′), Sph-CPX-A (5′-TAGCAAGCATGCCTATTTA AGGGGTTTCAGTAC-3′), Hind-CPQ-S (5′-AGAA AAAAGCTTAATATGTGGAGGCTGAAGGTGGGA-3′), Sph-CPQ-A (5′-AGCAGGCATGCTCATTCAGTAA GAACCCGATG-3′), Sac-CPR-S′ (5′-GCTAGAGCTCAA CATGTGGACCCTCAAATTCTCC-3′) and Not-CPR-A′ (5′-AATATTTGCGGCCGCCTATTCTTGACGTTTCA GAAC-3′). With each set of primers and cDNA pool as template, PCRs were performed with the same condition as our previous paper.[25] The obtained full length cDNA clones, *CPX*, *CPQ* and *CPR*, were sequenced in both strands. These sequences have been submitted to DDBJ sequence-database, and are available under accession numbers: *CPX*; AB116237, *CPQ*; AB116238 and *CPR*; AB116239.

Each of the 2.3 kb PCR products was digested with appropriate restriction enzyme sites and ligated into the corresponding sites of yeast expression vector pYES2 (Invitrogen) to construct the plasmid pOSC-CPX, pOSC-CPQ and pOSC-CPR.

3.3. Expression in *S. cerevisiae* and preparation of crude enzyme solutions

Each plasmid was transferred to *S. cerevisiae* strain *GIL77*,[19] using Frozen-EZ Yeast Transformation II™ kit (ZYMO RESEARCH). The transformant with pOSC-CPX was inoculated in 20 ml synthetic complete medium without uracil (SC-U), containing ergosterol (20 μg/ml), hemin (13 μg/ml) and Tween 80 (5 mg/ml), and incubated at 30 °C for 2 days. Then, media were changed to SC-U with the same supplements and 2% galactose in place of glucose. Cells were incubated at the same condition for one day, harvested by centrifugation at 500*g* for 5 min, resuspended in 0.5 ml of 0.1 M potassium phosphate buffer (pH 7.4, containing 0.45 M sucrose, 1 mM EDTA and 1 mM dithiothreitol), and broken by vortex with acid-washed glass beads (Sigma, #G-8772). Cell homogenates were centrifuged at 18,400×*g* for 20 min, and the supernatant served as the enzyme preparation.

3.4. In vitro oxidosqualene cyclase assay in the transformant by pOSC-CPX

Radio labeled substrate, (3*S*)-[^{14}C]-2,3-oxidosqualene (26 Ci/mol) was biosynthetically prepared by feeding [1-^{14}C] sodium acetate (Amersham Life Science, CFA.13).[32]

(3*S*)-[^{14}C]-2,3-oxidosqualene (0.17 nmol, 10,000 dpm in 10 μl ethyleneglycol monomethylether), 100 μl enzyme fraction (described above), and 890 μl phosphate buffer (100 mM potassium phosphate, pH 7.4, containing 0.1% Triton-X100) were incubated at 30 °C for 3 h. Reaction products were extracted with 1 ml of hexane, separated by silica gel TLC (Merck #11798) (benzene/acetone=19:1), and analyzed by an Imaging Plate Analyzer (BAS1500, Fuji) (data not shown). The spots corresponding to authentic triterpene monoalcohols were scraped off the plate and extracted with acetone. Reaction products were subjected to HPLC analysis on ODS-120T column (4.6×200 mm, Tosoh, with 95% CH_3CN, 1.5 ml/min, at 40 °C). The eluates were collected every minute, and radioactivities counted with a liquid scintillation counter. 80.5% of radioactivity associated with the fractions (36–38 min) corresponding to cycloartenol, and 19.5% with the early fractions (7–9 min) not corresponding to any one of cucurbitadienol, cycloartenol, lupeol and β-amyrin.

3.5. LC-APCIMS analysis of the CPQ products accumulated in GIL77 transformants

The transformants were cultured for 2 days and expression of OSC was induced at the same condition as described above. Then cells were collected and resuspended in the same volume of 0.1 M potassium phosphate buffer (pH 7.0) supplemented with 2% glucose and hemin (13 μg/ml) and further incubated for 24 h at 30 °C. Cells were collected and refluxed with 2 ml of 20% KOH/50% EtOH aq. for 5 min. After extraction with the same volume of hexane, the extract was concentrated and applied onto TLC plate (Merck

#11798) which was developed with benzene/acetone=19:1. The band migrating slightly forward than triterpene monoalcohol was scraped off and extracted with acetone. The extract was concentrated and applied to LC-APCIMS (LCQ, Thermo Quest). HPLC was carried out at the same condition described above. The authentic cucurbitadienol and isolated compound gave the base peak ion at *m/z* 409 $[M+H-H_2O]^+$ in APCIMS analysis (data not shown). For rigorous identification of triterpene products, MS/MS spectrum was measured (*m/z* 409 as the parent ion), which showed the identical patterns as shown in Figure 3.

3.6. NMR analysis of the CPQ products accumulated in GIL77 transformants

For preparative scale culture for transformant with pOSC-CPQ, 2000 ml culture was prepared. Induction and resting culture was performed as described above. After refluxing with 50 ml of 20% KOH/50% EtOH aq. for 1 h, the mixture was extracted with 50 ml of hexane for three times, combined and concentrated. The extract was purified by silica gel column chromatography with benzene as an eluent. The fractions corresponding to the slightly less polar spot than triterpene monoalcohol on TLC were collected (8 mg).

^1H and ^{13}C NMRs were measured in $CDCl_3$ (JEOL JSX-500) with TMS as an internal standard.

^1H NMR (500 MHz, $CDCl_3$): δ 0.80 (3H, s), 0.85 (3H, s), 0.90 (3H, d, *J*=6.5 Hz), 0.91 (3H, s), 1.02 (3H, s), 1.13 (3H, s), 1.60 (3H, s), 1.68 (3H, s), 3.47 (1H, br t, *J*=2.5 Hz), 5.09 (1H, m), 5.59 (1H, br d, *J*=6.1 Hz).

^{13}C NMR (125 MHz, $CDCl_3$): δ 15.3, 17.6, 17.8, 18.6, 21.1, 24.4, 24.8, 25.4, 25.7, 27.2, 27.9, 28.0, 28.9, 30.4, 32.3, 34.4, 34.7, 35.8, 36.4, 37.8, 41.4, 43.6, 46.2, 49.1, 50.4, 76.6, 121.5, 125.2, 130.9, 141.2.

These values were identical to those of reported.[29]

3.7. Mutagenesis of the 488th leucine and the 489th isoleucine in cucurbitadienol synthase

Mutant clones were constructed using PCR method. Following primers were used as a sense mutation primer. CPQ-L488P: 5′-TGGATGGCCCATCTCCGACTGTAC GGCTGAG-3′, CPQ-I489V: 5′-TGGATGGCTCGTCTCC GACTGTACGGCTGAG-3′, CPQ-LI489PV: 5′-CATC CGGCTATAACACCACATTTTAGC-3′. First PCR was performed with 1 μl (1 μg) of C-terminal primer (Sph-CPQ-A) and 1 μl (1 μg) mutation primer with 1 μl (0.05 μg) of pOSC-CPQ as a template. The reaction was carried out for 20 cycles with a program (94 °C, 1 min, 58 °C, 1 min, 72 °C, 1 min, and final extension at 72 °C, 10 min). The resulting 800 bp fragment was separated on agarose gel (2%) electrophoresis and purified as described above. Second PCR was carried out with this fragment as an anti-sense primer, and 1 μl (1 μg) of N-terminal primer (Hind-CPQ-S) with 1 μl (0.05 μg) of pOSC-CPQ as a template. The reaction was carried out for 20 cycles with a program (94 °C, 1 min, 58 °C, 2 min, 72 °C, 3 min, and final extension at 72 °C, 10 min). The resulting 2.3 kb band corresponding to full length cDNA fragments were digested with each restriction enzymes and ligated into pYES2 digested with the same restriction enzymes. For sequencing, the full-length clones were subcloned into pT7Blue and completely sequenced on both strands.

Each plasmid and the plasmid containing human lanosterol synthase cDNA[39] as positive control, were transferred to *S. cerevisiae* strain GIL77,[25] as described as above. The transformants were inoculated onto SC-U agar medium, containing hemin (13 μg/ml) and Tween 80 (5 mg/ml), or the same media supplemented with ergosterol (20 μg/ml), and incubated at 37 °C for 2 days. All transformants except one with human lanosterol synthase cDNA did not grow on the media without ergosterol.

Each transformant was cultured, and products were analyzed by the same method described above. In LC-APCIMS analysis, the product derived from each transformant gave exactly the same LC-profile and MS-fragmentation as those of the wild-type cucurbitadienol synthase clone CPQ. And, in vitro enzyme analysis by the same method as described above did not show the significant difference among mutant and wild-type CPQs.

3.8. Phylogenetic analysis

The phylogenetic tree was constructed from the amino acid sequences of all the known plant OSCs by the Neighbor-Joining method[40] followed by drawing with Tree View.[41] The accession numbers of the sequences on EMBL, GenBank and DDBJ sequence-data banks used in this analysis are as follows, *CAS1* cycloartenol synthase (*A. thaliana*);[42] U02555, *PSX* cycloartenol synthase (*Pisum sativum*);[43] D89619, *PNX* cycloartenol synthase (*P. ginseng*);[25] AB009029, *GgCAS1* cycloartenol synthase (*G. glabra*);[26] AB025968, *LcCAS1* cycloartenol synthase (*L. cylindrica*);[31] AB033334, *BPX* and *BPX2* cycloartenol synthases (*B. platyphylla*);[32] AB055509 and AB055510, *LUP1* lupeol synthase (*A. thaliana*);[18] U49919, *OEW* lupeol synthase (*Olea europaea*);[30] AB025343, *TRW* lupeol synthase (*T. officinale*);[30] AB025345, *BPW* lupeol synthase (*B. platyphylla*);[32] AB055511, *PNY* β-amyrin synthase (*P. ginseng*);[25] AB009030, *PNY2* β-amyrin synthase (*P. ginseng*);[44] AB014057, *PSY* β-amyrin synthase (*P. sativum*);[15] AB034802, *GgbAS1* β-amyrin synthase (*G. glabra*);[45] AB037203, *BPY* β-amyrin synthase (*B. platyphylla*);[32] AB055512, *MtAMY1* β-amyrin synthase (*Medicago truncatula*);[22,46] AF78453 and AJ430607, *PSM* mixed amyrin synthase (*P. sativum*);[15] AB034803, *LjAMY2* mixed amyrin synthase (*Lotus japonicus*);[22] AF78455, *YUP8H12R.43* multifunctional triterpene synthase (*A. thaliana*);[16] AC002986, *LcIMS1* isomultiflorenol synthase (*L. cylindrica*);[27] AB058643, *PNZ* putative oxidosqualene cyclase (*P. ginseng*);[25] AB009031, *TRV* putative oxidosqualene cyclase (*T. officinale*);[30] AB025346, *LcOSC2* putative oxidosqualene cyclase (*L. cylindrica*);[27] AB033335.

Acknowledgements

The authors are grateful to Dr. K. Yasukawa (College of Pharmacy, Nihon University) for a gift of authentic

cucurbitadienol. A part of this research was financially supported by a Grant-in-Aid for Scientific Research (B) (No. 14380285) to M. S. and a Grant-in-Aid for Scientific Research on Priority Area (A) (No. 12045213) to Y. E. from the Ministry of Education, Culture, Sports, Science and Technology, Japan.

References and notes

1. Lavie, D.; Glotter, E. *Fortshcr. Chem. Org. Naturst.* **1971**, *29*, 307.
2. Zander, J. M.; Wigfield, D. C. *J. Chem. Soc. Chem. Commun.* **1970**, 1599.
3. Konoshima, T.; Takasaki, M.; Kozuka, M.; Nagao, T.; Okabe, H.; Irino, N.; Nakasumi, T.; Tokuda, H.; Nishino, H. *Biol. Pharm. Bull.* **1995**, *18*, 284–287.
4. Peters, R. R.; Farias, M. R.; Ribeiro-do-Valle, R. M. *Planta Medica* **1997**, *63*, 525–528.
5. Konoshima, T.; Kashiwada, Y.; Takasaki, M.; Kozuka, M.; Yasuda, I.; Cosentino, L. M.; Lee, K. H. *Bioorg. Med. Chem. Lett.* **1994**, *4*, 1323–1326.
6. Tallamy, D. W.; Powell, B. E.; McClafferty, J. A. *Behav. Ecol.* **2002**, *13*, 511–518.
7. Sarker, S. D.; Whiting, P.; Sik, V.; Dinan, L. *Phytochemistry* **1999**, *50*, 1123–1128.
8. de Kock, W. T.; Enslin, P. R.; Barton, D. H. R.; Sklarz, B.; Bothner-By, A. A. *J. Chem. Soc.* **1963**, 3828–3845.
9. Lavie, D.; Shvo, Y.; Gottlieb, O. R.; Glotter, E. *J. Org. Chem.* **1963**, *28*, 1790–1795.
10. Calvert, M. J.; Ashton, P. R.; Allemann, R. K. *J. Am. Chem. Soc.* **2002**, *124*, 11636–11641.
11. Lin, X.; Hezari, M.; Koepp, A. E.; Floss, H. G.; Croteau, R. *Biochemistry* **1996**, *35*, 2968–2977.
12. Wigfield, D. C.; Zander, J. M. *J. Chem. Soc. Sec. D Chem. Commun.* **1970**, *23*, 1599–1600.
13. Balliano, G.; Caputo, O.; Viola, F.; Delprino, L.; Cattel, L. *Phytochemistry* **1983**, *22*, 909–913.
14. Balliano, G.; Caputo, O.; Viola, F.; Delprino, L.; Cattel, L. *Phytochemistry* **1983**, *22*, 915–921.
15. Morita, M.; Shibuya, M.; Kushiro, T.; Masuda, K.; Ebizuka, Y. *Eur. J. Biochem.* **2000**, *267*, 3453–3460.
16. Kushiro, T.; Shibuya, M.; Masuda, K.; Ebizuka, Y. *Tetrahedron Lett.* **2000**, *41*, 7705–7710.
17. Husselstein-Muller, T.; Schaller, H.; Benveniste, P. *Plant Mol. Biol.* **2001**, *45*, 75–92.
18. Herrera, J. B. R.; Bartel, B.; Wilson, W. K.; Matsuda, S. P. T. *Phytochemistry* **1998**, *49*, 1905–1911.
19. Kushiro, T.; Shibuya, M.; Ebizuka, Y. *J. Am. Chem. Soc.* **1999**, *121*, 1208–1216.
20. Kushiro, T.; Shibuya, M.; Masuda, K.; Ebizuka, Y. *J. Am. Chem. Soc.* **2000**, *122*, 6816–6824.
21. Segura, M. J. R.; Meyer, M. M.; Matsuda, S. P. T. *Org. Lett.* **2000**, *2*, 2257–2259.
22. Iturbe-Ormaetxe, I.; Haralampidis, K.; Papadopoulou, K.; Osbourn, A. E. *Plant Mol. Biol.* **2003**, *51*, 731–743.
23. Meyer, M. M.; Xu, R.; Matsuda, S. P. T. *Org. Lett.* **2002**, *4*, 1395–1398.
24. Segura, M. J. R.; Lodeiro, S.; Meyer, M. M.; Patel, A. J.; Matsuda, S. P. T. *Org. Lett.* **2002**, *4*, 4459–4462.
25. Kushiro, T.; Shibuya, M.; Ebizuka, Y. *Eur. J. Biochem.* **1998**, *256*, 238–244.
26. Hayashi, H.; Hiraoka, N.; Ikeshiro, Y.; Kushiro, T.; Morita, M.; Shibuya, M.; Ebizuka, Y. *Biol. Pharm. Bull.* **2000**, *23*, 231–234.
27. Hayashi, H.; Huang, P.; Inoue, K.; Hiraoka, N.; Ikeshiro, Y.; Yazaki, K.; Tanaka, S.; Kushiro, T.; Shibuya, M.; Ebizuka, Y. *Eur. J. Biochem.* **2001**, *268*, 6311–6317.
28. Frohman, M. A.; Dush, M. K.; Martin, G. R. *Proc. Natl. Acad. Sci. U.S.A.* **1988**, *85*, 8998–9002.
29. Itoh, T.; Tamura, T.; Jeong, T. M.; Tamura, T.; Matsumoto, T. *Lipids* **1980**, *15*, 122–123.
30. Shibuya, M.; Zhang, H.; Endo, A.; Shishikura, K.; Kushiro, T.; Ebizuka, Y. *Eur. J. Biochem.* **1999**, *266*, 302–307.
31. Hayashi, H.; Hiraoka, N.; Ikeshiro, Y.; Yazaki, K.; Tanaka, S.; Kushiro, T.; Shibuya, M.; Ebizuka, Y. *Plant Physiol.* **1999**, *121*, 1384.
32. Zhang, H.; Shibuya, M.; Yokota, S.; Ebizuka, Y. *Biol. Pharm. Bull.* **2003**, *26*, 642–650.
33. Pascal, S.; Taton, M.; Rahier, A. *J. Biol. Chem.* **1993**, *268*, 11639–11654.
34. Darneta, S.; Bardb, M.; Rahiera, A. *FEBS Lett.* **2001**, *508*, 39–43.
35. Taton, M.; Rahier, A. *Biochem. J.* **1991**, *277*, 32944–32950.
36. Bishop, G. J.; Nomura, T.; Yokota, T.; Harrison, K.; Noguchi, T.; Fujioka, S.; Takatsuto, S.; Jones, J. D. G.; Kamiya, Y. *Proc. Natl. Acad. Sci. U.S.A.* **1999**, *96*, 1761–1766.
37. Choe, S. W.; Dilkes, B. P.; Fujioka, S.; Takatsuto, S.; Sakurai, A.; Feldmann, K. A. *Plant Cell* **1998**, *10*, 231–243.
38. Konopa, J.; Matuszki, A.; Hrabowsk, M.; Onoszka, K. *Arzneimittel Forschung* **1974**, *24*, 1741–1743.
39. Sung, C.-K.; Shibuya, M.; Sankawa, U.; Ebizuka, Y. *Biol. Pharm. Bull.* **1995**, *18*, 1459–1461.
40. Saitou, N.; Nei, M. *Mol. Biol. Evol.* **1987**, *4*, 406–425.
41. Page, R. D. M. *Comput. Appl. Biosci.* **1996**, *12*, 357–358.
42. Corey, E. J.; Matsuda, S. P. T.; Bartel, B. *Proc. Natl. Acad. Sci. U.S.A.* **1993**, *90*, 11628–11632.
43. Morita, M.; Shibuya, M.; Lee, M. S.; Sankawa, U.; Ebizuka, Y. *Biol. Pharm. Bull.* **1997**, *20*, 770–775.
44. Kushiro, T.; Shibuya, M.; Ebizuka, Y. Towards Natural Medicine Research in the 21st Century. In *Excerpta Medica International Congress Series 1157*; Ageta, H., Aimi, N., Ebizuka, Y., Fujita, T., Honda, G., Eds.;, 1998; pp 421–428.
45. Hayashi, H.; Huang, P.; Kirakosyan, A.; Inoue, K.; Hiraoka, N.; Ikeshiro, Y.; Kushiro, T.; Shibuya, M.; Ebizuka, Y. *Biol. Pharm. Bull.* **2001**, *24*, 912–916.
46. Suzuki, H.; Achnine, L.; Xu, R.; Matsuda, S. P. T.; Dixon, R. A. *The Plant J.* **2003**, *32*, 1033–1048.

Available online at www.sciencedirect.com
SCIENCE DIRECT®
Tetrahedron
Tetrahedron 60 (2004) 7005–7013

Emission of 2-phenylethanol from its β-D-glucopyranoside and the biogenesis of these compounds from [$^2H_8$] L-phenylalanine in rose flowers

Shunsuke Hayashi,[a] Kensuke Yagi,[a] Takashi Ishikawa,[a] Miwa Kawasaki,[a] Tatsuo Asai,[a] Joanne Picone,[b] Colin Turnbull,[b] Jun Hiratake,[c] Kanzo Sakata,[c] Masayasu Takada,[d] Koji Ogawa[d] and Naoharu Watanabe[a,*]

[a]*Faculty of Agriculture, Shizuoka University, 836 Ohya, Shizuoka 422-8529, Japan*
[b]*Department of Agricultural Sciences, Imperial College at Wye, University of London, Wye, Ashford, Kent TN25 5AH, UK*
[c]*Institute for Chemical Research, Kyoto University, Uji, Kyoto 611-0011, Japan*
[d]*Nihon Shokuhin Kako Co., Ltd., 30 Tajima, Fuji, Shizuoka 417-8530, Japan*

Received 5 August 2003; revised 26 October 2003; accepted 26 October 2003

Available online 25 June 2004

Abstract—The hydrolysis of 2-phenylethyl β-D-glucopyranoside (**3**) was found to be partially inhibited by feeding with 2-phenyl-*N*-glucosyl-acetamidiumbromide (**8**), a β-glucosidase inhibitor, resulting in a decrease in the diurnal emission of 2-phenylethanol (**2**) from *Rosa damascena* Mill. flowers. Detection of [1,1,2,2′,3′,4′,5′,6′-$^2H_8$]-**2** and [1,2,2′,3′,4′,5′,6′-$^2H_7$]-**2** from *R.* 'Hoh-Jun' flowers fed with [1,1,2,2′,3′,4′,5′,6′-$^2H_8$]-**3** suggested that β-glucosidase, alcohol dehydrogenase, and reductase might be involved in scent emission. Comprehensive GC-SIM analyses revealed that [1,2,2,2′,3′,4′,5′,6′-$^2H_8$]-**2** and [1,2,2,2′,3′,4′,5′,6′-$^2H_8$]-**3** must be biosynthesized from [1,2,2,2′,3′,4′,5′6′-$^2H_8$] L-phenylalanine ([$^2H_8$]-**1**) with a retention of the deuterium atom at α-position of [$^2H_8$]-**1**.

1. Introduction

Floral scent compounds, such as monoterpenoids, shikimate derived compounds, and fatty acids-derived compounds, are synthesized in some flowers. These compounds are emitted to attract pollinators,[1−7] to attract or to deter herbivores,[8] and/or to prevent bacterial and fungal infections.

2-Phenylethanol (**2**) is one of the dominant floral scent compounds emitted from roses such as *Rosa damascena* spp and *R.* 'Hoh-Jun'. Rhythmic cycles in the emission of **2** are observed in *R.* 'Hoh-Jun' as shown in Figure 2, although *R. damascena* Mill. transiently emits **2** (cf. Fig. 5). It has been proposed that glycosidically bound volatiles act as aroma precursors,[9−12] and their hydrolysis may be responsible for the rhythmic emission pattern observed in *R.* 'Hoh-Jun'.[13] In *R. damascena* Mill. flowers, the amount of 2-phenylethyl β-D-glucoside (**3**) is greater during the stages of early development and decreases during the unfurling process, whilst levels of the free form generally increased over the unfurling.[14] In *Narcissus* flowers, β-glucosidase activity was found to be involved in the scent emission detected by gas sensors.[15] To date, attempts to correlate concentrations of glucosides with rhythmic cycles in volatile emission have been unsuccessful.[16,17] Synchronous diurnal rhythms have been detected in the concentration of both **2** and its acetate, but not in the concentration of **3**, in the *Trifolium repens* flowers.[17]

Although there has been much progress in elucidating biosynthetic pathways and characterizing enzymes, the underlying biosynthetic route of **2** in flowers has yet to be fully understood. We recently reported the biogenesis of **2** from L-phenylalanine (**1**) in rose flowers.[18] In that study, [1,2,2,2′,3′,4′,5′,6′-$^2H_8$]-**1** ([$^2H_8$]-**1**) was fed to *R.* 'Hoh-Jun' and *R. damascena* Mill. flowers throughout maturation, and feeding was terminated at full bloom stage. On the basis of GC-MS analyses, we found that [$^2H_8$]-**1** was incorporated into both **2** and **3** when the flowers were fed until full bloom. In both rose species, the labeling pattern of **2** was almost identical to that of **3**, and indicated the presence of both [$^2H_7$]- and [$^2H_8$]-**2**, and [$^2H_7$]- and [$^2H_8$]-**3**. This may be ascribed to the equilibrium established between **2** and **3**. Although the labeling pattern for **2** and **3** established that these compounds were produced from **1** via several routes as

Keywords: Rose flower; L-Phenylalanine; Biogenesis; β-Glucosidase; 2-Phenylethanol; 2-Phenylethyl β-D-glucopyranoside.
* Corresponding author. Tel./fax: +81-54-238-4870; e-mail address: acnwata@agr.shizuoka.ac.jp

0040–4020/$ - see front matter © 2004 Elsevier Ltd. All rights reserved.
doi:10.1016/j.tet.2003.10.130

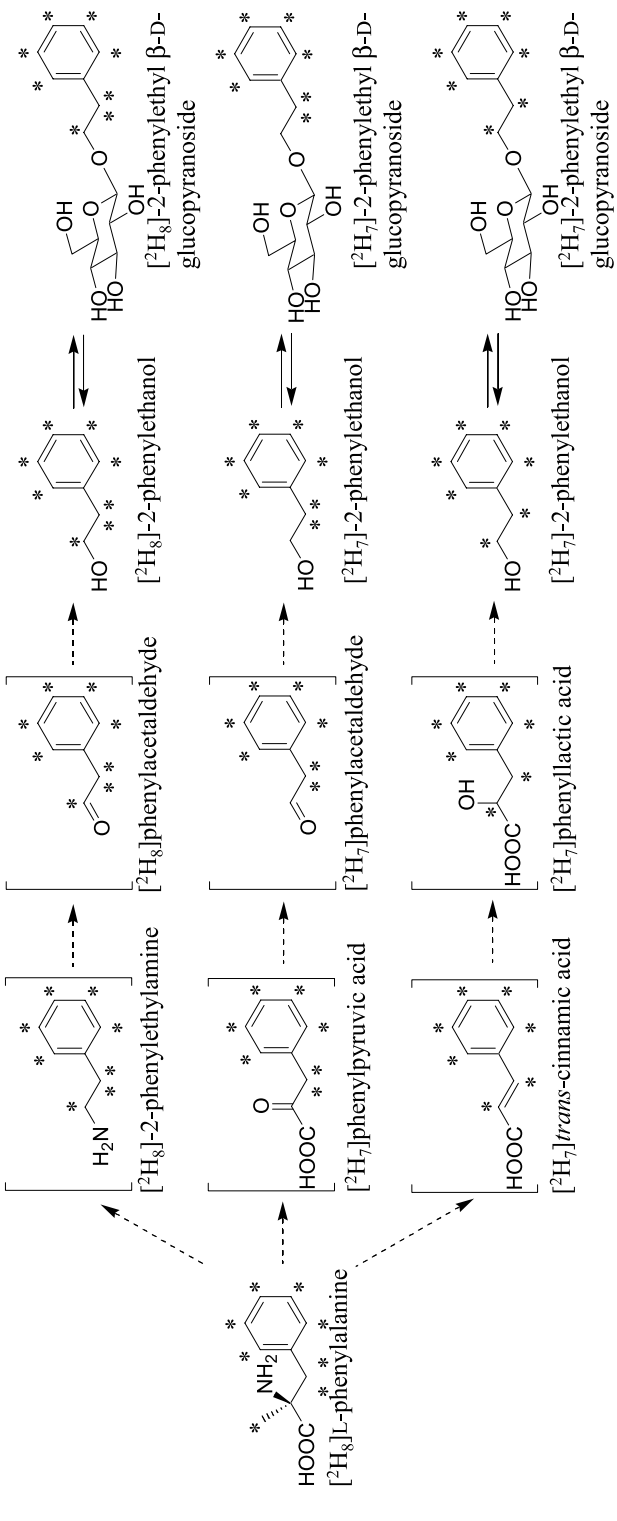

Figure 1. Hypothetical biogenetic pathway for 2-phenylethanol (**2**) and 2-phenylethyl β-D-glucopyranoside (**3**) from L-phenylalanine (**1**). Asterisk denotes the position of a ^{2}H atom.

shown in Figure 1, the route involving phenylpyruvic acid (**4**) was thought to be the major one. However, the detection of [$^2H_8$]-**2** and [$^2H_8$]-**3** strongly suggested the presence of a biosynthetic route involving the intermediate 2-phenylethylamine (**6**).

In this paper, we describe the involvement of β-glucosidase in the emission of **2**, based on experiments using a β-glucosidase inhibitor and feeding with [1,1,2,2′,3′,4′,5′,6′-$^2H_8$]-**3**, as well as details of the biosynthetic pathways of **2**, deduced from feeding with [$^2H_8$]-**1**, in *R. damascena* Mill. and *R.* 'Hoh-Jun' flowers.

2. Results and discussion

In *R. damascena* Mill. flowers, the amount of **3** is greater in early development and declines over the unfurling process, whereas levels of the free form generally increased over the unfurling process under natural conditions.[14] As shown in Figures 2 and 5, we found that **2** was emitted in higher concentrations when exposed to light than when kept in the dark at a constant temperature. Loughrin[16] has suggested that changes in the rate of the glycoside hydrolysis may be responsible for the emission of scent compounds. We therefore attempted to verify the involvement of β-glucosidase and its substrate **3** in the production of **2** in *R. damascena* Mill. flowers.

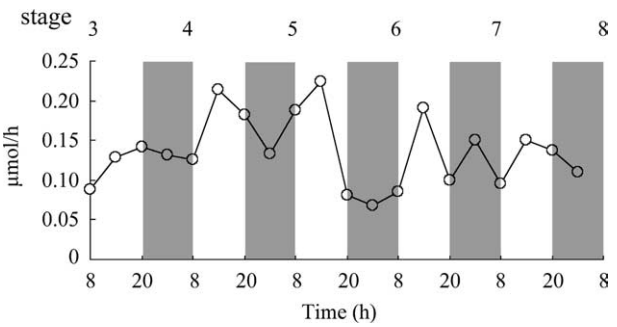

Figure 2. 2-Phenylethanol (**2**) emission during the unfurling process in *Rosa* 'Hoh-Jun' flowers of intact plants maintained under a 12-h photo period at constant temperature (22 °C) and relative humidity (75%). Shaded and non-shaded areas correspond to exposure to dark and light, respectively. Stages of flowers are defined in the text.

We examined the effect of 2-phenyl-*N*-β-glucosyl-acetamidiniumbromide (**8**, Fig. 3), a glucosidase inhibitor,[19,20] on the hydrolytic activity of crude enzymes prepared from flower petals. The crude enzymes (prepared from 100 to 400 mg of flower petals) released 1.3 μmol of **2** in 1 h from 5 μmol of **3**, and more than 95% of the hydrolytic activity was inhibited by 0.6 μmol of **8**. As each flower accumulated 15 μmol of **3** at stage 3, it was expected that more than 2.0 μmol of **8** would inhibit the hydrolysis of **3** in each flower. Therefore, 300 μl of an aqueous solution of **8** (10 mM) was fed to *R. damascena* Mill. flowers at stage 3. As shown in Figure 4b, the level of **3** gradually decreased by 7 μmol/flower in the control group, whereas the level in the fed group was almost constant (16–14 μmol/flower) during the dark period (6–18 h after the feeding commenced). During the day-time (18–30 h after the feeding commenced) the level of **3** remained fairly constant (13–17 μmol/flower) in the fed group, but decreased by 5 μmol/flower in the control group. The concentration of **2** in the tissue increased gradually to reach its maximal level (17 μmol/flower) 24 h after the feeding commenced in the control group, but the concentration did not exceed 5 μmol/flower during the unfurling process in the fed group (Fig. 4a).

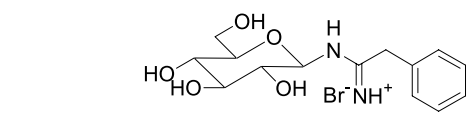

Figure 3. 2-Phenyl-*N*-β-glucopyranosyl-acetamidiumbromide (**8**), a β-glucosidase inhibitor.

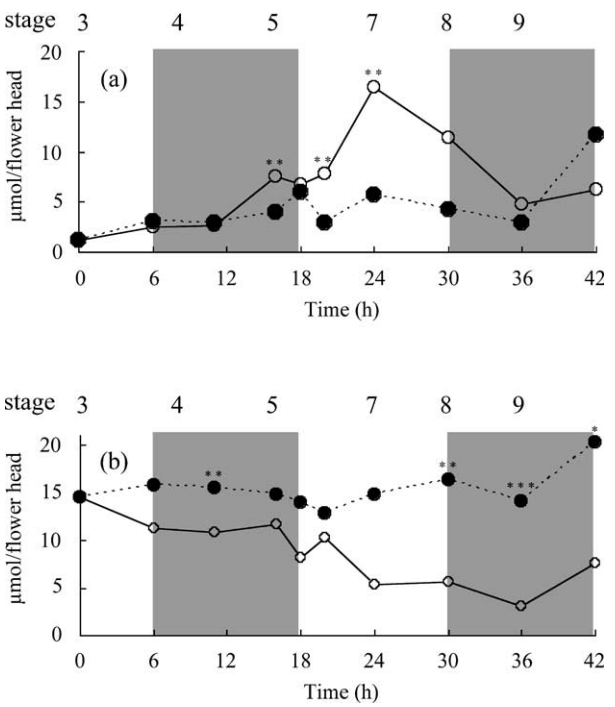

Figure 4. Effect of 2-phenyl-*N*-β-glucopyranosyl-acetamidiumbromide (**8**) on the accumulation of 2-phenylethanol (**2**) (a) and 2-phenylethyl β-D-glucopyranoside (**3**) (b) accumulated in the flowers of *Rosa damascena* Mill. during the unfurling process. ○, Control group; ●, fed **8**. Intact plants were exposed to the same conditions as in Figure 2. Shaded and non-shaded areas correspond to exposure to dark and light, respectively. $^{***}P<0.01$, $^{**}P<0.05$, $^{*}P<0.1$ for paired comparisons of the control versus the fed group. Stages of flowers are defined in the text.

As shown in Figure 5, diurnal emission reached its maximum level at 21 h after feeding commenced in the control group, whereas a peak was not observed in the fed group. β-Glucosidase activity increased between stages 4 and 6 (Fig. 5). The increase in β-glucosidase activity was observed prior to the increase in the concentration of **2** in the control flowers. As **8** does not bind to β-glucosidase via a covalent bond,[20] similar level of β-glucosidase activity was detected in the crude extract even in the fed group. Although the high β-glucosidase activity at stage 9 cannot be rationally explained, these observations strongly suggest that β-glucosidase activity is involved in both the production and the emission of **2**. We therefore, focus our research on the effect of the inhibitor, **8**, on the rhythmic emission of **2** observed in *R.* 'Hoh-Jun' and *R. damascena* semperflorens quatra saisons[21] flowers

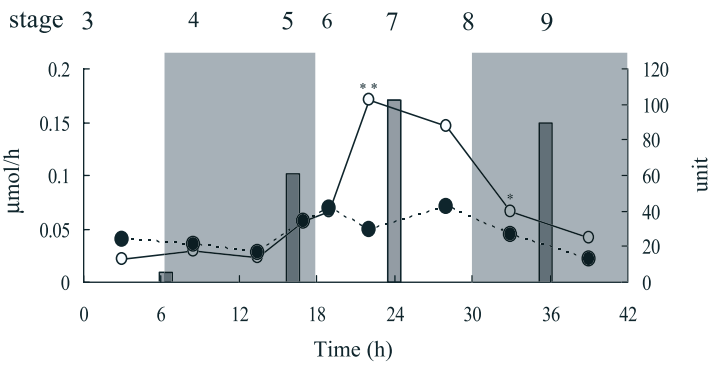

Figure 5. Effect of 2-phenyl-*N*-β-glucopyranosyl-acetamidiumbromeide (**8**) on 2-phenylethanol (**2**) emission from *Rosa damascena* Mill. flowers, and changes in β-glucosidase activity during the unfurling process *R. damascena* Mill. flowers. ○, Control group; ●, fed **8**. Bar indicates β-glucosidase activity. Intact plants were exposed to the same conditions as in Figure 2. Shaded and non-shaded areas correspond to exposure to dark and light, respectively. $^{**}P<0.05$, $^{*}P<0.1$ for paired comparisons of the control versus the fed group. Stages of flowers are defined in the text.

During the study, [1,1,2,2′,3′,4′,5′,6′-$^2H_8$]-**3** was fed to *R.* 'Hoh-Jun' flowers at stage 3 to confirm the emission of [1,1,2,2′,3′,4′,5′,6′-$^2H_8$]-**2**. As shown in Figure 6, [1,1,2,2′,3′,4′,5′,6′-$^2H_8$]-**2** and [1,2,2′,3′,4′,5′,6′-$^2H_7$]-**2** were detected in sample of the head-space gas, and the ratio of the [1,1,2,2′,3′,4′,5′,6′-$^2H_8$]-**2** to [1,2,2′,3′,4′,5′,6′-$^2H_7$]-**2** decreased during the unfurling process until senescence stage (between stages 3 and 8). This observation strongly suggests that [1,1,2,2′,3′,4′,5′,6′-$^2H_8$]-**2**, once produced by endogenous β-glucosidase, is transformed to [1,2,2′,3′,4′,5′,6′-$^2H_7$]-phenylacetaldehyde (**5**) by alcohol dehydrogenase, and subsequently interconverted into [1,2,2′,3′,4′,5′,6′-$^2H_7$]-**2**. In our preliminary experiments, we detected alcohol dehydrogenase activities toward **2** in the crude enzymes prepared from *R.* 'Hoh-Jun' petal tissues (data not shown). This indicates that the oxidation–reduction process is a significant factor involved in regulating the production and emission of **2**.

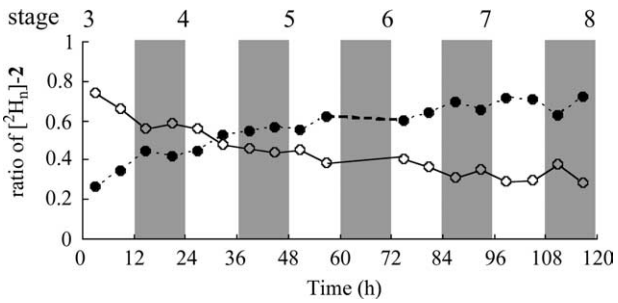

Figure 6. Changes in the ratio of [1,1,2,2′,3′,4′,5′,6′-$^2H_8$]-**2** to [1,2,2′,3′,4′,5′,6′-$^2H_7$]-**2** emitted from the flowers of *Rosa* 'Hoh-Jun' after feeding with [1,1,2,2′,3′,4′,5′,6′-$^2H_8$]-**3**. ○, [1,1,2,2′,3′,4′,5′,6′-$^2H_8$]-**2**; ●, [1,2,2′,3′,4′,5′,6′-$^2H_7$]-**2**. Intact plants were exposed to the same conditions as in Figure 2. Stages of flowers are defined in the text.

We recently found that [$^2H_8$]-**1** is transformed to **2** and its β-D-glucopyranoside **3** via **4**, and we proposed that this is the main biosynthetic pathway of **2** and **3** in *R. damascena* Mill. and *R.* 'Hoh-Jun' flowers.[18] The proposed pathway and the labeling pattern are illustrated in Figure 1;[18] this pathway has been already observed in yeasts and various plant tissues.[22–24] In our experiments, not only [$^2H_7$]-**2** and [$^2H_7$]-**3**, the primary isotopomers of the deuterium labeled compounds, but also [$^2H_8$]-**2** and [$^2H_8$]-**3** were detected as minor components in the flowers. This suggests that the flowers can produce **2** and **3** from **1** via several pathways from **1**. As shown in Figure 6, one deuterium atom of [1,2,2′,3′,4′,5′,6′-$^2H_8$]-**2** was lost during the oxidation–reduction reaction yielding [2,2′,3′,4′,5′,6′-$^2H_7$]-**2**. This prompted us to reconsider the biosynthetic route from **1** to **2** during feeding with [$^2H_8$]-**1**, because [$^2H_7$]-**2** and [$^2H_7$]-**3** are likely to be derived from [$^2H_8$]-**2** and [$^2H_8$]-**3**, respectively. Below, we examined the effects of [$^2H_8$]-**1** feeding over a short unfurling process in order to elucidate the actual biosynthetic route of **2** by tracing changes in the labeling patterns of [^2H_n]-**2** and [^2H_n]-**3**.

Initially, we attempted to confirm the transformation of [$^2H_8$]-**1** to [^2H_n]-**2** and [^2H_n]-**3** by increasing the concentration of [$^2H_8$]-**1** that was fed. Compound [$^2H_8$]-**1** was fed to the flowers for 48 h after unfurling initiated (stage 3), and the flower petals were collected and extracted with pentane in a microwave oven. In the previous paper,[18] all [^2H_n]-**2** were detected at the same t_R, but in this study, each [^2H_n]-**2** isotopomers was detected at different t_Rs (18.23, 18.30, and 18.32 min for [$^2H_8$]-**2**, [$^2H_7$]-**2**, and [$^2H_6$]-**2**, respectively, due to the isotope effects under the conditions used (see Section 3). Therefore, the amount of each isotopomer of [^2H_n]-**2** was estimated from the GC-SIM traces at *m/z* 130 for [$^2H_8$]-**2**, *m/z* 129 for [$^2H_7$]-**2**, and *m/z* 128 for [$^2H_6$]-**2** at each t_R. The ratio of [^2H_n]-**2** plus [^2H_n]-**3** to **2** plus **3** increased as the concentration of [$^2H_8$]-**1** increased (measured ratio 0.00033, 0.0010, 0.0032, 0.0036, 0.0073, and 0.013 at a concentration of 2.1, 4.3, 8.7, 17.3, 34.5, and 69.0 mM, respectively). This indicated that **1** is an actual precursor of **2** in the flowers. The overall yield of [^2H_n]-**2** plus [^2H_n]-**3** was ca. 1.1% when all of the [$^2H_8$]-**1** fed was absorbed in the flowers. As [$^2H_8$]-**1** contains ca. 15% of [$^2H_7$]- and/or [$^2H_6$]-**1** on the basis of ^1H NMR analyses of the methyl ester, the total empirical peak height for [$^2H_7$]-**2** must be subtracted by 15% of each value. The amount of [$^2H_6$]-**2** was not considered because the peak (which accounted for less than 5% of the total amount of [^2H_n]-**2**) for [$^2H_6$]-**2** might have originated from [$^2H_6$]-**1** at the initial feeding stage. On the basis of the prerequisite condition, the ratio ([$^2H_8$]-/[$^2H_7$]-**2**=50–58/40–42, [$^2H_8$]-/[$^2H_7$]-**3**=50–58/40–42) remained almost

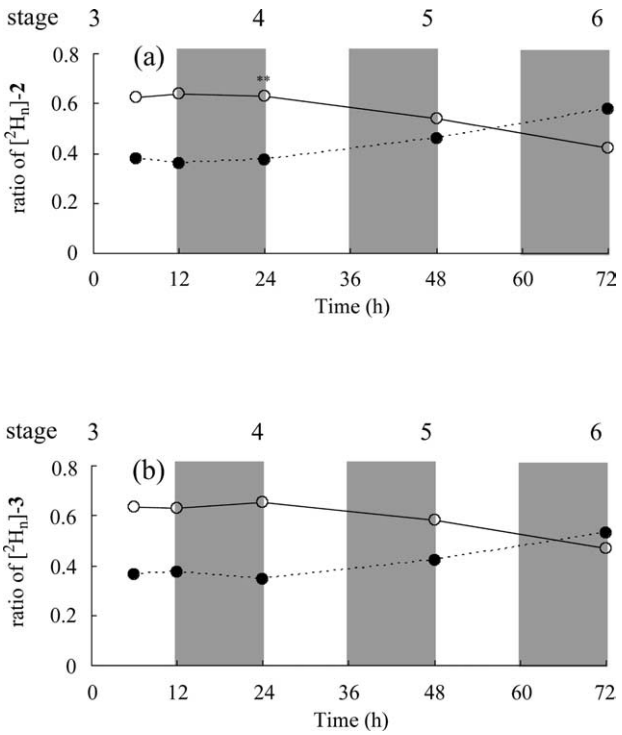

Figure 7. Changes in the ratio of [$^2H_8$]-**2** to [$^2H_7$]-**2** detected in the volatile fraction (a) and as the aglycone of **3** (b) in the flowers of *Rosa* 'Hoh-Jun' after feeding with [$^2H_8$]-**1**. ○, [$^2H_8$]-**2**; ●, [$^2H_7$]-**2**. Intact plants were exposed to the same conditions as in Figure 2.

identical, regardless of the increase in the concentration of the fed [$^2H_8$]-**1**.

We next compared changes in the $^2H_8$]-**2**/[$^2H_7$]-**2** and [$^2H_8$]-**3**/[$^2H_7$]-**3** ratios over time. Feeding of [$^2H_8$]-**1** was started at stage 3 of the *R*. 'Hoh-Jun' flower, and the flowers were subsequently collected at 6, 12, 24, 48, and 72 h after feeding began. Most of the [$^2H_8$]-**1** solution was absorbed by 72 h. The flowers were successively extracted by pentane and ethyl acetate in a microwave oven yielding volatile and glycosidic fractions as previously reported by Oka et al.[14]

As shown in Figure 7(a) and (b), changes in the ratio of [$^2H_8$]-**2**/[$^2H_7$]-**2** change corresponded to those in the ratio of [$^2H_8$]-**3**/[$^2H_7$]-**3** throughout the unfurling process (between stages 3 and 6). The ratio of [$^2H_8$]-**2**/[$^2H_7$]-**2** and [$^2H_8$]-**3**/[$^2H_7$]-**3** was 63/37, and 62/38, respectively, at the initial sampling point, but had decreased to reach 42/58 and 47/53, respectively, by 72 h after the feeding commenced. This correlation indicates that an equilibrium exists between **2** and **3** in the petal tissue, and abstracting one of the deuterium atoms from [$^2H_8$]-**2** by the action of alcohol dehydrogenase caused a decline in the ratio. The difference between the current value and the previously reported ratio [$^2H_8$]-**2**/[$^2H_7$]-**2**=[$^2H_8$]-**3**/[$^2H_7$]-**3**=10–20/90–80)[18] must be due to this abstraction of a deuterium atom from the initial isotopomer, [$^2H_8$]-**2**, during longer duration of the previous study. Therefore, **2** must be converted from **1** without the loss of a hydrogen atom at the α-position.

Interestingly, the postulated intermediates, [$^2H_8$]-**5** and [$^2H_8$]-**6**,[25] were not detected in *R*. 'Hoh-Jun' flowers upon feeding with [$^2H_8$]-**1**. This might be due to the rapid metabolism of [$^2H_8$]-**1** to [$^2H_8$]-**2** in the flower petals. Therefore, we fed 34.5 μmol of [1,1,2,2,2′,3′,4′,5′,6′-$^2H_9$]-**6**, to the *R*. 'Hon-Jun' flowers at stage 4 for 96 h to verify whether **2** and/or **3** would be produced via **6**. The flowers were extracted successively with pentane and ethyl acetate to test for [$^2H_8$]-**2** and/or [$^2H_8$]-**3**. [$^2H_8$]-**2** was not detected in the volatile fraction, although [1,2,2,2′,3′,4′,5′,6′-$^2H_8$]-**3** was detected in a trace amounts (0.0072 μmol, yield=0.021%). This yield was significantly lower than that (11%) from [$^2H_8$]-**1**, indicating that **6** might not be involved in the biosynthesis of **2** from **1**.

As previously reported[26], **5**, a key intermediate in the biosynthetic pathway, has been synthesized from **1** by a myeloperoxidase/hydrogen peroxide/chloride system derived from neutrophils. In a cell-free system, **5** is also non-enzymatically produced from **1** in the presence of the *ortho*-quinone of catechin, during which Schiff-base formation with **1** has been proposed as an intermediate.[27] Recently, a cytochrome P450 dependent oxidase,

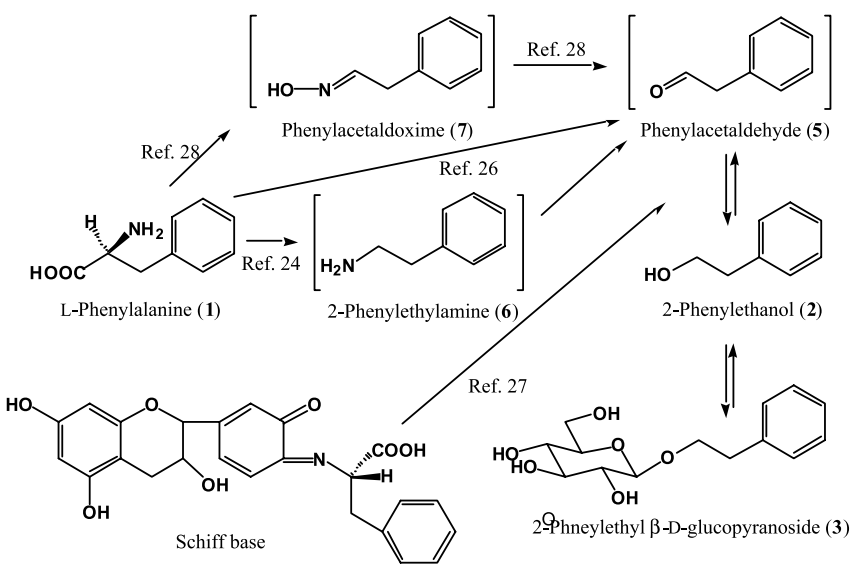

Figure 8. Possible biogenetic pathways for **2** from **1** in the rose flowers.

CYP79A2, has been characterized in *Arabidopsis* and has been shown to oxidize **1**, yielding phenylacetaldoxime (**7**).[28] Compound **7** can be enzymatically or non-enzymatically oxidized yielding **5**. In these cases, a deuterium atom at the α-position of [$^2H_8$]-**1** must be retained to yield [$^2H_8$]-**5**, which then subsequently yields [$^2H_8$]-**2**. Furthermore, **7** has been identified among volatile compounds in the flower concrete of *Michelia champaca* L.[29] We therefore, examined whether **7** is an intermediate in the biosynthetic pathway in *R.* 'Hoh-Jun' flowers. We injected [1,2,2′,3′,4′,5′,6′-$^2H_7$]-**7** (14 μmol/μl of DMSO) into *R.* 'Hoh-Jun' flowers. The overall yield (0.82 μmol, 5.8%) of [1,2,2′,3′,4′,5′,6′-$^2H_7$]-**2** (0.4%) and [1,2,2′,3′,4′,5′,6′-$^2H_7$]-**3** (5.4%) from [1,2,2′,3′,4′,5′,6′-$^2H_7$]-**7** was determined on the basis of the GC-MS analyses of the pentane and ethyl acetate fractions extracted from flowers detached 24 h after injection, suggesting that **7** is involved in the biosynthesis of **2**. Although the transformation of deuterium labeled **5** has not been confirmed yet, we can propose a plausible biosynthetic pathway for **2** as shown in Figure 8, on the basis of the results so far.

We are now focusing on the identification of the hypothesized intermediates, such as [$^2H_8$]-**5** and [$^2H_8$]-**7**, in order to clarify the exact pathway that yields [$^2H_8$]-**2** and [$^2H_8$]-**3** from [$^2H_8$]-**1** in rose petals.

In conclusion, β-glucosidase is thought to be partly involved in controlling diurnal emission of **2** in the *R. damascena* Mill. flowers. In addition, our analyses of the flower tissue after feeding have enabled us to propose a novel biosynthetic pathway for **2** and **3** via [$^2H_8$]-**5** from [$^2H_8$]-**1** in rose flowers.

3. Experimental

3.1. Chemicals and biochemicals

2,3,3,2′,3′,4′,5′,6′-[$^2H_8$] L-Phenylalanine ([$^2H_8$]-**1**, 98 atom% ^2H, Aldrich) was used. In the ^1H NMR spectral analyses of the methyl ester of [$^2H_8$]-**1**, the $^2H/H$ ratio was evaluated to be 17/83, 3/97, and 4/96 for H-2,3,3, and 2′-6′, respectively. 2-Phenyl-*N*-glucosyl-acetamidiumbromide (**8**) was synthesized by the method of Hiratake et al.[19,20] β-Glucosidase (EC 3.2.121, 500 units/mg from almond, Sigma) and naringinase (300 units/mg from *Penicillium decumbens*, Sigma) were used for enzymatic hydrolysis of glycoconjugated volatile compounds.

3.1.1. Synthesis of [1,1,2,2′,3′,4′,5′,6′-$^2H_8$]-2-phenylethyl β-D-glucopyranoside ([1,1,2,2′,3′,4′,5′,6′-$^2H_8$]-3) [1,1,2,2′,3′,4′,5′,6′-$^2H_8$]-**2** was synthesized by reduction with 9-BBN (30 mmol) in THF (10 ml) from [1,1,2,2′,3′,4′,5′,6′-$^2H_8$] styrene (2.00 g, 17.8 mmol, 98 atom% ^2H, Cambridge Isotope Laboratories, MA, USA), although the labeling pattern is not exactly the same as one of the isotopomers, [1,2,2,2′,3′,4′,5′,6′-$^2H_8$]-**2**, produced from [$^2H_8$]-**1**. The reaction mixture was treated with 6 M aq. NaOH (30 ml) and 35% H_2O_2 (30 ml). The desired compound was obtained after silica gel chromatography (hexane–EtOAc) yielding 2.38 g of a fraction containing both [1,1,2,2′,3′,4′,5′,6′-$^2H_8$]-**2** and the solvent. The fraction (1.00 g, 42% of the total) was dissolved in MeCN, and stirred for 24 h at ambient temperature in the presence of 10.4 g (25.0 mmol) of 2,3,4,6-tetra-*O*-acetyl-1-bromo α-glucose (Sigma), $Hg(CN)_2$ (2.80 g, Sigma), and molecular sieves (4 Å). After purification, [1,1,2,2′,3′,4′,5′,6′-$^2H_8$]-2-phenylethyl 2,3,4,6-tetra-*O*-acetyl β-D-glucolyranoside, it was treated with 5 ml of MeONa (1 M) in MeOH–$CHCl_3$ (1:1), followed by Dowex 50W-×4 (H^+ from), and the product was purified by silica gel chromatography ($CHCl_3$–MeOH) to yield [1,1,2,2′,3′,4′,5′,6′-$^2H_8$]-**3** (889 mg, 3.00 mmol, 40.1% from [1,1,2,2′,3′,4′,5′,6′-$^2H_8$] styrene). FABMS (pos.) analyses gave an ion peak at *m/z* 293 $[M+H]^+$. ^1H NMR (500 MHz, CD_3OD) δ_H: 2.93 (1H, s, H-2), 3.22 (1H, dd, *J*=8.7, 8.9 Hz, H-2″), 3.35 (1H, t, *J*=8.9 Hz, H-4″), 3.39 (1H, ddd, *J*=8.9, 5.4, 2.2 Hz, H-5″), 3.45 (1H, t, *J*=8.9 Hz, H-3″), 3.69 (1H, dd, *J*=11.7, 5.4 Hz, H-6″a), 3.99 (1H, dd, *J*=11.7, 2.2 Hz, H-6″b), 4.45 (1H, d, *J*=8.7 Hz, H-1″); ^{13}C NMR (125 MHz, CD_3OD) δ_C: 37.4 (t, *J*=19.2 Hz, C-2), 63.6 (C-6″), 72.4 (C-4″), 72.7 (quin. *J*=21.6 Hz, C-1), 75.9 (C-2″), 78.6 (C-3″), 78.6 (C-5″), 105.1 (C-1″), 128.8 (t, *J*=25.8 Hz, C-6′), 131.0 (2C, t, *J*=23.8 Hz, C-5′,7′), 131.4 (2C, t, *J*=24.8 Hz, C-4′,8′), 141.2 (C-3′). GC-MS analyses gave ion peaks at *m/z* 130 $[M]^+$ (100%) and *m/z* 129 $[M-1]^+$ (19%) for [1,1,2,2′,3′,4′,5′,6′-$^2H_8$]-**2**, and peaks at *m/z* 122 $[M]^+$ (100%) and *m/z* 123 $[M+1]^+$ (8.3%) for **2**, respectively. On the basis of these data, the ratio of the [$^2H_7$]-isotopomer in [1,1,2,2′,3′,4′,5′,6′-$^2H_8$]-**2** was calculated to be 17%. The ratio of [$^2H_7$]-isotopomer (17%) in [1,1,2,2′,3′,4′,5′,6′-$^2H_8$]-**3** was also estimated by GC-MS of the products obtained from [1,1,2,2′,3′,4′,5′,6′-$^2H_8$]-**3** after hydrolysis with β-glucosidase (from almond).

3.1.2. Synthesis of [1,1,2,2,2′,3′,4′,5′,6′-$^2H_9$]-2-phenyletylamine (6). $LiAlD_4$ (207 mg, 4.95 mmol, Aldrich) and anhydrous $AlCl_3$ (264 mg, 1.98 mmol, Sigma) were added to diethyl ether (6 ml), and stirred for 1 h under ice-cooling. [1,1,2′,3′,4′,5′,6′-$^2H_7$]-Phenylacetonitrile (204 mg, 1.65 mmol, Aldrich) was added and stirred for 1 h at ambient temperature. [1,1,2,2,2′,3′,4′,5′,6′-$^2H_9$]-**6** was obtained after treatment with 1 M NaOH and extraction with diethyl ether (197 mg, 1.50 mmol, yield 91%). EIMS analyses gave a peak at *m/z* 131 $[M]^+$; ^{13}C NMR (125 MHz, CD_3OD) δ_C: 39.1 (quin., *J*=19.1 Hz, C-2), 43.3 (quin., *J*=21.0 Hz, C-1), 126.7 (t, *J*=24.3 Hz, C-4′), 129.0 (2C, t, *J*=24.3 Hz, C-2′, 6′), 129.3 (2C, t, *J*=23.8 Hz, C-3′,5′), 140.7 (s, C-1′). The deuterium ratio was not estimated.

3.1.3. Synthesis of [1,2,2′,3′,4′,5′,6′-$^2H_7$]-phenylacetaldoxime (7). [1,2,2′,3′,4′,5′,6′-$^2H_7$]-phenylacetaldoxime (**7**) was prepared from [1,2,2′,3′,4′,5′,6′-$^2H_7$]-1-nitrostyrene[30] according to the method of Sera et al.[31] [1,2,2′,3′,4′,5′,6′-$^2H_7$]-1-Nitrostyrene (500 mg, 3.3 mmol) was treated by lead powder (5.5 g, 33 mmol) in acetic acid-DMF (1.5:20 v/v, 21.5 ml) for 2 h at ambient temperature. The reaction mixture was added to water (20 ml) and extracted with diethyl ether (20 ml×3 times) yielding crude extract, which was then purified by column chromatography on silica gel (hexane–diethyl ether) to yield [1,2,2′,3′,4′,5′,6′-$^2H_7$]-**7** (340 mg, 2.4 mmol, yield 73%). EIMS *m/z* 142 $[M]^+$; ^{13}C NMR (125 MHz, CD_3OD) δ_C: 31.1 (t, *J*=19.5 Hz, C-2 of *Z*-isomer), 35.4 (t, *J*=19.5 Hz, C-2 of *E*-isomer), 129.0 (2C, t, *J*=24.4 Hz, C-2′, 6′), 129.1 (2C, t, *J*=23.9 Hz, C-3′, 5′),

135.0 (s, C-1′ of *E*-isomer), 135.2 (s, C-1′ of *Z*-isomer), 150.5 (t, *J*=26.8 Hz, C-1 of *E*-isomer), 150.7 (t, *J*=26.8 Hz, C-1 of *Z*-isomer). The deuterium ratio of [1,2,2′,3′,4′,5′,6′-$^2H_7$]-**7** was not estimated. The ratio (3:1) of *Z*- to *E*-isomers was determined on the basis of the ^1H NMR spectrum of **7**, prepared from 1-nitrostyrene[30] according to the method mentioned above. ^1H NMR (500 MHz, CD_3OD) of **7**; δ_H: 3.54 (0.25H, d, *J*=12.0 Hz H-2 of *E*-isomer), 3.75 (0.75H, d, *J*=10.0 Hz, H-2 of *Z*-isomer), 6.89 (0.75H, t, *J*=10.0 Hz, H-1 of *Z*-isomer), 7.54 (0.25H, t, *J*=12.0 Hz, H-1 of *E*-isomer), 7.20–7.36 (5H, H-2′-6′).

3.2. Plant materials

Rosa damascena Mill. and *Rosa* 'Hoh-Jun' plants were grown on the University Farm, Faculty of Agriculture, Shizuoka University, Japan under natural conditions in 5-l pots, watered daily and fed weekly with a nutrient solution. Each plant bore 30–50 (*R. damascena*) and 1–4 (*R.* 'Hoh-Jun') flowers at various stages. *R.* 'Hoh-Jun' is a cultivar that produces flowers throughout the year, whereas *R. damascena* produces flowers from the end of April until mid-May in Shizuoka, Japan. Plants were acclimatized for 7 days to a constant temperature of 22±2 °C and a 12 h/12 h light/dark (LD) cycle in a controlled environment growth room with a natural light source (approximately 300 μmol m^{-2} s^{-1}). In subsequent experiments, plants were acclimatized to 22±2 °C, 75±5% humidity and 12 h photoperiods (300 μmol m^{-2} s^{-1}, provided by fluorescent lamps) in a controlled environment growth room.

The stages of floral growth are defined as follows: stage 1, immature flowers, sepals tightly closed; stage 2, sepals retracting, petal whorl tightly closed, petals beginning to lighten in color; stage 3, commencement of petal unfurling (4 days after stage 1), sepals fully retracted, outer petal whorl beginning to loosen; stage 4, outer petal whorl opened, inner petal whorl beginning to loosen; stage 5, inner petal whorl partly opened but reproductive organs not yet visible; stage 6, inner and outer whorls open, reproductive organs not visible; stage 7, full bloom flower, inner and outer whorls open, reproductive organs visible; stage 8, inner and outer whorls completely open, 30 h (*R. damascena*) or 5 days (*R.* 'Hoh-Jun') after stage 3; stage 9, senescence stage, anthers dried and darkened, petals pale.

3.3. Phenyl-*N*-glucosyl-acetamidiumbromide (8) feeding in *R. damascena* Mill. flowers

Feeding studies done in April to May of 2002 and 2003 were conducted on opening flowers at stage 3 in intact *R.* 'Hoh-Jun' plants as described above. A thin needle with a cotton thread (50 mm in length) was inserted at 2 p.m. on day 0 through the top of the ovary, just above the ovules. This thread acted as a wick enabling the absorption of an aqueous solution of **8** (10 mM, 300 μl) from an Eppendorf tube attached to the stem. A control group was evaluated in parallel in which water was fed instead of **8**. The total amount of **8** absorbed by the plant was not evaluated. Three treated flower heads at 6, 12, 16, 18, 20, 24, 30, 36, and 42 h after feeding startted were detached just below the ovary of the flower. The calyx was removed and the petal parts of each flower head were crushed in liquid nitrogen and stored at −80 °C until use.

3.4. [1,1,2,2′,3′,4′,5′,6′-$^2H_8$]-2-Phenylethyl β-D-glucopyranoside (3) feeding in *R.* 'Hoh-Jun' flowers

A solution of [1,1,2,2′,3′,4′,5′,6′-$^2H_8$]-**3** (3.4 mM, 1500 μl) was fed to the flowers at stage 3 in intact *R.* 'Hoh-Jun' plants as described above. The floral scent compounds emitted from the flowers were trapped by the dynamic head space method using automatic sampling system equipped with a time controller and six air-valves developed by the authors. A Tenax-TA column (150 mg, 3 mm i.d. ×100 mm) was used as an absorbent with an air at flow rate of 500 ml/min. Scent compounds were eluted from the column with CH_2Cl_2–diethyl ether (1:1, v/v) and concentrated at 40 °C. The concentrated materials were directly analyzed by GC-SIM.

3.5. [1,2,2,2′,3′,4′,5′,6′-$^2H_8$] L-Phenylalanine (1), [$^2H_8$]-1 feeding in *R.* 'Hoh-Jun' flowers

Feeding studies done in October and November 2002 were conducted on flowers at stage 3 in intact *R.* 'Hoh-Jun' plants as described above. An aqueous solution of [1,2,2,2′,3′,4′,5′,6′-$^2H_8$]-**1** at each concentration, 1.1, 2.1, 4.3, 8.7 and 17.3 mM, 1.5 ml was fed as described above. The total amount of [$^2H_8$]-**1** absorbed by the plant was not evaluated. Three of the treated flower heads were detached just below the ovary of the flower at 48 h after feeding started. The petal parts were crushed in liquid nitrogen and stored −80 °C. [^2H_n]-**2/2** and [^2H_n]-**3/3** were extracted by pentane and ethyl acetate, respectively. The ratio of [^2H_n]-**2/2** and [^2H_n]-**3/3** in the tissues were estimated from the GC-SIM data.

In May, 2003, [$^2H_8$]-**1** (17.3 mM, 1.5 ml) was fed to five flowers at stage 3 in intact *R.* 'Hoh-Jun' plants as described above. The flowers were detached at 6, 12, 24, 48, and 72 h after feeding started and were treated as described above. Changes in the ratio of [$^2H_8$]-**2**/[$^2H_7$]-**2** and [$^2H_8$]-**3**/[$^2H_7$]-**3** during the unfurling process were estimated from the GC-SIM data.

3.6. [1,1,2,2,2′,3′,4′,5′,6′-$^2H_9$]-2-Phenylethylamine (6) feeding in *R.* 'Hoh-Jun' flowers

In May, 2003, [1,1,2,2,2′,3′,4′,5′,6′-$^2H_9$]-**6** (23 mM solution, pH 6.8 as HCl salt, 1500 μl) was fed to five immature flowers at stage 3 for 96 h until the full bloom stage (stage 7) of *R.* 'Hoh-Jun' by the method just described above. The flowers were detached at 96 h after feeding started and were treated as described in Section 3.3.

3.7. [1,2,2′,3′,4′,5′,6′-$^2H_7$]-2-Phenylacetaldoxime (7) feeding in *R.* 'Hoh-Jun' flowers

In June, 2003, 1 μl of [1,2,2′,3′,4′,5′,6′-$^2H_7$]-**7** (14 mM of DMSO solution) was injected to the top of the ovary, just above the ovules of three immature flowers at stage 3. The flowers were detached at 24 h after injection and treated as described in Section 3.3.

3.8. Extraction of the volatile compounds and glycoconjugates

A portion (equivalent to one flower head) of each type of frozen flower petal was extracted twice with pentane (20 ml each) and then twice with EtOAc (20 ml each) in a microwave oven according to the method of Oka et al.[11] Ethyl octanoate (20 μg) and phenyl β-D-glucopyranoside (20 μg) were used as internal standards in the GC, GC-MS and GC-SIM analyses. The pentane extract was concentrated and directly analyzed by GC-MS and GC-SIM revealing the presence of **2** and [^2H_n]-**2**. The EtOAc extract was evaporated in vacuo and the resulting residue was re-dissolved in a citrate buffer (10 mM, pH 6.0) and hydrolyzed by a mixture of β-glucosidase (2500 units) and naringinase (3000 units) yielding the volatile compounds. After extraction with an azeotropic mixture (bp 38 °C) of pentane–CH_2Cl_2 (2:1),[12] the resulting extract was analyzed by GC-MS and GC-SIM to evaluate the amount of **2** and [^2H_n]-**2** as an aglycone part of **3** and [^2H_n]-**3**, respectively. To quantify **3** in the flower tissues, the ethyl acetate extract was directly analyzed for pertrifluoroacetates (TFA) derivatives by GC.

3.9. GC analyses

Ethyl acetate extract (from 100 to 500 mg of fresh flower petals) was concentrated and analyzed by GC after conversion into TFA-derivatives by treatment with *N*-methyl-bis(trifluoroacetamide-pyridine. A HITACHI G-3000 gas chromatograph was used for the analyses. A TC-1 column (df=0.25 mm), dimensions 0.25 mm i.d.×30 m, was used; the column temperature was raised from 150 to 280 °C (increment 2 °C/min); the injection temperature was 230 °C. For identification and quantitative analysis, **3** was analyzed as its TFA-derivative, and 0.1 μl of the reaction mixture was injected onto the GC column. Identification and quantification were carried out based on the peak area and the relative retention time (t'_R=2.957 for tetra *O*-TFA-**3**) relative to phenyl β-D-glucopyranoside-tetra-*O*-TFA, which was used as an internal standard (t_R=11.32 min).

3.10. GC-MS and GC-SIM analyses

The GC-MS analysis was conducted with a SHIMADZU QP505A gas chromatograph-mass spectrometer equipped with a SHIMADZU GC-17A. The column was a 30 m TC-WAX type with 0.25 mm i.d.×30 m; the column temperature was elevated from 100 to 170 °C (2 °C/min); the injector temperature was 250 °C; the ionizing voltage was 70 eV; the scanning speed was 0.5 scan/s with the range of *m/z* 40–250. 1 μl of each concentrate of solvent extract from petal tissues and of eluate from a TENAX columns was injected to the GC-MS. The identification of **2** and [^2H_n]-**2** was established by comparing their MS spectra with authentic samples as previously described by Watanabe et al.[18] Quantitative analyses of **2** and [^2H_n]-**2** were carried out from the SIM traces at *m/z* 130 [M^+] of [$^2H_8$]-**2**, *m/z* 129 [M^+] of [$^2H_7$]-**2**, *m/z* 128 [M^+] of [$^2H_6$]-**2**, *m/z* 98 [$C_7D_7^+$], *m/z* 97 [$C_7D_6H^+$], *m/z* 96 [$C_7D_5H_2^+$] and at *m/z* 122 [M^+] and *m/z* 91 [$C_7H_7^+$] for **2**. GC-SIM conditions were the same as mentioned above. Authentic [1,1,2,2′,3′,4′,5′,6′-$^2H_8$]-**2** (MW 130) and **2** were detected at t_R=18.23 and 18.48 min, respectively.

3.11. Estimation of β-glucosidase activity in the petal tissues during unfurling process of *R. damascena* Mill

2 ml of citrate buffer (50 mM, pH 6.0, containing 5 mM EDTA 2 Na, 2 mM dithiothreitol, 10 mM ascorbic acid, and 1% Triton X-100) was added to 0.1 g of liquid nitrogen powder (prepared from flower petals at the onset of unfurling) and stirred for 30 min at 4 °C, and was then centrifuged at 2000*g* for 10 min at 4 °C. The supernatant was passed through a membrane filter (0.45 μm) to give a crude enzyme solution. The β-glucosidase activity of the crude enzyme solution was evaluated as follows: (1) 50 mM of **3**, 100 μl in citrate buffer, plus crude enzyme, 200 μl; (2) citrate buffer, 100 μl, plus crude enzyme, 200 μl; (3) 50 mM of **3**, 100 μl in the citrate buffer plus citrate buffer, 200 μl. The three mixtures were incubated for 360 min at 37 °C, and the **2** released from **3** was extracted 5 times with pentane–CH_2Cl_2 (2:1) in the presence of ethyl decanoate (10 μg). The combined extract was concentrated and analyzed by GC-MS. The conditions were the same as described in Section 3.10. The activity was expressed as the amount of **2** (μmol) released from **3** in the initial 60 min of the incubation period. The inhibitory effect of **8** (6.0×10^{-9}, 1.0×10^{-8}, 6.0×10^{-8}, 1.0×10^{-7}, and 6.0×10^{-7} mol) toward the crude enzymes prepared from flower petals (0.1, 0.2, and 0.4 g fresh weight of the petals) at stage 6 was examined as described above. The hydrolysis of **3** was inhibited by 95% at a dose of 6.0×10^{-7} mol of **8**.

Acknowledgements

This work was supported in part by a grant-in-aid to N. W. for scientific research on priority areas (A)(2) from the Ministry of Education, Science, Sports and Culture of Japan, and by grant-aid to N.W. for the development of innovative plants and animals using transformation and Cloning from the Ministry of Forestry Fisheries and Agricultural Sciences of Japan. We also express our many thanks to Prof. Y. Ebizuka of the University of Tokyo for his informative discussions on the biogenesis of floral scent compounds.

References and notes

1. Knudsen, J. T.; Tollsten, L.; Bergström, L. G. *Phytochemistry* **1993**, *33*, 253–280.
2. Schiestl, F. P.; Ayasse, M.; Paulus, H. F.; Erdmann, D.; Francke, W. *J. Chem. Ecol.* **1997**, *23*, 2881–2895.
3. Borg-Karlson, A. K.; Valterova, I.; Nilsson, L. A. *Phytochemistry* **1994**, *46*, 1169–1172.
4. Ervik, F.; Tollsten, L.; Knudsen, J. T. *Plant Syst. Evol.* **1999**, *217*, 279–297.
5. Odell, E.; Raguso, R. A.; Jones, K. N. *Am. Midl. Nat.* **1999**, *142*, 257–265.
6. Jurgens, A.; Webber, A. C.; Gottsberger, G. *Phytochemistry* **2000**, *55*, 551–558.
7. Miyake, T.; Yamaoka, R.; Yahara, T. *J Plant Res.* **1998**, *111*, 199–205.
8. Omura, H.; Honda, K.; Hayashi, N. *J. Chem. Ecol.* **2000**, *26*, 655–666.

9. Francis, M. O.; Banthorpe, D. V.; Le Patourel, G. N. J. *Nature* **1970**, *228*, 1005–1006.
10. Francis, M. O. J.; O'Connell, M. *Phytochemistry* **1969**, *8*, 1705–1708.
11. Banthorpe, D. V.; Le Patourel, G. N. J.; Francis, M. J. O. *Biochem. J.* **1972**, *130*, 1045–1054.
12. Akermann, I. E.; Banthorpe, D. V.; Fordham, W. D.; Kinder, J. P.; Poots, I. *J. Plant Physiol.* **1989**, *134*, 567–572.
13. Loughrin, J. H.; Hamilton-Kemp, T. R.; Andersen, R. A.; Hildebrand, D. F. *Physiol. Plant* **1991**, *83*, 492–496.
14. Oka, N.; Ohishi, H.; Hatano, T.; Hornberger, M.; Sakata, K.; Watanabe, N. *Z. Naturforsch.* **1999**, *54c*, 889–895.
15. Reuveni, M.; Sagi, Z.; Evnor, D.; Hetzroni, A. *Plant Sci.* **1999**, *147*, 19–24.
16. Loughrin, J. H.; Hamilton-Kemp, T. R.; Burton, H. R.; Andersen, R. A.; Hildebrand, D. F. *Phytochemistry* **1992**, *31*, 1537–1540.
17. Jakobsen, H. B.; Christensen, L. P. *Plant Cell Env.* **2002**, *25*, 773–781.
18. Watanabe, S.; Hayashi, K.; Yagi, K.; Asai, T.; MacTavish, H.; Picone, J.; Turnbull, C.; Watanabe, N. *Biosci. Biotechnol. Biochem.* **2002**, *66*, 943–947.
19. Guo, W.; Hiratake, J.; Ogawa, K.; Yamamoto, M.; Ma, S. J.; Sakata, K. *Bioorg. Med. Chem. Lett.* **2001**, *11*, 467–470.
20. Inoue, K.; Hiratake, J.; Mizutani, M.; Takada, M.; Yamamoto, M.; Sakata, K. *Carbohydr. Res.* **2003**, *338*, 1477–1490.
21. Picone, M. J.; Clery, R. A.; Watanabe, N.; MacTavish, H. S.; Turnball, C. G. N. *Planta*, in press.
22. Albertazzi, E.; Cardillo, R.; Servi, S.; Zucchi, G. *Biotech. Lett.* **1994**, *16*, 491–496.
23. Robins, R. J.; Woolley, J. G.; Ansarin, M.; Eagles, J.; Goodfellow, B. J. *Planta* **1994**, *194*, 86–94.
24. Dickinson, J.; Salgado, L. E.; Hewlins, J. E. *J. Biol. Chem.* **2003**, *278*, 8028–8034.
25. Walsch, C. *Enzymatic Reaction Mechanisms*; W.H. Freeman and Co: New York, 1978; Chapter 14, pp 451–454.
26. Hazen, S.; d'Avignon, A.; Anderson, M. M.; Hsu, F. F.; Heinecke, J. W. *J. Biol. Chem.* **1998**, *273*, 4997–5005.
27. Saijo, R. *Jpn. Agric. Res. Q.* **1973**, *7*, 202–207.
28. Wittstock, U.; Halkier, B. A. *J. Biol. Chem.* **2000**, *275*, 14659–14666.
29. Kaiser, R. *J. Ess. Oil Res.* **1991**, *3*, 129–146.
30. Campos, P. J.; Garcia, B.; Rodriguez, M. A. *Tetrahedron Lett.* **2000**, *41*, 979–982.
31. Sera, A.; Yamauchi, H.; Yamada, H.; Itoh, K. *Synlett* **1990**, 477–478.

Available online at www.sciencedirect.com
SCIENCE DIRECT®
Tetrahedron 60 (2004) 7015–7023
Tetrahedron

New phlegmarane-type, cernuane-type, and quinolizidine alkaloids from two species of *Lycopodium*

Hiroshi Morita,[a] Yusuke Hirasawa,[a] Takakazu Shinzato[b] and Jun'ichi Kobayashi[a,*]

[a]*Graduate School of Pharmaceutical Sciences, Hokkaido University, Sapporo 060-0812, Japan*
[b]*Faculty of Agriculture, University of the Ryukyus, Okinawa 905-1427, Japan*

Received 18 August 2003; revised 10 September 2003; accepted 10 September 2003

Available online 2 July 2004

Abstract—Two new phlegmarane-type alkaloids, cermizines A (**1**) and B (**2**), three new quinolizidine alkaloids, cermizine C (**3**) and senepodines G (**4**) and H (**5**), and a new $C_{16}N_2$ type alkaloid consisting of a quinolizidine and a piperidine ring, cermizine D (**6**), as well as two new cernuane-type alkaloids, cernuine *N*-oxide (**7**) and lycocernuine *N*-oxide (**8**), have been isolated together with cernuine (**9**) and lycocernuine (**10**) from the club moss *Lycopodium cernuum* and *L. chinense*. The relative stereochemistry of **1**–**4** and **6**, and the absolute stereochemistry of **5**, **7**, and **8** were elucidated by combination of NOESY correlations, modified Mosher's method, chemical transformations, and computational methods. Cermizine D (**6**) might be a biosynthetic intermediate of cernuane-type alkaloids such as **7**–**10**.

1. Introduction

Plants of *Lycopodium* species produce a number of structurally diverse alkaloids, which often possess unusual skeletons, and many of them continue to be of interest from biogenetic[1,2] and biological[3] points of view as well as challenging targets for total synthesis.[4] For example, huperzines A and B, potent reversible inhibitors of acetylcholinesterase, have been studied well so far.[3] Recently, we have isolated serratezomine A[5] with a seco-serratinine-type skeleton from *Lycopodium serratum* var. *serratum*, complanadine A[6] with a lycodine-dimeric skeleton and lyconadin A[7] from *L. complanatum*, and senepodines A–E,[8,9] lyconesidines A–C,[10] and himeradine A[11] from *L. chinense*. Biomimetic transformation from serratinine into serratezomine A through a modified Polonovski reaction has also been reported.[12] Our interest has been focused on isolation of structurally interesting alkaloids and biosynthetic intermediates to clarify the biogenetic pathway. Investigation on extracts of *Lycopodium cernuum* and *L. chinense* (Lycopodiaceae) resulted in the isolation of eight new alkaloids, cermizines A–C (**1**–**3**) and D (**6**), senepodines G (**4**) and H (**5**), cernuine *N*-oxide (**7**), and lycocernuine *N*-oxide (**8**), together with known related alkaloids, cernuine (**9**)[13] and lycocernuine (**10**).[13] This paper describes the isolation and structure elucidation of **1**–**8**.

1.1. Isolation and structure elucidation of 1–8

The club moss of *L. cernuum* was extracted with MeOH, and the extract was partitioned between EtOAc and 3% tartaric acid. Water-soluble materials, which were adjusted at pH 10 with satd Na_2CO_3, were extracted with $CHCl_3$ and then BuOH. $CHCl_3$-soluble materials were subjected to an amino silica gel column (hexane/EtOAc, 1:0→0:1, and then

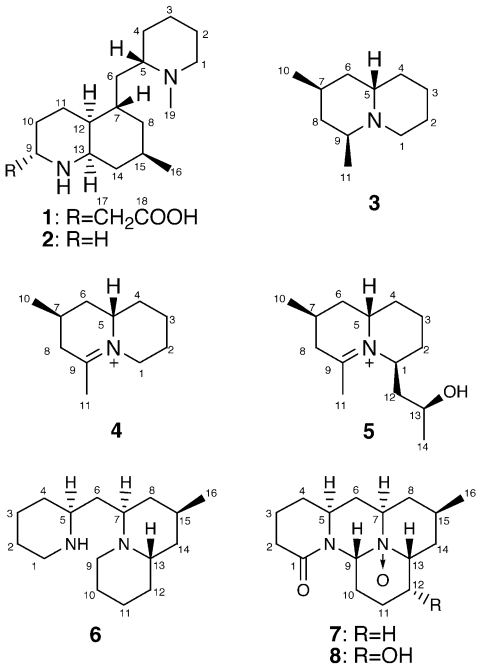

Keywords: Alkaloids; Phlegmarane; Cernuane; Quinolizidine.
* Corresponding author. Tel.: +81-11-706-3239; fax: +81-11-706-4985; e-mail address: jkobay@pharm.hokudai.ac.jp

0040–4020/$ - see front matter © 2004 Elsevier Ltd. All rights reserved.
doi:10.1016/j.tet.2003.09.106

Table 1. ^{1}H NMR data [δ_H (J, Hz)] of cermizines A (**1**) and B (**2**) in CD_3OD at 300 K

	1			**2**		
	^{1}H	^{13}C	HMBC	^{1}H	^{13}C	HMBC
1a	2.29(1H, ddd, 11.7, 11.7, 3.9)	57.6	2, 3b, 19	2.17(1H, ddd, 11.1, 11.1, 3.6)	57.9	19
1b	2.91(1H, ddd, 11.7, 4.0, 4.0)			2.84(1H, brd, 11.1)		
2a	1.61(1H, m)	25.8	1, 4b	1.41(1H, m)	26.7	1b
2b	1.61(1H, m)			1.60(1H, m)		
3a	1.34(1H, m)	24.6	1b, 4a	1.32(1H, m)	25.0	1
3b	1.74(1H, m)			1.73(1H, m)		
4a	1.27(1H, m)	31.4	6b	1.24(1H, m)	32.0	
4b	1.80(1H, m)			1.78(1H, m)		
5	2.08(1H, ddd, 9.2, 9.2, 3.7)	63.7	1b, 3b, 4a, 6, 19	1.92(1H, m)	64.0	1b, 4a, 6, 19
6a	1.24(1H, m)	36.4	4a, 5, 8a	1.19(1H, m)	37.0	8a
6b	1.99(1H, ddd, 13.6, 9.6, 3.7)			1.97(1H, m)		
7	1.69(1H, m)	37.6	5, 6b	1.56(1H, m)	38.6	6
8a	1.24(1H, m)	33.2	6b, 14a, 16	1.18(1H, m)	33.9	14a, 16
8b	1.40(1H, brd, 14.1)			1.32(1H, m)		
9a	3.44(1H, ddd, 8.6, 8.3, 4.3)	49.6	10, 11	2.67(1H, brd, 12.6)	40.5	
9b				2.78(1H, ddd, 12.6, 12.6, 2.9)		
10	1.51(1H, m)	30.6	7b, 11b	1.52(1H, m)	27.7	9
	1.88(1H, m)			1.66(1H, m)		
11	1.51(1H, m)	25.2		1.38(1H, m)	26.3	9a
	1.89(1H, m)			1.76(1H, m)		
12	1.77(1H, m)	39.7	8b, 10b, 14a	1.61(1H, m)	42.1	8b, 11a
13	3.62(1H, ddd, 12.2, 4.8, 4.8)	52.8	9, 11, 12, 14	3.09(1H, ddd, 12.1, 4.5, 4.5)	51.7	9a, 11a, 14b
14	1.65(1H, m)	32.9	8, 16	1.41(1H, m)	34.8	8b, 16
	1.69(1H, m)			1.61(1H, m)		
15	1.72(1H, m)	27.6	8, 14, 16	1.63(1H, m)	28.1	16
16	0.98(3H, d, 6.3)	22.6	14a	0.94(3H, d, 6.2)	23.0	
17	2.37(1H, dd, 16.2, 8.6)	41.2	10a			
	2.42(1H, dd, 16.2, 4.3)					
18		178.2	17			
19	2.33(3H, s)	42.5	1a	2.26(3H, s)	43.1	

$CHCl_3$/MeOH, 1:0→0:1), in which a fraction eluted with MeOH was purified by a silica gel column ($CHCl_3$→MeOH) to afford cermizines B (**2**, 0.00005%), C (**3**, 0.00008%), and D (**6**, 0.0002%) together with cernuine (**9**, 0.01%)[13] and lycocernuine (**10**, 0.004%).[13] BuOH-soluble materials were subjected to an ODS column (H_2O→MeOH) followed by an amino silica gel column ($CHCl_3$/MeOH, 15:1) and then a silica gel column ($CHCl_3$/MeOH, 10:1→0:1) to give cermizine A (**1**, 0.0002%), cernuine *N*-oxide (**7**, 0.002%), and lycocernuine *N*-oxide (**8**, 0.003%).

$CHCl_3$-soluble materials[9–11] prepared from the club moss of *L. chinense* were subjected to an amino silica gel column (hexane/EtOAc, 1:0→0:1), in which a fraction eluted with hexane/EtOAc (3:2) was purified by a silica gel column ($CHCl_3$/MeOH→$CHCl_3$/MeOH/TFA) and then C_{18} HPLC to afford senepodines G (**4**, 0.00005%) and H (**5**, 0.00003%) together with senepodine A–E,[9] lyconesidines A–C,[10] lycodoline,[14] and lucidine B.[15]

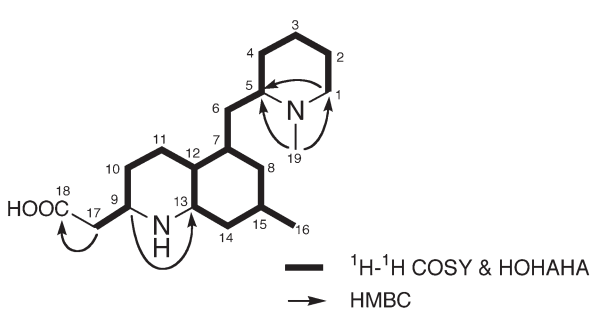

Figure 1. Selected 2D NMR correlations for cermizine A (**1**).

Cermizine A (**1**) showed the pseudomolecular ion peak at m/z 323 $(M+H)^+$ in the FABMS, and the molecular formula, $C_{19}H_{34}N_2O_2$, was established by HRFABMS [m/z 323.2683, $(M+H)^+$, Δ −1.5 mmu]. IR absorptions implied the presence of carboxylate (1580 cm^{-1}) functionality. ^{1}H and ^{13}C NMR data (Table 1) revealed nineteen carbon signals due to one sp^2 quaternary carbon, six sp^3 methines, ten sp^3 methylenes, and two methyl groups. Among them, three methines (δ_C 63.7; δ_H 2.08, δ_C 49.6; δ_H 3.44, and δ_C 52.8; δ_H 3.62), one methylene (δ_C 57.6; δ_H 2.29 and 2.91), and one methyl (δ_C 42.5; δ_H 2.33) were ascribed to those bearing a nitrogen. Since one out of four elements of unsaturation was accounted for, **1** was inferred to possess three rings. A partial structure (C-1–C-17) was deduced from detailed analyses of 2D NMR data (^{1}H–^{1}H COSY and HOHAHA) of **1** (Fig. 1). Connections among the partial structure, one isolated methyl (C-19) which was attached to a nitrogen, and one carbonyl carbon (δ_C 178.2, C-18) were implied by HMBC cross-peaks for H_3-19 to C-1 and C-5, and H_2-17 to C-18, respectively. The HMBC correlation of H-9 to C-13 (δ_C 52.8) through a nitrogen revealed that the nitrogen was attached to C-9 and C-13. HMBC correlations listed in Table 1 verified compound **1** to have phlegmarane-type skeleton consisting of a decahydroquinoline ring (C-7–C-15 and N-9) with a methyl group (C-16) at C-15 and a carboxymethyl group (C-17 and C-18) at C-9 and a piperidine ring (C-1–C-5 and N-1) with an *N*-methyl group (C-19) through a methylene bridge (C-6). The relative stereochemistry of **1** was elucidated from NOESY correlations as shown in computer-generated 3D drawing (Fig. 2). The *cis* junction of the decahydroquinoline ring with a chair-form and the presence of an α-oriented C_2 unit at C-9

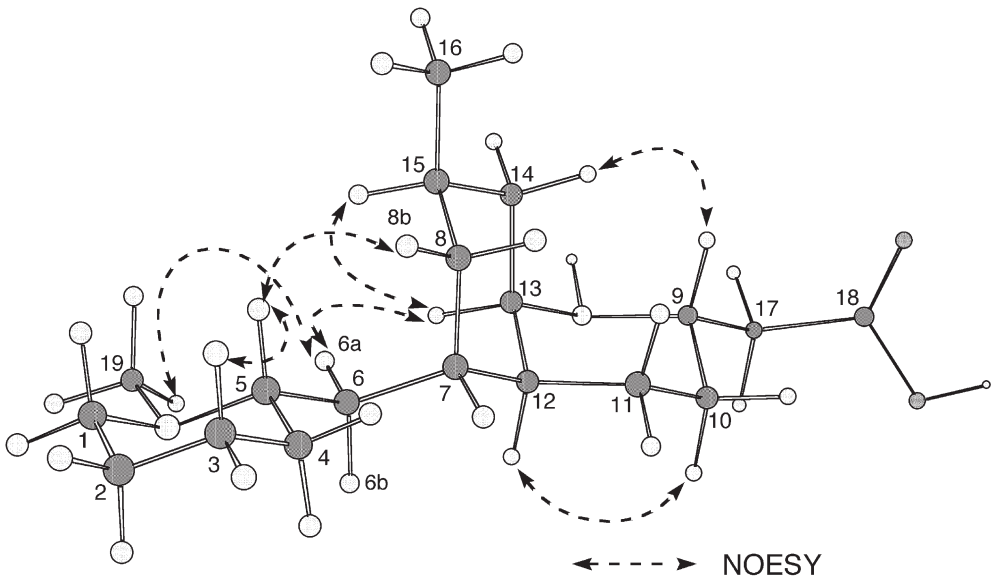

Figure 2. Selected NOESY correlations and relative stereochemistry for cermizine A (**1**).

were elucidated by the NOESY correlation of H-9/H14a, although known phlegmarane-type alkaloids[16] possess a *trans* junction for that ring. In addition, NOESY correlations of H-6a/H-13 and H-5/H-8b and ^3J coupling constants ($J_{5/6b}$=9.6 Hz, $J_{6b/7}$=3.7 Hz) indicated that the two heterocyclic ring systems did not rotate freely. Thus, the relative stereochemistry of cermizine A (**1**) was assigned as shown in Figure 2.

HRFABMS data [*m/z* 265.3108, $(M+H)^+$, Δ −0.5 mmu] of cermizine B (**2**) established the molecular formula to be $C_{17}H_{32}N_2$, which was smaller than that of cermizine A (**1**) by a $C_2H_2O_2$ unit. ^1H and ^{13}C NMR data (Tables 1) of **2** were analogous to those of **1**, although ^1H and ^{13}C signals of a C_2 unit (δ_H 2.37 and 2.42, δ_C 41.2 and 178.2) at C-9 observed for **1** were absent for **2**. Cermizine B (**2**) was elucidated to be a decarboxymethyl form at C-9 of **1** by 2D NMR (^1H–^1H COSY, HOHAHA, HMQC, and HMBC) data. The relative stereochemistry of **2** was deduced from the same NOESY correlations as those of **1**.

Cermizine C (**3**) was revealed to have the molecular formula, $C_{11}H_{21}N$, by HRESIMS [*m/z* 168.1745 $(M+H)^+$, Δ −0.7 mmu]. ^1H and ^{13}C NMR data (Table 2) for **3**

Table 2. ^1H NMR data [δ_H (*J*, Hz)] of cermizines C (**3**) and D (**6**) in CD_3OD at 300 K

	3			**6**		
	^1H	^{13}C	HMBC	^1H	^{13}C	HMBC
1a	3.08(1H, ddd, 13.7, 13.5, 2.7)	49.9		3.05(1H, ddd, 12.2, 11.8, 2.3)	46.0	3b
1b	3.65(1H, brd, 13.7)			3.42(1H, brd, 12.2)		
2a	1.69(1H, m)	18.4	3	1.69(1H, m)	23.2	1
2b	1.79(1H, m)			1.93(1H, m)		
3a	1.65(1H, m)	23.8	1b	1.70(1H, m)	23.1	1
3b	1.94(1H, m)			1.91(1H, m)		
4a	1.62(1H, m)	24.6	6a	1.57(1H, m)	31.0	3b
4b	2.17(1H, brq, 13.3)			2.01(1H, m)		
5	3.60(1H, brd, 13.2)	61.4	1b, 4b, 6a	3.30(1H, m)	54.2	1, 3b, 4a, 6b
6a	1.56(1H, ddd, 14.1, 14.1, 5.1)	38.4	5, 8a, 10	1.66(1H, m)	36.3	
6b	1.79(1H, m)			2.32(1H, m)		
7	1.96(1H, m)	25.4	5, 6a, 8a, 10	3.96(1H, brt, 10.7)	51.5	6, 8a, 9a
8a	1.21(1H, q, 13.2)	41.8	6, 10, 11	1.17(1H, q, 12.8)	38.9	6b, 14b, 16
8b	1.95(1H, m)			2.22(1H, brd, 13.4)		
9a	3.82(1H, m)	51.1	1a, 5, 8a, 11	3.14(1H, ddd, 12.8, 12.4, 3.2)	50.0	6b
9b				3.71(1H, brd, 12.8)		
10a	0.95(3H, d, 6.2)	21.6		1.73(1H, m)	18.6	9a, 11
10b				1.82(1H, m)		
11a	1.31(3H, d, 6.3)	17.6		1.65(1H, m)	23.7	9b
11b				1.93(1H, m)		
12a				1.69(1H, m)	24.7	
12b				2.17(1H, brq, 13.0)		
13				3.68(1H, brd, 13.0)	62.4	9b, 11b, 14a
14a				1.60(1H, m)	38.0	8b, 16
14b				1.80(1H, m)		
15				1.97(1H, m)	24.9	8, 14, 16
16				0.98(3H, d, 6.3)	21.6	

Table 3. ^{1}H [δ_H (J, Hz)] and ^{13}C (δ_C) NMR data and HMBC correlations of senepodines G (**4**) and H (**5**) in CD_3OD at 300 K

	4			**5**		
	^{1}H	^{13}C	HMBC	^{1}H	^{13}C	HMBC
1a	3.52(1H, brt, 12.9)	56.0	3b	4.90(1H, ddd, 10.5, 4.9, 4.4)	61.3	3a, 12b
1b	4.50(1H, brd, 12.9)					
2a	1.75(1H, m)	27.5	1a, 4b	1.89(1H, m)	31.4	4a, 12b
2b	2.01(1H, m)			1.98(1H, m)		
3a	1.80(1H, m)	24.7	1b, 4b	1.75(1H, m)	19.9	4b
3b	1.94(1H, m)			2.01(1H, m)		
4a	1.85(1H, m)	34.7	2, 6b	1.89(1H, m)	34.8	2a, 6
4b	1.91(1H, m)			1.89(1H, m)		
5	3.96(1H, m)	64.8	1b, 3b, 4a, 6a	4.17(1H, m)	58.0	1, 3a, 6
6a	1.76(1H, m)	35.5	10	1.72(1H, m)	35.5	10
6b	1.82(1H, m)			1.84(1H, brd, 14.1)		
7	2.02(1H, m)	21.9	6, 10	2.02(1H, m)	21.2	6a, 10
8a	2.45(1H, m)	43.7	6, 10, 11	2.52(1H, dd, 20.8, 9.9)	43.7	6b, 10, 11
8b	2.98(1H, dd, 19.9, 3.8)			3.04(1H, dd, 20.8, 2.9)		
9		189.1	1, 5, 11		187.0	1, 5, 8, 11
10	1.04(3H, d, 6.7)	20.4		1.04(3H, d, 6.6)	20.3	6b
11	2.44(3H, s)	23.6		2.58(3H, s)	24.3	
12a				1.65(1H, ddd, 14.9, 10.6, 4.4)	39.7	14
12b				2.39(1H, ddd, 14.9, 10.5, 2.6)		
13				3.54(1H, ddq, 10.6, 2.6, 6.1)	64.4	12, 14
14				1.24(3H, d, 6.1)	24.3	

suggested the presence of three sp^3 methines, six sp^3 methylenes, and two methyl groups. Among them, two methines (δ_c 61.4 and 51.1) and one methylene (δ_c 49.9) were ascribed to those bearing a nitrogen. The $^{1}H-^{1}H$ COSY and HOHAHA spectra revealed the presence of a quinolizidine ring (C-1–C-9) with two methyl groups (C-10 and C-11) at C-7 and C-9, respectively. Connections among C-1 (δ_C 49.9), C-5 (δ_C 61.4), and C-9 (δ_C 51.1) through a nitrogen were suggested by HMBC correlations for H-1b of C-5, H-1a of C-9, and H-5 of C-9. Thus, cermizine C (**3**) was elucidated to be 1,3-dimethyl quinolizidine. The relative stereochemistry was deduced from cross-peaks observed in the phase sensitive NOESY spectrum as shown in computer-generated 3D drawing (Fig. 4). Chair conformations of the two six-membered rings in the *cis* quinolizidine moiety with two methyls at C-7 and C-9 equatorially oriented were suggested by NOESY correlations of H-1b/H-5 and H-3b, H-5/H-3b, H-9/H-2a and H-7, and H-4a/H-2a and H-7.

Senepodines G {**4**, $[\alpha]_D$ −35° (*c* 0.3, MeOH)} and H {**5**, $[\alpha]_D$ −35° (*c* 0.2, MeOH)} were revealed to have the molecular formula, $C_{11}H_{20}N$ and $C_{14}H_{26}NO$, respectively, by HRFABMS [**4**: *m/z* 166.1596 $(M)^+$, Δ 0.0 mmu; **5**: 224.2032 $(M)^+$, Δ +1.8 mmu]. IR absorptions implied the presence of an imine (1685 cm^{-1}) group for **4** and **5**, and a hydroxy (3380 cm^{-1}) group for **5**. ^{1}H and ^{13}C NMR data (Table 3) for **4** suggested the presence of two sp^3 methines, six sp^3 methylenes, two methyl, and one sp^2 quaternary carbon. Among them, one methine (δ_c 64.8) and one methylene (δ_c 56.0) were ascribed to those bearing a nitrogen. The $^{1}H-^{1}H$ COSY and HOHAHA spectra of **4** clearly revealed connectivities of C-1–C-8 and C-10 as shown in Figure 3. The presence of an iminium carbon (C-9) with a methyl group (C-11) was elucidated by HMBC correlations for H_3-11 to C-8 and C-9. Connections among C-1 (δ_C 56.0), C-5 (δ_C 64.8), and C-9 (δ_C 189.1) through a nitrogen were suggested by HMBC correlations for H_2-1 of C-5 and C-9 and H-5 of C-9. Thus, the gross senepodine G (**4**) was elucidated to be an imine form at C-9 and N-1 of **3**. The IR and NMR data (Fig. 3) revealed that **5** is an analog of **4**, having an additional 2-hydroxypropyl group (C-12–C-14) at C-1.

The relative stereochemistry of **4** and **5** was deduced from cross-peaks observed in the phase sensitive NOESY spectra as shown in computer-generated 3D drawing (Fig. 4). The chair conformation of a piperidine ring (N-1 and C-1–C-5) in **4** was suggested by NOESY correlations of H-1b/H-5 and H-3b, and H-2a/H-4a. In the rotation models for C-1–C-12

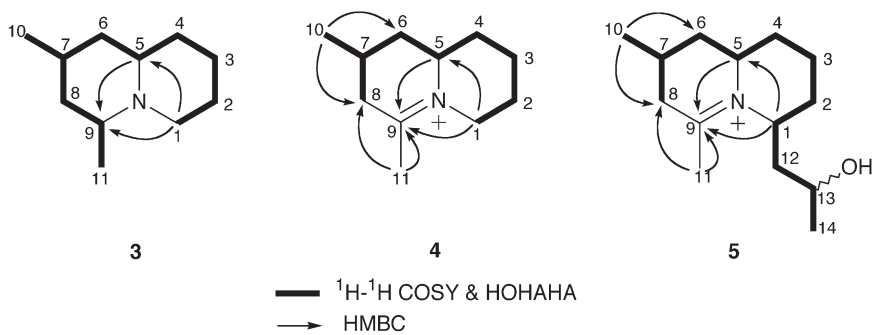

Figure 3. Selected 2D NMR correlations for cermizine C (**3**), and senepodines G (**4**) and H (**5**).

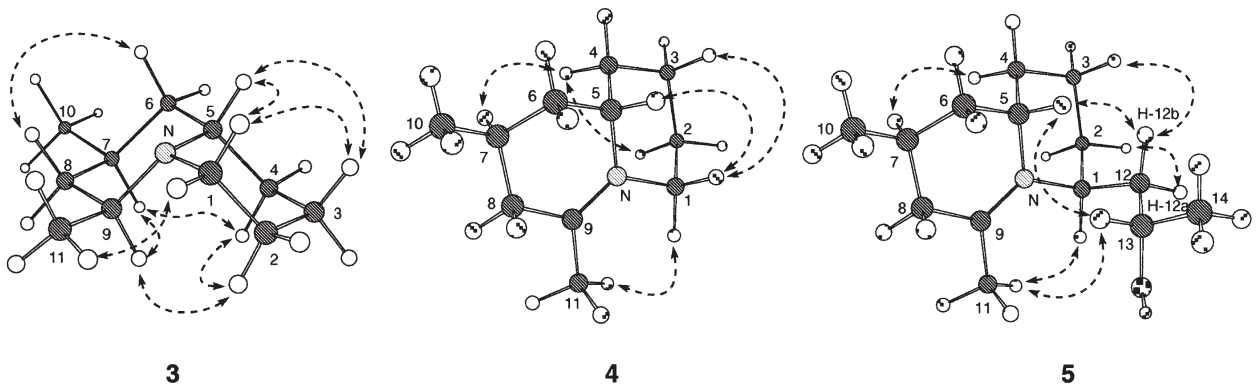

Figure 4. Selected NOESY correlations and stereochemistry for cermizine C (**3**), and senepodines G (**4**) and H (**5**).

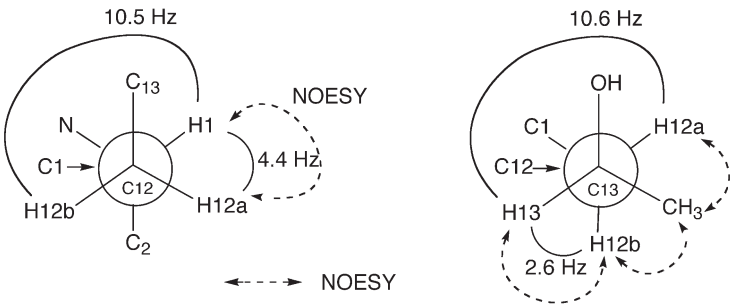

Figure 5. Rotation models for C-1–C-12 and C-12–C-13 of senepodine H (**5**).

and C-12–C-13 of **5**, the ^3J (H-1, H-12b) (10.5 Hz) and ^3J (H-12a, H-13) (10.6 Hz) were typical values for *anti* relationship, while the ^3J (H-1, H-12a) (4.4 Hz) and ^3J (H-12b, H-13) (2.6 Hz) were those for *gauche* relationship (Fig. 5). NOESY correlations of H-1/H-12a, H-12b/H-13, H-12b/H_3-14, and H-12a/H_3-14 also corroborated these rotation models. Inspection of these molecular models by Monte Carlo simulation[17] using MMFF force field[18] gave the same results.

To determine the absolute configuration at C-13, senepodine H (**5**) was treated with sodium borohydride and then converted into its (*S*)- and (*R*)-2-methoxy-2-trifluoromethylphenylacetic acid (MTPA) esters (**5a** and **5b**, respectively). $\Delta\delta$ values ($\delta_S-\delta_R$) of H-1, H-7, H-9, H_3-10, H_3-11, and H_2-12 showed positive values, while those of H-13 and H_3-14 were negative (Fig. 6), suggesting that C-13 possessed *S*-configuration. Thus, the absolute configuration of **5** was assigned as 1*S*,5*S*,7*S*, and 13*S*.

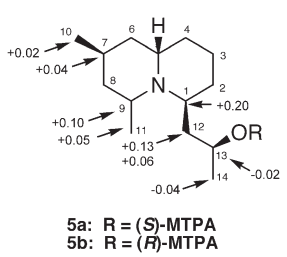

Figure 6. $\Delta\delta$ values [$\Delta\delta$ (in ppm)$=\delta_S-\delta_R$] obtained for (*S*)- and (*R*)-MTPA esters (**5a** and **5b**, respectively) of hydrosenepodine H.

^{1}H and ^{13}C NMR data of cermizine D {**6**, $[\alpha]_D$ −33° (*c* 0.6, MeOH)} were analogous to those of cermizine C (**3**), except for an additional piperidine unit (C-1–C-5) at C-6. 2D NMR data (Fig. 7) revealed the presence of a quinolizidine ring (C-7–C-8, C-9–C-15, and N-7) with a methyl group (C-16) at C-15 and a piperidine ring (C-1–C-5 and N-1) through a

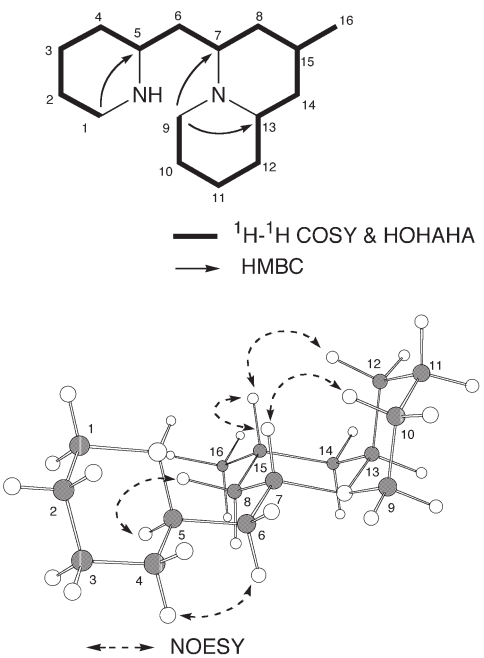

Figure 7. Selected 2D NMR correlations and relative stereochemistry for cermizine D (**6**).

Table 4. ^{1}H NMR data [δ_H (J, Hz)] of cernuine *N*-oxide (**7**), lycocernuine *N*-oxide (**8**), cernuine (**9**), and lycocernuine (**10**) in CD_3OD at 300 K

	7	8	9	10
2a	2.38 (1H, m)	2.38 (1H, m)	2.35 (1H, m)	2.35 (1H, m)
2b	2.45 (1H, m)	2.46 (1H, m)	2.36 (1H, m)	2.36 (1H, m)
3a	1.65 (1H, m)	1.69 (1H, m)	1.65 (1H, m)	1.65 (1H, m)
3b	1.90 (1H, m)	1.90 (1H, m)	1.82 (1H, m)	1.80 (1H, m)
4a	1.65 (1H, m)	1.62 (1H, m)	1.48 (1H, dddd, 11.2, 11.2, 11.2, 3.0)	1.50 (1H, m)
4b	2.03 (1H, m)	2.04 (1H, m)	2.02 (1H, m)	2.04 (1H, m)
5	3.78 (1H, m)	3.84 (1H, m)	3.64 (1H, m)	3.67 (1H, m)
6a	1.52 (1H, ddd, 13.7, 3.1, 3.1)	1.50 (1H, ddd, 13.7, 3.1, 3.1)	1.20 (1H, ddd, 12.7, 12.2, 11.8)	1.16 (1H, m)
6b	2.02 (1H, m)	1.95 (1H, m)	1.73 (1H, ddd, 12.7, 3.0, 2.9)	1.72 (1H, m)
7	4.03 (1H, dddd, 11.8, 11.8, 3.1, 3.0)	4.36 (1H, dddd, 11.8, 11.8, 3.1, 3.1)	3.24 (1H, dddd, 11.8, 11.7, 2.9, 2.8)	3.76 (1H, m)
8a	1.46 (1H, m)	1.43 (1H, brd, 13.7)	0.81 (1H, ddd, 12.1, 12.1, 11.7)	0.84 (1H, m)
8b	1.65 (1H, m)	1.69 (1H, m)	1.66 (1H, m)	1.70 (1H, m)
9	5.64 (1H, dd, 13.1, 3.6)	5.67 (1H, dd, 13.5, 3.2)	5.44 (1H, dd, 12.5, 2.6)	5.47 (1H, dd, 12.0, 2.3)
10a	1.72 (1H, m)	2.74 (1H, dddd, 13.9, 13.9, 13.5, 3.5)	1.19 (1H, m)	1.21 (1H, m)
10b	2.42 (1H, m)	1.60 (1H, m)	2.12 (1H, dddd, 12.8, 12.8, 12.5, 4.2)	2.42 (1H, m)
11a	1.77 (1H, m)	1.90 (1H, m)	1.66 (1H, m)	1.90 (1H, m)
11b	1.95 (1H, m)	1.99 (1H, m)	1.94 (1H, m)	2.39 (1H, m)
12a	1.74 (1H, m)	4.12 (1H, brs)	1.12 (1H, brd, 14.6)	3.78 (1H, m)
12b	2.22 (1H, dddd, 13.5, 13.5, 13.5, 3.1)		1.89 (1H, m)	
13	3.43 (1H, brd, 13.5)	3.29 (1H, brd, 5.9)	3.07 (1H, brd, 12.2)	2.97 (1H, brd, 6.6)
14a	1.46 (1H, m)	1.66 (1H, m)	1.40 (1H, ddd, 13.0, 12.9, 5.2)	1.40 (1H, m)
14b	2.32 (1H, ddd, 13.1, 13.1, 4.4)	2.29 (1H, ddd, 13.1, 13.1, 5.9)	1.58 (1H, brd, 13.0)	1.79 (1H, m)
15	1.92 (1H, m)	2.54 (1H, m)	1.78 (1H, m)	2.45 (1H, m)
16	0.93 (3H, d, 6.5)	0.90 (3H, d, 6.5)	0.89 (3H, d, 6.4)	0.88 (3H, d, 6.5)

methylene bridge (C-6). The relative stereochemistry was deduced from cross-peaks observed in the phase sensitive NOESY spectrum as shown in computer-generated 3D drawing (Fig. 7).

Compounds **7** {$[\alpha]_D$ −38° (*c* 0.2, MeOH)} and **8** {$[\alpha]_D$ −23° (*c* 1.0, MeOH)} were revealed to have the molecular formula, $C_{16}H_{26}N_2O_2$ and $C_{16}H_{26}N_2O_3$, respectively, by HRFABMS [**7**: *m/z* 279.2094 $(M+H)^+$, Δ +2.2 mmu; **8**: 295.2008 $(M+H)^+$, Δ −1.4 mmu]. IR absorptions implied the presence of an amide carbonyl (1680 and 1650 cm^{-1}, respectively) group for **7** and **8**, and a hydroxyl (3260 cm^{-1}) group for **8**. ^{1}H and ^{13}C NMR data (Tables 4 and 5, respectively) for **7** suggested the presence of five sp^3 methines, nine sp^3 methylenes, one methyl, and one sp^2 quaternary carbon. Among them, four methines (δ_c 50.9, 59.0, 82.0, and 75.9) were ascribed to those bearing a nitrogen. 2D NMR data of **7** clearly revealed the presence of a cernuane-type skeleton[13] consisting of a fused tetracyclic ring system containing two nitrogen atoms, with a methyl group at C-15. Detailed analyses of ^{13}C NMR data (Table 5) and comparison of ^{13}C chemical shifts of C-7, C-9, and C-13 (δ 59.0, 82.0, and 75.9, respectively) in **7** with those (δ 47.6, 68.7, and 59.2, respectively) of cernuine (**9**)[19] indicated the presence of an *N*-oxide functionality. Oxidation of cernuine (**9**) with hydrogen peroxide afforded the *N*-oxide derivative (**7**), whose spectral data and the $[\alpha]_D$ value were identical with those of compound **7**. Thus, **7** was concluded to be an *N*-oxide form of cernuine (**9**). Compound **8** was also elucidated to be the *N*-oxide derivative of lycocernuine (**10**) by detailed analyses of NMR data and comparison with those of lycocernuine (**10**).[19] Chemical transformation of lycocernuine (**10**) into compound **8** by oxidation with hydrogen peroxide led to the conclusion that **8** was an *N*-oxide form of lycocernuine (**10**).

Table 5. ^{13}C NMR data (δ_C) of cernuine *N*-oxide (**7**), lycocernuine *N*-oxide (**8**), cernuine (**9**), and lycocernuine (**10**) in CD_3OD at 300 K

	7	8	9	10
1	172.1	172.8	171.1	171.3
2	33.7	33.8	33.7	33.7
3	19.4	19.3	19.9	19.7
4	30.2	30.1	31.2	31.0
5	50.9	51.1	52.1	52.2
6	34.7	35.0	41.7	41.8
7	59.0	62.5	47.6	51.1
8	36.0	35.6	42.5	42.0
9	82.0	82.4	68.7	68.7
10	26.8	22.3	21.6	17.7
11	23.6	32.4	25.6	33.7
12	28.3	71.2	23.5	70.3
13	75.9	76.9	59.2	60.6
14	34.7	34.2	40.0	38.6
15	25.3	25.7	26.3	26.7
16	21.8	22.4	22.6	23.0

1.2. Plausible biogenesis of 1–8

Biogenetically, cermizines A (**1**) and B (**2**), a new type of phlegmarane alkaloids with a *cis* decahydroquinoline ring, may be generated from pelletierine through intermediates **A** and **B** (path a)[20] followed by coupling with Δ^1-piperideine, while cermizine C (**3**) and senepodine G (**4**) may be derived from the intermediate **A** (path b) (Scheme 1).[1c,2] On the other hand, senepodine H (**5**) might be generated from pelletierine through coupling with a C_6 unit derived from two moles of acetone dicarboxylic acid[2] (path c). Cernuane-type alkaloids such as **7**–**10** might be generated from cermizine C (**3**) through coupling with Δ^1-piperideine to form cermizine D (**6**) followed by coupling between N-1 and C-9.

1.3. Bioactivities of 1–8

Cermizines A (**1**), B (**2**) and D (**6**), senepodines G (**4**) and H

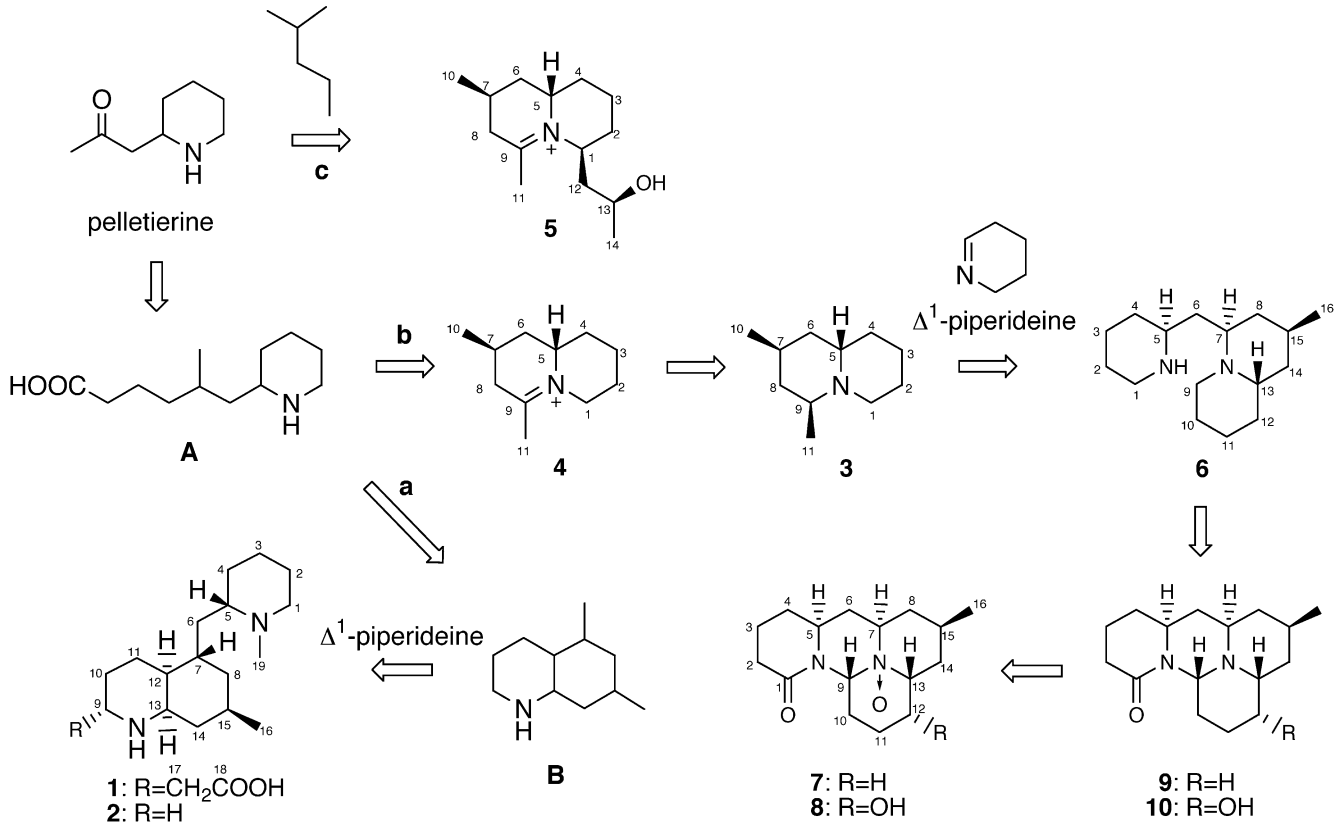

Scheme 1.

(**5**), cernuine *N*-oxide (**7**), and lycocernuine *N*-oxide (**8**) exhibited cytotoxicity against murine lymphoma L1210 cells (IC_{50} 4.9, 5.5, 7.5, 7.8, 8.2, 6.5, and 8.9 μg/ml, respectively) in vitro, while cermizine C (**3**) did not show cytotoxicity at 10 μg/ml. Cernuine *N*-oxide (**7**) and cernuine (**9**) inhibited acetylcholinesterase (from electric eel) at IC_{50} 330 and 220 μM, respectively,[21,22] whereas the other alkaloids did not show such activity (IC_{50}>1000 μM).

2. Experimental

2.1. General methods

^{1}H and 2D NMR spectra were recorded on a 600 MHz spectrometer at 300K, while ^{13}C NMR spectra were measured on a 150 MHz spectrometer. Each NMR sample of **1**–**10** was prepared by dissolving 1.0 mg in 30 μl of CD_3OD in 2.5 mm micro cells (Shigemi Co. Ltd) and chemical shifts were reported using residual CD_2HOD (δ_H 3.31) for ^{1}H NMR and CD_3OD (δ_C 49.0) for ^{13}C NMR as internal standards. Standard pulse sequences were employed for the 2D NMR experiments. COSY, HOHAHA, and NOESY spectra were measured with spectral widths of both dimensions of 4800Hz, and 32 scans with two dummy scans were accumulated into 1K data points for each of 256 t_1 increments. NOESY and HOHAHA spectra in the phase sensitive mode were measured with a mixing time of 800 and 30 ms, respectively. For HMQC spectra in the phase sensitive mode and HMBC spectra, a total of 256 increments of 1K data points were collected. For HMBC spectra with *Z*-axis PFG, a 50 ms delay time was used for long-range C–H coupling. Zero-filling to 1K for F_1 and multiplication with squared cosine-bell windows shifted in both dimensions were performed prior to 2D Fourier transformation. FABMS was measured by using glycerol as a matrix.

2.2. Material

The club moss *Lycopodium cernuum* was collected in Okinawa in 2001. The club moss *Lycopodium chinense* was collected at Kiyosato in Hokkaido in 2001. The voucher specimens have been deposited in the herbarium of Hokkaido University.

2.3. Extraction and isolation

The club moss (2.75 kg) of *L. cernuum* was extracted with MeOH (10 L×3). The MeOH extract (220 g) was partitioned between EtOAc and 3% tartaric acid. Water-soluble materials, after being adjusted at pH 10 with satd Na_2CO_3, were partitioned with $CHCl_3$ and then BuOH. $CHCl_3$ soluble materials (2.6 g) were subjected to an amino silica gel column (hexane/EtOAc, 1:0→0:1, and then $CHCl_3$/MeOH, 1:0→0:1). The fraction eluted with MeOH was separated by a silica gel column ($CHCl_3$→MeOH) to afford cermizines B (**2**, 1.4 mg, 0.00005%), C (**3**, 2.2 mg, 0.00008%), and D (**6**, 5.5 mg, 0.0002%) together with cernuine (**9**, 275 mg, 0.01%)[13] and lycocernuine (**10**, 110 mg, 0.004%).[13] BuOH soluble materials (6.1 g) were subjected to an ODS column (H_2O→MeOH) followed by an

amino silica gel column ($CHCl_3$/MeOH, 15:1), and then a silica gel column ($CHCl_3$/MeOH, 10:1→0:1) to give cermizine A (**1**, 5.5 mg, 0.0002%), cernuine *N*-oxide (**7**, 55 mg, 0.002%), and lycocernuine *N*-oxide (**8**, 83 mg, 0.003%).

The club moss (2 kg) of *L. chinense* was extracted with MeOH (10 L×3). The MeOH extract (146 g) was partitioned between EtOAc and 3% tartaric acid. Water-soluble materials, after being adjusted at pH 10 with satd Na_2CO_3, were partitioned with $CHCl_3$. $CHCl_3$ soluble materials (2.4 g) were subjected to an amino silica gel column (hexane/EtOAc, 1:0→0:1, and then $CHCl_3$/MeOH, 1:0→0:1). The fraction eluted with hexane/EtOAc (3:2) was separated by a silica gel column ($CHCl_3$/MeOH→ $CHCl_3$/MeOH/EtOAc) and then C_{18} HPLC (Mightysil RP-18 GP 250−20, 5 μm, Kanto Chemical Co., 10×250 mm; eluent, 14−35% CH_3CN/0.1% TFA; flow rate, 2 ml/min; UV detection at 205 nm) to afford senepodines G (**4**, 1.0 mg, 0.00005%) and H (**5**, 0.6 mg, 0.00003%) together with senepodine A (60 mg, 0.003%), lyconesidines A (40 mg, 0.002%), B (100 mg, 0.005%), and C (60 mg, 0.003%), lycodoline (20 mg, 0.001%), and lucidine B (20 mg, 0.001%).

2.3.1. Cermizine A (1). Colorless solid; $[\alpha]_D^{27}$ +3° (*c* 1.0, MeOH);[23] IR (neat) ν_{max} 2930, 1580, and 1390 cm^{-1}; ^1H and ^{13}C NMR data (Table 1); FABMS *m/z* 323 $(M+H)^+$; HRFABMS *m/z* 323.2683 (M+H; calcd for $C_{19}H_{35}N_2O_2$, 323.2698).

2.3.2. Cermizine B (2). Colorless solid; $[\alpha]_D^{27}$ −2° (*c* 0.6, MeOH);[23] IR (neat) ν_{max} 3370, 2930, and 1460 cm^{-1}; ^1H and ^{13}C NMR data (Table 1); FABMS *m/z* 265 $(M+H)^+$; HRFABMS *m/z* 265.2638 (M+H; calcd for $C_{17}H_{33}N_2$, 265.2644).

2.3.3. Cermizine C (3). Colorless solid; $[\alpha]_D^{25}$ +4° (*c* 0.8, MeOH)[23]; IR (neat) ν_{max} 2930, 1460, and 800 cm^{-1}; ^1H and ^{13}C NMR data (Table 1); ESIMS *m/z* 168 $(M+H)^+$; HRESIMS *m/z* 168.1745 (M+H; calcd for $C_{11}H_{22}N$, 168.1752).

2.3.4. Senepodine G (4). Colorless solid; $[\alpha]_D^{26}$ −35° (*c* 0.3, MeOH) (with TFA); IR (neat) ν_{max} 3516, 3390, 2930, 1685, 1195, and 1125 cm^{-1}; ^1H and ^{13}C NMR data (Table 1); FABMS *m/z* 166 $(M)^+$; HRFABMS *m/z* 166.1596 (M; calcd for $C_{11}H_{20}N$, 166.1596).

2.3.5. Senepodine H (5). Colorless solid; $[\alpha]_D^{27}$ −35° (*c* 0.2, MeOH) (with TFA); IR (neat) ν_{max} 3380, 2930, 1686, 1195, and 1125 cm^{-1}; ^1H and ^{13}C NMR data (Table 1); FABMS *m/z* 224 $(M)^+$; HRFABMS *m/z* 224.2032 (M; calcd for $C_{14}H_{26}NO$, 224.2014).

2.3.6. Cermizine D (6). Colorless solid; $[\alpha]_D^{25}$ −33° (*c* 0.6, MeOH); IR (neat) ν_{max} 3370, 2930, 1450, and 720 cm^{-1}; ^1H and ^{13}C NMR data (Table 1); FABMS *m/z* 251 $(M+H)^+$; HRFABMS *m/z* 251.2511 (M+H; calcd for $C_{16}H_{31}N_2$, 251.2487).

2.3.7. Cernuine *N*-oxide (7). Colorless solid; $[\alpha]_D^{27}$ −18° (*c* 1.0, MeOH); IR (neat) ν_{max} 3450, 3295, 2927, 1680, 1195, and 1128 cm^{-1}; ^1H and ^{13}C NMR data (Table 1); FABMS *m/z* 279 $(M+H)^+$; HRFABMS *m/z* 279.2094 (M+H; calcd for $C_{16}H_{27}N_2O_2$, 279.2072).

2.3.8. Lycocernuine *N*-oxide (8). Colorless solid; $[\alpha]_D^{22}$ −23° (*c* 1.0, MeOH); IR (neat) ν_{max} 3260, 2960, 1650, and 750 cm^{-1}; ^1H and ^{13}C NMR data (Table 1); FABMS *m/z* 295 $(M+H)^+$; HRFABMS *m/z* 295.2008 (M+H; calcd for $C_{16}H_{27}N_2O_3$, 295.2022).

2.4. (*S*)-MTPA ester (5a) of hydrosenepodine H

To a solution of **5** (0.05 mg) in methanol (50 μl) was added sodium borohydride (0.004 mg). The mixture was allowed to stand for 1 h. After addition of acetone (10 μl) and evaporation of solvent, to the residue in methylene chloride (50 μl) was added (*R*)-(−)-MTPACl (0.2 μl), *N*,*N*-dimethylaminopyridine (10 μg), and triethylamine (0.25 μl). The mixture was allowed to stand for 3 h. After addition of *N*,*N*-dimethylamino-1,3-propandiamine (2 μl) and evaporation of solvent, the residue was dissolved in $CHCl_3$ and washed with Na_2CO_3 aq. After evaporation of solvent, the (*S*)-MTPA ester (**5a**, 0.05 mg) was obtained. **5a**: colorless oil; ^1H NMR ($CDCl_3$) δ 0.97 (3H, d, 6.4, H-10), 1.43 (3H, d, 6.2, H-14), 1.48 (3H, d, 6.3, H-11), 1.84 (1H, m, H-7), 2.10 (1H, m, H-12a), 2.94 (1H, brd, 12.3, H-12b), 3.52 (1H, m, H-9), 3.66 (1H, m, H-1), 5.30 (1H, m, H-13). FABMS *m/z* 442 $(M+H)^+$; HRFABMS *m/z* 442.2572 (M+H; calcd for $C_{24}H_{35}NO_3F_3$, 442.2569).

2.5. (*R*)-MTPA ester (5b) of hydrosenepodine H

Senepodine H (**5**, 0.05 mg) was treated with sodium borohydride, followed by the (*S*)-(+)-MTPACl (0.2 μl) by the same procedure as described above to afford the (*R*)-MTPA ester (**5b**, 0.05 mg). **5b**: colorless oil; ^1H NMR ($CDCl_3$) δ 0.95 (3H, d, 6.4, H-10), 1.43 (3H, d, 6.3, H-11), 1.47 (3H, d, 6.1, H-14), 1.80 (1H, m, H-7), 1.97 (1H, m, H-12a), 2.88 (1H, brd, 14.5, H-12b), 3.42 (1H, m, H-9), 3.46 (1H, m, H-1), 5.32 (1H, m, H-13). FABMS *m/z* 442 $(M+H)^+$; HRFABMS *m/z* 442.2585 (M+H; calcd for $C_{24}H_{35}NO_3F_3$, 442.2569).

2.6. Computational methods

Conformational searching was carried out using Pseudo Monte Carlo simulation in Macromodel program for **5**. Three thousand Monte Carlo steps were performed, yielding 71 unique conformations in the energy region of 0−10 kcal/mol. Each conformer was finally minimized by molecular mechanics calculation of MMFF force field with solvation method. The lowest energy conformation was depicted in Figures 4 and 5.

2.7. Oxidation of cernuine (9) and lycocernuine (10)

30% H_2O_2 aq (60 μl) was added to a stirred solution of cernuine (**9**, 1 mg) in MeOH (0.5 ml) at room temperature. The mixture was stirred at room temperature for 1 day, and then concentrated to give white needles (1 mg). The residue was subjected to silica gel column chromatography ($CHCl_3$/MeOH, 10:1) to give the *N*-oxide derivative (0.8 mg) of **9**,

whose spectral data and $[\alpha]_D$ value were identical with those of **7**. Oxidation of lycocernuine (**10**) was carried out by the same procedure as described above to give the *N*-oxide of **10**, whose spectral data and $[\alpha]_D$ value were identical with those of **8**.

Acknowledgements

The authors thank Dr. Takakazu Shinzato, Faculty of Agriculture, University of the Ryukyus for the botanical identification of *L. cernuum*, Mr. N. Yoshida, Health Sciences University of Hokkaido for the botanical identification of *L. chinense*, and Mrs. S. Oka and Miss M. Kiuchi, Center for Instrumental Analysis, Hokkaido University, for measurements of FABMS. This work was partly supported by a Grant-in-Aid for Scientific Research from the Ministry of Education, Culture, Sports, Science, and Technology of Japan.

References and notes

1. For reviews of the *Lycopodium* alkaloids, see: (a) Kobayashi, J.; Morita, H. *The Alkaloids*; Cordell, G. A., Ed., in press. (b) Ayer, W. A.; Trifonov, L. S. *The Alkaloids*; Cordell, G. A., Brossi, A., Eds.; Academic: New York, 1994; Vol. 45, p 233. (c) Ayer, W. A. *Nat. Prod. Rep.* **1991**, *8*, 455. (d) MacLean, D. B. *The Alkaloids*; Brossi, A., Ed.; Academic: New York, 1985; Vol. 26, p 241. (e) MacLean, D. B. *The Alkaloids*; Manske, R. H. F., Ed.; Academic: New York, 1973; Vol. 14, p 348. (f) MacLean, D. B. *The Alkaloids*; Manske, R. H. F., Ed.; Academic: New York, 1968; Vol. 10, p 305.
2. (a) Hemscheidt, T.; Spenser, I. D. *J. Am. Chem. Soc.* **1996**, *118*, 1799–1800. (b) Hemscheidt, T.; Spenser, I. D. *J. Am. Chem. Soc.* **1993**, *115*, 3020–3021.
3. Liu, J. S.; Zhu, Y. L.; Yu, C. M.; Zhou, Y. Z.; Han, Y. Y.; Wu, F. W.; Qi, B. F. *Can J. Chem.* **1986**, *64*, 837–839.
4. (a) Yen, C.-F.; Liao, C.-C. *Angew. Chem., Int. Ed.* **2002**, *41*, 4090–4093. (b) Cassayre, J.; Gagosz, F.; Zard, S. Z. *Angew. Chem., Int. Ed.* **2002**, *41*, 1783–1785. (c) Sha, C.-K.; Lee, F.-K.; Chang, C.-J. *J. Am. Chem. Soc.* **1999**, *121*, 9875–9876. (d) Williams, J. P.; St. Laurent, D. R.; Friedrich, D.; Pinard, E.; Roden, B. A.; Paquette, L. A. *J. Am. Chem. Soc.* **1994**, *116*, 4689–4696. (e) Hirst, G. C.; Johnson, T. O.; Overman, L. E. *J. Am. Chem. Soc.* **1993**, *115*, 2992–2993, and references cited therein.
5. Morita, H.; Arisaka, M.; Yoshida, N.; Kobayashi, J. *J. Org. Chem.* **2000**, *65*, 6241–6245.
6. Kobayashi, J.; Hirasawa, Y.; Yoshida, N.; Morita, H. *Tetrahedron Lett.* **2000**, *41*, 9069–9073.
7. Kobayashi, J.; Hirasawa, Y.; Yoshida, N.; Morita, H. *J. Org. Chem.* **2001**, *66*, 5901–5904.
8. Morita, H.; Hirasawa, Y.; Yoshida, N.; Kobayashi, J. *Tetrahedron Lett.* **2001**, *42*, 4199–4201.
9. Hirasawa, Y.; Morita, H.; Kobayashi, J. *Tetrahedron* **2003**, *59*, 3567–3573.
10. Hirasawa, Y.; Morita, H.; Kobayashi, J. *Tetrahedron* **2002**, *58*, 5483–5488.
11. Morita, H.; Hirasawa, Y.; Kobayashi, J. *J. Org. Chem.* **2003**, *68*, 4563–4566.
12. Morita, H.; Kobayashi, J. *J. Org. Chem.* **2002**, *67*, 5378–5381.
13. Braekman, C.; Nyembo, L.; Bourdoux, P.; Kahindo, N.; Hootele, C. *Phytochemistry* **1974**, *13*, 2519–2528.
14. Ayer, W.; Iverach, G. G. *Can. J. Chem.* **1964**, *42*, 2514–2522.
15. (a) Ayer, W.; Browne, L. M.; Nakahara, Y.; Tori, M. *Can. J. Chem.* **1979**, *57*, 1105–1107. (b) Tori, M.; Shimoji, T.; Takaoka, S.; Nakashima, K.; Sono, M.; Ayer, W. A. *Tetrahedron Lett.* **1999**, *40*, 323–324. (c) Tori, M.; Shimoji, T.; Shimura, E.; Takaoka, S.; Nakashima, K.; Sono, M.; Ayer, W. A. *Phytochemistry* **2000**, *503*, 509.
16. (a) Leniewski, A.; Szychowski, J.; MacLean, D. B. *Can. J. Chem.* **1981**, *59*, 2479–2490. (b) Leniewski, A.; MacLean, D. B.; Saunders, J. K. *Can. J. Chem.* **1981**, *59*, 2695–2702.
17. Conformational search and molecular mechanics calculations were conducted by Macromodel program and energetically stable conformer was shown in Figure 4: Mohamadi, F.; Richards, N. G. J.; Guida, W. C.; Liskamp, R.; Lipton, M.; Caufield, C.; Chang, G.; Hendrickson, T.; Still, W. C. *J. Comput. Chem.* **1990**, *11*, 440–467.
18. Halgren, T. *J. Am. Chem. Soc.* **1990**, *112*, 4710–4723.
19. ^{1}H and ^{13}C NMR assignments of cernuine (**9**) and lycocernuine (**10**) were conducted by 2D NMR analysis, since there were no reports on their assignments.
20. Nyembo, L.; Goffin, A.; Hootele, C.; Braekman, J.-C. *Can. J. Chem.* **1978**, *56*, 851–856.
21. (a) Zhou, M.; Diwu, Z.; Panchuk-Voloshina, N.; Haugland, R. P. *Anal. Biochem.* **1997**, *253*, 162–168. (b) Mohanty, J. G.; Jaffe, J. S.; Schulman, E. S.; Raible, D. G. *J. Immunol. Methods* **1997**, *202*, 133–141.
22. (±)-Huperzine A inhibited acetylcholinesterase with an IC_{50} value of 1.6 μM.
23. $[\alpha]_D$ values of **1**–**3** were not reliable due to small amount of samples and small values of optical rotations.

Available online at www.sciencedirect.com
SCIENCE DIRECT®
Tetrahedron 60 (2004) 7025–7033
Tetrahedron

Taveuniamides: new chlorinated toxins from a mixed assemblage of marine cyanobacteria

R. Thomas Williamson, Inder Pal Singh and William H. Gerwick*

College of Pharmacy, Oregon State University, Corvallis, OR 97331, USA

Received 30 August 2003; revised 21 February 2004; accepted 21 February 2004

Available online 25 June 2004

Abstract—Brine shrimp toxicity guided fractionation of the extracts from two mixed Fijian collections of the cyanobacteria *Lyngbya majuscula* and *Schizothrix* sp. led to the isolation of eleven novel chlorinated lipids. All of these metabolites show an intriguing constellation of unsaturation (olefinic and acetylenic bonds) and chlorination at the two termini of a 15-carbon chain. The central carbon atom of the chain (C-8) is substituted in each case with an *N*-acetate function. Taveuniamides A–E have an adjacent carbomethoxy group at C-9 to form a protected β-amino acid while taveuniamides F–K have a methylene group at this position. A standard assortment of 2D NMR techniques in concert with mass spectrometry and other analytical techniques were used to define the structures of these novel metabolites. Taveuniamides F, G and K were the most potent brine shrimp toxins with LD_{50}s between 1.7–1.9 μg/mL.

1. Introduction

Marine cyanobacteria continue to be an exceptionally rich source of metabolites with unusual structural features as well as interesting biological activities.[1,2] In particular, *Lyngbya majuscula* Gomont (Oscillatoriaceae) has been the subject of extensive research in our laboratory and elsewhere.[3,4] We have isolated a number of structurally unique compounds from *L. majuscula*, including such classes of compounds as the curacins,[5] the malyngamides,[6] antillatoxins,[7] barbamides,[8] the carmabins,[9] and grenadadiene.[10] Curacin A, which was isolated as a potent brine shrimp toxin, has shown promising antiproliferative activity due to its inhibition of tubulin polymerization, a known mechanism for the treatment of neoplastic disorders,[11] and promising analog structures have recently been chemically synthesized.[12] Others have reported from this species such diverse natural products as the microcolins (immunosuppressant activity),[13] ypaoamide (fish antifeedant),[14] the majusculamides (antifungal agents),[15] and the lyngbyatoxins (pro-inflammatory agents and tumor promoters).[16]

In a continuing discovery program for bioactive compounds from *L. majuscula*, a number of lipid extracts were screened for brine shrimp toxicity and we encountered one with potent activity from a *L. majuscula*/*Schizothrix* sp. mixture collected from the Taveuni and Yanuca islands in Fiji. Bioassay-guided isolation of the active compounds resulted in the isolation and characterization of eleven new chlorinated compounds, named the 'taveuniamides'. This paper describes the isolation, structure elucidation and brine shrimp toxicity of the taveuniamides (**1**–**11**). These new metabolites are structurally related to a series of polychlorinated acetamides reported from the same or a related organism (described as *Microcoleus lyngbyaceus*) during late stages of the current study, and collectively, give additional insight into the unique metabolic processes at work in their construction.[17]

2. Results and discussion

The CH_2Cl_2/MeOH (2:1) extract (2.9 g) of a mixed assemblage of *L. majuscula* and *Schizothrix* sp. collected from the Taveuni Islands of Fiji (code # VTI-9 Feb 97-02) was subjected to repeated chromatography on Si gel and ODS followed by HPLC on ODS to give taveuniamides A (**1**, 17.3 mg, 0.606%), B (**2**, 1.5 mg, 0.05%), C (**3**, 0.8 mg, 0.03%), D (**4**, 1.2 mg, 0.04%), E (**5**, 7.4 mg, 0.3%), F (**6**, 17.8 mg, 0.6%), G (**7**, 5.1 mg, 0.2%), H (**8**, 0.6 mg, 0.02%), I (**9**, 0.4 mg, 0.01%), and J (**10**, 3.2 mg, 0.1%). Another mixed collection of the same two cyanobacteria from the Yanuca Islands of Fiji (VYI-2 Feb 97-01) yielded a crude extract (215 mg) that was similarly chromatographed to give **1** (1.0 mg, 0.465%), **5** (3.3 mg, 2%), **6** (2.0 mg, 0.9%), **9** (1.0 mg, 0.5%) and taveuniamide L (**11**, 1.5 mg, 0.7%). All of the taveuniamides showed very similar UV absorptions (λ_{max} 244 or 238 nm), indicating chromophores due to conjugated double and triple bonds. Additionally, the IR

Keywords: Taveuniamide; Lyngbya majuscula; Dichloroenyne.
* Corresponding author. Tel.: +1-541-737-5801; fax: +1-541-737-3777; e-mail address: bill.gerwick@orst.edu

0040–4020/$ - see front matter © 2004 Elsevier Ltd. All rights reserved.
doi:10.1016/j.tet.2004.02.076

spectra of these metabolites possessed absorptions for acetylenic (ν_{max} 2220 cm^{-1}) and amide bonds (ν_{max} 1650 cm^{-1}), whereas taveuniamides A–E (**1**–**5**) showed an additional absorption band at 1730 cm^{-1} due to an ester group.

Positive ion FAB-MS of taveuniamide A (**1**) showed a molecular ion cluster at *m/z* 424/426/428/430 suggesting the presence of three chlorine atoms.[18a] HRFABMS of **1** defined a molecular formula of $C_{19}H_{28}{}^{35}Cl_3NO_3$, indicating five degrees of unsaturation. The ^{13}C NMR and DEPT spectra of **1** showed all nineteen carbon atoms and included two methyl groups, eight methylenes, five methines, and four quaternary carbons. Chemical shifts indicated that two of the methine carbons were associated with an olefinic bond (δ 129.2, 114.1) and three were aliphatic. Two quaternary carbons belonged to ester or amide carbonyl groups (δ 176.1, 169.9) and two others could be assigned to acetylenic carbons (δ 92.7, 76.4). A highly shielded carbon signal at δ 19.1 was attributed to a methylene adjacent to an acetylenic carbon.[19] Chemical shifts indicated that one methyl was a methoxy group (δ_C 51.9) whereas the other was part of an acetate functionality (δ_H 2.00).

The ^1H NMR of **1** showed two mutually coupled low-field protons at δ 6.43 (d, J=13.7 Hz) and δ 5.90 (dt, J=13.7, 2.4 Hz) that were assigned to a double bond. Another low-field triplet at δ 5.73 (J=6.4 Hz, corresponding carbon δ_C 73.5) could be assigned to a dichloromethyl adjacent to a methylene group on the basis of chemical shifts. Besides these, the ^1H NMR also showed signals due to an NH (δ 6.32, d, J=9.7 Hz), two additional methines (δ 4.17 and 2.54) and sixteen methylene protons [(δ 1.2–1.7 (12H), 2.17 (2H), 2.31 (2H)].

The structure of **1** was established by 2D NMR experiments, including HSQC, HMBC, ^1H–^1H COSY, and HSQC-TOCSY. A doublet signal at δ 6.43 (H-1) showed HMBC correlations with carbons at δ 114.1 (C-2) and 76.2 (C-3). Another signal at δ 5.90 (H-2) was correlated to carbons at δ 129.0 (C-1) and δ 92.5 (C-4). A high-field methylene signal at δ 2.31 (H-5) showed HMBC correlations with C-1, C-2, C-3, C-4 and two other methylene carbons at δ 25.0 (C-6) and 33.6 (C-7). ^1H–^1H COSY also connected the protons between H-1 and H_2-7, in part because H-2 was coupled to H-5 by 2.4 Hz, which is diagnostic for an enyne system.[18b]

Similar long range couplings (^4J and ^5J) were observed between the H_2-5 protons to C-1 and C-2 by HMBC. These data led to a partial structure **1A** consisting of a heteroatom-substituted conjugated enyne system.

A methine proton at δ 4.17 showed HMBC correlations with two singlet carbons at δ 169.9 (–N*C*OCH$_3$) and 176.1 (–*C*OOCH$_3$), a doublet carbon (δ 48.2, C-9), and three triplets at 25.0 (C-6), 30.0 (C-10), and 33.6 (C-7). Another methine signal at δ 2.54 was correlated with a doublet carbon at δ 48.9 (C-8, δ_H 4.17), the singlet at δ 176.1, and two triplets at δ 27.1 (C-11) and 30.0 (C-10). These data, supported by ^1H–^1H COSY as shown in **1B**, suggested a partial structure having *N*-acetyl and carbomethoxy groups on adjacent carbon atoms and two sets of methylene groups to either side.

A downfield triplet at δ 5.73 ($CHCl_2$, H-15) was connected with methylene protons at δ 2.17 (δ_C 43.4, C-14) that were sequentially connected with methylenes at C-13, C-12, and C-11 on the basis of HSQC-TOCSY data. This suggested partial structure **1C** in which a terminal dichloromethyl group (–$CHCl_2$) was connected to four contiguous methylene groups. Partial structures **1A**, **1B**, and **1C**, which accounted for all of the atoms in taveuniamide A (**1**), were connected using a combination of ^1H–^1H COSY, HMBC, and HSQC-TOCSY experiments (Figure 1). Taveuniamide A was therefore characterized as a C-15 chain having a conjugated monochloro-enyne group, an *N*-acetyl group at C-8, a carbomethoxy group at C-9 and a terminal dichloro-methine group. The strong electron withdrawing effect of the C-1 vinyl chloride significantly reduced the magnitude of the $^3J_{HH}$ vicinal coupling.[20] The value of 13.7 Hz was indicative of an *E* geometry for the C-1-C-2 olefin. This geometry was confirmed by DPFGSE 1D-NOE experiments on H-1 and H-2.[21]

The molecular formula of taveuniamide B (**2**) ($C_{19}H_{27}{}^{35}Cl_4NO_3$) indicated that one proton in **1** was replaced by a chlorine atom. The ^{13}C NMR spectrum of **2** was very similar to that of **1**; however, important differences were observed in the ^1H NMR spectrum, which showed only three low-field protons. The signal at δ 5.92 (H-2) appeared as a triplet (J=2.1 Hz) instead of the doublet of triplets observed for **1**, indicating that H-2 was only coupled across the C-3–C-4 acetylenic bond to the methylene protons at C-5; hence, one proton at C-1 was replaced by a chlorine

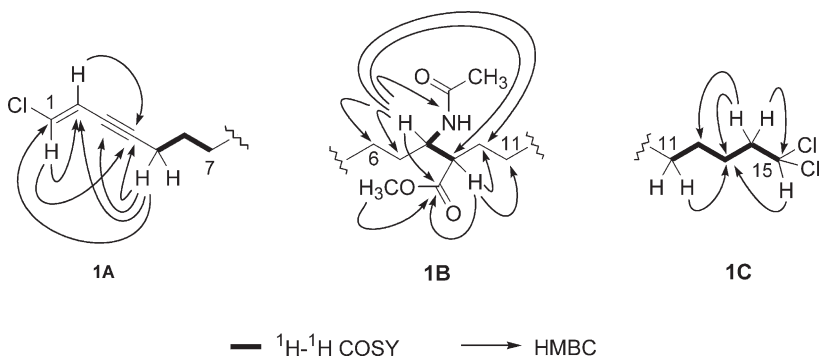

Figure 1. Partial structures of taveuniamide A (**1**) and key ^1H–^1H COSY and HMBC correlations.

atom. The remainder of taveuniamide B (**2**) was identical to that of taveuniamide A (**1**), and this was confirmed by additional 2D NMR (COSY, HSQC, HMBC) experiments.

High-resolution FAB-MS of taveuniamide C (**3**) determined a molecular formula $C_{19}H_{25}{}^{35}Cl_4NO_3$ implying six degrees of unsaturation. Two-dimensional NMR experiments confirmed a partial structure (C-10 through C-15) in **3** that was identical to C-1 to C-6 of taveuniamide B (**2**). The high field methylene group at H_2-10 was next to the same constellation of *N*-acetyl- and carbomethoxy-bearing methines; however, in the opposite orientation. Specifically, COSY correlations showed the H_2-10 protons were coupled with the higher field H-9 proton (δ 2.82) which in turn was coupled to the lower field H-8 methine proton (δ 4.20). ^{1}H and ^{13}C NMR data indicated that the other half of the molecule possessed one disubstituted olefinic bond (δ_H 5.59 and 5.46) that was adjacent to a methylene group (δ 2.85) that in turn was next to a terminating dichloromethine group (δ_H 5.69). To the other side of the olefinic bond were three sequential high field methylene groups and then the low field H-8 methine proton. A large coupling constant (J=15.1 Hz) between H-3 and H-4 indicated *E* geometry for this double bond. Hence, taveuniamide C (**3**) was related to taveuniamide B in which close analogs of the two side chains were disposed to opposite sides of the central β-amino acid functionality.

Taveuniamide D (**4**) possessed a molecular formula $C_{19}H_{24}{}^{35}Cl_4NO_3$ as determined by high resolution FAB-MS, and possessed structural features similar to taveuniamide C (**3**) except that the C-3 double bond was replaced by a triple bond as demonstrated by the absence of olefinic protons and the appearance of ^{13}C NMR resonances at δ 83.7 and 73.4 for C-3 and C-4, respectively.

Positive ion FAB-MS of taveuniamide E (**5**) ($[M+H]^+$ at *m/z* 418) indicated the presence of three chlorine atoms from a characteristic molecular ion cluster, and HRFAB-MS defined a molecular formula of $C_{19}H_{22}^{35}Cl_3NO_3$ for eight degrees of unsaturation. The ^{13}C NMR and HSQC spectra of **5** showed all 19 carbon atoms, including two CH_3's, five CH_2's, five CH's and seven quaternary carbons. By ^{13}C NMR chemical shift reasoning, these 19 carbons comprised of four sp, six sp^2 and only 9 sp^3 carbons instead of the 13 sp^3 carbons observed for **1** and **2**. Consistent with these assignments, the ^{1}H NMR of **5** showed three vinyl protons (δ 6.45, 5.93 and 5.90), ten methylene protons, one acetate methyl group (δ 2.01) and one methoxy group (δ 3.72), and two methine protons (δ 4.21 and 2.84). These data suggested the presence of two conjugated enyne moieties in **5**.

The structure of **5** was elucidated using 2D NMR experiments. Methylene protons at δ 2.52 and 2.43 (H-11, δ_C 17.6) showed a wealth of HMBC correlations including carbons at δ 130.9 (C-15), 111.0 (C-14), 76.2 (C-13), 97.4 (C-12), 28.4 (C-10) and 46.7 (C-9). A fine triplet at δ 5.93 (H-14, J=2.2 Hz, δ_C 111.0) was correlated with C-12. A methine signal at δ 2.84 (H-9, δ_C 46.7) was correlated with carbons at δ 175.5 ($COOCH_3$) and δ 48.1 (C-8) as well as C-10 and C-11. These correlations yielded a partial structure composed of a dichloroenyne terminus and a carbomethoxy group at C-9.

Methylene protons at δ 2.32 (H-5, δ_C 19.1) showed HMBC cross-peaks with carbons at δ 129.0 (C-1, CHCl), 92.4 (C-4), 33.4 (C-7), and 25.0 (C-6). A methine proton at δ 4.21 showed HMBC correlations with a carbon at δ 169.8 ($NHCOCH_3$), C-9, C-6, and C-7. These and other HMBC correlations confirmed this second partial structure as possessing a monochloro enyne terminus and an *N*-acetyl group. The two partial structures were connected using additional HMBC and HSQC-TOCSY data. Taveuniamide E (**5**) was therefore deduced to have a monochloroenyne moiety, a dichloroenyne moiety, a carbomethoxy group at C-9, and an *N*-acetyl group at C-8. A coupling constant of 13.6 Hz between H-1 and H-2 indicated an *E* geometry for the C-1–C-2 double bond, and this was also confirmed by a 1D-NOE experiment.

The relative stereochemistry of the adjacent chiral carbons (C-8 and C-9) was determined using the *J*-based configuration analysis which uses carbon–proton spin coupling constants ($^{2,3}J_{C,H}$) and proton–proton spin coupling constants ($^3J_{H,H}$).[22] In acyclic systems, such as **5**, the configuration of adjacent asymmetric centers can be represented by staggered rotamers (shown in Figure 2 together with the anticipated magnitude of coupling constants). Except for **5**–**1** and **5**–**6**, each rotamer has a unique set of $^{2,3}J_{C,H}$ and $^3J_{H,H}$ coupling constants such that their relative stereochemistry can be determined. The heteronuclear coupling constants of **5** were determined using the HSQMBC method ($^3J_{(H\text{-}9,H\text{-}8)}$-sm, $^3J_{(H\text{-}8,C\text{-}10)}$-sm, $^3J_{(H\text{-}8,CO)}$-lg, $^2J_{(H\text{-}9,C\text{-}8)}$-sm).[23] These values correspond only to those shown for rotamer **5**–**5** in Figure 2 (e.g., *R*,*S* or *S*,*R*). This assignment was confirmed by NOE enhancements between protons at C-8 and C-9 observed using the DPFGSE 1D-NOE experiment.

A few general conclusions can be inferred from the ^{1}H NMR data of this series of metabolites; (a) conjugated dichloroenyne moieties are characterized by the appearance of a triplet vinyl proton at δ 5.9 with a very small coupling constant, usually 2–3 Hz, (b) conjugated monochloroenyne moieties are characterized by a doublet of triplets around δ 5.9 with one large and one small coupling constant, usually 13–15 Hz and 2–3 Hz, and (c) terminal dichloromethyl moieties are characterized by a triplet around δ 5.7 (J=4–6 Hz).

Taveuniamides F (**6**)–L (**12**) were also composed of fifteen carbon chains; however, in contrast to compounds **1**–**5**, they possessed only an *N*-acetyl group at C-8 and lacked a carbomethoxy group at C-9. This latter feature in compounds **6**–**12** was clearly revealed by the lack of an IR absorption band at 1730 cm^{-1} as well as the absence of an ^{1}H NMR resonance at δ 3.7 for the carbomethoxy group.

The molecular formula of taveuniamide F (**6**) was established as $C_{17}H_{26}{}^{35}Cl_3NO$ by high resolution FAB-MS. The ^{13}C NMR spectrum of **6** showed only two vinyl and two acetylenic carbons in addition to nine methylene carbons. The ^{1}H NMR spectrum of **6** showed two protons for a single enyne system [δ 6.44 (d, J=13.5 Hz) and 5.94 (dt, J=13.5, 2.2 Hz)], and thus indicated it was a monochloro-enyne. Another triplet at δ 5.74 (δ_C 73.5, C-15) indicated a terminal $-CHCl_2$ group. Additional two-dimensional NMR

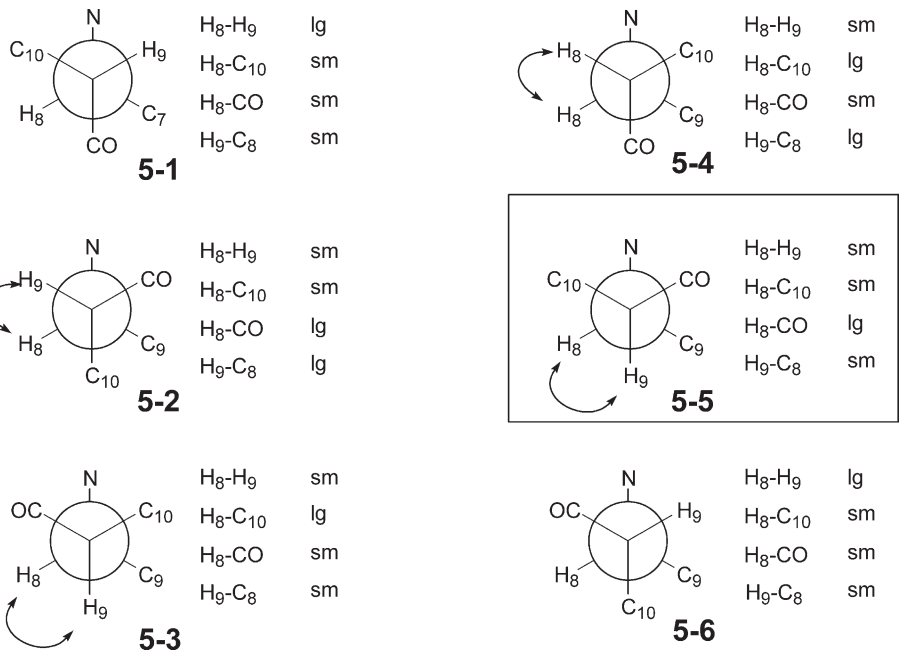

Figure 2. *J*-based configurational analysis of six possible rotamers of taveuniamide E (**5**) to determine the relative stereochemistry.

experiments (^{1}H–^{1}H COSY, HSQC, and HMBC) established a structure that was identical to taveuniamide A, including the geometry of the C-1-C-2 olefin, except for the absence of a carbomethoxy group at C-9; in taveuniamide F (**6**), this C-9 this substituent was replaced by a hydrogen atom.

The molecular formula ($C_{17}H_{21}{}^{35}Cl_4NO$) of taveuniamide G (**7**) showed many of the same NMR bands observed for taveuniamide D (**4**) including those for a terminal gem-dichloro enyne functionality, a dichloromethyl group appearing as a triplet (δ_H 5.76, J=5.9 Hz) adjacent to a methylene group (δ_H 3.06), an isolated acetylenic bond (δ_C 73.9 and 83.9), and an *N*-acetate group (δ_H 1.99). The only difference between these metabolites, similar to the relationship between taveuniamide A (**1**) and F (**6**), was the absence of the carbomethoxy ester in **7** and its replacement with a hydrogen atom to form the C-9 methylene group.

Gas chromatography–mass spectrometry (GC–MS) of taveuniamide H (**8**) gave a molecular ion at *m/z* 325 which in concert with NMR data indicated a molecular formula of $C_{17}H_{21}{}^{35}Cl_2NO$ (7 degrees of unsaturation). The ^{1}H and ^{13}C NMR of **8** indicated that it was symmetric (e.g. only 10 ^{13}C NMR resonance lines, Table 2). By comparison with taveuniamide A (**1**), it was clear that taveuniamide H (**8**) possessed the same C-1 to C-7 monochloroenyne fragment, and that this fragment constituted both termini of the 15-carbon chain. Both of the terminal double bonds possessed *E* geometry (J=13.6 Hz).

Positive ion FAB-MS of taveuniamide I (**9**) indicated the presence of three chlorine atoms, and high-resolution mass measurement defined a molecular formula of $C_{17}H_{20}{}^{35}Cl_3NO$ for 7 degrees of unsaturation. The ^{13}C NMR and DEPT spectra of **9** again indicated 17 carbons including four acetylenic, four ethylenic, six methylenes, one methine, one carbonyl and a methyl carbon. The ^{1}H NMR spectrum of taveuniamide I (**9**) was very similar to that of taveuniamide E (**5**) except for the lack of signals due to the carbomethoxy group. Ethylenic signals at δ 6.44 (d, J=13.1 Hz) and 5.90 (dt, J=13.1, 2.2 Hz) indicated a monochloroenyne moiety, whereas a triplet at δ 5.93 (J=2.2 Hz) suggested a dichloroenyne arrangement. Besides these signals, compound **9** also showed a doublet at δ 5.17 that was assigned to the *N*-acetyl NH as well as signals due to twelve methylene protons and a methyl group. A signal at δ 3.97 was assigned to the methine proton on the carbon bearing the *N*-acetyl group.

Two partial structures (**9A** and **9C**, Fig. 3) in taveuniamide I (**9**) identical to the two termini in taveuniamide E (**5**) were confirmed by 2D NMR experiments. The methine proton at δ 3.97 showed HMBC correlations with carbons at C-6, C-7, C-9, and C-10 while methylene protons at δ 2.41 (H_2-5) showed correlations with C-6 and C-7. Additionally, the methylene protons at δ 2.35 (H_2-11) were also correlated with C-9 and C-10. Hence three contiguous methylene groups were positioned on either side of the methine carbon carrying the *N*-acetyl group; this was confirmed by TOCSY (**9B**). These three partial structures were connected using HMBC and HSQC-TOCSY experiments. A coupling constant of 13.1 Hz was indicative of *E* geometry for the C-14-C-15 double bond.

The molecular formula $C_{17}H_{19}{}^{35}Cl_4NO$ of taveuniamide J

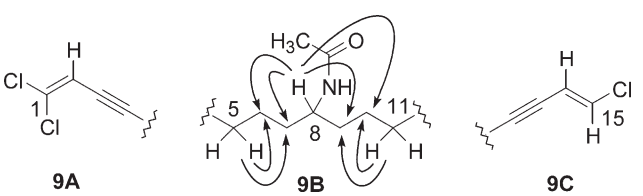

Figure 3. Key HMBC correlations for taveuniamide I (**9**).

(**10**) suggested that one hydrogen in **9** was replaced by an additional chlorine in **10**. Additionally, ^{1}H and ^{13}C NMR spectra of **10** indicated that it was symmetric. The ^{13}C NMR and DEPT spectra of **10** showed only 10 carbon resonances, including four quaternary carbons (one carbonyl, one olefinic, and two acetylenic), two methines (one methine and one ethylenic), three methylenes, and one methyl group. Importantly, the ^{1}H NMR spectrum of **10** showed only one olefinic signal for two protons at δ 5.94, and these were long-range coupled to four methylene protons across acetylenic bonds (2H, t, J=2.0 Hz). Hence, this downfield signal was assigned to H-2 and H-14. Further 2D NMR experiments (HSQC, HMBC, and COSY) led to a structure that was similar to **9** except that the vinylic proton at C-15 was replaced by a chlorine atom giving rise to a structure symmetric about C-8.

High-resolution mass measurement of taveuniamide K (**11**) defined a molecular formula of $C_{17}H_{23}{}^{35}Cl_3NO$. A combination of ^{13}C NMR and HSQC data indicated the presence of six olefinic, two acetylenic, six methylene and one methine carbons. The ^{1}H NMR spectrum showed the presence of five downfield protons that were assigned to a conjugated diene and an enyne system. $^{1}H-^{1}H$ COSY connected protons at C-2 through C-5 for the conjugated diene (λ_{max}=246 nm) and then extended through to a methylene at C-11. From ^{1}H and ^{13}C NMR data (Table 2 and Section 3), a monochloroenyne system formed the other terminus, similar to that present in **9**. However, a series of 1D DPFGSE NOE experiments with taveuniamide K (**11**) established a Z relationship between H-14 and H-15 (J=11.3 Hz) as well as between H-3 and H-4 (J=12.7 Hz).

Taveuniamides A–K (**1**–**11**) were tested for toxicity to brine shrimp (*Artemia salina*) and the LD_{50} and ED_{50} values of the taveuniamides are summarized in Table 3.[24] Taveuniamides F (**6**), G (**7**), and K (**11**) showed somewhat greater potency (LD_{50}=1.8, 1.9, and 1.7 μg/mL, respectively) while taveuniamides A–E (**1**–**5**) showed moderate activity (LD_{50} 3–5 μg/mL). Taveuniamides G (**8**), I (**9**), and J (**10**) were essentially inactive at a concentration of 10 μg/mL.

This report complements an earlier report on related polychlorinated acetamides from another cyanobacterium, *M. lyngbyaceus*.[17] It should be noted that it is not clear from our studies whether the taveuniamides are produced by *L. majuscula* or *Schizothrix* sp. However, taken together, these two reports suggest a biogenesis of these metabolites from a polyketide pathway with several unique transformations and tailoring reactions. First, it is important to note that the pendant carboxyl functionality at C-9 in taveuniamide A–E is a feature not observed in the metabolites reported from *M. lyngbyaceus*. The carbon chain of taveuniamides A–E (**1**–**5**) can thus be envisioned as arising from either: (1) a octaketide that undergoes terminal decarboxylation and addition of a pendant carbon to C-9 (discussed below), or (2) the novel joining together of two tetraketides through the C-1 carboxyl function of one chain to the alpha C-2 carbon of the second chain. If the first of the two hypotheses is correct, and irrespective of which terminus is chosen as the initiation of the polyketide, then this pendant carbon atom is attached to the C-1 position of the polyketide backbone (assuming an acetate starter unit), and hence, suggests that it may derive from C-2 of a pendant acetate group as for the cyclopropyl methylene carbon of curacin A (unreported observations). However, this would be the first report wherein such a pendant C-2 carbon would be present as an oxidized carboxylic acid functionality.

Second, the pendant amino functionality in almost all of these metabolites is distinctively placed in the middle of the lipid chain; it seems likely this occurs from an amino transferase functioning on a ketone precursor. However, if the first hypothesis above on the origin of the polyketide chain is correct, then this amine is positioned at a C-2 deriving position of the polyketide chain, and an oxidation must precede the amine transfer reaction. Third, the presence of dichloromethyl groups and terminal dichloroenynes (note, all halogen atoms are introduced at the termini and not at interior carbon sites) suggests the operation of a halogenase similar to that observed in the production of barbamide, another metabolite from *L. majuscula* which possesses a trichloromethyl group.[8] In this latter example, it appears that a novel halogenase acting via a radical-type mechanism is involved in the chlorination, and hints that such an enzyme may be involved in formation of the taveuniamides.[25] Lastly, the distinctive terminal unsaturation in conjugation with a carbon–carbon triple bond indicates the functioning of unusual desaturases. The fact that such functionalities occur at both termini (e.g. taveuniamide E, **5**) suggests that this occurs either in the modular environment of the polyketide synthase, or possibly after release of the substrate from the multi-enzyme complex. In this regard, detection of non-halogenated acetamides in the *M. lyngbyaceus* report suggests that release from the multienzyme occurs prior to introduction of the halogen atoms and unsaturations. Alternatively, if the taveuniamide backbone arises from two distinct tetraketides, then this functionality is present singly in each precursor chain, and could be introduced at any stage of its construction.

3. Experimental

3.1. General experimental procedures

Optical rotations were measured with a Perkin–Elmer Model 141 polarimeter. Ultraviolet spectra were recorded on a Hewlett–Packard 8452A diode array spectrophotometer and IR on a Nicolet 510 spectrophotometer. Nuclear magnetic resonance (NMR) spectra were recorded at 600 MHz (Bruker DRX 600) or a 300 MHz (Bruker AC 300) in $CDCl_3$ and ^{13}C NMR at 150 MHz (Bruker DRX 600) or 75 MHz (Bruker AC 300). All chemical shifts are reported relative to TMS as an internal standard, or are referenced to δ 7.27 (^{1}H NMR) and δ 77.2 (^{13}C NMR) for residual chloroform. Low-resolution mass spectra (LRMS) were obtained using a Hewlett–Packard GC (Model 5810) connected to a Hewlett–Packard mass selective detector (Model 5971), while high-resolution mass spectra (HRMS) were obtained on a Kratos MS 50 TC. High performance liquid chromatography was performed using a Waters 6000A pump and a Lambda-Max 480 lc spectrophotometer. TLC grade (10–40 μm) silica gel was used for vacuum liquid chromatography and Merck aluminum backed TLC

sheets (silica gel 60 F_{254}) were used for thin layer chromatography. Molecular modeling was done using the PC Spartan molecular modeling program using an MM2 force field.

3.2. Biological material

The marine cyanobacteria *L. majuscula*/*Schizothrix* sp. (voucher specimens available from WHG as VTI-9 Feb 97-02 and VYI-2 Feb 97-01) were collected using SCUBA diving from a depth of 13 m in Taveuni and Yanuca islands in Fiji and stored in 2-propanol at low temperature until work-up.

3.3. Extraction and isolation

A total of 87.2 g (dry wt) of an assemblage of *L. majuscula*/*Schizothrix* (VTI-9 Feb 97-02) was extracted twice with CH_2Cl_2/MeOH (2:1) to yield 3.27 g of the crude extract. A portion of this extract (2.9 g) was subjected to vacuum liquid chromatography (VLC) on Si gel (TLC grade) to yield five fractions. Fraction 2 was again separated on silica gel to yield nine fractions (2A–2I). Fraction 2I was subjected to VLC on reversed phase C_{18} silica gel to give seven fractions (2I-1 to 2I-7). Fraction 2I-2 was subjected to NP-HPLC (Phenomenex, Maxsil, 10 m, 500×10 mm, 9.5 mL/min, UV detection at 254 nm, hexanes–EtOAc, 60:40) to yield seven fractions 2I-2-A to 2I-2-G. Fraction 2I-2-B was subjected to RP-HPLC (Phenomenex, Sphereclone 5 μm, ODS, 250×10.0 mm, 3.5 mL/min, UV detection at 254 nm, MeOH–H_2O, 80:20) to yield taveuniamides A (17.3 mg), B (1.5 mg), and C (0.8 mg). Following HPLC using the same conditions, fraction 2I-2-D yielded taveuniamides D (1.2 mg), E (7.4 mg), and F (17.8 mg). Fraction 2I-2-F was subjected to HPLC under the same conditions to give four peaks. Peak 2 was further purified to yield taveuniamides G (0.4 mg) and H (0.6 mg). Peaks 3 and 4 were characterized as taveuniamides I (5.1 mg) and J (3.2 mg).

A total of 22.6 g (dry wt) of *L. majuscula*/*Schizothrix* sp. (VYI-2 Feb 97-01) was extracted twice with CH_2Cl_2/MeOH (2:1) to yield 250 mg of crude extract. A portion of this (215 mg) was fractionated using vacuum liquid chromatography (VLC) on Si gel by a stepwise gradient of hexanes–EtOAc and EtOAc–MeOH to give ten fractions. Fractions A–E were 100 mL each while fractions F–J were 50 mL each. Fraction F (32 mg, EtOAc) showed very potent (65% dead and the rest visually immobile) brine shrimp activity at 1 μg/mL. Fraction F was subjected to HPLC (Phenomenex, Sphereclone 5 μm, ODS, 250×10.0 mm, 2 mL/min, UV detection at 254 nm, MeOH–H_2O, 80:20) to yield taveuniamides A (**1**, 1.0 mg), E (**5**, 3.3 mg), F (**6**, 2.0 mg), and K (**11**, 1.5 mg). Fraction G (6 mg, EtOAc–MeOH, 90:10) showed 90% activity against brine shrimp at 10 μg/mL and was subjected to HPLC under the same conditions as fraction F to yield taveuniamide I (**9**, 1.0 mg).

3.3.1. Taveuniamide A (1). $[\alpha]_D^{25>}$ +11.7° (*c* 0.4, $CHCl_3$); ORD $[\alpha]_{589}$ +11.7°, $[\alpha]_{578}$ +11.5°, $[\alpha]_{546}$ +12.0°, $[\alpha]_{436}$ +20.5°, $[\alpha]_{365}$ +1870° (*c* 0.4, $CHCl_3$); UV (EtOH) λ_{max} 236 (6700); IR ν_{max} (neat) 3366, 3325, 2217, 1731, 1652, 1540, 1201, 930 cm^{-1}; ^1H NMR ($CDCl_3$, 600 MHz) δ 6.43 (1H, d, *J*=13.7 Hz, H-1), 6.32 (1H, d, *J*=9.6 Hz, NH), 5.90 (1H, dt, *J*=13.7, 2.4 Hz, H-2), 5.73 (1H, t, *J*=6.4 Hz, H-15), 4.17 (1H, tt, *J*=9.6, 4.8 Hz, H-8), 3.70 (3H, s, OCH_3), 2.54 (1H, ddd, *J*=9.6, 6.5, 3.6 Hz, H-9), 2.31 (2H, m, H-5), 2.17 (2H, m, H-14), 2.00 (3H, s, CH_3), 1.65 (1H, m, H-10a), 1.58 (2H, m, H-6), 1.55 (4H, m, H-7a, 10b, 13), 1.45 (1H, m, H-7b), 1.35 (3H, m, H-11a, 12), 1.25 (1H, m, H-11b); ^{13}C NMR see Table 1; GC-EIMS (70 eV) t_R=15.82 min, obs. *m*/*z* (rel. int) 423 (8), 388 (13), 332 (10), 280 (19), 254 (67), 222 (11), 198 (30), 157 (100), 139 (12), 121 (58), 60 (46); HRFABMS *m*/*z* 424.1175 (calcd for $C_{19}H_{29}{}^{35}Cl_3NO_3$, 424.1213).

Table 1. ^{13}C NMR data (δ) for taveuniamides A–E (**1**–**5**)

Position	**1**[a,b]	**2**[c]	**3**[c]	**4**[c]	**5**[b]
1	129.0 CH	130.3	72.7	70.3	129.0
2	114.1 CH	111.3	46.3	33.4	114.1
3	76.2 C	73.3	123.4	83.7	76.0
4	92.5 C	98.8	135.9	73.4	92.4
5	19.1 CH_2	19.2	31.8	18.0	19.1
6	25.0 CH_2	25.0	25.5	25.0	25.0
7	33.6 CH_2	33.4	33.5	33.3	33.4
8	48.9 CH	48.8	48.5	48.1	48.1
9	48.2 CH	48.3	46.5	46.8	46.7
10	30.0 CH_2	29.9	28.2	28.3	28.4
11	27.1 CH_2	27.1	17.5	17.4	17.6
12	28.3 CH_2	28.3	97.5	75.8	97.4
13	25.6 CH_2	25.6	75.9	97.4	76.2
14	43.4 CH_2	43.4	111.0	111.0	111.0
15	73.5 CH	73.4	130.7	130.7	130.9
16	176.1 C	175.4	176.0	175.3	175.5
16-OCH_3	51.7 CH_3	51.6	51.7	51.7	51.9
NH*C*O	169.9 C	169.8	169.8	169.8	169.8
NHCO*C*H_3	23.5 CH_3	23.4	23.4	23.3	23.4

[a] Multiplicity assigned by DEPT experiment.
[b] 150 MHz.
[c] 75 MHz.

3.3.2. Taveuniamide B (2). $[\alpha]_D^{25}$ +10.4° (*c* 0.1, $CHCl_3$); ORD $[\alpha]_{589}$ +10.4°, $[\alpha]_{578}$ −1.6°, $[\alpha]_{546}$ +0.8°, $[\alpha]_{436}$ +9.2°, $[\alpha]_{365}$ +14.7° (*c* 0.1, $CHCl_3$); UV (EtOH) λ_{max} 244 (18,300); IR ν_{max} (neat) 3293, 2218, 1731, 1651, 1540, 1170, 933 cm^{-1}; ^1H NMR ($CDCl_3$, 600 MHz) δ 6.32 (1H, d, *J*=9.6 Hz, NH), 5.92 (1H, t, *J*=2.1 Hz, H-2), 5.74 (1H, t, *J*=5.9 Hz, H-15), 4.17 (1H, *J*=dddd, *J*=9.4, 9.4, 3.5, 3.5 Hz, H-8), 3.72 (3H, s, OCH_3), 2.55 (1H, ddd, *J*=9.4, 6.5, 3.7 Hz, H-9), 2.40 (2H, m, H-5), 2.17 (2H, m, H-14), 2.02 (3H, s, CH_3), 1.64 (1H, m, H-10a), 1.59 (3H, m, H-7, 8a), 1.53 (3H, m, H-10b, 13), 1.43 (1H, m, H-6, 7a), 1.40 (2H, m, H-11), 1.33 (2H, m, H-12); ^{13}C NMR see Table 1; GC-EIMS (70 eV) t_R=16.36 min, obs. *m*/*z* (rel. int) 457 (10), 417 (21), 280 (30), 254 (91), 232 (39), 190 (100), 157 (91), 115 (54), 64 (86); HRFABMS *m*/*z* 458.0802 (calcd for $C_{19}H_{28}{}^{35}Cl_4NO_3$, 458.0823).

3.3.3. Taveuniamide C (3). $[\alpha]_D^{25}$ +24.0° (*c* 0.03, $CHCl_3$); ORD $[\alpha]_{589}$ +24.0°, $[\alpha]_{578}$ +59.3°, $[\alpha]_{546}$ +94.3°, $[\alpha]_{436}$ +52.6°, $[\alpha]_{365}$ +41.3° (*c* 0.03, $CHCl_3$); UV (EtOH) λ_{max} 244 (15,400); IR ν_{max} (neat) 3303, 2218, 1732, 1650, 1540, 1165, 930 cm^{-1}; ^1H NMR ($CDCl_3$, 600 MHz) δ 6.25 (1H, d, *J*=9.8 Hz, NH), 5.93 (1H, t, *J*=2.0 Hz, H-2), 5.69 (1H, t, *J*=5.9 Hz, H-15), 5.59 (1H, dt, *J*=15.1, 7.2 Hz, H-12), 5.46 (1H, dt, *J*=15.1, 7.5 Hz, H-13), 4.20 (1H, m, H-8), 3.71 (3H, s, OCH_3), 2.85 (2H, t, *J*=5.9 Hz, H-14), 2.82 (1H, m, H-7), 2.55 (1H, m, H-5a), 2.45 (1H, m, H-5b), 2.05 (2H, m, H_2-11), 2.01 (3H, s, CH_3), 1.89 (1H, dddd, *J*=14.0, 7.0, 7.0,

7.0 Hz, H-6a), 1.77 (1H, dddd, *J*=14.0, 7.0, 7.0, 7.0 Hz, H-6b), 1.42 (4H, m, H-9, 10); ^{13}C NMR see Table 1; GC-EIMS (70 eV) t_R=15.11 min, obs. *m/z* (rel. int) 455 (7), 422 (7), 398 (35), 290 (14), 254 (42), 248 (14), 218 (45), 194 (100), 157 (26), 115 (40), 60 (86); HRFABMS *m/z* 456.0615 (calcd for $C_{19}H_{26}{}^{35}Cl_4NO_3$, 456.0667).

3.3.4. Taveuniamide D (4). $[\alpha]_D^{25}$ +5.3° (*c* 0.09, $CHCl_3$); ORD $[\alpha]_{589}$ +5.3°, $[\alpha]_{578}$ +0°, $[\alpha]_{546}$ +3.3°, $[\alpha]_{436}$ +4.8°, $[\alpha]_{365}$ +5.3° (*c* 0.09, $CHCl_3$); UV (EtOH) λ_{max} 244 (16,500); IR ν_{max} (neat) 3286, 2220, 1728, 1658, 1549, 1165, 931 cm^{-1}; ^{1}H NMR ($CDCl_3$, 600 MHz) δ 6.27 (1H, d, *J*=10.3 Hz, NH), 5.94 (1H, t, *J*=2.2 Hz, H-2), 5.76 (1H, t, *J*=6.1 Hz, H-15), 4.20 (1H, dddd, *J*=9.2, 9.2, 4.1, 4.1 Hz, H-8), 3.7 (3H, s, OCH_3), 3.05 (2H, dt, *J*=6.0, 2.2 Hz, H-14), 2.83 (1H, ddd, *J*=7.5, 7.5, 3.5 Hz, H-7), 2.51 (1H, dddd, *J*=17.3, 7.4, 7.4, 2.2 Hz, H-5a), 2.43 (1H, dddd, *J*=17.3, 6.8, 6.8, 2.2 Hz, H-5b), 2.22 (2H, m, H-11), 2.0 (3H, s, CH_3), 1.89 (1H, dddd, *J*=14.0, 7.0, 7.0, 7.0 Hz, H-6a), 1.78 (1H, dddd, *J*=14.0, 7.0, 7.0, 7.0 Hz, H-6b), 1.59 (1H, m, H-9a), 1.56 (2H, m, H-10), 1.54 (1H, m, H-9b); ^{13}C NMR see Table 1; GC-EIMS (70 eV) t_R=14.62 min, obs. *m/z* (rel. int) 453 (2), 396 (8), 248 (7), 212 (22), 193 (28), 139 (31), 95 (65), 56 (100); HRFABMS *m/z* 454.0492 (calcd for $C_{19}H_{24}{}^{35}Cl_4NO_3$, 454.0510).

3.3.5. Taveuniamide E (5). $[\alpha]_D^{25}$ +2.1° (*c* 0.3, $CHCl_3$); ORD $[\alpha]_{589}$ +2.1°, $[\alpha]_{578}$ +1.8°, $[\alpha]_{546}$ +2.1°, $[\alpha]_{436}$ +3.5°, $[\alpha]_{365}$ +8.1° (*c* 0.3, $CHCl_3$); UV (EtOH) λ_{max} 242 (7,200); IR ν_{max} (neat) 3307, 3076, 2218, 1730, 1650, 1550, 1165, 932 cm^{-1}; ^{1}H NMR ($CDCl_3$, 600 MHz) δ 6.45 (1H, d, *J*=13.6 Hz, H-1), 6.28 (1H, d, *J*=10.3 Hz, NH), 5.93 (1H, t, *J*=2.2 Hz, H-14), 5.90 (1H, dt, *J*=13.6, 2.2 Hz, H-2), 4.21 (1H, tt, J=9.2, 4.6 Hz, H-8), 3.72 (3H, s, OCH_3), 2.84 (1H, ddd, *J*=7.5, 7.5, 3.5 Hz, H-9), 2.52 (1H, ddt, *J*=17.3, 2.2, 8.3 Hz, H-11a), 2.43 (1H, ddt, *J*=17.3, 2.2, 6.8 Hz, H-11b), 2.32 (2H, m, H-5), 2.01 (3H, s, CH_3), 1.89 (1H, dddd, *J*=14.3, 7.6, 7.6, 7.6 Hz, H-10a), 1.78 (1H, dddd, *J*=13.8, 6.8, 6.8, 6.8 Hz, H-10b), 1.58 (2H, m, H-6), 1.55 (1H, m, H-7a), 1.50, (1H, m, H-7b); ^{13}C NMR see Table 1; GC-EIMS (70 eV) t_R=14.10 min, obs. *m/z* (rel. int) 417 (11), 382 (21), 263 (16), 240 (22), 212 (37), 180 (38), 157 (100), 121 (54), 99 (53), 56 (77); HRFABMS *m/z* 418.0743 (calcd for $C_{19}H_{23}{}^{35}Cl_3NO_3$, 418.0744).

3.3.6. Taveuniamide F (6). $[\alpha]_D^{25}$ −5.2° (*c* 0.4 $CHCl_3$); ORD $[\alpha]_{589}$ −5.2°, $[\alpha]_{578}$ −5.0°, $[\alpha]_{546}$ −5.0°, $[\alpha]_{436}$ −6.0°, $[\alpha]_{365}$ −8.0° (*c* 0.4, $CHCl_3$); UV (EtOH) λ_{max} 238 (9,100); IR ν_{max} (neat) 3284, 3084, 2216, 1643, 1552, 918 cm^{-1}; ^{1}H NMR ($CDCl_3$, 600 MHz) δ 6.44 (1H, d, *J*=13.5 Hz, H-1), 5.94 (1H, dt, *J*=13.5, 2.3 Hz, H-2), 5.74 (1H, t, *J*=6.0 Hz, H-15), 5.13 (1H, d, *J*=9.2 Hz, NH), 3.93 (1H, m, H-8), 2.32 (2H, td, *J*=6.1, 2.3 Hz, H-5), 2.18 (2H, m, H-14), 2.02 (3H, s, CH_3), 1.61 (1H, m, H-7a), 1.55 (2H, m, H-6), 1.53 (2H, m, H-13), 1.47 (1H, m, H-9a), 1.40 (1H, m, H-7b), 1.34 (1H, m, H-9b), 1.32 (6H, m, H-10, 11, 12); ^{13}C NMR see Table 2; GC-EIMS (70 eV) t_R=14.35 min, obs. *m/z* (rel. int) 365 (2), 330 (17), 222 (46), 216 (17), 196 (82), 157 (38), 139 (16), 112 (49), 99 (100), 79 (28), 60 (51); HRFABMS *m/z* 366.1144 (calcd for $C_{17}H_{27}{}^{35}Cl_3NO$, 366.1158).

3.3.7. Taveuniamide G (7). $[\alpha]_D^{25}$ +0.3° (*c*.04, $CHCl_3$); ORD $[\alpha]_{589}$ +0.3°, $[\alpha]_{578}$ −12.5°, $[\alpha]_{546}$ −5.5°, $[\alpha]_{436}$ −6.5°, $[\alpha]_{365}$ −10.0° (*c* 0.04, $CHCl_3$); UV (EtOH) λ_{max} 244 (21,100); IR ν_{max} (neat) 3307, 2215, 1642, 1552, 1170, 931 cm^{-1}; ^{1}H NMR ($CDCl_3$, 600 MHz) δ 5.93 (1H, t, *J*=2.2 Hz, H-2), 5.76 (1H, t, *J*=5.9 Hz, H-15), 5.14 (1H, d, *J*=9.7 Hz, NH), 3.97 (1H, m, H-8), 3.06 (2H, dt, *J*=11.9, 2.3 Hz, H-14), 2.40 (2H, td, *J*=2.2, 5.9 Hz, H-5), 2.22 (2H, tt, *J*=6.7, 2.3 Hz, H-11), 1.99 (3H, s, CH_3), 1.65 (2H, m, H-7a, 9a), 1.59 (2H, m, H_2-6), 1.54 (2H, m, H-10), 1.48 (2H, m, H-7b, 9b); ^{13}C NMR see Table 2; GC-EIMS (70 eV) t_R=13.52 min, obs. *m/z* (rel. int) 395 (3), 360 (13), 318 (10), 260 (10),218 (46), 193 (50), 164 (58), 148 (57), 99 (66), 95 (100); HRFABMS *m/z* 396.0456 (calcd for $C_{17}H_{22}{}^{35}Cl_4NO$, 396.0456).

3.3.8. Taveuniamide H (8). $[\alpha]_D^{25}$ +0° (*c* 0.04, $CHCl_3$); UV (EtOH) λ_{max} 238 (10,300); IR ν_{max} (neat) 3287, 2216, 1642, 1552, 2200, 1656, 931 cm^{-1}; ^{1}H NMR ($CDCl_3$, 600 MHz) δ 6.45 (2H, d, *J*=13.6 Hz, H-1, 15), 5.91 (2H, dt, *J*=13.6, 2.1 Hz, H-2, 14), 5.11 (1H, d, *J*=9.3 Hz, NH), 3.97 (1H, m, H-8), 2.33 (4H, td, *J*=7.2, 2.1 Hz, H-5, 11), 2.00 (3H, s, CH_3), 1.62 (2H, m, H-7a, 9a), 1.56 (4H, m, H-6, 10), 1.44 (2H, m, H-7b, 9b); ^{13}C NMR see Table 2; GC-EIMS (70 eV) t_R=10.95 min, obs. *m/z* (rel. int) 325 (3), 290 (42), 248 (12), 182 (42), 175 (43), 157 (74), 120 (64), 103 (67), 91 (100), 77 (70), 60 (68).

3.3.9. Taveuniamide I (9). $[\alpha]_D^{25}$ −2.0° (*c* 0.4, $CHCl_3$); ORD $[\alpha]_{589}$ −2.0°, $[\alpha]_{578}$ −2.5°, $[\alpha]_{546}$ −2.2°, $[\alpha]_{436}$ −2.0°, $[\alpha]_{365}$ −3.0° (*c* 0.4, $CHCl_3$); UV (EtOH) λ_{max} 242 (37,500); IR ν_{max} (neat) 3294, 2215, 1639, 1383, 1043 cm^{-1}; ^{1}H NMR ($CDCl_3$, 600 MHz) δ 6.44 (1H, d, *J*=13.1 Hz, H-15), 5.93 (1H, t, *J*=2.2 Hz, H-2), 5.90 (1H, dt, *J*=13.1, 2.2 Hz, H-14), 5.17 (1H, d, *J*=9.4 Hz, NH), 3.97 (1H, m, H-8), 2.41 (2H, dt, *J*=2.2, 7.0 Hz, H-5), 2.32 (2H, dt, *J*=2.2, 7.0 Hz, H-11), 1.99 (3H, s, CH_3), 1.67 (2H, m, H-7a, 9a), 1.58 (4H, m, H-6, 10), 1.45 (2H, m, H-7b, 9b); ^{13}C NMR see Table 2; GC-EIMS (70 eV) t_R=11.82 min, obs. *m/z* (rel. int) 359 (7), 324 (36), 216 (25), 191 (53), 157 (42) 146 (57), 99 (90), 91 (100), 60(83); HRFABMS *m/z* 360.0689 (calcd for $C_{17}H_{21}{}^{35}Cl_3NO$, 360.0689).

Table 2. ^{13}C NMR data (δ) for taveuniamides F–K (**6**–**11**)

Position	**6**[a]	**7**[a]	**8**[a]	**9**[b]	**10**[b]	**11**[a]
1	128.7	130.2	129.0	130.4 C	130.2 C	119.3
2	113.9	111.2	113.9	111.3 CH	111.3 CH	128.9
3	73.5	75.1	75.9	75.3 C	75.4 C	125.0
4	92.5	99.2	92.4	98.9 C	99.0 C	137.9
5	19.1	19.3	19.0	19.4 CH_2	19.5 CH_2	32.7
6	24.7	24.4	24.6	24.7 CH_2	24.7 CH_2	25.3
7	34.4	34.2	34.4	34.3 CH_2	34.4 CH_2	35.0
8	48.7	48.2	48.1	48.3 CH	48.3 CH	48.7
9	35.2	34.2	34.4	34.5 CH_2	34.4 CH_2	34.5
10	25.6	24.7	24.6	24.8 CH_2	24.7 CH_2	24.9
11	29.0	18.2	19.0	19.2 CH_2	19.5 CH_2	19.3
12	28.3	73.9	92.4	92.5 C	99.0 C	92.7
13	25.7	83.9	75.9	76.2 C	75.4 C	76.6
14	43.3	34.5	113.9	114.1 CH	111.3 CH	114.5
15	73.5	70.5	129.0	129.0 CH	130.2 C	129.1
NH*C*O	169.5	169.5	169.4	169.7 C	169.7 C	169.8
NHCO*C*H_3	23.2	23.3	23.3	23.5 CH_3	23.5 CH_3	23.7

Multiplicity assigned by DEPT experiment.
[a] 75 MHz.
[b] 150 MHz.

3.3.10. Taveuniamide J (10). $[\alpha]_D^{25}$ +0° (*c* 0.25, $CHCl_3$); UV (EtOH) λ_{max} 244 (37,700); IR ν_{max} (neat) 3300, 2216, 1636, 1542, 933 cm^{-1}; ^1H NMR ($CDCl_3$, 600 MHz) δ 5.94 (2H, t, *J*=2.0 Hz, H-2, 14), 5.13 (1H, d, *J*=9.4 Hz, NH), 3.98 (1H, nonet, *J*=4.5 Hz, H-8), 2.41 (4H, dt, *J*=2.4, 6.9 Hz, H-5, 11), 2.00 (3H, s, CH_3), 1.67 (2H, m, H-7a, 9a), 1.56 (4H, m, H-6, 10), 1.49 (2H, m, H-7b, 9b); ^{13}C NMR see Table 2; GC-EIMS (70 eV) t_R=12.87 min, obs. *m/z* (rel. int) 393 (1), 360 (6), 216 (37), 191 (50), 154 (55), 133 (65), 73 (84), 60 (100); HRFABMS *m/z* 394.0287 (calcd for $C_{17}H_{20}{}^{35}Cl_4NO$, 394.0299).

3.3.11. Taveuniamide K (11). $[\alpha]_D^{25}$ +2.4° (*c* 0.1, $CHCl_3$); ORD $[\alpha]_{589}$ +2.4°, $[\alpha]_{578}$ +2.8°, $[\alpha]_{546}$ +2.4°, $[\alpha]_{436}$ +3.4°, $[\alpha]_{365}$ +10.0° (*c* 0.1, $CHCl_3$); UV (EtOH) λ_{max} 242 (18200), 246 (18200); IR ν_{max} (neat) 3280, 2215, 1640, 1580, 1400, 915, 890 cm^{-1}; ^1H NMR ($CDCl_3$, 600 MHz) δ 6.43 (1H, d, *J*=11.3 Hz, H-15), 6.36 (1H, d, *J*=8.6 Hz, H-2), 6.16 (1H, dd, *J*=12.7, 8.6 Hz, H-3), 5.89 (1H, dt, *J*=11.3, 1.7 Hz, H-14), 5.79 (1H, dt, *J*=12.7, 5.9 Hz, H-4), 5.07 (1H, d, *J*=7.5 Hz, NH), 3.94 (1H, m, H-8), 2.32 (2H, t, *J*=5.3 Hz, H-11), 2.13 (2H, m, H-5), 1.98 (3H, s, H-17), 1.60 (1H, m, H-9a), 1.42 (1H, m, H-9b), 1.56 (2H, m, H-10), 1.50 (1H, m, H-7a), 1.35 (1H, m, H-7b), 1.44 (2H, m, H-6); ^{13}C NMR see Table 2; GC-EIMS (70 eV) t_R=12.95 min, obs. *m/z* (rel. int) 361 (8), 326 (10), 220 (13), 175 (20), 148 (60), 113 (95), 99 (66), 77 (73), 60(100); HRFABMS *m/z* 362.0849 (calcd for $C_{17}H_{23}{}^{35}Cl_3NO$, 363.0845).

3.4. Brine shrimp toxicity assay

The screening for brine shrimp toxicity was performed using a slight modification of the original method.[24] Approximately fifteen hatched brine shrimp (*A. salina*) in ca. 0.5 mL seawater were added to each well containing different concentrations of sample in 50 μL of EtOH and 4.5 mL of artificial seawater to make a total volume of ca. 5 mL. Samples and controls were run in duplicate. After 24 h at 28 °C, the number of alive, immobile and dead brine shrimp were counted under a dissecting light microscope. The activity is expressed in terms of LD_{50} and ED_{50} to account for a significant number of brine shrimp which were alive but visually affected and their movements inhibited (Table 3).

Table 3. Brine shrimp toxicities of taveuniamides A–K (**1**–**11**) in μg/mL

Taveuniamide	Cmpd #	LD_{50}	ED_{50}
A	**1**	4.2	3.2
B	**2**	3.3	1.5
C	**3**	3.1	1.5
D	**4**	[a]	3.5
E	**5**	3.5	3.5
F	**6**	1.8	1.5
G	**7**	1.9	1.0
H	**8**	[a]	[a]
I	**9**	[a]	[a]
J	**10**	[a]	[a]
K	**11**	1.7	1.6

[a] Inactive.

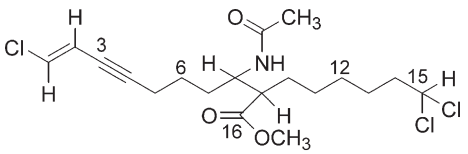

Taveuniamide A (**1**)

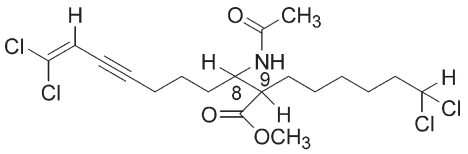

Taveuniamide B (**2**)

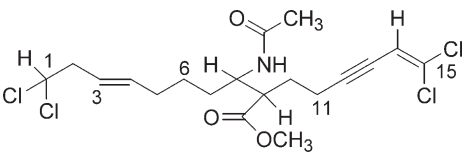

Taveuniamide C (**3**)

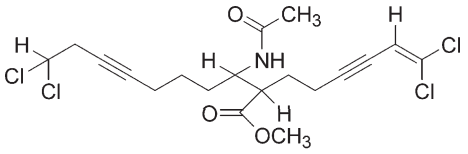

Taveuniamide D (**4**)

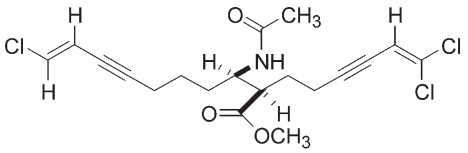

Taveuniamide E (**5**)

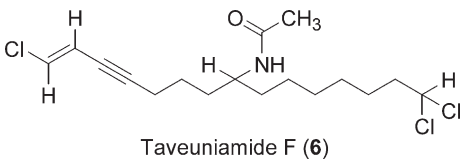

Taveuniamide F (**6**)

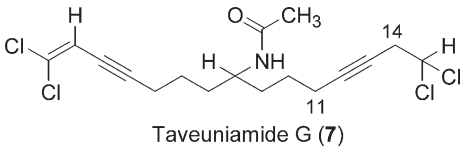

Taveuniamide G (**7**)

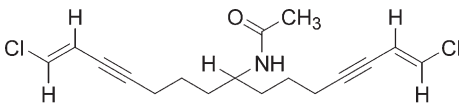

Taveuniamide H (**8**)

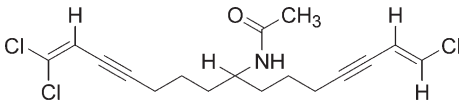

Taveuniamide I (**9**)

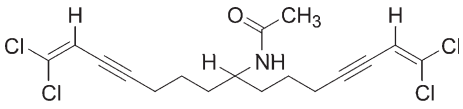

Taveuniamide J (**10**)

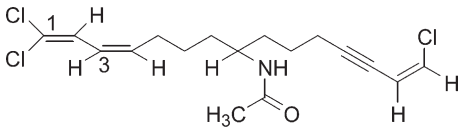

Taveuniamide K (**11**)

Acknowledgements

We thank the government of Fiji for permission to make these cyanobacterial collections, M. Graber and G. Hooper for making the collections, and K. McPhail for critically reading the manuscript. We thank V. Hsu and the Department of Biochemistry and Biophysics (OSU) for use of the Bruker 600 MHz NMR and R. Kohnert and the Department of Chemistry for use of the Bruker 300 and 400 MHz NMR instruments. We also gratefully acknowledge the OSU Environmental Health Sciences Center for use of the mass spectrometry facility. The MFBS Center at OSU (ES 03850) and NIH (GM 86354 and CA 52955) is acknowledged for financial support of this work.

References and notes

1. Gerwick, W. H.; Tan, L. T.; Sitachitta, N. *The Alkaloids*; Cordell, G. A., Ed.; Academic: San Diego, 2001; Vol. 57, pp 75–184.
2. Burja, A. M.; Banaigs, B.; Abou-Mansour, E.; Burgess, J. G.; Wright, P. C. *Tetrahedron* **2001**, *57*, 9347–9377.
3. Nogle, L. M.; Gerwick, W. H. *Org. Lett.* **2003**, *5*, 3–6.
4. Williams, P. G.; Yoshida, W. Y.; Moore, R. E.; Paul, V. J. *J. Nat. Prod.* **2003**, *66*, 1006–1009.
5. (a) Gerwick, W. H.; Proteau, P. J.; Nagle, D. G.; Hamel, E.; Blokhin, A.; Slate, D. L. *J. Org. Chem.* **1994**, *59*, 1243–1245. (b) Yoo, H. D.; Gerwick, W. H. *J. Nat. Prod.* **1995**, *58*, 1961–1965. (c) Marquez, B.; Verdier-Pinard, P.; Hamel, E.; Gerwick, W. H. *Phytochemistry* **1998**, *49*, 2387–2389.
6. (a) Orjala, J.; Nagle, D. G.; Gerwick, W. H. *J. Nat. Prod.* **1995**, *58*, 764–768. (b) Wu, M.; Milligan, K. E.; Gerwick, W. H. *Tetrahedron* **1997**, *53*, 15983–15990.
7. (a) Orjala, J.; Nagle, D. G.; Hsu, V. L.; Gerwick, W. H. *J. Am. Chem. Soc.* **1995**, *117*, 8281–8282. (b) Yokokawa, F.; Fujiwara, H.; Shiori, T. *Tetrahedron Lett.* **1999**, *40*, 1915.
8. Orjala, J.; Gerwick, W. H. *J. Nat. Prod.* **1996**, *59*, 427–430.
9. Hooper, G. J.; Orjala, J.; Schatzman, R. C.; Gerwick, W. H. *J. Nat. Prod.* **1998**, *61*, 529–533.
10. Sitachitta, N.; Gerwick, W. H. *J. Nat. Prod.* **1998**, *61*, 681–684.
11. Verdier-Pinard, P.; Sitachitta, N.; Rossi, J. V.; Sackett, D. L.; Gerwick, W. H.; Hamel, E. *Arch. Biochem. Biophys.* **1999**, *370*, 51–58.
12. Wipf, P.; Reeves, J. T.; Balachandran, R.; Day, B. W. *J. Med. Chem.* **2002**, *45*, 1901–1917.
13. Koehn, F. E.; Longley, R. E.; Reed, J. K. *J. Nat. Prod.* **1992**, *55*, 613–619.
14. Nagle, D. G.; Paul, V. J.; Roberts, M. A. *Tetrahedron Lett.* **1996**, *37*, 6263–6266.
15. (a) Marner, F. J.; Moore, R. E.; Hirotsu, K.; Clardy, J. *J. Org. Chem.* **1977**, *42*, 2815–2819. (b) Carter, D. C.; Moore, R. E.; Mynderse, J. S.; Niemczura, W. P.; Todd, J. S. *J. Org. Chem.* **1984**, *49*, 236–241.
16. (a) Cardellina, J. H., II; Marner, F. J.; Moore, R. E. *Science* **1979**, *204*, 193–195. (b) Aimi, N.; Odaka, H.; Skai, S. I.; Fujiki, H.; Suganuma, M.; Moore, R. E.; Patterson, G. M. L. *J. Nat. Prod.* **1990**, *53*, 1593–1596.
17. Orsini, M. A.; Pannell, L. K.; Erickson, K. L. *J. Nat. Prod.* **2001**, *64*, 572–577.
18. (a) Silverstein, R. M.; Bassler, G. C.; Morril, T. C. *Spectrometric Identification of Organic Compounds*; 4th ed.; Wiley: New York, 1981; p 35. (b) Silverstein, R. M.; Bassler, G. C.; Morril, T. C. *Spectrometric Identification of Organic Compounds*; 4th ed. Wiley: New York, 1981; p 235.
19. Breitmaier, E.; Voelter, W. *^{13}C NMR Spectroscopy*; 1st ed.; Chemie: Weinheim, 1974; p 129.
20. Gunther, H. *NMR Spectroscopy—Basic Principles, Concepts, and Application in Chemistry*; 2nd ed.; Wiley: New York, 1995; p 519.
21. Stott, K.; Keeler, J.; Van, Q. N.; Shaka, A. J. *J. Magn. Res.* **1997**, *125*, 302–304.
22. Matsumori, N.; Kaneno, D.; Murata, M.; Nakamura, H.; Tachibana, K. *J. Org. Chem.* **1999**, *64*, 866–876.
23. Williamson, R. T.; Marquez, B.; Kover, K. E.; Gerwick, W. H. *Magn. Res. Chem.* **2000**, *38*, 265–273.
24. Meyer, B. N.; Ferrigni, J. E.; Putnam, J. E.; Jacobson, L. B.; Nichols, D. E.; Mclaughlin, J. L. *Planta Med.* **1982**, *45*, 31–34.
25. Chang, Z.; Flatt, P.; Gerwick, W. H.; Nguyen, V.-A.; Willis, C. L.; Sherman, D. H. *Gene* **2002**, *296*, 235–247.

Available online at www.sciencedirect.com
SCIENCE DIRECT®
Tetrahedron 60 (2004) 7035–7039
Tetrahedron

Capisterones A and B from the tropical green alga *Penicillus capitatus*: unexpected anti-fungal defenses targeting the marine pathogen *Lindra thallasiae*

Melany P. Puglisi, Lik Tong Tan, Paul R. Jensen and William Fenical*

Center for Marine Biotechnology and Biomedicine, Scripps Institution of Oceanography, University of California, San Diego, La Jolla, CA 92093-0204, USA

Received 29 August 2003; revised 14 October 2003; accepted 14 October 2003

Available online 25 June 2004

Abstract—The mechanism by which marine algae show resistance to pathogenic microorganisms remains poorly understood. To examine the possible role that algal secondary metabolites play in the prevention of infection, we examined the abundant green alga *Penicillus capitatus*, one of the major shallow water algae found in the Tropical Atlantic Ocean. Both aqueous and EtOAc extracts of this alga were found to be potent inhibitors of the well-known marine algal pathogen *Lindra thallasiae*. Using *L. thallasiae* in bioassay-guided fractionation, we isolated two new triterpene sulfate esters, capisterones A (**1**) and B (**2**). The capisterones are potent inhibitors of *L. thallasiae* at natural and below natural concentrations. The structures of the capisterones, with relative stereochemistry only, were assigned by comprehensive spectral analyses that relied heavily on 2D NMR methods.

1. Introduction

There is clear evidence that pathogenic microorganisms pose a serious threat to the health of benthic marine organisms on coral reefs.[1] Although this threat can result in high levels of marine plant mortality over short periods of time,[2,3] episodic disease events appear to be rare occurrences suggesting that marine plants maintain effective defenses against disease causing microorganisms. While the mechanism of resistance remains poorly known, antibiotic activity, albeit generally not against marine pathogens, has been reported from some species.[4,5] Thus, we hypothesize that algal defenses may include the use of selectively-active secondary metabolites. Despite the observations of antimicrobial activities, there is little evidence that algal secondary metabolites target marine pathogens or are effective at naturally occurring concentrations.[6,7]

Recently, we initiated a program to investigate the hypothesis that marine plants produce secondary metabolites that function in antimicrobial chemical defense. Using bioassays developed to test the antibiotic activity of plant extracts and purified compounds against ecologically relevant and potentially harmful marine microorganisms, it has been possible to demonstrate that seagrass[8] and algal[9] metabolites effectively inhibit the growth of ecologically relevant microbial pathogens. Although algal secondary metabolite chemistry has been extensively studied, these assays have led to the discovery of unprecedented new compounds[9] and a better understanding of the potential ecological roles of algal metabolites in antimicrobial chemical defense.

In this study, we report the results of an investigation of the tropical green alga *Penicillus capitatus* (Bryopsidales) collected in the Bahamas. The crude aqueous and EtOAc extracts of this common Tropical Atlantic alga showed potent inhibition of the ubiquitous marine fungal pathogen *Lindra thallasiae*.[10,11] Using bioassay-guided fractionation, we isolated two new triterpene sulfate esters, capisterones A

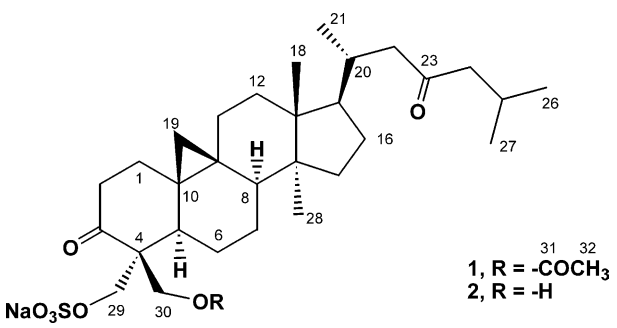

Keywords: *Penicillus capitatus*; *Lindra thallasiae*; Antifungal defense; Triterpenoid sulfate.
* Corresponding author. Tel.: +1-858-534-2133; fax: +1-858-558-3702; e-mail address: wfenical@ucsd.edu

0040–4020/$ - see front matter © 2004 Elsevier Ltd. All rights reserved.
doi:10.1016/j.tet.2003.10.131

(**1**) and B (**2**), which are solely responsible for the potent antifungal properties of this alga.

2. Results and discussion

Extracts of the green alga *P. capitatus* were identified as containing potent fungal growth inhibitors during a broad survey of anti-microbial activity in Caribbean algae (Puglisi et al. in preparation). The EtOAc and H_2O partitions from the crude extract displayed selective activity against the pathogen *L. thallasiae*, inhibiting growth by 97 and 100%, respectively, when tested at whole tissue (natural) concentrations. Capisterones A (**1**) and B (**2**) were isolated from the EtOAc-soluble material by multiple chromatographic steps involving C-18 reversed-phase VLC and HPLC methods. Additional quantities of capisterone B (**2**) were isolated in a similar manner from the H_2O partition.

Capisterone A (**1**), isolated as an amorphous white solid, gave an $[M]^+$ ion at *m/z* 639.2895 by high-resolution positive-ion MALDI-FTMS, thereby establishing the molecular formula of **1** as $C_{32}H_{49}NaO_8S$ (eight units of unsaturation). The IR spectrum of **1** displayed strong absorption bands at 1650 and 1250 cm^{-1} indicative of the presence of carbonyl and a sulfate groups, respectively.

Table 1. ^1H and ^{13}C NMR spectral data for capisterone A (**1**) in DMSO[a]

Position	^1H mult. (*J* in Hz)	^{13}C	HMBC
1a	1.52 m	31.7	C-9, C-10
1b	1.80 m		C-9, C-10
2a	2.19 m	37.9	C-4, C-10
2b	2.66 ddd (14.1, 6.3)		C-1, C-3
3		208.2	
4		56.0	
5	2.20 m	42.3	C-4, C-10, C-30
6	1.78 m	20.8	
7	1.20 m	25.7	C-6, C-8
8	1.54 m	47.1	C-9, C-10, C-14, C-28
9		21.3	
10		24.6	
11ab	1.23 m	25.7	C-8, C-9, C-13
12a	1.60 m	32.2	C-13, C-14, C-18
12b	1.80 m		C-13, C-14, C-18
13		44.7	
14		48.2	
15ab	1.27 m	35.0	C-16, C-28
16	1.26 m	27.7	
17	1.61 m	51.5	C-13, C-14, C-18
18	0.99 s	17.9	C-12, C-13, C-14, C-17
19ab	0.67 brs	29.1	C-1, C-5, C-7, C-8, C-9, C-10
20	1.82 m	32.0	
21	0.80 d	19.1	C-17, C-20, C-22
22a	2.41 brd (16.0)	49.7	C-21, C-23
22b	2.14 m		C-21, C-23
23		209.7	
24ab	2.26 d (7.2)	51.4	C-23, C-25, C-26, C-27
25	2.01 m	23.8	C-24
26	0.88 d (6.2)	22.2	C-24, C-25, C-27
27	0.84 d (6.2)	22.3	C-24, C-25, C-26
28	0.90 s	19.0	C-8, C-13, C-14, C-15
29a	3.71 d (9.9)	63.8	C-3, C-4, C-5
29b	4.09 d (9.9)		C-3, C-4, C-5
30a	4.03 d (11.7)	63.3	C-3, C-4, C-29, C-31
30b	4.70 d (11.7)		C-3, C-4, C-29, C-31
31		169.6	
32	1.92 s	20.4	C-31

[a] Spectra obtained at 400 MHz. Assignments were facilitated by DEPT, COSY and HMBC 2D NMR measurements.

Three carbonyl carbons were identified in the ^{13}C NMR spectrum of capisterone A, accounting for three units of unsaturation (Table 1). Four oxygens could be assigned to an ester and two ketones by interpretation of ^{13}C NMR data. The remaining four oxygens were assigned to a sulfate group. Using additional data derived by ^{13}C DEPT measurements, capisterone A was concluded to contain five quaternary carbons, one ester, two ketone carbonyls, five methine carbons, 13 methylene carbons and six methyl carbons, for a total of 32 carbons.

The planar structure of capisterone A (**1**) was established by the analysis of 1D and 2D NMR data (Table 1). The ^1H NMR spectrum was indicative of a steroidal-like structure with two methyl singlets (δ 0.90, δ 0.99) characteristic of methyl groups at the C–D ring juncture and three methyl doublets (δ 0.80, δ 0.84, δ 0.88) characteristic of the expected isoprene-derived side chain positioned on ring D. HMBC NMR correlations between the methyl proton at δ 0.99 (H_3-18) and C-12, C-13, C-14 and C-17 and between the methyl proton at δ 0.90 (H_3-28) and C-8, C-13, C-14 and C-15 further supported that the methyl singlets were attached to a ring juncture. The methyl group at δ 0.80 (H_3-21) showed HMBC correlations to C-17, C-20 and C-22. The location of a methyl group at C-20 was also established by ^1H NMR COSY correlations between δ 0.80 (H_3-21) and δ 1.82 (H-20). The methyl doublet at δ 0.84 (H_3-27) showed HMBC correlations with C-24, C-25, and C-26. The doublet methyl at δ 0.88 (H_3-26) showed HMBC correlations with C-24, C-25, and C-27. HMBC correlations between the methylene protons at H_2-22ab and H_2-24ab to the ketone functionality at C-23 provided the remaining data needed to establish the structure of the side chain. An HMBC correlation between H-20 and C-11 established the position of the side chain on ring D. Further evidence to support the position of the ketone at C-23 in the modified sterol side chain was the McLafferty rearrangement fragmentation ion ([M−*m/z* 43 (C_3H_7)]) observed in the negative EI-MS spectrum.[12]

Also prominent in the ^1H NMR spectrum were four downfield doublets belonging to two pairs of methylene protons at δ 3.71 (H-29a) and δ 4.09 (H-29b) and δ 4.03 (H-30a) and δ 4.70 (H-30b). These assignments were supported by HMQC and COSY correlations. All four protons showed HMBC correlations to the carbonyl at δ 208.2 (C-3) and the quaternary carbon at δ 56.0 (C-4) establishing a partial structure for a modified A-ring where the expected hydroxyl group at C-3 has been oxidized to the ketone functionality. The methylene protons at δ 4.03 and 4.70 also showed HMBC correlations to the acetate carbonyl at δ 169.9 (C-31). An HMBC correlation between the singlet methyl protons at δ 1.92 (H_3-32) and C-31 allowed the assignment of this methyl as part of the acetyl group. The methylene protons at δ 3.71 (H-29a) and δ 4.09 (H-29b) showed no further HMBC or COSY correlations. By the process of elimination, and considering the presence of a methylene carbon with a ^{13}C NMR shift of δ 63.8, the sulfate group was assigned to C-29. The chemical shift for this primary sulfate carbon (C-29), however, is considerably upfield shifted (δ 63.8) in comparison with an analogous structural array observed at δ 69.9 in a triterpenoid isolated from the green alga *Tydemannia*.[20] We rationalize this

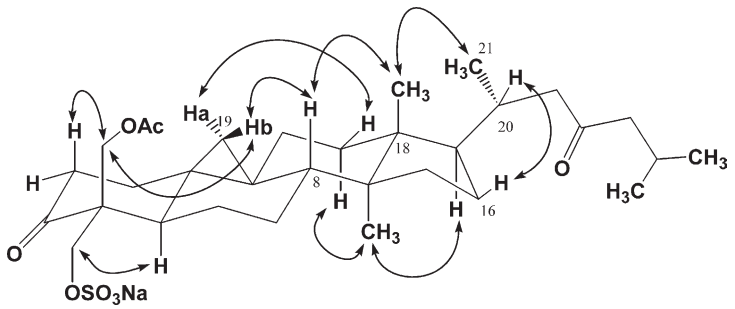

Figure 1.

shielding effect a as consequence of the proximate (C-30) acetoxyl functionality in capisterone A, which is lacking in this latter metabolite.

Another interesting chemical shift in the ^{1}H NMR spectrum of **1** was a broad upfield shifted methylene singlet at δ 0.67 (^{13}C NMR δ 29.1). When the ^{1}H NMR spectrum was acquired in CD_3OD, the broad singlet seen in the DMSO ^{1}H NMR spectrum split into two methylene doublets, δ 0.75 and δ 0.82 (J=3.9 Hz), characteristic of an isolated cyclopropyl methylene group in cycloartane-type triterpenes.[13–15] The methylene protons at δ 0.67 showed HMBC correlations to C-1, C-5, C-7, C-8, C-9, and C-10 establishing the cyclopropane ring at C-9 and C-10.

The relative stereochemistry of **1**, determined by the analysis of ROESY NMR data, was identical to the known cycloartanes (Fig. 1). The stereocenter at C-20 was assigned as R^* as expected for this class of triterpenoids. This was supported by ROESY correlations between δ 0.80 (H_3-21) and δ 0.99 (H_3-18), and between protons at δ 1.61 (H_2-16) on the D-ring to δ 1.82 (H-20) on the side chain of the molecule. The axial position of the cyclopropyl methylene group was supported by ROESY correlations between H_3-18 and H-8 as well as from H-8 to H_2-19. Additional ROESY correlations showed the carbon skeleton of capisterone A to possess typical *trans–anti* AB, BC and CD ring junctures, typical of the triterpenoids.

Capisterone B (**2**), isolated as a white amorphous solid, gave a $[M-Na]^+$ ion at m/z 550.6339 by high-resolution positive-ion MALDI-FTMS, thereby establishing the molecular formula of **2** as $C_{30}H_{47}NaO_7S$. The IR spectrum of **2** was identical to **1** except for a strong, broad absorbance band at 3400 cm^{-1} indicative of a hydroxyl group. The ^{1}H NMR spectrum (Table 2) of **2** differed from **1** by the appearance of a double doublet at δ 4.50 (OH-30, J=6.4, 11.6 Hz) coupled to the methylene protons on C-30, which split into quartets and shifted upfield to δ 3.55 and δ 4.05. In addition, the singlet methyl protons at δ 1.92 were no longer present. The ^{13}C NMR spectrum of **2** lacked the carbonyl at δ 169.6 and the methyl carbon at δ 20.4 in **1** that corresponded to the acetate ester. COSY correlations between OH-30 and the H_2-30ab methylene protons indicated that the acetate at C-30 was replaced by a hydroxyl group in capisterone B (**2**). This was confirmed by acetylation of **2**, which produced **1** in high yield.

Triterpenoids of the cycloartane class are common in terrestrial plants, most often occurring as glycosides,[16,17] but they are only rarely isolated from marine sources.[18–21] Exceptions include the related cycloartanol triterpene sulfate esters reported from the Indo Pacific green alga *Tydemania expeditionis*[20] and the red alga *Tricleocarpa fragilis*.[21] The triterpene sulfate esters from *T. expeditionis*[20] and *T. fragilis*[21] differ from the capisterones at C-3 by the substitution of a sulfate group. In addition, the compounds from *T. expeditionis* have a second sulfate group at C-29.[20] Comparison of 1D NMR chemical shifts of the present compounds with these related molecules confirmed the sterol core of the capisterones. While the compounds from *T. expeditionis* have been reported to inhibit protein tyrosine

Table 2. ^{1}H and ^{13}C NMR spectral data for capisterone B (**2**) in DMSO[a]

Position	^{1}H mult. (J in Hz)	^{13}C	HMBC
1a	1.52 m	32.0	C-9, C-10
1b	1.80 m		C-9, C-10
2a	2.19 m	38.1	C-4, C-10
2b	2.66 ddd (14.1, 6.3)		C-1, C-3
3		209.5	
4		58.6	
5	2.20 m	42.9	C-4, C-10, C-30
6	1.78 m	21.0	
7	1.20 m	25.9	C-6, C-8
8	1.54 m	47.1	C-9, C-10, C-14, C-28
9		21.0	
10		25.0	
11ab	1.23 m	25.9	C-8, C-9, C-13
12a	1.60 m	32.4	C-13, C-14, C-18
12b	1.80 m		C-13, C-14, C-18
13		44.8	
14		48.3	
15ab	1.27 m	35.0	C-16, C-28
16	1.26 m	27.7	
17	1.55 m	51.5	C-13, C-14, C-18
18	0.99 s	17.9	C-12, C-13, C-14, C-17
19ab	0.67 brs	29.4	C-1, C-5, C-7, C-8, C-9, C-10
20	1.82 m	32.0	C-17, C-20, C-22
21	0.80 d	19.1	C-21, C-23
22a	2.41 brd (16.0)	49.7	C-21, C-23
22b	2.14 m		
23		209.8	C-23, C-25, C-26, C-27
24ab	2.26 d (7.2)	51.4	C-24
25	2.01 m	23.8	C-24, C-25, C-27
26	0.88 d (6.2)	22.2	C-24, C-25, C-26
27	0.84 d (6.2)	22.4	C-8, C-13, C-14, C-15
28	0.90 s	19.0	C-3, C-4, C-5
29a	3.81 d (10)	64.9	C-3, C-4, C-5
29b	4.11 d (10)		C-3, C-4, C-29
30a	3.55 dd (5.6, 11.6, 16.8)	61.3	C-3, C-4, C-29
30b	4.05 dd (6.4, 10.8, 17.6)		
OH-30	4.50 t (6.4, 11.6)		

[a] Spectra obtained at 400 MHz. Assignments were facilitated by DEPT, COSY and HMBC 2D NMR measurements.

kinase pp60v-src,[20] the ecological function of cycloartane-type triterpenes in marine algae is unknown.

Tropical green algae in the order Bryopsidales, including those of the genera *Avrainvillea*, *Caulerpa*, *Halimeda*, *Penicillus*, and *Udotea*, *inter alia*, are noted for the production of sesqui- and diterpenoids.[22] A previous chemical investigation, in 1984, of *P. capitatus* from the same region of the Bahamas resulted in the isolation of a series of sesquiterpenoid enol acetates, **3** and **4**, which are representative of a widely-distributed class of metabolites in these green algae. Compounds **3** and **4** were reported to be active against the marine bacterium *Serratia marinorubra* and the marine fungi *Leptosphaeria* sp., *Lulworthia* sp., and *Alternaria* sp.[23] While these compounds showed some activity, their potencies were very poor in comparison with the antifungal properties of capisterones A and B. Curiously, although *P. capitatus* is very easily recognized, collections made more recently lacked the terpenoid enol acetate metabolites previously reported.

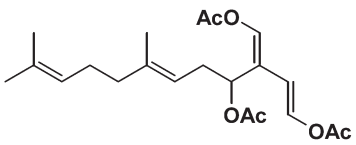

3

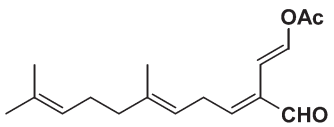

4

The discovery of the capisterones from this previously studied alga was unexpected and may be due to the highly selective activity of these compounds against *L. thallasiae*. This finding supports the use of diverse, ecologically meaningful test strains as a method of natural product discovery.

Capisterones A (**1**) and B (**2**) are potent antifungal compounds that have the potential to protect *P. capitatus* from the indiscriminate marine pathogen *L. thallasiae*. They inhibited the growth of this fungus at LD_{50} concentrations of 0.03 and 0.94 μg/mL, respectively. These concentrations are well below those at which the compounds occur in extracts of whole algal tissue (25 and 20 μg/mL, respectively). The substitution of a hydroxyl group for the acetyl group at C-30 in **1** decreased the LD_{50} approximately 30-fold indicating that the acetyl functionality is an part of the overall pharmacophore.

The results of this study provide further evidence that marine plants are chemically defended against potential pathogens. It seems clear that the continued application of ecologically relevant bioassays will lead to the discovery of new antimicrobial compounds and a better understanding of the role of these compounds in antimicrobial chemical defense.

3. Experimental

3.1. General procedures

The capisterones (**1** and **2**) were purified by HPLC using a Waters 6000A solvent delivery system coupled to a differential refractometer, a Waters model R401 detector. ^1H and ^{13}C NMR spectra were acquired using a Varian 400 MHz spectrometer, while all 2D NMR experiments were run using a Varian 300 MHz spectrometer. HRMS data were obtained from The Scripps Research Institute using an IonSpec FT mass spectrophotometer. IR spectra were acquired using a Perkin Elmer 1600 FTIR spectrophotometer. Optical rotations were measured using a Rudulph Autopol III polarimeter at 589 nm.

3.2. Algae collection

Approximately 25 individuals of *P. capitatus* (collection # BA01-13) were collected by hand, snorkeling on March 8, 2001 at Cat Cay, Bahamas at a depth of 5–10 in. behind a fringing reef. The algae were frozen, voucher specimens were prepared, and the preserved material was returned to Scripps Institution of Oceanography, San Diego, CA for extraction.

3.3. Extraction and isolation

The thawed algal material (360 mL by volume) was homogenized in acetone and subsequently extracted in MeOH and MeOH–CH_2Cl_2 (1:1, v/v) over 36 h. The extracts were filtered, combined, and the solvents removed in vacuo to yield a green residue, which was partitioned between EtOAc and H_2O. The EtOAc and H_2O partitions, at natural volumetric concentrations, inhibited the growth of *L. thallasiae* by 97 and 100%, respectively. The EtOAc partition (6.8 g) was fractionated using C-18 reversed-phase vacuum–liquid chromatography (VLC) employing a step-wise gradient solvent system of MeOH in H_2O followed by EtOAc in MeOH. Fractions eluting in 50 and 75% MeOH in H_2O inhibited the growth of *L. thallasiae* by 95%. These fractions were combined and further fractionated by C-18 reversed-phase VLC. The active fractions were then fractionated by C-18 (Dynamax 60A) HPLC, eluting with MeOH–H_2O (70:30), to yield capisterones A (**1**, 6.6 mg) and B (**2**, 3.0 mg). The H_2O partition (7.4 g) was fractionated by LH-20 chromatography (100% MeOH). The active fractions were combined and further fractionated by C-18 reversed-phase VLC. Fractionation by C-18 (Dynamax 60A) HPLC using MeOH–H_2O (50:50), yielded additional capisterone B (**2**, 3.0 mg).

3.3.1. Capisterone A (1). An amorphous solid, showed $[\alpha]_D^{25}$ −9.6° (*c* 1.9×10^{-2}, MeOH); IR (neat) ν_{max} 2520, 2150, 1650, 1455, 1250, 1088, 695 cm^{-1}; ^1H NMR (400 MHz, DMSO-d_6) and ^{13}C NMR (400 MHz, DMSO-d_6), see Table 1; EI-MS (negative) *m/z* 594 (100), 551 (15), 537 (47), 525 (35), 491 (36), 353 (5); HR-MALDI FTMS (positive ion, methanol) *m/z* 639.2895 (calcd for $C_{32}H_{49}NaO_8S$ [(M+Na)$^+$], 639.7739).

3.3.2. Capisterone B (2). An amorphous solid, showed $[\alpha]_D^{25}$ +0.19° (*c* 5.2×10^{-3}, MeOH); IR (neat) ν_{max} 3400,

2520, 2150, 1650, 1455, 1250, 1088, 695 cm^{-1}; ^1H NMR (400 MHz, DMSO-d_6) and ^{13}C NMR (400 MHz, DMSO-d_6), see Table 2; EI-MS (negative) *m/z* 593 (62), 551 (100), 527 (10), 513 (11), 481 (23), 423 (9); HR-MALDI FTMS (positive ion, methanol) *m/z* 550.6339 (calcd for $C_{30}H_{47}O_7S$ $[M-Na]^+$, 550.7492).

3.4. Acetylation of capisterone B (2)

To 0.5 mg of **2** were added three drops of pyridine followed by three drops of acetic anhydride. The reaction was stirred in a vial at room temperature for 16 h and the solvent was then removed in vacuo to yield capisterone B acetate in quantitative yield.

3.5. Antifungal assay

Extracts and pure compounds were assayed against the marine pathogen *L. thallasiae* as previously described.[9] Briefly, extracts were dissolved in methanol (final concentration 5%) and incorporated into YPM media (0.25% yeast, 0.25% peptone, 0.5% mannitol, 1 L seawater, 16 g agar) at natural volumetric concentrations of the whole algal tissue. The whole tissue concentration of the extract derived from *P. capitatus* was determined by solvent displaced with the algal mass, as measured in a graduated cylinder. Using this method, the volumetric concentration of the crude extract from *P. capitatus* was determined to be 39 mg/mL. The EtOAc and H_2O partitions were assayed at 19 and 21 mg/mL, respectively. Four hundred microlitres of extract-treated YPM media and controls (5% MeOH) were poured into 24-well plates. *L. thallasiae* was inoculated into the center of the control (solvent only) and treated wells. After 36–72 h, when the growth of the fungus in the control wells covered 100% of the agar surface, the treated wells were scored as percent of growth relative to the controls.

Acknowledgements

This work is the result of financial support from the National Science Foundation, Chemistry Division, under grant CHE 01-11270. We thank Professor Joseph Pawlik, University of North Carolina at Wilmington, for the opportunity to participate in an expedition to the Bahamas (funded by the NSF under grant # OCE-0095724), and Robert Feling for assistance with field collections.

References and notes

1. Harvell, C. D.; Kim, K.; Burkholder, J. M.; Colwell, R. R.; Epstein, P. R.; Grimes, D. J.; Hofmann, E. E.; Lipp, E. K.; Osterhaus, A. D. M. E.; Overstreet, R. M.; Porter, J. W.; Smith, G. W.; Vasta, G. R. *Science* **1999**, *285*, 1505–1510.
2. Littler, M. M.; Littler, D. S. *Science* **1995**, *267*, 1356–1360.
3. Martin, Y.; Bonnefont, J. L.; Chancerelle, L. *Water Res.* **2002**, *36*, 779–782.
4. Rinehart, K. L.; Shaw, P. D.; Shield, L. S.; Gloer, J. B.; Harbour, G. C.; Koker, M. E. S.; Samain, D.; Schwartz, R. E.; Tymiak, A. A.; Weller, D. L.; Carter, G. T.; Munro, M. H. G.; Hughes, J. R. G.; Renis, H. E.; Swynenberg, E. B.; Stringfellow, D. A.; Varva, J. J.; Coats, J. H.; Zurenko, G. E.; Kuentzel, S. L.; Li, L. H.; Bakus, G. J.; Brusca, R. C.; Craft, L. L.; Young, D. N.; Connor, J. L. *Pure Appl. Chem.* **1981**, *53*, 795–817.
5. Pesando, D. In *Introduction to Applied Phycology*; Akatsuka, I., Ed.; SPB Academic: The Hague, 1990; pp 3–26 Chapter 1.
6. Hay, M. E. *J. Exp. Mar. Biol. Ecol.* **1996**, *200*, 103–134.
7. Engel, S.; Jensen, P. R.; Fenical, W. *J. Chem. Ecol.* **2002**, *28*, 1971–1985.
8. Jensen, P. R.; Jenkins, K. M.; Porter, D.; Fenical, W. *Appl. Environ. Microbiol.* **1998**, *64*, 1490–1496.
9. Kubanek, J.; Jensen, P. R.; Keifer, P. A.; Sullards, C.; Fenical, W. *Proc. Natl. Acad. Sci.* **2003**, *100*(12), 6916–6921.
10. Kohlmeyer, J.; Kohlmeyer, E. *Marine Mycology: The Higher Fungi*; Academic: New York, 1979.
11. Miller, J. D.; Jones, E. B. G. *Bot. Mar.* **1983**, *26*, 345–351.
12. McLafferty, F. W. *Anal. Chem.* **1959**, *31*, 82–87.
13. Banskota, A. H.; Tezuka, Y.; Tran, K. Q.; Tenaka, K.; Saiki, I.; Kadota, S. *J. Nat. Prod.* **2000**, *63*, 57–64.
14. Gutierrez-Lugo, M.-T.; Singh, M. P.; Maiese, W. M.; Timmerman, B. N. *J. Nat. Prod.* **2002**, *65*, 872–875.
15. Ju, J.-h.; Liu, D.; Lin, G.; Zhang, Y.; Yang, J.; Lu, Y.; Gong, N.; Zheng, Q.-T. *J. Nat. Prod.* **2002**, *65*, 147–152.
16. Boar, R. B.; Romer, C. R. *Phytochemistry* **1975**, *14*, 5–6.
17. Kennelly, E. J.; Suttsri, R.; Kinghorn, A. D. *Adv. Exp. Med. Biol.* **1996**, *405*, 13–24.
18. Paul, V. J.; Fenical, W.; Raffii, S.; Clardy, J. *Tetrahedron Lett.* **1982**, *23*, 3459–3462.
19. Makarieva, T. N.; Stonik, V. A.; Kapustina, I. I.; Boguslavsky, V. M.; Dmitrenok, A. S.; Kalinin, V. I.; Cordeiro, M. L.; Djerassi, C. *Steroids* **1993**, *58*, 508–512.
20. Govindan, M.; Abbas, S. A.; Schmitz, F. J.; Lee, R. H.; Papkoff, J. S.; Slate, D. L. *J. Nat. Prod.* **1994**, *57*, 74–78.
21. Horgen, F. D.; Sakamoto, B.; Scheuer, P. J. *J. Nat. Prod.* **2000**, *63*, 210–216.
22. Faulkner, D. J. *Nat. Prod. Rep.* **2002**, *19*, 1–48, and references cited therein.
23. Paul, V. J.; Fenical, W. *Tetrahedron* **1984**, *40*, 2913–2918.

Available online at www.sciencedirect.com
SCIENCE DIRECT®
Tetrahedron 60 (2004) 7041–7048
Tetrahedron

Climacostol, a defense toxin of *Climacostomum virens* (protozoa, ciliata), and its congeners

Miyuki Eiraku Masaki,[a] Shouji Hiro,[a] Yoshinosuke Usuki,[a] Terue Harumoto,[b] Masayo Noda Terazima,[b] Federico Buonanno,[c] Akio Miyake[c] and Hideo Iio[a,*]

[a]*Department of Material Science, Graduate School of Science, Osaka City University, Osaka 558-8585, Japan*
[b]*Graduate School, Nara Women's University, Nara 630-8506, Japan*
[c]*Department of Molecular, Cellular and Animal Biology, University of Camerino, Camerino (MC) 62032, Italy*

Received 22 July 2003; revised 17 September 2003; accepted 17 September 2003

Available online 19 June 2004

Abstract—Climacostol (**1**), a defense toxin of the heterotrich ciliate *Climacostomum virens* was established as 5-(*Z*)-non-2-enyl-benzene-1,3-diol. The structure was rigorously confirmed by the total synthesis. The two congeners of climacostol contained in this ciliate were determined as 5-(*Z*,*Z*)-undeca-2,5-dienyl-benzene-1,3-diol (**2**) and 5-(*Z*,*Z*,*Z*)-undeca-2,5,8-trienyl-benzene-1,3-diol (**3**).

1. Introduction

The heterotrich ciliates *Stentor coeruleus* and *Blepharisma japonicum*, respectively, have a blue pigment stentorin[1] and red pigments blepharismins[2] in their extrusive organelles (pigment granules).[3] These pigments have been studied as photoreceptors,[4] but recently we showed that they also have the function of chemical defense against predators.[5] In another heterotrich ciliate *Climacostomum virens*, we found a defense toxin contained in its colorless extrusive organelles (cortical granules),[6] identified it as 5-(*Z*)-non-2-enyl-benzene-1,3-diol, and named it climacostol.[7] We also found that this ciliate has two congeners of climacostol. In this paper, we describe isolation, characterization and synthesis of climacostol and the structural elucidation of its congeners in detail.

2. Result and discussion

2.1. Isolation of climacostol and its congeners

Whole cells (0.8 mL) of *Climacostomum virens* were dipped in aqueous 75% EtOH (39 mL). After removal of the cells by filtration and concentration of the filtrate, the residue was partitioned between dichloromethane and water. From the organic layer, a biologically active fraction which is highly toxic against the raptorial ciliate *Dileptus margaritifer* was obtained by preparative TLC on silica gel developed with MeOH/CH_2Cl_2 7:93. The biologically active fraction contained climacostol and compounds **A** and **B**. The mixture were further purified by preparative TLC impregnated with 15% silver nitrate which was prepared in CH_3CN[8] (developing solvent MeOH/CH_2Cl_2 1:9) to give three fractions **A** (R_f value=0.31), **B** (R_f value=0.17) and **C** (R_f value=0.05). The fraction **A** (1.0 mg), the fraction **B** (0.1 mg) and the fraction **C** (0.2 mg) consisted, respectively, of mostly pure climacostol (**1**), a 1:1 mixture of **1** and new compound **2**, and mostly pure new compound **3**. We have quitted further purification of the fraction B due to its scarcity. LD_{50} of **1** for *D. margaritifer* (D3-I) was 0.71 μg/ml.[6]

2.2. Structure of climacostol and its congeners

The molecular formula of climacostol (**1**) was estimated as $C_{15}H_{22}O_2$ by high-resolution mass spectroscopy (HRMS): *m/z* $[M]^+$ found 234.1630, calcd 234.1620. In the preliminary study, the ^1H and ^{13}C NMR spectra of a mixture of climacostol (**1**), **2** and **3** had been recorded on the machine for 500 MHz, and the result was published in the preliminary paper.[7] Herein, pure climacostol (**1**) was submitted to measure the ^1H and ^{13}C NMR spectra on the machine for 600 MHz. The ^1H and ^{13}C NMR spectra (Table 1) showed the presence of two phenolic OH protons and the close resemblance of chemical shifts of the aromatic protons at δ 6.25 (2H, d, *J*=1.9 Hz, H-4, 6) and 6.18 (1H, t, *J*=1.9 Hz, H-2) and carbons at δ 156.8 (2C, C-1, 3), 144.4 (C-5), 108.0 (2C, C-4, 6) and 100.4 (C-2) of **1** to that of olivetol (5-pentyl-benzene-1,3-diol) suggested that **1** is a derivative of 5-alkenyl resorcinol. The $^1H-^1H$ COSY

Keywords: Biologically active compounds; Toxins; Phenols; Resorcinol; Cobalt compounds.
* Corresponding author. Tel.: +81-6-6605-2562; fax: +81-6-6605-3152; e-mail address: iio@sci.osaka-cu.ac.jp

0040–4020/$ - see front matter © 2004 Elsevier Ltd. All rights reserved.
doi:10.1016/j.tet.2003.09.105

Table 1. ^{1}H NMR (600 MHz) and ^{13}C NMR (150 MHz) data for climacostol (**1**) in $CDCl_3$

Position	δ_H	δ_C	COSY	HMBC	NOEsy
1,3	—	156.8 (2C)			
2	6.18 (1H, t, *J*=1.9 Hz)	100.4		1, 3, 4, 6	
4,6	6.25 (2H, d, *J*=1.9 Hz)	108.0 (2C)	1′	1, 2, 3, 1′	
5	—	144.4			
1′	3.28 (2H, d, *J*=6.1 Hz)	33.2	4, 6, 2′	4, 5, 6, 2′, 3′	4′
2′	5.50 (1H, m)	127.3	1′	1′, 4′	
3′	5.51 (1H, m)	131.5	4′	1′, 4′, 5′	
4′	2.11 (2H, q, *J*=6.9 Hz)	27.3	3′, 5′	2′, 3′, 5′	1′
5′	1.35–1.41 (2H, m)	29.7	4′	3′, 4′, 6′, 7′	
6′	1.25–1.34 (2H, m)	29.0		5′, 7′, 8′	
7′	1.25–1.34 (2H, m)	31.8		5′, 6′, 8′, 9′	
8′	1.25–1.34 (2H, m)	22.6	9′	6′, 7′, 9′	
9′	0.89 (3H, t, *J*=6.9 Hz)	14.1	8′	7′, 8′	
1,3 –OH	4.70 (2H, s)				

spectrum of **1** indicated that the presence of Ar–CH_2–CH=CH–CH_2. The olefinic protons at δ 5.50 (1H, m, H-2′) and 5.51 (1H, m, H-3′) were correlated with the protons at δ 3.28 (2H, d, *J*=6.1 Hz, H-1′) and 2.11 (2H, q, *J*=6.9 Hz, H-4′), which deduced the presence of a 2′-non-enyl group as the side chain attached to resorcinol at the 5-position. The side chain of **1**, in especially C-6′, 7′, 8′ was assigned by the HMQC and HMBC spectra (Table 1). The EI-MS/MS experiment was carried out in positive mode by choosing the $[M]^+$ ion (*m*/*z* 234) as the precursor ion. The fragment ion peaks of the EI-MS/MS spectrum were observed at *m*/*z* 219 $[M-CH_3]^+$, 205 $[M-C_2H_5]^+$, 191 $[M-C_3H_7]^+$, 177 $[M-C_4H_9]^+$, 163 $[M-C_5H_{11}]^+$, 149 $[M-C_6H_{13}]^+$, 124 $[M+H-CH=CHC_6H_{13}]^+$, which confirmed the presence of double bonds at $\Delta^{2,3}$ as shown in Figure 1. The *Z*-configuration of $\Delta^{2',3'}$-olefin was determined by the observation of NOE between the 1′- and 4′-methylene protons. Thus, the structure of a new toxic compound climacostol (**1**) was determined to be 5-(*Z*)-non-2-enyl-benzene-1,3-diol. Previously, the structure of 5-(*Z*)-heptadec-2-enyl-benzene-1,3-diol, a derivative of 5-(2′-alkenyl)-resorcinol, was reported as a possible dermatitis allergen from the latex of a mango.[9] The position of the olefin was assumed from the chemical shifts of ^{1}H NMR (CCl_4, 60 MHz) δ 5.33 (2H, br t, H-2′, 3′), 2.25–2.60 (2H, m, H-1′), 1.80–2.20 (2H, m, H-4′), and fragment peaks of MS. The incompatibility of the data to that of climacostol suggests the necessity of reinvestigating the structure of the compound from the mango. To our best knowledge, climacostol is the first example of 5-alkenylresorcinol having a double bond at the 2′-position.

Analysis of ^{1}H NMR for compound **2** was carried out in the 1:1 mixture of climacostol and **2**. The ^{1}H NMR spectra (Table 2) of **2** showed the presence of two phenolic OH protons, and the aromatic protons at δ 6.26 (2H, d, *J*=2.3 Hz, H-4, 6) and 6.18 (1H, t, *J*=2.3 Hz, H-2) suggested that **2** is also a derivative of 5-alkenyl resorcinol. The ^{1}H

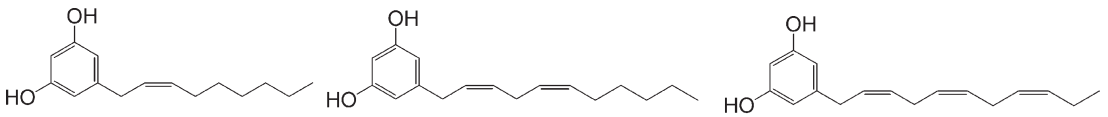

1 (Climacotol) **2** **3**

Figure 1. Climacostol and its congeners from *Climacostomum virens*.

Table 2. ^{1}H NMR (600 MHz) data of **2** and **3** in $CDCl_3$

	2		**3**		
Position	δ_H	NOEsy	δ_H	COSY	NOEsy
2	6.18 (1H, t, *J*=2.3 Hz)		6.19 (1H, t, *J*=2.3 Hz)	4,6	
4,6	6.26 (2H, d, *J*=2.3 Hz)		6.25 (2H, d, *J*=2.3 Hz)	2	1′
1′	3.31 (2H, d, *J*=6.3 Hz)	4′	3.32 (2H, d, *J*=6.6 Hz)	2′	6,4′
2′	5.47–5.56 (1H, m)		5.51–5.55 (1H, m)	1′	
3′	5.47–5.56 (1H, m)		5.51–5.55 (1H, m)	4′	
4′	2.87 (2H, t, *J*=6.5 Hz)	1′, 7′	2.91 (2H, t, *J*=5.6 Hz)	3′, 5′	1′, 7′
5′	5.34–5.44 (1H, m)		5.38–5.42 (1H, m)	4′	
6′	5.34–5.44 (1H, m)		5.38–5.42 (1H, m)	7′	
7′	2.04–2.08 (2H, m)	4′	2.82 (2H, t, *J*=5.5 Hz)	6′, 8′	4′, 10′[a]
8′	ND		5.31–5.36 (1H, m)	7′	
9′	ND		5.38–5.42 (1H, m)	10′	
10′	ND		2.06–2.08 (2H, m)	9′, 11′	7′[a]
11′	ND		0.97 (3H, t, *J*=7.5 Hz)	10′	
1,3 –OH	4.67 (2H, s)		4.68 (2H, s)		

ND, not determined.
[a] Observed in benzene-d_6.

NMR spectrum also showed the presence of the olefinic protons at δ 5.47–5.56 (2H, m, H-2′, 3′), 5.34–5.44 (2H, m, H-5′, 6′), the benzylic methylene protons at δ 3.31 (2H, d, *J*=6.3 Hz, H-1′), the double-allylic methylene protons at δ 2.87 (2H, t, *J*=6.5 Hz, H-4′), and the allylic methylene protons at δ 2.04–2.08 (2H, m, H-7′), indicating that the presence of a dienyl group as the side chain attached to resorcinol. Although the carbon length of **2** could not be determined from the ^{1}H NMR spectrum, comparison of the LC/ESI-MS/MS spectrum (vide infra) with that of **3** allowed us to elucidate the side chain of **2**. The LC/ESI-MS spectrum showed *m/z* 259 $[M-H]^-$ ion peak, which suggested the carbon length of the side chain as C11. The LC/ESI-MS/MS experiment was carried out on negative ions by choosing the $[M-H]^-$ ion (*m/z* 259) as the precursor ion. The fragment ion peaks of the LC/ESI-MS/MS spectrum were observed at *m/z* 244 $[M-H-CH_3]^-$, 230 $[M-H-C_2H_5]^-$, 215 $[M-2H-C_3H_7]^-$, 201 $[M-2H-C_4H_9]^-$, 187 $[M-2H-C_5H_{11}]^-$, 161 $[M-2H-CH{=}CHC_5H_{11}]^-$, 147 $[M-2H-CH_2CH{=}CHC_5H_{11}]^-$, 122 $[M-H-CH{=}CHCH_2CH{=}CHC_5H_{11}]^-$, 108 $[M-H-CH_2CH{=}CHCH_2CH{=}CHC_5H_{11}]^-$, which confirmed the presence of double bonds at $\Delta^{2,3}$ and $\Delta^{5,6}$ as shown in Figure 1. The configuration of the double bonds was determined to be both *cis* by the observation of NOE's between the 1′- and 4′-methylene protons, and the 4′- and 7′-methylene protons. Thus, the structure of **2** was established as 5-(*Z*,*Z*)-undeca-2,5-dienyl-benzene-1,3-diol.

The molecular formula of compound **3** was estimated as $C_{17}H_{21}O_2$ by FAB-HRMS (*m/z* $[M-H]^-$ found 257.1528 calcd 257.1542). The ^{1}H NMR spectra (Table 2) showed the presence of two phenolic OH protons, and the aromatic protons at δ 6.25 (2H, d, *J*=2.3 Hz, H-4, 6) and 6.19 (1H, t, *J*=2.3 Hz, H-2), suggested that **3** is also a derivative of 5-alkenyl resorcinol. The ^{1}H–^{1}H COSY NMR spectrum of **3** showed that the olefinic proton at δ 5.51–5.55 (1H, m, H-2′), the olefinic protons at δ 5.51–5.55 (1H, m, H-3′) and 5.38–5.42 (1H, m, H-5′), the olefinic protons at δ 5.38–5.42 (1H, m, H-6′) and 5.31–5.36 (1H, m, H-8′), and the olefinic proton at δ 5.38–5.42 (1H, m, H-9′) were correlated, respectively, to the benzylic protons at δ 3.32 (2H, d, *J*=6.6 Hz, H-1′), the double-allylic methylene protons at δ 2.91 (2H, t, *J*=5.6 Hz, H-4′), the double-allylic methylene protons at δ 2.82 (2H, t, *J*=5.5 Hz, H-7′), and the allylic methylene protons at δ 2.06–2.08 (2H, m, H-10′), which suggested the side chain of **3** is the skipped triene at $\Delta^{2',3'}$, $\Delta^{5',6'}$ and $\Delta^{8',9'}$ with the carbon length of C11. The protons at δ 2.06–2.08 (2H, m, H-10′) and the triplet protons at δ 0.97 (3H, t, *J*=7.5 Hz, H-11′) showed the terminal ethyl function. Thus, the undeca-2′,5′,8′-trienyl group is added to resorcinol at the 5-position as the side chain. The *Z*-configuration of $\Delta^{2',3'}$-olefin, $\Delta^{5',6'}$-olefin and $\Delta^{8',9'}$-olefin were determined, respectively, by the observation of NOE between the 1′- and 4′-protons, 4′- and 7′-protons, and 7′- and 10′-protons. The proposed structure was further supported by LC/ESI-MS/MS spectrum. The LC/ESI-MS/MS experiment was carried out on negative ions by choosing the $[M-H]^-$ ion (*m/z* 257) as the precursor ion. The fragment peaks in the LC/ESI-MS/MS spectrum of **3** were observed at *m/z* 227 $[M-2H-C_2H_5]^-$, 202 $[M-H-CH{=}CHC_2H_5]^-$, 187 $[M-2H-CH_2-CH{=}CHC_2H_5]^-$, 161 $[M-2H-CH{=}CHCH_2CH{=}CHC_2H_5]^-$, 147 $[M-2H-CH_2CH{=}CHCH_2CH{=}CHC_2H_5]^-$, 122 $[M-H-CH{=}CHCH_2CH{=}CHCH_2CH{=}CHC_2H_5]^-$, 108 $[M-H-CH_2CH{=}CHCH_2CH{=}CHCH_2CH{=}CHC_2H_5]^-$, which confirmed the position of three olefins at $\Delta^{2',3'}$, $\Delta^{5',6'}$ and $\Delta^{8',9'}$. Thus, the structure of **3** was determined to be 5-(*Z*,*Z*,*Z*)-undeca-2,5,8-trienyl-benzene-1,3-diol.

2.3. Synthesis of climacostol

The structure and biological activity of climacostol were confirmed by the synthesis of **1**.[10] The synthesis of climacostol (**1**) was achieved in six steps (Scheme 1). Phenolic hydroxyl groups of commercially available 3,5-dihydroxybenzaldehyde was protected with *tert*-butyldimethylsilyl groups, and reacted with 1-octyne using *n*-BuLi at −78 °C to give the acetylenic adduct **5** in 91% yield. Reductive removal of the hydroxyl group at C1′ of the adduct **5** was unsuccessful, because of migration of the unsaturated bond. The triple bond of **5** was protected by treatment with dicobalt octacarbonyl to afford the corresponding cobalt complex **6** in 64% yield. The hydroxyl group at the benzylic position of **6** was activated by complexation of triple bond with dicobalt octacarbonyl and the reduction of the hydroxyl group with triethylsilane in the presence of $BF_3{\cdot}OEt_2$[11] proceeded to afford **7** in 89% yield.

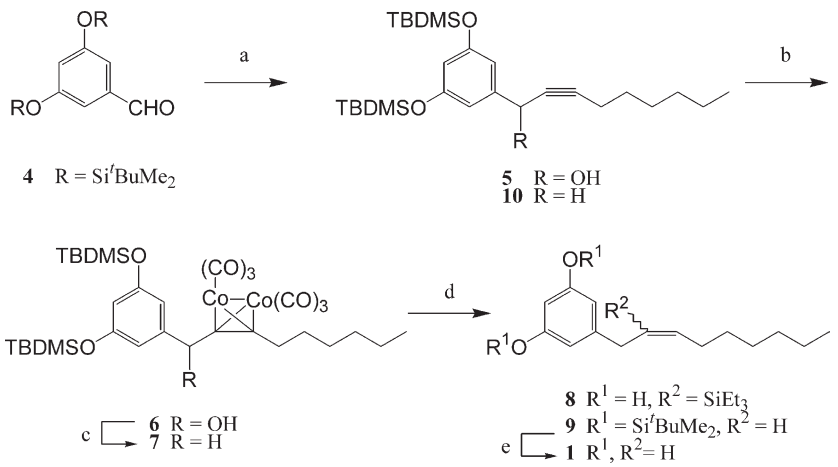

Scheme 1. Reagents and conditions. (a) 1-octyne, *n*-BuLi, THF, −78 °C, 91%. (b) $Co_2(CO)_8$, Et_2O, −20 °C→25 °C, 64%. (c) Et_3SiH, $BF_3{\cdot}OEt_2$, CH_2Cl_2, 89%. (d) *n*-Bu_3SnH, benzene, 65 °C, 93%. (e) 70% HF·pyridine, THF, 86%.

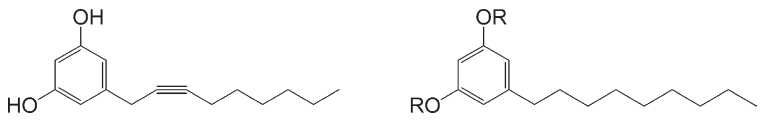

11

12 R = Si^{t}BuMe$_2$
13 R = H

Figure 2. Synthetic analogues of climacostol.

In this reaction, a regio- and stereoselective hydrosilylation product was also formed as a minor side product, whose structure was confirmed by leading to **8**. The configuration of the olefin in **8** has not been determined. The hydrosilylation of an acetylene cobalt complex was also reported by Isobe et al.[12] The *Z*-olefin **9** was obtained by reductive decomplexation of the cobalt carbonyl under the Isobe's conditions[13] in 93%. Climacostol (**1**) was finally synthesized by deprotection of the silyl group of **9** in HF·pyridine. Synthetic climacostol (**1**) exhibited identical properties to those for the natural product. The toxic activity against *D. margaritifer* was as high as that of the natural product. Recently, Mori et al. reported a simpler synthesis of climacostol based on the Wittig reaction method starting from [3,5-bis-(*tert*-butyl-dimethyl-silanyloxy)-phenyl]-acetic acid methyl ester.[14]

The alkynyl and alkyl derivatives of climacostol were also synthesized from **7** and **9**, respectively, in order to do the biological evaluation. Thus, **7** was oxidized with I_2 to yield **10** in 90% yield, followed by deprotection of the silyl group by HF·pyridine to afford the alkynyl derivative **11** in quantitative yield. *Z*-olefin **9** was reduced with 10 wt% palladium-on-charcoal as a catalyst to give **12** in 80% yield, and deprotection of the silyl group afforded the alkyl derivatives **13** in 83% yield (Fig. 2).

2.4. The biosynthesis and the biological activity of climacostol

We consider that there is a close relation between the biosynthesis of climacostol and that of stentorin, a toxic pigment from *Stentor coeruleus*, though the chemical structure of them is considerably different to each other. A hypothetical pathway for the biosynthesis of long-chain resorcinolic lipids[15] would be also true for the biosynthesis of climacostol and its congeners. Namely, climacostol (C_{15}) and its congeners (C_{17}) would be synthesized from the C_{16}- and C_{18}-polyketide, respectively, with the cyclization and the decarboxylation, as shown in Figure 3. Stentorin is also likely generated from C_{16}-polyketide accompanied by the addition reaction of C_1 to form isopropyl group resulting 2,4,5,7-tetrahydroxy-3-isopropylanthrone, and followed by the dimerization reaction of the anthrone.[2a,16] The finding of

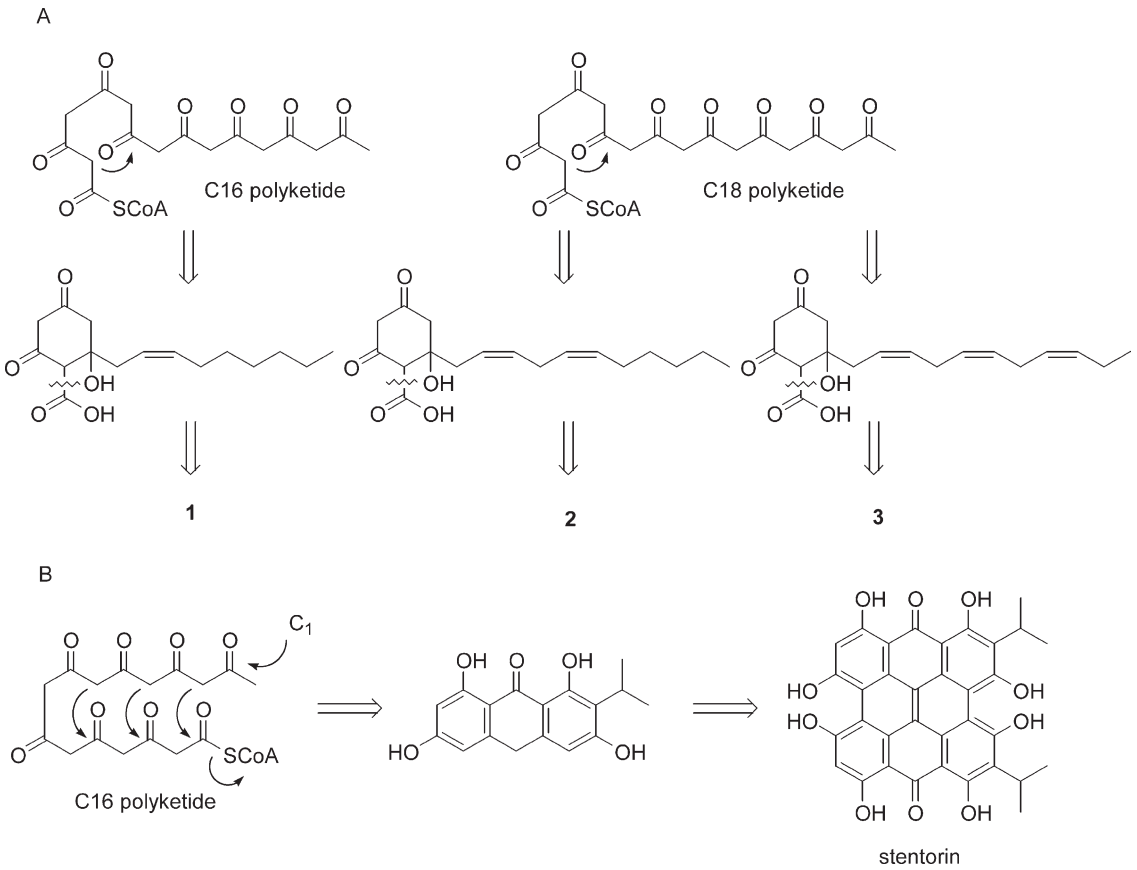

Figure 3. The putative biosynthesis of climacostol (**1**) and its congeners, and stentorin.

climacostol as defense toxin of *C. virens* is consisting with the suggestion that the primary function of stentorin and blepharismin is the defense against the predator rather than photoreception.[5b,17]

Cell–cell interaction by means of extrusomes (extrusive organelles in protist) in ciliates was reviewed by Miyake.[17] Secondary metabolites of ciliates were scarcely studied except the pigments mentioned above, keronopsin from *Pseudokeronopsis rubra*,[18] and euplotin,[19] raikovenal[20] and epoxyfocardin[21] from *Euplotes* species. The structure, synthesis and biological activity of resorcinolic lipids were recently reviewed in detail.[15,22] More than 100 of 5-alkyl and 5-alkenylresorcinol homologues have been found mainly from a variety of higher plants, including those in the *Proteaceae*, *Anacardiaceae*, *Ginkogoaceaen* and *Graminae* families, but rarely found in animal and microorganism. Resorcinolic lipids are reported to show significant biological activities,[15,22] including antibacterial, antiparasitic and cytotoxic activity as growth regulator, inhibition of DNA and RNA synthesis,[23] inhibitory effect on enzymes,[24] nematicidal activities,[25] interaction with biological membranes, and as modulator of lipid oxidation. In recent studies, climacostol was found to cleave DNA in the presence of $CuCl_2$,[26] and also climacostol specifically inhibits the respiratory chain complex I in mitochondria.[27]

Biological activities including lethal toxicity against the predatory ciliate *D. margaritiefer* of the congeners **2** and **3**, and the synthetic alkyl and alkynyl derivatives will be reported in due course.

3. Conclusion

A potent toxin against *D. margaritifer* was found in the 75% ethanol extract of *C. virens*. A new toxin climacostol of *C. virens*, a lethal toxin against the predator, was isolated and its structure was determined. The two congeners of climacostol were also isolated and their structures were determined. Furthermore, the synthesis of climacostol was carried out and the structure of the natural product was confirmed.

4. Experimental

4.1. General

^1H and ^{13}C NMR spectra were recorded on a Bruker DRX-600 for 600 MHz, Varian Unity-500 for 500 MHz, JEOL JNM-LA400 for 400 MHz or JEOL JNM-LA300 for 300 MHz. Chemical shifts (δ) are given in ppm relative to tetramethysilane (δ 0.00) or $CHCl_3$ (δ 7.26) for ^1H NMR and δ 77.0 for ^{13}C NMR as internal standard. Mass spectra were obtained on a JEOL JMS-700T. IR spectra were obtained on a JUSCO A-100. Reaction solvents were reagent grade. Diethyl ether and tetrahydrofuran (THF) were distilled from sodium benzophenone ketyl. Dichloromethane (CH_2Cl_2) was distilled from phosphorous oxide. Dimethyformamide (DMF) was distilled from calcium hydride. Analytical thin-layer chromatography (TLC) was performed on Merck silica gel plates (Art5715 Kiesel gel $60F_{254}$ 0.25 mm), and preparative TLC was done on Merck silica gel plates (Art5744 Kiesel gel $60F_{254}$ 0.5 mm). Silica gel column chromatography was carried out on Daisogel IR-60 (63/210 μm).

4.2. Microbial material

Stock W-24 of *Climacostomum virens*, provided by Dr. Tavrovskaya (see Acknowledgement), was originally green due to symbiotic algae. By culturing in the dark, colorless clones (200–300 μm in length, 150–200 μm in width) were obtained. Stock D3-I of *D. margaritifer* (ca. 800 μm in length, ca. 60 μm in width) formerly *D. anser*, provided by Dr. Tavrovskaya, was used as a predator of *C. virens*. Both ciliates were grown on *Sathrophilus* sp., a small ciliate grown on the boiled lettuce medium, and concentrated by centrifugation, washed by and suspended in SMB-III,[28] a balanced salt solution (called SMB below).[6] Culture, handling of ciliates and experiments were performed at 24±1 °C.

4.3. Biological assay

Toxicity-test of climacostol: Ten cells of a ciliate were placed in 250 μL of SMB solution of climacostol of various concentrations, kept in a dark moist chamber, and the number of surviving cells were counted after 24 h. The LD_{50} concentration of climacostol for a ciliate was obtained based on the concentration–survival curve of the ciliate. At the late stage of this work, we noticed that the way to dilute the stock solution of climacostol (5 mg/mL ethanol solution) influences the result of toxicity measurement of climacostol. For example, if the ethanol solution was first diluted at 100, 10, and 5 μg/mL and then further diluted, measured LD_{50} concentrations for *D. margaritifer* (D3-I) were 1.8, 0.88, and 0.71 μg/mL, respectively.[6]

4.4. Extraction and isolation

Whole cells (0.8 mL) of *Climacostomum virens* were dipped in aqueous 75% EtOH (39 mL). After removal of the cells by filtration, the EtOH solution was concentrated under the reduced pressure. To the residue was added water and then extracted with CH_2Cl_2. The organic layer was washed with brine, dried over Na_2SO_4 and evaporated under reduced pressure. The residue was subjected to the preparative TLC (developed with MeOH/CH_2Cl_2, 7:93), and then eluted with MeOH/CH_2Cl_2, 1:4. The biologically active fraction was further purified by the preparative TLC impregnated with 15% silver nitrate which was prepared in CH_3CN.[8] The residue was dissolved in CH_2Cl_2, charged on the preparative TLC impregnated with 15% silver nitrate in CH_3CN. The plate was developed with MeOH/CH_2Cl_2, 1:9. Three fractions were observed by 2.5% $FeCl_3{\cdot}6H_2O$ in EtOH. Each of fractions was scraped off and eluted with MeOH/CH_2Cl_2, 1:4 to give climacostol (**1**) (1.0 mg, R_f value=0.31), a 1:1 mixture of **1** and **2** (0.1 mg, R_f value=0.17), and **3** (0.2 mg, R_f value=0.05).

4.4.1. Climacostol (1). ^1H NMR ($CDCl_3$, 600 MHz) and ^{13}C NMR ($CDCl_3$, 150 MHz), see Table 1; EI-MS *m/z* 234 $[M]^+$; EI-MS/MS *m/z* 219 $[M-CH_3]^+$, 205 $[M-C_2H_5]^+$, 191 $[M-C_3H_7]^+$, 177 $[M-C_4H_9]^+$, 163 $[M-C_5H_{11}]^+$, 149

$[M-C_6H_{13}]^+$, 124 $[M+H-CH{=}CHC_6H_{13}]^+$. HRMS (FAB^+) calcd for $C_{15}H_{22}O_2$ $[M]^+$ 234.1620, found 234.1630.

4.4.2. 5-(*Z*,*Z*)-Undeca-2,5-dienyl-benzene-1,3-diol (2). ^1H NMR ($CDCl_3$, 600 MHz), see Table 2; LC/ESI-MS (in negative mode) *m/z* 259 $[M-H]^-$; LC/ESI-MS/MS (in negative mode) *m/z* 244 $[M-H-CH_3]^-$, 230 $[M-H-C_2H_5]^-$, 215 $[M-2H-C_3H_7]^-$, 201 $[M-2H-C_4H_9]^-$, 187 $[M-2H-C_5H_{11}]^-$, 161 $[M-2H-CH{=}CHC_5H_{11}]^-$, 147 $[M-2H-CH_2CH{=}CHC_5H_{11}]^-$, 122 $[M-H-CH{=}CHCH_2CH{=}CHC_5H_{11}]^-$, 108 $[M-H-CH_2CH{=}CHCH_2CH{=}CHC_5H_{11}]^-$. HRMS ($EI^+$) calcd for $C_{17}H_{24}O_2$ $[M]^+$ 260.1776, found 260.1763.

4.4.3. 5-(*Z*,*Z*,*Z*)-Undeca-2,5,8-trienyl-benzene-1,3-diol (3). ^1H NMR ($CDCl_3$, 600 MHz), see Table 2; LC/ESI-MS (in negative mode) *m/z* 257 $[M-H]^-$; LC/ESI-MS/MS (in negative mode) *m/z* 227 $[M-2H-C_2H_5]^-$, 202 $[M-H-CH{=}CHC_2H_5]^-$, 187 $[M-2H-CH_2CH{=}CHC_2H_5]^-$, 161 $[M-2H-CH{=}CHCH_2CH{=}CHC_2H_5]^-$, 147 $[M-2H-CH_2CH{=}CHCH_2CH{=}CHC_2H_5]^-$, 122 $[M-H-CH{=}CHCH_2CH{=}CHCH_2CH{=}CHC_2H_5]^-$, 108 $[M-H-CH_2CH{=}CHCH_2CH{=}CHCH_2CH{=}CHC_2H_5]^-$. HRMS ($FAB^-$) calcd for $C_{17}H_{21}O_2$ $[M-H]^-$ 257.1542, found 257.1528.

4.5. Synthesis of climacostol and its derivatives

4.5.1. 1-[3,5-Bis-(*tert*-butyl-dimethyl-silanyloxy)-phenyl]-non-2-yn-1-ol (5). 1-Octyne (720 mg, 6.5 mmol) was dissolved in THF (13 mL) and cooled to −78 °C under an argon atmosphere, and *n*-BuLi (1.6 M solution in hexane, 3.4 mL, 5.5 mmol) was added dropwise. After the mixture was stirred for 1.5 h at −78 °C, a solution of 3,5-bis-(*tert*-butyl-dimethyl-silanyloxy)-benzaldehyde (**4**) (2.0 g, 5.5 mmol) in THF (10 mL) was added at −78 °C. The reaction temperature was gradually raised to 25 °C and stirred overnight. To the reaction mixture was added saturated aqueous NH_4Cl and extracted with diethyl ether. The organic layer was washed with brine, and dried over Na_2SO_4. The solvent was removed under reduced pressure to give **5** (2.36 g, 91%): ^1H NMR ($CDCl_3$, 400 MHz) δ 6.66 (2H, d, *J*=2.2 Hz, H-2, 6), 6.28 (1H, t, *J*=2.2 Hz, H-4), 5.31 (1H, br s, H-1′), 2.263 (1H, t, *J*=7.1 Hz, H-4′), 2.258 (1H, t, *J*=7.1 Hz, H-4′), 2.04 (1H, br s, 1′-OH), 1.50–1.57 (2H, m, H-5′), 1.36–1.43 (2H, m), 1.26–1.34 (4H, m), 0.98 (18H, s, Si–C$(CH_3)_3$), 0.88 (3H, H-9′), 0.20 (12H, s, Si–CH_3); ^{13}C NMR ($CDCl_3$, 100 MHz) δ 156.6 (2C), 143.3, 111.70, 111.65 (2C), 87.4, 79.8, 64.6, 31.3, 28.6 (2C), 25.7 (6C), 22.5, 18.8, 18.2 (2C), 14.0, −4.4 (4C); IR (neat) 2980, 2955, 2925, 2880, 1605, 1465, 1405, 1380, 1350, 1270, 1175, 1040, 1015, 990, 950, 840, 790, 750, 690, 675 cm^{-1}; EI-MS *m/z* 476 $[M]^+$; HRMS (FAB^+) calcd for $C_{27}H_{48}O_3Si_2$ $[M]^+$ 476.3142, found 476.3157.

4.5.2. 1-[3,5-Bis-(*tert*-butyl-dimethyl-silanyloxy)-phenyl]-non-2-yn-1-ol cobalt complex (6). To a solution of **5** (2 g, 4.2 mmol) in diethyl ether (5 mL) was added a solution of $Co_2(CO)_8$ (2.1 g, 6.1 mmol) in diethyl ether (20 mL) at −20 °C under an argon atmosphere. The cooling bath was removed and the reaction mixture was stirred for 17.5 h at room temperature. The reaction mixture was washed with 1 M HCl. The organic layer was dried over Na_2SO_4, evaporated under reduced pressure, and the residue was purified by silica gel column chromatography (*n*-hexane/AcOEt, 9:1) to give **6** (2.06 g, 64%): ^1H NMR ($CDCl_3$, 400 MHz) δ 6.54 (2H, d, *J*=1.7 Hz, H-2, 6), 6.23 (1H, t, *J*=1.7 Hz, H-4), 5.76 (1H, d, *J*=3.2 Hz, H-1′), 2.77 (1H, t, *J*=5.6 Hz, H-4′), 2.74 (1H, t, *J*=6.0 Hz, H-4′), 2.23 (1H, d, *J*=3.2 Hz, –OH), 1.58–1.69 (2H, m, H-5′), 1.42–1.49 (2H, m), 1.31–1.38 (4H, m), 0.98 (18H, s, Si–C$(CH_3)_3$), 0.91 (3H, t, *J*=7.1 Hz, H-9′), 0.185 (6H, s, Si–CH_3), 0.179 (6H, s, Si–CH_3); ^{13}C NMR ($CDCl_3$, 100 MHz) δ 199.9 (3C), 199.5 (3C), 156.8 (2C), 146.2, 111.6, 110.3 (2C), 101.5, 98.9, 73.9, 33.7, 31.9, 31.6, 29.3, 25.6 (6C), 22.6, 18.2 (2C), 14.0, −4.4 (4C); IR (nujol) 2975, 2950, 2880, 2120, 2080, 2050, 1603, 1470, 1390, 1350, 1265, 1180, 1040, 1020, 845, 790, 730 cm^{-1}; FAB-MS *m/z* 678 $[M-3CO]^+$ 650 $[M-4CO]^+$, 622 $[M-5CO]^+$, 594 $[M-6CO]^+$; HRMS (FAB^+) calcd for $C_{30}H_{48}O_6Si_2Co_2$ $[M-3CO]^+$ 678.1653, found 678.1664.

4.5.3. 1,3-Bis-(*tert*-butyl-dimethyl-silanyloxy)-5-non-2-ynyl-benzene cobalt complex (7). To a solution of **6** (1.1 g, 1.4 mmol) and Et_3SiH (0.22 mL, 1.4 mmol) in CH_2Cl_2 (14 mL) was added $BF_3{\cdot}OEt_2$ (0.16 mL, 1.4 mmol) dropwise under the argon atmosphere. After the mixture was refluxed for 30 min, the reaction mixture was added to saturated aqueous $NaHCO_3$, extracted with CH_2Cl_2. The organic layer was washed with brine, dried over Na_2SO_4, and the solvent was removed under reduced pressure to give **7** (960 mg, 89%), and the hydrosilylation product as a minor product whose *tert*-butyldimethysilyl groups were removed by HF·pyridine to afford **8**; data for **7**: ^1H NMR ($CDCl_3$, 400 MHz) δ 6.36 (2H, d, *J*=2.1 Hz, H-4,6), 6.22 (1H, t, *J*=2.1 Hz, H-2), 3.95 (2H, s, H-1′), 2.78–2.82 (2H, m, H-4′), 1.59–1.67 (2H, m, H-5′), 1.42–1.48 (2H, m), 1.31–1.37 (4H, m), 0.98 (18H, s, Si–C$(CH_3)_3$), 0.91 (3H, t, *J*=7.3 Hz, H-9′), 0.18 (12H, s, Si–CH_3); ^{13}C NMR ($CDCl_3$, 100 MHz) δ 199.9 (3C), 199.5 (3C), 156.75, 156.67, 146.1, 111.5, 110.3 (2C), 101.5, 98.9, 73.9, 33.9, 31.9, 31.6, 29.3, 25.6 (6C), 22.6, 18.1 (2C), 14.0, −4.5 (4C); IR (nujol) 2975, 2950, 2880, 2120, 2075, 2050, 1603, 1480, 1470, 1390, 1350, 1265, 1180, 1040, 1020, 840, 790 cm^{-1}; FAB-MS *m/z* 662 $[M-3CO]^+$, 635 $[M-3CO+H]^+$, 606 $[M-5CO]^+$, 461 $[M-Co_2(CO)_6+H]^+$; HRMS (FAB^+) calcd for $C_{30}H_{48}O_5Si_2Co_2$ $[M-3CO]^+$ 662.1704, found 662.1714; data for **8**: ^1H NMR ($CDCl_3$, 400 MHz) δ 6.20 (2H, d, *J*=1.7 Hz, H-4,6), 6.15 (1H, t, *J*=1.7 Hz, H-2), 5.92 (2H, t, *J*=6.8 Hz, H-3′), 4.66 (2H, s, OH), 3.37 (2H, s, H-1′), 2.14 (2H, q, *J*=6.8 Hz, H-4′), 1.37–1.45 (2H, m, H-5′), 1.20–1.30 (6H, m, H-6′, 7′, 8′), 0.87 (3H, t, *J*=7.1 Hz, H-9′), 0.83 (9H, t, *J*=7.9 Hz, Si–CH_2CH_3), 0.46 (6H, q, *J*=7.9 Hz, Si–CH_2CH_3).

4.5.4. 1,3-Bis-(*tert*-butyl-dimethyl-silanyloxy)-5-non-2-enyl-benzene (9). To a solution of **7** (130 mg, 0.17 mmol) in benzene (1.7 mL) was added *n*-Bu_3SnH (0.09 mL, 0.34 mmol). After the reaction mixture was stirred for 3 h at 65 °C, the solvent was evaporated and then the residue was purified by silica gel column chromatography with *n*-hexane to give **9** (73 mg, 93%): ^1H NMR ($CDCl_3$, 400 MHz) δ 6.30 (2H, d, *J*=2.2 Hz, H-4, 6), 6.17 (1H, t, *J*=2.2 Hz, H-2), 5.50 (2H, t, *J*=4.8 Hz, H-2′, 3′), 3.27 (2H,

d, J=4.8 Hz, H-1′), 2.12 (2H, m, H-4′), 1.42–1.52 (2H, m, H-5′), 1.21–1.41 (6H, m, H-6′, 7′, 8′), 0.98 (18H, s, Si–C(CH$_3$)$_3$), 0.90 (3H, m, H-9′), 0.18 (12H, s, Si–CH$_3$); ^{13}C NMR (CDCl$_3$, 100 MHz) δ 156.4 (2C), 143.2, 131.0, 127.8, 113.5 (2C), 109.5, 33.4, 31.8, 29.7, 29.0, 27.3, 25.7 (6C), 22.7, 18.2 (2C), 14.1, −4.5 (4C). IR (neat) 2950, 2925, 2850, 1590, 1450, 1335, 1250, 1160, 1020, 1000, 830, 775 cm^{-1}; FAB-MS m/z 463 [M+H]$^+$, HRMS (FAB$^+$) calcd for $C_{27}H_{50}O_2Si_2$ [M]$^+$ 462.3349, found 462.3342.

4.5.5. 5-(*Z*)-Non-2-enyl-benzene-1,3-diol (climacostol (1)). To a solution of **9** (87.7 mg, 0.19 mmol) in THF (1.1 mL) was added 70% HF·pyridine (0.19 mL) at 0 °C under an argon atmosphere. After the mixture was stirred for 1 h at 0 °C, the reaction temperature was gradually raised to 25 °C. The reaction mixture was added to saturated aqueous $NaHCO_3$, and extracted with diethyl ether. The organic layer was washed with 1 M HCl, dried over Na_2SO_4, and evaporated under reduced pressure. The residue was purified by silica gel column chromatography (*n*-hexane/AcOEt, 1:1) to give climacostol (**1**) (38.3 mg, 86%). ^{1}H NMR and ^{13}C NMR spectra were identical with those of natural **1**; IR (nujol) 2980, 2960, 2880, 1615, 1480, 1390, 1350, 1320, 1170, 1020, 980, 850 cm^{-1}; LC/ESI-MS/MS (in negative mode) m/z 217 [M−2H−CH$_3$]$^-$, 203 [M−2H−C$_2$H$_5$]$^-$, 189 [M−2H−C$_3$H$_7$]$^-$, 175 [M−2H−C$_4$H$_9$]$^-$, 161 [M−2H−C$_5$H$_{11}$]$^-$, 147 [M−2H−C$_6$H$_{13}$]$^-$, 122 [M−H−CH=CHC$_6$H$_{13}$]$^-$, 108 [M−H−CH$_2$CH=CHC$_6$H$_{13}$]$^-$.

4.5.6. 1,3-Bis-(*tert*-butyl-dimethyl-silanyloxy)-5-non-2-ynyl-benzene (10). To a solution of **7** (211 mg, 0.28 mmol) in THF (5 mL) was added I_2 (0.50 g, 3.94 mmol) in THF (10 mL). After the mixture was stirred at 25 °C for 2 h, was added saturated aqueous $NaHCO_3$ and saturated aqueous $NaHSO_3$ at 0 °C, and extracted with diethyl ether. The organic layer was washed with brine, and dried over anhyd. $MgSO_4$. The solvent was removed under reduced pressure and then purified by silica gel column chromatography (*n*-hexane/diethyl ether, 40:1) to give **10** (117 mg, 90%): ^{1}H NMR (CDCl$_3$, 400 MHz) δ 6.46 (2H, d, J=2.2 Hz, H-4, 6), 6.19 (1H, t, J=2.2 Hz, H-2), 3.45 (2H, t, J=2.4 Hz, H-1′), 2.18–2.23 (2H, m, H-4′), 1.48–1.54 (2H, m, H-5′), 1.34–1.44 (2H, m, H-6′), 1.27–1.34 (4H, m, H-7′, 8′), 0.97 (18H, s, Si–C(CH$_3$)$_3$), 0.89 (3H, t, J=7.0 Hz, H-9′), 0.19 (12H, s, Si–CH$_3$).

4.5.7. 5-Non-2-ynyl-benzene-1,3-diol (11). To a solution of **10** (210 mg, 0.46 mmol) in THF (15 mL) dissolved in the Teflon vial was added 70% HF·pyridine (1.24 mL) dropwise using the Teflon syringe at 0 °C under an argon atmosphere. After the reaction temperature was gradually raised to 25 °C over 2 h, the reaction was quenched with saturated aqueous $NaHCO_3$, and was added 1 M HCl, and then extracted with AcOEt. The organic layer was dried over anhyd. $MgSO_4$, evaporated under reduced pressure and then purified by silica gel column chromatography (*n*-hexane/AcOEt, 5:2) to give **11** (106 mg, quant): ^{1}H NMR (CDCl$_3$, 400 MHz) δ 6.42 (2H, d, J=2.3 Hz, H-4, 6), 6.22 (1H, t, J=2.3 Hz, H-2), 4.79 (2H, s, OH), 3.47 (2H, t, J=2.4 Hz, H-1′), 2.21 (2H, tt, J=2.4, 7.1 Hz, H-4′), 1.48–1.56 (2H, m, H-5′), 1.37–1.43 (2H, m, H-6′), 1.24–1.36 (4H, m, H-7′, 8′), 0.89 (3H, t, J=7.0 Hz, H-9′).

4.5.8. 1,3-Bis-(*tert*-butyl-dimethyl-silanyloxy)-5-nonyl-benzene (12). To a solution of **9** (334 mg, 0.72 mmol) in MeOH (14 mL) was added 10% palladium-on-charcoal catalyst and the mixture was stirred under a hydrogen atmosphere at 25 °C for 1 h. The reaction mixture was filtered through the Celite pad, and the filtrate was evaporated under reduced pressure and then purified by silica gel column chromatography (*n*-hexane/diethyl ether, 40:1) to give **12** (270 mg, 80%): ^{1}H NMR (CDCl$_3$, 400 MHz) δ 6.28 (2H, d, J=2.1 Hz, H-4, 6), 6.16 (1H, t, J=2.1 Hz, H-2), 2.46 (2H, t, J=7.8 Hz, H-1′), 1.24–1.30 (14H, m, H-2′, 3′, 4′, 5′, 6′, 7′, 8′), 0.97 (18H, s, Si–C(CH$_3$)$_3$), 0.88 (3H, t, J=6.8 Hz, H-9′), 0.18 (12H, s, Si–CH$_3$).

4.5.9. 5-Nonyl-benzene-1,3-diol (13). To a solution of **12** (250 mg, 0.54 mmol) in THF (18 mL) dissolved in the Teflon vial was added 70% HF·pyridine (1.46 mL) dropwise using the Teflon syringe at 0 °C under an argon atmosphere. After the reaction temperature was gradually raised to 25 °C over 2 h, the reaction mixture was quenched with saturated aqueous $NaHCO_3$, added 1 M HCl and then extracted with AcOEt. The organic layer was dried over anhyd. $MgSO_4$, evaporated under reduced pressure and then purified by silica gel column chromatography (*n*-hexane/AcOEt, 5:2) to give **13** (105 mg, 83%): ^{1}H NMR (CDCl$_3$, 400 MHz) δ 6.25 (2H, d, J=2.2 Hz, H-4, 6), 6.18 (1H, t, J=2.2 Hz, H-2), 4.82 (2H, s, OH), 2.48 (2H, t, J=7.8 Hz, H-1′), 1.56 (2H, m, H-2′), 1.23–1.29 (12H, m, H-3′, 4′, 5′, 6′, 7′, 8′), 0.88 (3H, t, J=7.0 Hz, H-9′).

Acknowledgements

Thanks are due to the Analytical Division at Osaka City University for analyses, mass spectra measurements and 600 MHz NMR measurements. We thank Dr. M. Tavrovskaya, Institute of Cytology, Russian Academy of Sciences, St. Petersburg for the strain of *Climacostomum virens* and the strain of *D. margaritifer*. This work was partially supported by Grand-in-Aid for Scientific Research of MEXT Japan, and Italian MURST, which are gratefully appreciated.

References and notes

1. Tao, N.; Orlando, M.; Hyon, J.-S.; Gross, M.; Song, P.-S. *J. Am. Chem. Soc.* **1993**, *115*, 2526–2528.
2. (a) Checcucci, G.; Shoemaker, R. S.; Bini, E.; Cerny, R.; Tao, N.; Hyon, J.-S.; Gioffre, D.; Ghetti, F.; Lenci, F.; Song, P.-S. *J. Am. Chem. Soc.* **1997**, *119*, 5762–5763. (b) Maeda, M.; Naoki, H.; Matsuoka, T.; Kato, Y.; Kotsuki, H.; Utsumi, K.; Tanaka, T. *Tetrahedron Lett.* **1997**, *38*, 7411–7414. (c) Spitzner, D.; Hofle, G.; Klein, I.; Pohlan, S.; Ammermann, D.; Jaenicke, L. *Tetrahedron Lett.* **1998**, *39*, 4003–4006.
3. (a) Tartar, V. *The Biology of Stentor*; Pergamon: New York, 1961. (b) Giese, A. C. *Blepharisma*; Stanford University Press: California, 1973.
4. (a) Song, P.-S. *Biochim. Biophys. Acta* **1981**, *639*, 1–29. (b) Scevoli, P.; Bisi, F.; Colombetti, F.; Ghetti, F.; Lenci, F.; Pasarelli, V. *J. Photochem. Photobiol. B: Biol.* **1987**, *1*,

75–84. (c) Matsuoka, T.; Watanabe, Y.; Sagara, Y.; Takayanagi, M.; Kato, Y. *Photochem. Photobiol.* **1995**, *62*, 190–193.
5. (a) Miyake, A.; Harumoyo, T.; Iio, H. *Eur. J. Protistol.* **2001**, *37*, 77–88. (b) Harumoto, T.; Miyake, A.; Ishikawa, N.; Sugibayashi, R.; Zenfuku, K.; Iio, H. *Eur. J. Protistol.* **1998**, *34*, 458–470. (c) Terazima, M. N.; Iio, H.; Harumoto, T. *Photochem. Photobiol.* **1999**, *69*, 47–54. (d) Miyake, A.; Harumoto, T.; Salvi, B.; Rivola, V. *Eur. J. Protistol.* **1990**, *25*, 310–315.
6. Miyake, A.; Buonanno, F.; Saltalamacchia, P.; Masaki, M. E.; Iio, H. *Eur. J. Protistol.* **2003**, *39*, 25–36.
7. Masaki, M. E.; Harumoto, T.; Terazima, M. N.; Miyake, A.; Usuki, Y.; Iio, H. *Tetrahedron Lett.* **1999**, *40*, 8227–8229.
8. (a) Suzuki, Y.; Esumi, Y.; Hyakutake, H.; Kono, Y.; Sakurai, A. *Phytochemistry* **1996**, *41*, 1485–1489. (b) Suzuki, Y.; Esumi, Y.; Uramoto, M.; Kono, Y.; Sakurai, A. *Biosci. Biotech. Biochem.* **1997**, *61*, 480–486.
9. Bandyopadhyay, C.; Gholap, A. S.; Mamdapur, V. R. *J. Agric. Food Chem.* **1985**, *33*, 377–379.
10. For the synthesis of 5-alkylresorcinols, see: Alonso, E.; Ramon, D. J.; Yus, M. *J. Org. Chem.* **1997**, *62*, 417–421, and references cited therein.
11. (a) Arisawa, M.; Ohmura, K.; Kobayashi, A.; Morita, N. *Chem. Pharm. Bull.* **1989**, *37*, 2431–2434. (b) Warshawsky, A. M.; Patel, M. V.; Chen, T.-M. *J. Org. Chem.* **1997**, *62*, 6439–6440.
12. (a) Kira, K.; Isobe, M. *Tetrahedron Lett.* **2000**, *41*, 5951–5955. (b) Kira, K.; Tanda, H.; Hamajima, A.; Baba, T.; Takai, S.; Isobe, M. *Tetrahedron* **2002**, *58*, 6485–6492.
13. (a) Hosokawa, S.; Isobe, M. *Synlett* **1996**, 351–352. (b) Hosokawa, S.; Isobe, M. *Tetrahedron Lett.* **1998**, *39*, 2609–2612. (c) Shibuya, S.; Isobe, M. *Tetrahedron* **1998**, *54*, 6677–6698.
14. Abe, Y.; Mori, K. *Biosci. Biotech. Biochem.* **2001**, *65*, 2110–2112.
15. Kozubek, A.; Tyman, J. H. P. *Chem. Rev.* **1999**, *99*, 1–25.
16. Thomson, R. H. *Naturally Occurring Quinones*; 2nd ed.; Academic: New York, 1971; pp 576–633.
17. Miyake, A. *Jpn J. Protozool.* **2002**, *33*, 97–117, in Japanese.
18. (a) Hofle, G.; Pohlan, S.; Uhlig, G.; Kabbe, K.; Schumacher, D. *Angew. Chem. Int. Ed. Engl.* **1994**, *33*, 1495–1497. (b) Lueken, W.; Uhlig, G.; Kruppel, T. *J. Protozool.* **1989**, *36*, 350–353.
19. (a) Dini, F.; Guella, G.; Giubbilini, P.; Mancini, I.; Pietra, F. *Naturwissenschaften* **1993**, *80*, 84–86. (b) Ronald, A.; Raymond, L. *J. Am. Chem. Soc.* **2001**, *123*, 9455–9456.
20. (a) Guella, G.; Dini, F.; Pietra, F. *Helv. Chim. Acta* **1995**, *78*, 1747–1754. (b) Rosini, G.; Laffi, F.; Marotta, E.; Pagani, I.; Righi, P. *J. Org. Chem.* **1998**, *63*, 2389–2391.
21. Guella, G.; Dini, F.; Pietra, F. *Helv. Chim. Acta* **1996**, *79*, 439–448.
22. (a) Tyman, J. H. P. *Synthetic and Natural Phenols*; Elsevier: Amsterdam, 1996; pp 465–557. (b) Kozubek, A.; Zarnowski, R.; Stasiuk, M.; Gubernator, J. *Cell. Biol. Mol. Lett.* **2001**, *6*, 351–355.
23. (a) Lytollis, W.; Scannell, R. T.; An, H.; Murty, V. S.; Reddy, K. S.; Barr, J. R.; Hecht, S. M. *J. Am. Chem. Soc.* **1995**, *117*, 12683–12690. (b) Singh, U. S.; Scannell, R. T.; An, H.; Carter, B. J.; Hecht, S. M. *J. Am. Chem. Soc.* **1995**, *117*, 12691–12699.
24. Lee, J. S.; Cho, Y. S.; Park, E. J.; Kim, J.; Oh, W. K.; Lee, H. S.; Ahn, J. S. *J. Nat. Prod.* **1998**, *61*, 867–871.
25. Valcic, S.; Wachter, G. A.; Eppler, C. M.; Timmermann, B. N. *J. Nat. Prod.* **2002**, *65*, 1270–1273.
26. Terazima, M. N.; Iio, H.; Harumoto, H. *Jpn J. Protozool.* **2001**, *34*, 60.
27. Muto, Y.; Tanabe, Y.; Kawai, K.; Iio, H. *Jpn J. Protozool.* **2003**, *36*, 25–26.
28. Miyake, A. In *Sexual Interaction in Eukaryotic Microbes*; O'Day, D. H., Horgen, P. A., Eds.; Academic: New York, 1981; pp 95–129.

Available online at www.sciencedirect.com
SCIENCE DIRECT
Tetrahedron
Tetrahedron 60 (2004) 7049–7052

Orirubenones A, B and C, novel hyaluronan-degradation inhibitors from the mushroom *Tricholoma orirubens*

Hirokazu Kawagishi,[a,*] Yumiko Tonomura,[a] Hiroyuki Yoshida,[b] Shingo Sakai[b] and Shintaro Inoue[b]

[a]*Department of Applied Biological Chemistry, Faculty of Agriculture, Shizuoka University, 836 Ohya, Shizuoka 422-8529, Japan*
[b]*Basic Research Laboratory, Kanebo Ltd, 3-28, 5-Chome, Kotobuki-cho, Odawara, Kanagawa 250-0002, Japan*

Received 5 August 2003; revised 10 October 2003; accepted 10 October 2003

Available online 24 June 2004

Abstract—Three new compounds, orirubenone A (**1**), B (**2**) and C (**3**) were isolated from the mushroom *Tricholoma orirubens*. Their structures were determined by spectral analyses. These compounds inhibited hyaluronan-degradation by human skin fibroblasts.

1. Introduction

Hyaluronan (HA), a nonsulfated glycosaminoglycan composed of repeating disaccharide units of *N*-acetyl-glucosamine and glucuronic acid, plays an important role in inflammation, cell locomotion, and wound healing.[1] The skin has more than 50% of total body HA, and the half-life of HA is less than one day, suggesting that the velocity of HA production and depolymerization (degradation) in the skin is very rapid.[2] Moreover, HA has been reported to have many physiological activities corresponded to its different molecular size. Oligosaccharides of HA are known to stimulate angiogenesis,[3,4] and low-molecular-mass HA (less than 5×10^5 Da) has been shown to activate NF-κ B expression[5] and induce chemokine gene expression[6] and nitric-oxide synthase[7] in mouse macrophages, suggesting that the regulation of HA depolymerization is important during the process of skin inflammation. The mechanism of depolymerization in skin fibroblasts remains unclear. Some reports showed that HA bound to plasma membrane of fibroblasts,[8,9] while other reports clearly indicated an absence of lysosomal hyaluronidase activity in normal human skin fibroblasts.[10–12] Recently, five hyaluronidase genes and one pseudogene have been cloned.[13] Three (HYAL1, HYAL2 and HYAL3) of them are expressed in human skin fibroblasts.[14] HYAL1 is widely expressed in various tissues. However, its activity outside of lysosomes seems very little because of its sharp pH optimum around.[4,7,14] HYAL2 is localized in the lysosomes or cell membranes, and can degrade high-molecular-mass HA to intermediately sized products of 20 kDa under an acidic pH optimum.[15,16] However, no hyaluronidase activity was demonstrated in the lysate of either fibroblasts or HeLa cells transfected with human HYAL2.[15] The activity of HYAL3, which was found in chondrocytes, has not been characterized.[17] On the other hand, Nakamura et al. found that an extracellular-depolymerization enzyme, which did not produce oligo-HA as end-products like the lysosomal hyaluronidase, was at work in normal skin fibroblasts.[11] So far, there is no direct evidence that lysosomal hyaluronidase plays a role in depolymerization of HA in skin fibroblasts. Therefore, inhibitors toward HA-depolymerization by skin fibroblasts can be useful tools for the study of the HA-depolymerization. In the present study, we screened for inhibitory activity of extracts of various mushrooms against the extracellular HA depolymerization of [^{3}H]-HA in human skin fibroblast culture. Among the mushroom extracts tested, the extract from the mushroom *Tricholoma orirubens* showed the most potent activity, therefore, we tried to isolate the active principles from the mushroom. We wish to report here the isolation, the structure determination and the inhibitory activity against HA-degradation of three novel phenols named orirubenone A (**1**), B (**2**), and C (**3**).

2. Result and discussion

The extract of *T. orirubens* was divided into a $CHCl_3$ fraction, an EtOAc soluble fraction and a water soluble fraction. Since only the EtOAc soluble fraction showed significant activity, this fraction was repeatedly chromatographed on the basis of the result of the bioassay. As a consequence, three new compounds were purified and named orirubenone A (**1**), B (**2**), and C (**3**).

Keywords: Mushroom; *Tricholoma orirubens*; Hyaluronan-degradation inhibitor.
* Corresponding author. Tel./fax: +81-542384885;
e-mail address: achkawa@agr.shizuoka.ac.jp

0040–4020/$ - see front matter © 2004 Elsevier Ltd. All rights reserved.
doi:10.1016/j.tet.2003.10.129

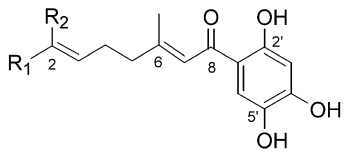

1 $R_1 = CH_3$, $R_2 = COOH$

2 $R_1 = COOH$, $R_2 = CH_3$

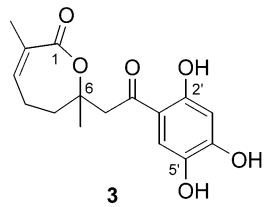

3

Orirubenone A (**1**) was isolated as yellow oil. FABMS of **1** showed a molecular ion peak at *m/z* 307 ($[M+H]^+$). Its molecular formula was determined as $C_{16}H_{18}O_6$ by HRESIMS, indicating the presence of eight degrees of unsaturation in the molecule. The ^1H NMR and ^{13}C NMR spectra of **1** along with DEPT and HMQC showed two methyls attached at sp^2 carbons [δ_H 1.85 (s), 2.11 (s); δ_C 12.9, 19.5], two methylenes attached at sp^2 carbons [δ_H 2.40 (t, *J*=6.9 Hz), 2.48 (dt, *J*=6.7, 6.9 Hz); δ_C 40.7, 27.7], four sp^2 methines [δ_H 6.28 (s), 6.62 (s), 6.74 (t, *J*=6.7 Hz), 7.17 (s); δ_C 104.1, 122.0, 140.9, 116.0], six sp^2 quaternary carbons (δ_C 113.8, 131.2, 139.3, 155.7, 157.2, 160.7), a conjugated carbonyl (δ_C 196.5), and a carboxyl (δ_C 173.0) (Table 1). The COSY spectrum indicated a contiguous sequence of coupled signals, $-CH{=}CH_2-CH_2-$ [δ_H 6.74 (t, *J*=6.7 Hz), 2.48 (dt, *J*=6.7, 6.9 Hz), 2.40 (t, *J*=6.9 Hz)]. The HMBC spectrum showed that the methine at δ_H 6.74 bound to a quaternary carbon (δ_C 131.2) bearing a methyl [δ_H 1.85 (s); δ_C 12.9], and a carboxyl (δ_C 173.0), and the metylene [δ_H 2.40 (t, *J*=6.9 Hz); δ_C 40.7] attached to the sequence of $-C(CH_3){=}CH-CO-$ (Table 2). Therefore, the structure of the side chain in **1** was determined as $HOOC-C(CH_3){=}CH-CH_2-CH_2-C(CH_3){=}CH-CO-$. The other unassigned parts, six carbons (two methines and four quaternary carbons), three oxygens and three hydrogens, comprised a benzene ring having three hydroxyls. The two methines appeared as singlets [δ_H 6.28 (s), 7.17 (s)] in the ^1H NMR spectrum, indicating these methines were located at *para*-positions each other. In the HMBC spectrum, a cross peak between the methine at δ_H 7.17 and the terminal carbonyl of the side chain (δ_C 196.5) appeared (Table 2). In addition, a hydroxyl gave a sharp singlet at δ_H 12.4 in

Table 1. ^1H and ^{13}C NMR data for orirubenones A (**1**), B (**2**) and C (**3**) (in CD_3OD)[a]

Position	**1**		**2**		**3**	
	δ_H (multiplicity, *J* in Hz)	δ_C	δ_H (multiplicity, *J* in Hz)	δ_C	δ_H (multiplicity, *J* in Hz)	δ_C
1		173.0		176.6		171.9
2		131.2		134.9		129.6
2-Me	1.85 (s)	12.9	1.84 (s)	13.7	1.78 (s)	12.4
3	6.74 (t, 6.7)	140.9	6.55 (t, 5.8)	137.3	6.73 (m)	142.6
4	2.48 (dt, 6.7, 6.9)	27.7	2.41 (dt, 5.8, 5.5)	27.3	2.33 (m)	24.0
5	2.40 (t, 6.9)	40.7	2.40 (t, 5.5)	40.6	1.74 (m), 1.88 (m)	38.7
6		157.2		155.8		81.7
6-Me	2.11 (s)	19.5	2.04 (s)	19.3	1.39 (s)	23.9
7	6.62 (s)	122.0	6.53 (s)	122.8	2.58 (d, 16.5), 2.71 (d, 16.5)	47.9
8		196.5		197.1		193.5
1′		113.8		111.3		113.5
2′		160.7		160.5		157.1
3′	6.28 (s)	104.1	6.25 (s)	104.1	6.31 (s)	104.7
4′		155.7		156.1		156.2
5′		139.3		139.5		141.7
6′	7.17 (s)	116.0	7.17 (s)	116.0	7.13 (s)	111.2

[a] These assignments were established by DEPT, HMQC and HMBC experiments.

Table 2. HMBC and NOESY correlations of orirubenones A (**1**), B (**2**) and C (**3**)

Position	**1**		**2**		**3**	
	HMBC	NOE	HMBC	NOE	HMBC	NOE
1	H-2-Me, 3		H-2-Me, 3		H-2-Me, 3	
2	H-2-Me, 4		H-2-Me, 4		H-2-Me, 3, 4	
2-Me	H-3	H-3		H-4	H-3	
3	H-2-Me, 4, 5	H-2-Me, 5	H-2-Me, 4, 5	H-5	H-2-Me, 4, 5	
4	H-3, 5		H-3, 5	H-2-Me	H-3, 5	H-6-Me
5	H-4, 6-Me, 7	H-3, 7	H-3, 4, 6-Me, 7	H-3, 7	H-3 4, 6-Me, 7	H-7
6	H-4, 5, 6-Me, 7		H-4, 5, 6-Me, 7		H-4, 5, 6-Me, 7	
6-Me	H-5, 7		H-5, 7		H-5, 7	H-4
7	H-5, 6-Me	H-5, 6′	H-5, 6-Me	H-5, 6′	H-5	H-5
8	H-7, 6′		H-7, 6′		H-7, 6′	
1′	H-3′		H-3′		H-3′, 6′	
2′	H-3′, 6′		H-3′, 6′		H-3′, 6′	
3′						
4′	H-3′, 6′		H-3′, 6′		H-3′, 6′	
5′	H-3′, 6′		H-3′, 6′		H-3′, 6′	
6′		H-7		H-7		

$CDCl_3$, suggesting the presence of a hydrogen bond between the hydroxyl and the carbonyl (data not shown). The NOESY spectrum showed correlations between H-2-Me and H-3, and H-5 and H-7. Thus, the structure of orirubenone A (**1**) was determined as (2*Z*,6*E*)-8-(2,4,5-trihydroxylphenyl)-2,6-dimethyl-8-oxo-2,6-octadienoic acid.

Orirubenone B (**2**) was obtained as yellow oil. This compound showed the same molecular formula, $C_{16}H_{18}O_6$, by HRESIMS as **1** and its ^1H and ^{13}C NMR data were very similar to those of **1** (Table 1). The HMBC and COSY correlations were almost same as those of **1**, suggesting **2** was a geometrical isomer of **1** (Table 2). Cross peaks between H-2-Me and H-4, and H-5 and H-7 were observed in the NOESY spectrum (Table 2). Therefore, the structure of orirubenone B (**2**) was determined to be (2*E*,6*E*)-8-(2,4,5-trihydroxylphenyl)-2,6-dimethyl-8-oxo-2,6-octadienoic acid.

Compound **3**, orirubenone C, was purified as yellow oil and its molecular formula determined by HRESIMS, $C_{16}H_{18}O_6$, was identical with those of **1** and **2**. This compound possessed a 2,4,5-trihydroxyphenone moiety like **1** and **2**; two methines [δ_H 6.31 (s), 7.31 (s); δ_C 104.7, 111.2], four quaternary carbons (δ_C 113.5, 141.7, 156.2, 157.1), a conjugated carbonyl (δ_C 193.5). However, the structure of the monoterpene unit in **3** was different from those of **1** and **2**. The ^1H NMR and ^{13}C NMR spectra of **3** showed that the unit had two methyls [δ_H 1.39 (s), 1.78 (s); δ_C 23.9, 12.4], three methylenes attached at sp^2 carbons [δ_H 1.74 (1H, m), 1.88 (1H, m), 2.33 (2H, m), 2.58 (1H, d, J=16.5 Hz), 2.71 (1H, d, J=16.5 Hz); δ_C 38.7, 24.0, 47.9], an sp^2 methine [δ_H 6.73 (m); δ_C 142.6], an sp^2 quaternary carbon (δ_C 129.6), an sp^3 quaternary carbon (δ_C 81.7), a conjugated carbonyl (δ_C 193.5), and a carboxyl (δ_C 171.9) (Table 1). The HMBC spectrum indicated that the sequence of the unit was $-OOC-C(CH_3)=CH-CH_2-CH_2-C(O-)(CH_3)-CH_2-CO-$. The molecular formula of **3**, the degrees of unsaturation of the molecule, and the chemical shift (δ_C 81.7) of the sp^3 quaternary carbon suggested the presence of a lactone in the unit. All the data allowed us to conclude that orirubenone C (**3**) was 6-(2′,4′,5′-trihydroxybenzoylmethyl)-2,6-dimethyl-2-hexen-6-olide. This compound has an asymmetric carbon (C-6), but is racemic since the CD spectrum of it showed a plane line. This compound was not artifact formed by intramolecular 1,4-addition of the carboxy anion to C-6 in **1**, because TLC and HPLC analyses showed that **3** existed in the MeOH soluble part obtained by extraction of the mushroom at −20 °C.

Orirubenone A (**1**), B (**2**) and C (**3**) were evaluated in a hyaluronan-degradation inhibition assay. All the compounds showed the inhibitory activity and the IC_{50} of **1**, **2** and **3** were 15, 21 and 57 μM, respectively.

3. Experimental

3.1. General

The ^1H NMR spectra (one- and two-dimensional) were recorded on a JEOL lambda-500 spectrometer at 500 MHz, while ^{13}C NMR spectra were recorded on the same instrument at 125 MHz. The FABMS spectra were recorded on a JEOL DX-303HF and the HRESIMS spectra were measured on a JMS-T100LC mass spectrometer. A JASCO grating infrared spectrophotometer was used to record the IR spectra. The CD spectrum was measured by using a JASCO J-500A spectropolarimeter. MPLC was done with a YAMAZEN MPLC-system (Japan) and an UltraPack ODS-S50D column (50×300 mm, YAMAZEN, Japan). HPLC separations were performed with a JASCO Gulliver system using an ODS column (Grandpack ODS-A S-5 YC, 20×300 mm, Masis, Japan). Silica gel plate (Merck F_{254}) and silica gel 60 N (Merck 100–200 mesh) were used for analytical TLC and for flash column chromatography, respectively. Preparative reverse-phase TLC was performed on C_{18} TLC plates (J. T. Baker, USA). Sephadex G50 and Sepharose CL-2B were purchased from Pharmacia Fine Chemicals (Sweden). Hyaluronan variants extracted from pigskin ($4–6\times10^4$ Da) and human umbilical cord ($8–12\times10^5$ Da) were obtained from Seikagaku Corporation (Japan).

3.2. Fungus materials

Mature fruiting bodies of *T. orirubens* Quél were collected at Narusawa village, Yamanashi Prefecture in Japan.

3.3. Extraction and isolation

Fresh fruiting bodies of *T. orirubens* (3.7 kg) were extracted with MeOH (6 l, four times) and then acetone (3 l, twice). The solvents were combined, concentrated under reduced pressure, and partitioned between $CHCl_3$ and H_2O. The H_2O layer was further partitioned between EtOAc and H_2O. The residue (1.5 g) obtained after removing EtOAc was fractionated by silica gel flash column chromatography (100, 70, 30% $CHCl_3$/acetone, 90, 50% $CHCl_3$/MeOH, MeOH, each 1 l) to obtain nine fractions. Fraction 5 (370.0 mg) was further separated by reversed-phase MPLC (60% MeOH) and 14 fractions were obtained. Fraction 5–6 (45.6 mg) was separated by reversed-phase HPLC (60% MeOH) and then by preparative reversed-phase TLC (60% MeOH) to afford compounds **1** (3.6 mg) and **2** (2.5 mg). On the other hand, fraction 5–4 (27.4 mg) was subjected to reversed-phase HPLC (40% MeOH) to purify compound **3** (10.1 mg).

3.3.1. Oribubenone A (1). IR (neat) ν_{max} cm^{-1}: 3367, 1686, 1636, 1524; FABMS (matrix, glycerol) *m/z* 307 $(M+H)^+$; HRESIMS *m/z* 329.0997 [Calcd for $C_{16}H_{18}O_6Na$ $(M+Na)^+$, 329.1001], 305.1011 [Calcd for $C_{16}H_{17}O_6$ $(M-H)^-$, 305.1025].

3.3.2. Oribubenone B (2). IR (neat) ν_{max} cm^{-1}: 3367, 1709, 1635, 1529; FABMS (matrix, glycerol) *m/z* 307 $(M+H)^+$; HRESIMS *m/z* 329.1001 [Calcd for $C_{16}H_{18}O_6Na$ $(M+Na)^+$, 329.1001], 305.1028 [Calcd for $C_{16}H_{17}O_6$ $(M-H)^-$, 305.1025].

3.3.3. Oribubenone C (3). IR (neat) ν_{max} cm^{-1}: 3368, 1732, 1464; FABMS (matrix, glycerol) *m/z* 307 $(M+H)^+$; HRESIMS *m/z* 329.0992 [Calcd for $C_{16}H_{18}O_6Na$ $(M+Na)^+$, 329.1001], 305.1034 [Calcd for $C_{16}H_{17}O_6$ $(M-H)^-$, 305.1025].

3.4. Bioassay

3.4.1. Cell lines and culture procedure. Detroit 551 human skin fibroblasts purchased from the American Type Culture Collection (USA) were grown to confluence on 12-well plates in Eagle's minimal medium (ICN Biomedicals Ltd, USA) supplemented with non-essential amino acids, 1 mM sodium pyruvate, and 10% (v/v) FBS (JRH Pharmaceutical Co, USA). Cultures were grown at 37 °C in a humidified atmosphere of 5% CO_2 and 95% air.

3.4.2. Preparation of [^{3}H]HA. [^{3}H]HA was prepared by the method described by Underhill and Tool with some modification.[8] Briefly, confluent Detroit 551 fibroblasts were incubated with 10 μCi/ml of [^{3}H]glucosamine (American Radiolabeled Chemicals Inc., USA) at 37 °C. The conditioned medium was pooled, digested with pronase (0.3 mg/ml) (Calbiochem, USA) at 37 °C for 24 h, and precipitated with four volumes of absolute ethanol (−20 °C). After suspending the resulting pellets with distilled H_2O and then centrifuging them, the supernatants were incubated at room temperature in 0.1% cetylpyridinium chloride and 0.4 M NaCl, centrifuged again, precipitated with four volumes of absolute ethanol (−20 °C), resolubilized, and applied to a Sepharose CL-2B column (1.0×60 cm) in 0.5 M NaCl. The void fractions were collected, precipitated with four volumes of absolute ethanol (−20 °C), and finally resolubilized with 5 mM phosphate buffer (pH 7.5). The uronic acid concentration was determined by the method of Rai et al.[15] The specific activity of isolated [^{3}H]HA (>10^6 Da) was 1.3×10^5 dpm/μg (2.2 kBq/μg). The isolated [^{3}H]HA was completely degraded by *Streptomyces* hyaluronidase (Seikagaku Kogyo Co., Japan), indicating that this material was pure.

3.4.3. Assay for [^{3}H]HA depolymerization. At confluence, the medium was changed to Eagle's minimal medium supplemented with non-essential amino acids and 1 mM sodium pyruvate without 10% (v/v) FBS. After one day, the fibroblasts were incubated with [^{3}H]HA and each sample at various concentrations at 37 °C in an atmosphere of 95% air and 5% CO_2. The concentration of added [^{3}H]HA was 0.4 μg/ml. After incubation with [^{3}H]HA (3 days), the medium was harvested, boiled, and applied to a Sepharose CL-2B column (1.0 cm×60 cm) eluted with 0.5% NaCl. The flow rate was 0.6 ml/min. The activity of each fraction (2.4 ml) was measured by a liquid scintillation counter (Aloka LSC-1000, Japan). The total radioactivities recovered in the medium were matched with that of cell-free culture and degraded completely by *Streptomyces* hyaluronidase. To determine activities of cellular HA depolymerization, the total radioactivities of high-molecular-mass fractions (fractions 1–8) were measured. The activities were given by as follows.

Depolymerizing activity (dpm/well)=cell free*−cultured** (cell free* is the total of the radioactivities of fractions 1–8 after culture without cells, and cultured** is the total of the radioactivities of fractions 1–8 of the CL-2B column after culture).

Acknowledgements

Financial support of this research was partially provided by a Grant-in-Aid for Scientific Research on Priority Areas 'Targeted Pursuit of Challenging Bioactive Molecules' (No. 12045232) from the Ministry of Education, Science, Sports and Culture of Japan, and a Grant-in-Aid for Scientific Research (No. 12490015) from the Japan Society for the Promotion of Science.

References and notes

1. Laurent, T. C.; Fraser, J. R. *J. FASEB* **1992**, *6*, 397–404.
2. Tammi, R.; Säämänen, A. M.; Maibach, H. I.; Tammi, M. *J. Invest. Dermatol.* **1991**, *97*, 126–130.
3. Trochon, V.; Mabilat, P. C.; Bertrand, P.; Legrand, Y.; Soria, J.; Soria, C.; Delpech, B.; Lu, H. *FEBS Lett.* **1997**, *418*, 6–10.
4. West, D. C.; Hampson, I. N.; Arnold, F.; Kumar, S. *Science* **1985**, *228*, 1324–1326.
5. Noble, P. W.; McKee, C. M.; Cowman, M.; Shin, H. S. *J. Exp. Med.* **1996**, *183*, 2373–2378.
6. McKee, C. M.; Penno, M. B.; Cowman, M.; Burdick, M. D.; Strieter, R. M.; Bao, C. E. A.; Noble, P. W. *J. Clin. Invest.* **1996**, *98*, 2403–2413.
7. McKee, C. M.; Lowenstein, C. J.; Horton, M. R.; Wu, J.; Bao, C.; Chin, B. Y.; Choi, A. M.; Noble, P. W. *J. Biol. Chem.* **1997**, *272*, 8013–8018.
8. Underhill, C. B.; Toole, B. P. *J. Cell. Biol.* **1979**, *82*, 475–484.
9. Bertolami, C. N.; Berg, S.; Messadi, D. V. *Matrix* **1992**, *11*, 11–21.
10. Arbogast, B.; Hopwood, J. J.; Dorfman, A. *Biochem. Biophys. Res. Commun.* **1975**, *67*, 376–382.
11. Nakamura, T.; Takagaki, K.; Kubo, K.; Morikawa, A.; Tamura, S.; Endo, M. *Biochem. Biophys. Res. Commun.* **1990**, *172*, 70–76.
12. Orkin, R. W.; Toole, B. P. *J. Biol. Chem.* **1980**, *255*, 1036–1042.
13. Csoka, A. B.; Scherer, S. W.; Stern, R. *Genomics* **1999**, *60*, 356–361.
14. Stair-Nawy, S.; Csoka, A. B.; Stern, R. *Biochem. Biophys. Res. Commun.* **1999**, *266*, 268–273.
15. Rai, S. K.; Duh, F. M.; Vigdorovich, V.; Danilkovitch-Miagkova, A.; Lerman, M. I.; Miller, A. D. *Proc. Natl. Acad. Sci. U.S.A.* **2001**, *98*, 4443–4448.
16. Lepperdinger, G.; Strobl, B.; Kreil, G. *J. Biol. Chem.* **1998**, *273*, 22466–22470.
17. Flannery, C. R.; Little, C. B.; Hughes, C. E.; Caterson, B. *Biochem. Biophys. Res. Commun.* **1998**, *251*, 824–829.

Available online at www.sciencedirect.com
SCIENCE DIRECT®
Tetrahedron
Tetrahedron 60 (2004) 7053–7059

Kendarimide A, a novel peptide reversing P-glycoprotein-mediated multidrug resistance in tumor cells, from a marine sponge of *Haliclona* sp.

Shunji Aoki,[a] Liwei Cao,[a] Kouhei Matsui,[a] Rachmaniar Rachmat,[b] Shin-ichi Akiyama[c] and Motomasa Kobayashi[a,*]

[a]*Graduate School of Pharmaceutical Sciences, Osaka University, Yamada-oka 1-6, Suita, Osaka 565-0871, Japan*
[b]*Research and Development Centre for Oceanology, LIPI, JL. Pasir Putih I, Ancol Timur, Jakarta 11048, Indonesia*
[c]*Department of Cancer Chemotherapy, Institute for Cancer Research, Faculty of Medicine, Kagoshima University, 8-35-1 Sakuragaoka, Kagoshima 890-8520, Japan*

Received 15 July 2003; revised 31 July 2003; accepted 31 July 2003

Available online 25 June 2004

Abstract—A novel modulator of multidrug resistance (MDR) in tumor cells, kendarimide A (**1**), was isolated from an Indonesian marine sponge of *Haliclona* sp. Compound **1** reversed MDR in KB-C2 cells mediated by P-glycoprotein (P-gp) at a 6 μM concentration, and the chemical structure of **1** was characterized to be a linear peptide composed of *N*-methylpyroglutamic acid (pyroMeGlu), *N*-methylated eight-membered cysteinyl-cysteine (ox-[MeCys-MeCys]) together with many *N*-methyl amino acid residues. The amino acid sequence of **1** was determined by 2D NMR and FAB MS analysis. The absolute configuration of the amino acid residues in **1** except for the MeCys part was determined to be L-form respectively, based on interpretation of the HPLC analysis of Marfey's derivatives of the hydrolysates of **1** and the synthetic method for the pyroMeGlu residue.

1. Introduction

Tumor cells, which acquired drug resistance to several anticancer drugs having unrelated action mechanisms and chemical structures, are called multidrug resistance (MDR) cells. In many cases, the major mechanism of MDR is the overexpression of the membrane glycoproteins as ATP-dependent pumps, which excrete anticancer drugs in tumor cells.[1] P-glycoprotein (P-gp) encoded by the MDR1 gene, which belongs to a super family of ATP-binding cassette (ABC) transporters, has been observed in various MDR cell lines and is closely related to drug resistance in clinical treatment. Substances which inhibit the function of P-gp and increase the concentration of antitumor agents in MDR cell, are expected to have high potential to realize successful cancer chemotherapy.[2] In the course of our screening of MDR-modulators from marine organisms, we isolated agosterols[3] as a potent reversing substance to both P-gp- and multidrug resistance associated protein (MRP1)-mediated MDR from a marine sponge of *Spongia* sp. and brianthein A[4] as a reversing substance to P-gp-mediated MDR from the Indonesian gorgonian *Briareum excavatum*. We further isolated a peptide named kendarimide A (**1**) exhibiting a reversing activity to P-gp-mediated MDR, from an Indonesian marine sponge. Here we report the detail of the structure analysis of kendarimide A (**1**).

2. Results and discussion

The MeOH extract of the titled dried sponge collected at Sulawesi Island, Indonesia, was partitioned into an H_2O–EtOAc mixture (1:1). The EtOAc-soluble portion, which showed a reversing activity against P-gp mediated MDR, was subjected to silica gel flash column chromatography ($CHCl_3$–MeOH). The active MeOH eluate was further separated by ODS column (Cosmosil 75C_{18}-OPN, MeOH–H_2O) chromatography. The 90% aq MeOH eluate was further purified by reversed-phase HPLC (Cosmosil 5C_{18}AR, 90% aq MeCN; Cosmosil 5Ph, 86% aq MeOH) to furnish kendarimide A (**1**) (16 mg, 0.0047% from the dried sponge) as an active substance.

Kendarimide A (**1**) was obtained as a colorless powder. The positive ion FAB MS of **1** gave a quasi-molecular ion [$(M+H)^+$] peak at *m*/*z* 1631 and the molecular formula of **1**

Keywords: Multidrug resistance; Marine sponge; *Haliclona* sp; Kendarimide A; *N*-methyl amino acid.
* Corresponding author. Tel.: +81-6-6879-8215; fax: +81-6-6879-8219; e-mail address: kobayasi@phs.osaka-u.ac.jp

0040–4020/$ - see front matter © 2004 Elsevier Ltd. All rights reserved.
doi:10.1016/j.tet.2003.07.020

was determined as $C_{83}H_{135}N_{14}O_{15}S_2$ by HR-FAB MS. The IR spectrum (ν_{max} 1640 cm^{-1}, amide groups) and the ^1H and ^{13}C NMR spectral data of **1** indicated it to be a highly *N*-methylated lipophilic peptide. The ^{13}C NMR and DEPT spectra of **1** revealed the presence of two phenyl groups, one oxymethylene carbon (δ_C 64.60), and 14 amide carbonyl carbons (δ_C 175.79, 173.00, 172.88, 172.47, 172.35, 171.72, 170.68, 170.61, 170.51, 170.46, 170.44, 170.11, 170.07 and 167.91). The ^1H NMR spectrum of **1** displayed the signals ascribable to two amide *N*-H protons (δ 7.37 and 6.46) and 12 *N*-methyl groups (δ 3.29, 3.06, 3.04, 3.03, 3.01, 3.001, 2.998, 2.986, 2.96, 2.95, 2.77 and 2.34). The detailed analysis of the 2D NMR (COSY, HOHAHA, HMQC, HMBC) spectra of **1** revealed the existence of 1 equiv. each of *N*-methylisoleucine (MeIle), phenylalanine (Phe), 2 equiv. each of *N*-methylalanine (MeAla) and *N*-methylcysteine (MeCys), and 6 equiv. of *N*-methylvaline (MeVal) together with *N*- and *C*-terminal residues.

The ^1H and ^{13}C NMR signals ascribable to the residue in the *C*-terminus were similar to those of phenylalanine except for the observation of an additional signal ascribable to an oxymethylene group [(δ 3.77, 3.60 (both 1H), δ_C 64.60)] instead of the carboxyl group. Then, the residue in the *C*-terminus was assigned to be phenylalaninol, while no correlation was observed between the oxymethylene signal and the other amino acid residue in the HOHAHA and HMBC spectra of **1**. In order to confirm the presence of the terminal alcohol moiety, the pyridine–DMF solution of **1** was treated with phthalic anhydride and DMAP to furnish a phthalic ester **2**.

On the other hand, the residue in the *N*-terminus of **1** was proposed to be *N*-methylglutamic acid (MeGlu); however, the HMBC correlation between *N*-Me (δ 2.77) and δ-CO (δ_C 175.79) assignable to the *N*-terminal residue indicated the presence of an intramolecular amide bond. Thus, the residue in the *N*-terminus was presumed to be not MeGlu but *N*-methylpyroglutamic acid (pyroMeGlu). However, the signals ascribable to β- and γ-protons of the pyroMeGlu residue were observed to be close to each other and it was difficult to confirm the structure of pyroMeGlu. Then, we synthesized a model compound **5** as shown in Scheme 1. The ^1H and ^{13}C signals assignable to the pyroMeGlu part in **5** were closely similar to those of **1**. Consequently, we could presume the presence of L-pyroMeGlu including the absolute configuration. Natural depsipeptides containing pyroGlu, such as didemnins H, D, E, have been isolated from tunicate,[5] while a peptide containing *N*-methylpyroglutamic acid (pyroMeGlu) has not been reported up to now.

From the detailed 2D NMR analysis of **1**, the presence of two continuous *N*-methylcysteine (MeCys) residues adjacent to the phenylalaninol residue at the *C*-terminus was revealed. Based on the HR-FAB MS analysis of **1** and **2**, the formation of the S–S bond was confirmed. The eight-membered cysteinyl-cysteine (ox-[Cys-Cys]) connected by a disulfide bond has been found in a few natural peptides such as bicyclic malformin,[6] catalytic domain of mercuric ion reductase[7] and nicotinic acetylcholine receptor,[8] while compound **1** was the first example of a peptide having *N*-methylated eight-membered cysteinyl-cysteine (ox-[MeCys-MeCys]) connected by a disulfide bond (Fig. 1).

The amino acid sequence of kendarimide A (**1**) was examined by NOESY experiment of **1**, which gave sequential information from the correlation between the amide protons or *N*-methyl protons and α-protons of the adjacent residue via the amide bond (Fig. 2). The same resolution was deduced from the HMBC correlations between the amide protons or *N*-methyl protons and its own the α-protons and carbonyl carbons of the adjacent residue, which were further correlated with α-protons of the adjacent residue (Fig. 2).

The amino acid sequence of **1** was further confirmed by FAB MS analysis of **1**. Thus, the positive ion FAB MS of **1** provided many fragment ion peaks containing the *N*-terminus, which were consistent with the amino acid sequence of **1** as shown in Figure 3. The assignment of the fragment ions of **1** was further confirmed in comparison with the fragmentation of the phthalic ester **2**, which gave a similar fragmentation in the positive ion FAB MS together with the quasi-molecular ion ($[M+Na]^+$) peak at *m*/*z* 1802, while the negative ion FAB MS of **2** did not give the expected fragment ion peaks containing the *C*-terminus.

In order to determine the absolute configuration of the amino acid sequence, **1** was hydrolyzed by 6 N HCl at

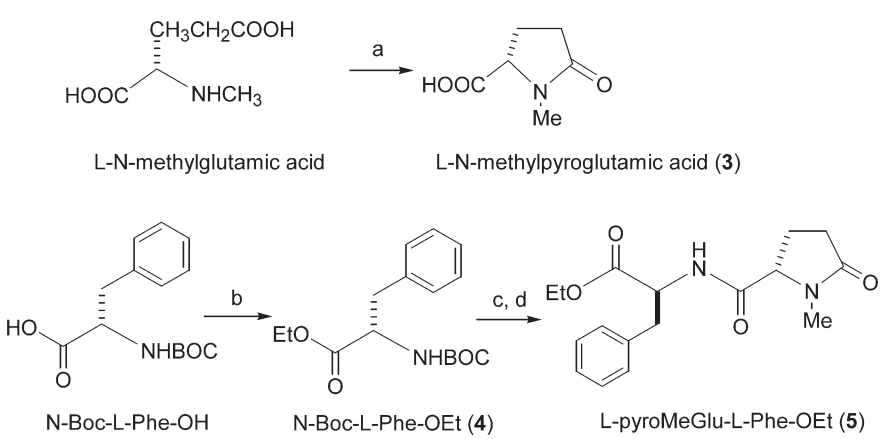

Scheme 1. Synthesis of L-pyroMeGlu-L-Phe-OEt. Conditions a: H_2O, 132 °C, 1.9 kg/cm^2 (autoclave), b: $NaHCO_3$, C_2H_5I, DMF, 98%, c: TFA, CH_2Cl_2, d: L-pyroMeGlu, DEPC, TEA, DMF, 0 °C.

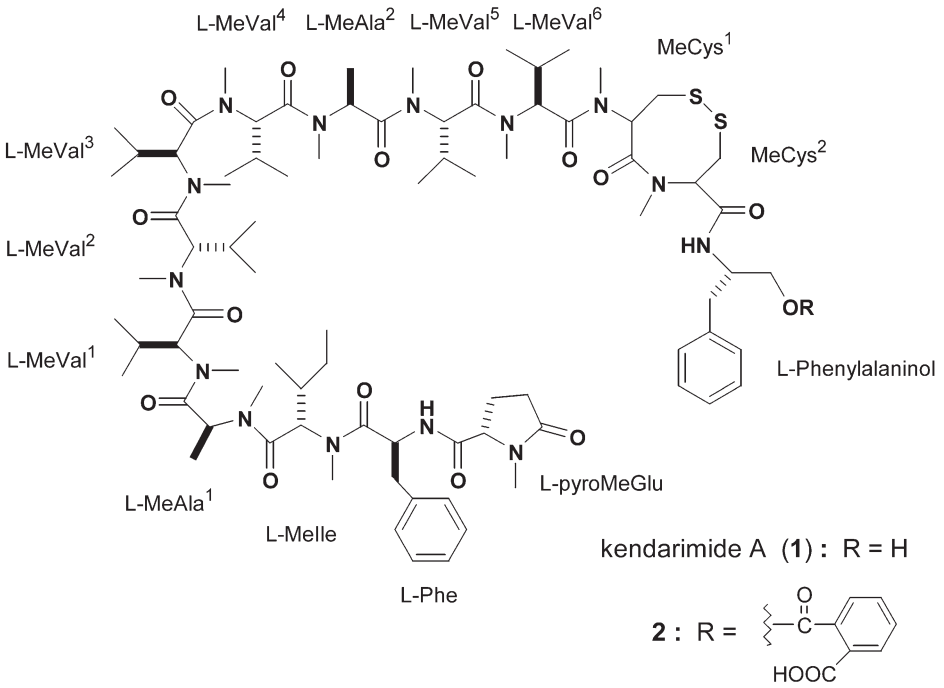

Figure 1. Chemical structure of kendarimide A (**1**).

110 °C for 20 h. Marfey's derivatives[9] of the resulting hydrolysates were analyzed by HPLC to reveal the presence of one each of L-MeGlu, L-Phe, L-MeIle, L-phenylalaninol, and two MeAla and six L-MeVal. L-PyroMeGlu was converted to L-MeGlu under this hydrolysis condition. Thus, Marfey's method was applicable to determine the absolute configuration of phenylalaninol. However, *N*-methylcysteines existing as an eight-membered disulfide form (ox-[MeCys-MeCys]) could not be analyzed by Marfey's method because of decomposition and racemization during acidic hydrolysis. Consequently, we were able to determine the absolute stereostructure of kendarimide A (**1**) except for the absolute configuration of two MeCys. The absolute configuration of two *N*-methylcysteine residues is under investigation by a synthetic method.

Kendarimide A (**1**) completely reversed the resistance to colchicine in KB-C2 cells,[10] human carcinoma cell line overexpressing P-gp, at a 6 μM concentration. Thus, the 6 μM of **1** showed a 87% growth inhibition against KB-C2 cells in the presence of 0.1 μg/mL of colchicine, while **1** showed no inhibitory activity against KB-3-1 cells at a 6 μM concentration. Interestingly, cyclosporin A,[11] a potent MDR modulator against P-gp, is also a peptide composed of

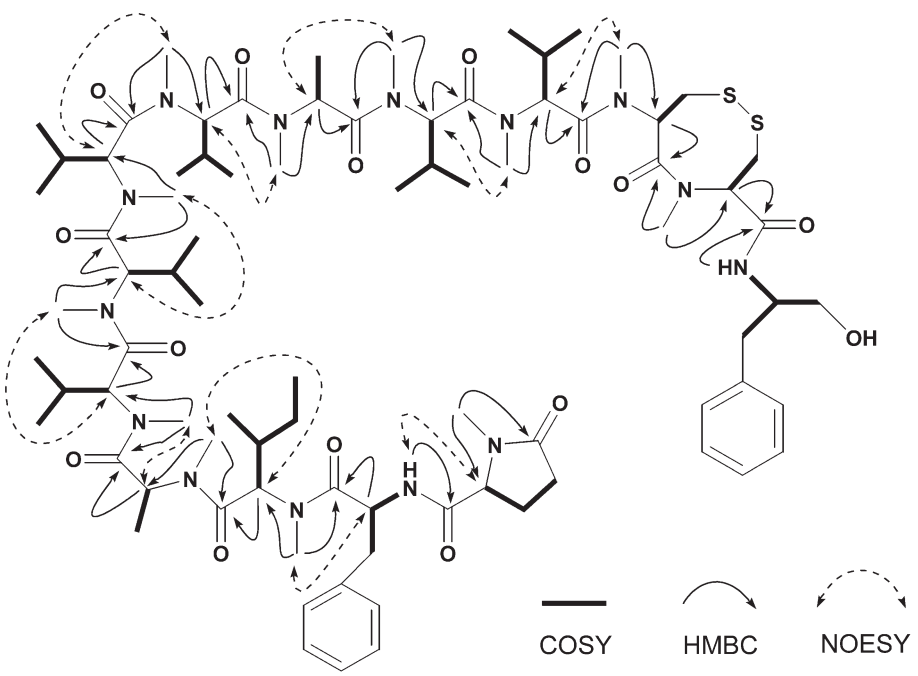

Figure 2. 2D NMR correlations for kendarimide A (**1**).

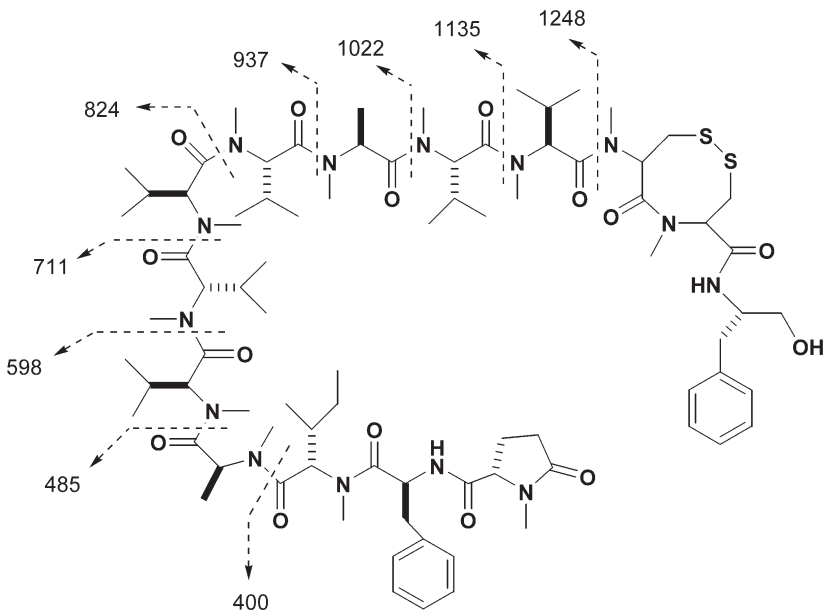

Figure 3. Fragment ion peaks observed in positive ion FAB MS for kendarimide A (**1**).

11 amino acid residues including many *N*-methyl residues. The similarity of these compounds may be related to the MDR reversing activity.

3. Experimental

3.1. General

3.1.1. Isolation of kendarimide A (1). The titled dried sponge (350 g) collected at Sulawesi Island, Indonesia, was extracted with MeOH (3×1 L) to obtain a MeOH extract (36 g). The MeOH extract was partitioned into an H_2O–EtOAc mixture (1:1), and the EtOAc layer was evaporated to afford an EtOAc extract (4.2 g). The EtOAc extract, which showed MDR reversing activity, was subjected to silica gel flash column chromatography ($CHCl_3$–MeOH and hexane–EtOAc). The active fraction was further separated by ODS column (Cosmosil 75C_{18}-OPN, MeOH–H_2O) chromatography and finally purified by reversed-phase HPLC (Cosmosil 5C_{18}AR 10ϕ×250 mm, 90% aq MeCN; Cosmosil 5Ph 10ϕ×250 mm, 86% aq MeOH) to furnish kendarimide A (**1**) (16 mg, 0.0047% from the dried sponge).

Kendarimide A (**1**): $[\alpha]_D^{25}=-273°$ (MeOH, c=0.3); IR (KBr) ν_{max} 3354, 3319, 1640 cm^{-1}; positive ion FAB MS: m/z 1631 $(M+H)^+$, see in Figure 3 for the fragment ion. HR-FAB MS: obsd; m/z 1631.9708. Calcd for $C_{83}H_{135}N_{14}O_{15}S_2$; m/z 1631.9743 $(M+H)^+$. ^1H NMR (600 MHz) and ^{13}C NMR (150 MHz) data in $CDCl_3$ are given in Table 1.

3.1.2. Phthalic ester 2 of kendarimide A (1). The DMF (20 μL) solution of **1** (0.5 mg, 0.3 μmol) was treated with phthalic anhydride (0.2 mg, 3 equiv.), DMAP (0.1 mg, 3 equiv.), and pyridine (5 μL) and stirred for 21 h at room temperature. After removal of the solvent under reduced pressure, the residue was dissolved in H_2O and extracted with EtOAc. The organic layer was washed with 0.5 N aq HCl and brine, dried over $MgSO_4$ and then evaporated in reduce pressure. The crude product was purified by reversed-phase HPLC (Mightysil RP-18 4.6ϕ×150 mm, 85% MeCN) to give phthalic ester **2**. Compound **2**: positive ion FAB MS: m/z 1802 $(M+Na)^+$, 1248, 1135, 1022, 937, 824, 711, 598, 485, 400. HR-FAB MS: obsd; m/z 1802.9645. Calcd for $C_{91}H_{138}N_{14}NaO_{18}S_2$; m/z 1802.9653 $(M+Na)^+$.

3.2. Determination of the absolute configurations of amino acids

(1) *Acid hydrolysis of kendarimide A* (**1**): compound **1** (1.0 mg) was treated with 0.5 mL of 6 N aq HCl and heated at 110 °C for 20 h. The reaction mixture was evaporated and dried under reduced pressure.

(2) *HPLC analysis of Marfey's derivatives*. The H_2O solution (50 μL) of the above hydrolysates was treated with 350 μL of 1-fluoro-2,4-dinitrophenyl-5-L-leucine amide (L-FDLA) in acetone (10 mg/mL) and 155 μL of 1 M aq Na_2CO_3 and the mixture was kept at 37 °C for 6 h. The 2 aq HCl (77 μL) was added, and the resulting solution was diluted with 400 μL of MeCN. An aliquot (5 μL) of the L-FDLA derivatives was analyzed by reversed-phase HPLC with two different conditions as shown below.

(a) A linear gradient from 0.1 M aq CH_3COONH_4 (containing 0.25% TFA)/MeCN (85:15) to 0.1 M aq CH_3COONH_4 (containing 0.25% TFA)/MeCN (55:45) over 45 min (flow rate: 1.0 mL/min) was used to separate the L-FDLA derivatives, which were detected by UV absorption at 340 nm. The system was allowed to equilibrate for 30 min at 15% MeCN prior to the next analysis. Mightysil RP-18 column (4.6ϕ×150 mm) was used for separation and maintained at 30 °C.

(b) A linear gradient from 0.5% aq TFA/MeCN (70:30) to

Table 1. NMR data for kendarimide A (**1**) in $CDCl_3$

C/H no.	δ_H (J in Hz)[a]	δ_C[b]	C/H no.	δ_H[a] (J in Hz)	δ_C[b]
pyroMeGlu			4	0.74, d (6.9)	17.71[m]
1	—	170.68	NMe	2.998[c], s	30.37[i]
2	3.88, dd (8.7, 4.3)	63.51	MeVal[4]		
3a	2.31	23.21	1		170.51[g]
3b	1.77, m	—	2	5.13, d (11)	58.33
4a	2.29	29.24	3	2.33	26.96
4b	2.35	—	3-Me	0.85 (overlapped)	19.37[k]
5		175.79	4	0.81, d (6.6)	18.13[l]
NMe	2.77, s	28.94	NMe	2.986,s	30.00[h]
Phe			MeAla[2]		
1		171.72	1		172.47
2	5.25, dd like	49.93	2	5.40, q (6.9)	49.15
3a	3.09 (overlapped)	38.63	3	1.24, (d, 6.9)	14.82
3b	2.86 (overlapped)	—	NMe	3.001[c], s	30.71
4		135.43	MeVal[5]		
5/9	7.15, m	129.16[d]	1		170.61
6/8	7.28, m	128.53[e]	2	5.11, d (11)	58.39
7	7.25, m	127.36	3	2.31	27.04
NH	6.46, (d, 8.7)	—	3-Me	0.87 (overlapped)	19.27
MeIle			4	0.81, d (6.6)	18.18[l]
1		170.07[f]	Nme	3.01, s	30.02[h]
2	5.21, d (11)	56.84	MeVal[6]		
3	2.09, m	33.21	1		172.88
3-Me	0.81, d (6.6)	15.20	2	5.28, d (11)	57.78
4	1.24 (overlapped)	24.14	3	2.27	27.72
5	0.84, t (7.7)	10.69	3-Me	0.96, d (6.5)	19.50
NMe	2.95, s	30.24	4	0.77, d (6.5)	17.98
MeAla[1]			Nme	2.96, s	30.30
1		172.35	MeCys[1]		
2	5.42, q (6.9)	49.31	1		173.00
3	1.23, (d, 6.9)	15.04	2	5.56, dd like	56.63
NMe	3.06, s	30.65	3a	3.23, dd (14, 12)	38.80
MeVal[1]			3b	2.86 (overlapped)	—
1		170.44[g]	Nme	3.29, s	32.50
2	5.18, d (11)	58.20[j]	MeCys[2]		
3	2.32	27.35	1		167.91
3-Me	0.86 (overlapped)	19.68	2	5.23, dd like	59.25
4	0.74, d (6.9)	17.66[m]	3a	3.33, dd (14, 3.8)	37.17
NMe	3.04, s	30.43	3b	2.85 (overlapped)	—
MeVal[2]			Nme	2.34, s	28.01
1		170.11[f]	Phenylalaninol		
2	5.19, d (11)	58.07	1a	3.77, dd (11, 3.0)	64.60
3	2.32	27.20	1b	3.60, dd (11, 4.1)	—
3-Me	0.85 (overlapped)	19.41[k]	2	4.28, m	52.94
4	0.73, d (6.8)	17.73[m]	3a	2.95 (overlapped)	37.02
NMe	3.03, s	30.35[i]	3b	2.83 (overlapped)	—
MeVal[3]			4	—	137.83
1		170.46[g]	5/9	7.21, m	129.20[d]
2	5.17, d (11)	58.22[j]	6/8	7.26, m	128.60[e]
3	2.33	27.20	7	7.20, m	126.55
3-Me	0.86 (overlapped)	19.37[k]	NH	7.37, d (8.7)	—

[a] Recorded at 600 MHz.
[b] Recorded at 150 MHz.
[c–m] Assignment may be interchangeable for items with identical superscript letters c–m.

0.5% aq TFA/MeCN (30:70) over 45 min (flow rate: 0.22 mL/min) and then to 0.5% aq TFA/MeCN (10:90) over 10 min was also used to separate the L-FDLA derivatives. The system was allowed to equilibrate for 80 min at 30% aq MeCN prior to the next analysis. YMC AS-3C2-3 column (2.0×150 mm) was used for separation and maintained at 30 °C.

Standard amino acids were derivatized as described above. The each peak was identified by co-injection with the respective FDLA derivative of L- or D-amino acid. Resulting data are given in Table 2.

3.2.1. L-Phenylalaninol-L-FDLA. ^{1}H NMR ($CDCl_3$, 500 MHz, δ): 8.95 (1H, s), 7.16–7.07 (5H, m), 5.77 (1H, s), 3.99 (1H, m), 3.86 (1H, m), 3.60 (1H, dd, J=11, 4.5 Hz), 3.53 (1H, dd, J=11, 4.5 Hz), 2.91 (1H, dd, J=14, 6.5 Hz), 2.82 (1H, dd, J=14, 6.5 Hz), 1.75 (3H, m), 0.95 (3H, d, J=5.5 Hz), 0.88 (3H, d, J=5.5 Hz).

3.2.2. D-Phenylalaninol-L-FDLA. ^{1}H NMR ($CDCl_3$, 500 MHz, δ): 8.99 (1H, s), 7.22–7.07 (5H, m), 5.59 (1H, s), 3.82 (2H, m), 3.60 (1H, dd, J=11.5, 4.5 Hz), 3.56 (1H, dd, J=11.5, 4.5 Hz), 2.96 (1H, dd, J=14, 6 Hz), 2.87 (1H, dd, J=14, 8 Hz), 1.72 (3H, m), 0.96 (3H, d, J=6 Hz), 0.88 (3H, d, J=6 Hz).

3.2.3. Synthesis of L-*N*-methylpyroglutamic acid (3). A

Table 2. HPLC analysis of the Marfey's derivatives of the hydrolysates of kendarimide A (**1**)

Amino acid	t_R of standard (min)		Amino acid found by co-injection
	Condition (a)	Condition (b)	
L-MeAla	30.13	42.97	✓
D-MeAla	32.65	44.25	
L-MeVal	35.53	51.16	✓
D-MeVal	44.69	57.28	
L-Phe	35.28	52.29	✓
D-Phe	37.63	59.79	
L-MeGlu	20.43	22.87	✓
D-MeGlu	24.47	25.20	
L-MeIle	39.68	54.89	✓
D-MeIle	49.73	60.94	
L-Phenylalaninol	54.55	53.16	✓
D-Phenylalaninol	64.15	59.71	

H_2O solution of L-*N*-methylglutamic acid (50 mg/100 μL) was autoclaved at 132 °C for 60 min. Water was evaporated under reduced pressure to give L-*N*-methylpyroglutamic acid (**3**). L-*N*-Methylpyroglutamic acid (**3**): FAB MS: *m*/*z* 144 $(M+H)^+$.

3.2.4. Synthesis[12] of *N*-Boc-L-Phe-OEt (4). To a suspension of *N*-Boc-L-Phe-OH (**3**) (265 mg, 1 mmol) and sodium hydrogen carbonate (168 mg, 2 mmol) in 5 mL of DMF, ethyl iodide (0.4 mL, 5 mmol) was added at room temperature. The reaction mixture was stirred for 24 h, and then partitioned into H_2O–EtOAc mixture. The organic phase was washed with H_2O, dried over sodium sulphate, evaporated under reduced pressure, and the crude product was purified by silica gel column chromatography [hexane–EtOAc (8:2)] to furnish *N*-Boc-L-Phe-OEt (**4**) (286 mg, 98%). Compound **4**: FAB MS, *m*/*z* 294 $(M+H)^+$. ^{1}H NMR ($CDCl_3$, 500 MHz, *δ*): 7.21 (5H, m), 7.09 (2H, m), 4.95 (1H, brd), 4.51 (1H, m), 4.11 (2H, q, *J*=7.5 Hz), 3.04 (2H, d, *J*=6 Hz), 1.37 (9H, s), 1.18 (3H, t, *J*=7.5 Hz).

3.2.5. Synthesis of L-pyroMeGlu-L-Phe-OEt (5). To a solution of **4** (50 mg, 0.17 mmol) in CH_2Cl_2 (1.5 mL) at 0 °C, TFA (1.5 mL) was added dropwise. The mixture was stirred at 0 °C for 2 h, and then concentrated in reduced pressure. The solution of the resulting amine salt and L-*N*-methylpyroglutamic acid (**2**) (25 mg, 0.17 mmol) in DMF (1 mL) was treated with diethyl phosphorocyanidate[13] (DEPC) (34 μL, 0.23 mmol) at 0 °C. After 15 min, triethylamine (TEA) (49 μL, 0.36 mmol) was added, and the mixture was stirred at 0 °C for 16 h. The reaction mixture was partitioned into EtOAc/benzene–H_2O mixture, and the organic layer was washed with ice-cold 1 M aq $KHSO_4$ solution, sat. $NaHCO_3$ solution, and brine, dried over $NaSO_4$, and concentrated in reduced pressure. The crude product was purified by silica gel column chromatography (hexane/EtOAc=1:2 then EtOAc) to give L-pyroMeGlu-L-Phe-OEt (**5**) as a white solid (38 mg, 81%). Compound **5**: $[\alpha]_D^{25}=-11.6°$ (MeOH, *c*=0.253). HR-FAB MS: obsd; *m*/*z* 319.1673. Calcd for $C_{17}H_{23}N_2O_4$; *m*/*z* 319.1658 $(M+H)^+$. ^{1}H NMR ($CDCl_3$, 500 MHz, *δ*): 7.26–7.23 (3H, m), 7.12 (2H, m), 6.41 (1H, d, *J*=8 Hz, NH), 4.91 (1H, dd-like, α-H of Phe), 4.20 (2H, q, *J*=7.5 Hz, Et), 3.88 (1H, brs, α-H of Glu), 3.24 (1H, dd, *J*=14, 5 Hz, β-H of Phe), 3.01 (1H, dd, *J*=14, 8 Hz, β-H of Phe), 2.76 (3H, s, N-Me), 2.27 (3H, m, β,γ-H of Glu), 1.73 (1H, t-like, β-H of Glu), 1.27 (3H, t, *J*=7.5 Hz, Et). ^{13}C NMR ($CDCl_3$, 125 MHz, δ_c): 175.81 (δ-C of Glu), 171.26 (CO of Phe), 170.92 (CO of Glu), 135.77, 129.08, 128.56, 127.22, 63.60 (α-C of Glu), 61.71 (Et), 52.58 (α-C of Phe), 37.72 (β-C of Phe), 29.23 (γ-C of Glu), 28.91 (N-Me), 23.09 (β-C of Glu), 14.08 (Et).

3.3. Bioassay

Human epidermoid carcinoma KB cells (KB-3-1) were used as the parental cell line for the present study. KB-3-1 cells were cultured in RPMI 1640 medium with 0.44 mg/mL of glutamine, 50 μg/mL of kanamycin sulfate, supplemented with 10% newborn calf serum. MDR cell line, KB-C2,[10] was selected from KB-3-1 cells and maintained in the medium containing 2 μg/mL of colchicine. Reversing activity and cytotoxicity were measured by means of MTT colorimetric assay performed in 96-well plates. Equal numbers of cells (10,000) were inoculated into each well with 100 μL of the culture medium. After 24 h preincubation (37 °C, 5% CO_2), a 50 μL solution of colchicine and testing sample were added to each well and the whole were further incubated for 48 h. Thereafter, 25 μL of MTT solution (2 mg/mL in PBS) was added to each well and incubated for further 3 h. After removing the medium by aspiration, the resulting formazan was dissolved in 200 μL of dimethylsulfoxide. The percentage of cell growth inhibition was calculated from the absorbance at 540 nm. The cytotoxic activity of the testing sample was also examined by MTT assay using parental KB 3-1 cells.

Acknowledgements

The authors are grateful to Prof. R.W.M. Soest, Zoologisch Museum, University of Amsterdam, for identification of the sponge. The authors are also grateful to the Takeda Science Foundation, the Houansha Foundation, the Tokyo Biochemical Research Foundation, the Uehara Memorial Foundation and the Ministry of Education, Culture, Sports, Science, and Technology of Japan for financial support.

References and notes

1. Horio, M.; Gottesman, M. M.; Pastan, I. *Prod. Natl. Acad. Sci. U.S.A.* **1988**, *85*, 3580–3584.
2. Krishna, R.; Louis, St., M.; Mayer, L. D. *Int. J. Cancer* **2000**, *85*, 131–141.
3. (a) Aoki, S.; Yoshioka, Y.; Miyamoto, Y.; Higuchi, K.; Setiawan, A.; Murakami, N.; Chen, Z. S.; Sumizawa, T.; Akiyama, S.; Kobayashi, M. *Tetrahedron Lett.* **1998**, *39*, 6303–6306. (b) Aoki, S.; Setiawan, A.; Yoshioka, Y.; Higuchi, K.; Fudetani, R.; Chen, Z. S.; Sumizawa, T.; Akiyama, S.; Kobayashi, M. *Tetrahedron* **1999**, *55*, 13965–13972. (c) Aoki, S.; Chen, Z. S.; Higashiyama, K.; Setiawan, A.; Akiyama, S.; Kobayashi, M. *Jpn. J. Cancer Res.* **2001**, *92*, 886–895.
4. Aoki, S.; Okano, M.; Matsui, K.; Itoh, T.; Satari, R.; Akiyama, S.; Kobayashi, M. *Tetrahedron* **2001**, *57*, 8951–8957.
5. Boulanger, A.; Abou-Mansour, E.; Badre, A.; Banaigs, B.;

Combaut, G.; Francisco, C. *Tetrahedron Lett.* **1994**, *35*, 4345–4348.
6. Bodanszky, M.; Stahl, G. L. *Prod. Natl. Acad. Sci. U.S.A.* **1974**, *71*, 2791–2794.
7. Schiering, N.; Kabsch, W.; Moore, M. J.; Distefano, M. D.; Walsh, C. T.; Pai, E. F. *Nature* **1991**, *352*, 168–172.
8. Creighton, C. J.; Reynolds, C. H.; Lee, D. H. S.; Leo, G. C.; Reitz, A. B. *J. Am. Chem. Soc.* **2001**, *123*, 12664–12669.
9. (a) Marfey, P. *Carlsberg Res. Commun.* **1984**, *49*, 591–596. (b) Fujii, K.; Ikai, Y.; Oka, H.; Susuki, M.; Harada, K. *Anal. Chem.* **1997**, *69*, 5146–5151.
10. Akiyama, S.; Fojo, J. A.; Hanover, J. A.; Pastan, I. H.; Gottesman, M. M. *Somat. Cell Mol. Genet.* **1985**, *11*, 117–126.
11. Hait, W. N.; Stein, J. M.; Koletsky, A. J.; Harding, M. W.; Handschumacher, R. E. *Cancer Commun.* **1989**, *01*, 35–43.
12. Bocchi, V.; Casnati, G.; Dossena, A.; Marchelli, R. *Synthesis* **1979**, 961–962.
13. Takuma, S.; Hamada, Y.; Shioiri, T. *Chem. Pharm. Bull.* **1982**, *30*, 3147–3153.

Available online at www.sciencedirect.com
SCIENCE DIRECT®
Tetrahedron
Tetrahedron 60 (2004) 7061–7066

Preparation and biological activities of optically active dehydroxymethylepoxyquinomicin, a novel NF-κB inhibitor

Yoshikazu Suzuki, Chie Sugiyama, Osamu Ohno and Kazuo Umezawa*

Department of Applied Chemistry, Faculty of Science and Technology, Keio University, 3-14-1 Hiyoshi, Kohoku-ku, Yokohama 223-0061, Japan

Received 27 June 2003; revised 28 January 2004; accepted 28 January 2004

Available online 25 June 2004

Abstract—NF-κB is a transcription factor that induces inflammatory cytokines and anti-apoptotic proteins. We have designed a new NF-κB inhibitor based on the structure of the antibiotic epoxyquinomicin C. The designed compound, dehydroxymethylepoxyquinomicin (DHMEQ) was synthesized as a racemic form from 2,5-dimethoxyaniline through 5 steps. Application of racemic DHMEQ onto the chiral column (Chiralpak AD) directly gave enantiomeric DHMEQ after purification. (−)-DHMEQ was more potent than its enantiomer. (−)-DHMEQ was found to inhibit NF-κB activity and macrophage differentiation induced by 12-*O*-tetradecanoylphorbol-13-acetate (TPA) in human monocyte THP-1 cells.

1. Introduction

1.1. Role and signal transduction of NF-κB

NF-κB was found in 1986 as a nucleoprotein bound to the enhancer region of the gene encoding the immunoglobulin κ chain.[1] NF-κB is typically a heterodimer consisting of p65 (Rel A) and p50 proteins.[2] NF-κB is the transcription factor that binds to the κB sequence. It promotes the transcription of the immunoglobulin κ chain, cytokines such as IL-1, IL-2, IL-6, IL-8, TNF-α and interferon γ; cell adhesion molecules such as E-selectin, ICAM-1, and VCAM-1; MHC proteins; and viral proteins. Therefore, NF-κB is mainly an inducer of inflammatory cytokines,[2] and so its inhibitors may be useful as anti-inflammatory agents. NF-κB also induces the transcription of anti-apoptotic proteins called inhibitor of apoptosis proteins. TNF-α is an apoptosis-inducing factor, and the TNF-α receptor contains the death domain like FAS. However, TNF-α does not induce apoptosis in most cases, because TNF-α induces NF-κB activation to inhibit apoptosis.[3] NF-κB is often constitutively activated in human carcinomas such as prostate carcinomas, bladder carcinomas, breast carcinomas, and melanomas and leukemias such as adult T-cell leukemia. The activation of NF-κB may provide additional malignant phenotypes. Therefore, NF-κB function inhibitors of low-molecular-weight should be useful as both anti-inflammatory and anticancer agents.

NF-κB is inactive without stimulation, and it is activated by extracellular signals such as TNF-α, IL-1, LPS, UV, and phorbol esters.[1] The signal transduction pathways from the TNF-α receptor to NF-κB activation have been extensively studied.[4] TNF-α acts through TNF-α receptor (TNFR), inducing its trimerization. The cytoplasmic region of TNFR binds to TRADD (TNFR-associated death domain protein). TRADD activates RIP (receptor interacting protein) and then TRAF-2 (TNFR-associated factor-2). TRAF-2 activates NIK (NF-κB-inducing kinase). NIK activates IKK, which induces phosphorylation of IκB. IκB is an inhibitory protein bound to NF-κB. Phosphorylation of IκB induces its release from its complex with NF-κB after ubiquitination and degradation by proteasomes. Liberated NF-κB molecules then enter the nucleus where they bind to the κB site of DNA.

1.2. Molecular design and synthesis of DHMEQ as an NF-κB inhibitor

Panepoxydone was isolated from the basidiomycete *Lentinus crinitu* and inhibited TNF-α-induced activation of NF-κB in a promoter-reporter assay using COS-7 cells.[5] Cycloepoxydon was also isolated from a deuteromycete strain as an NF-κB inhibitor.[6] On one hand, four novel 5,6-epoxycyclohexenone compounds, named epoxyquinomicins A, B, C and D, were isolated from *Amycolatopsis* as weak antibiotics.[7] Epoxyquinomicin C is the simplest in structure among them, having a 4-hydroxy-5,6-epoxycyclohexenone

Keywords: NF-κB; DHMEQ; Optical resolution; Nuclear transport; Inflammation; Apoptosis.
* Corresponding author. Tel.: +81-45-566-1558; fax: +81-45-566-1558; e-mail address: umezawa@applc.keio.ac.jp

0040–4020/$ - see front matter © 2004 Elsevier Ltd. All rights reserved.
doi:10.1016/j.tet.2004.01.103

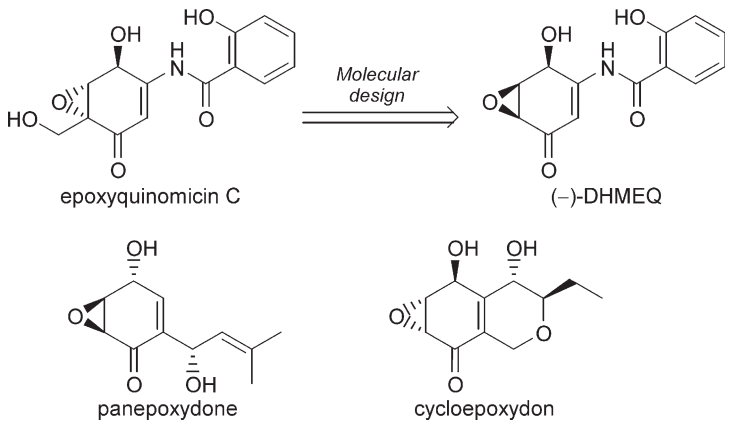

Figure 1. Molecular design of DHMEQ based on the structures of epoxyquinomicin C, panepoxydone, and cycloepoxydon.

structure like panepoxydone. Therefore, we tested the inhibitory activity on NF-κB. However, it did not inhibit activation of NF-κB. Epoxyquinomicin C has an additional hydroxymethyl group compared with panepoxydone. Therefore, we designed and synthesized DHMEQ as one of the 5-dehydroxymethyl derivatives of epoxyquinomicin C (Fig. 1).[8]

2. Results and discussion

2.1. Preparation of optically active DHMEQ

To prepare racemic DHMEQ, we largely modified each reaction reported in our previous communication.[8] These optimized reaction conditions are described in Section 4. Scheme 1 shows the synthetic route for DHMEQ. Salicylamide **2** was prepared from commercially available 2,5-dimethoxyaniline **3** and acetylsalicyloyl chloride. Treatment of **2** with iodobenzene diacetate in methanol formed bisdimethylacetal **3** temporarily and following selective hydrolysis of the vinylogous amide dimethylacetal group gave partially protected quinone **4** in 63% yield base on **2**. Epoxidation of **4** with H_2O_2 and aq NaOH in THF gave epoxyquinonedimethylacetal **5** in 80% yield. Fortunately, the salicyl group remained intact during epoxidation unlike in the case of acetamide.[9] The masked carbonyl group of **5** was deacetalized. Treatment of **5** with BF_3-OEt_2 in CH_2Cl_2

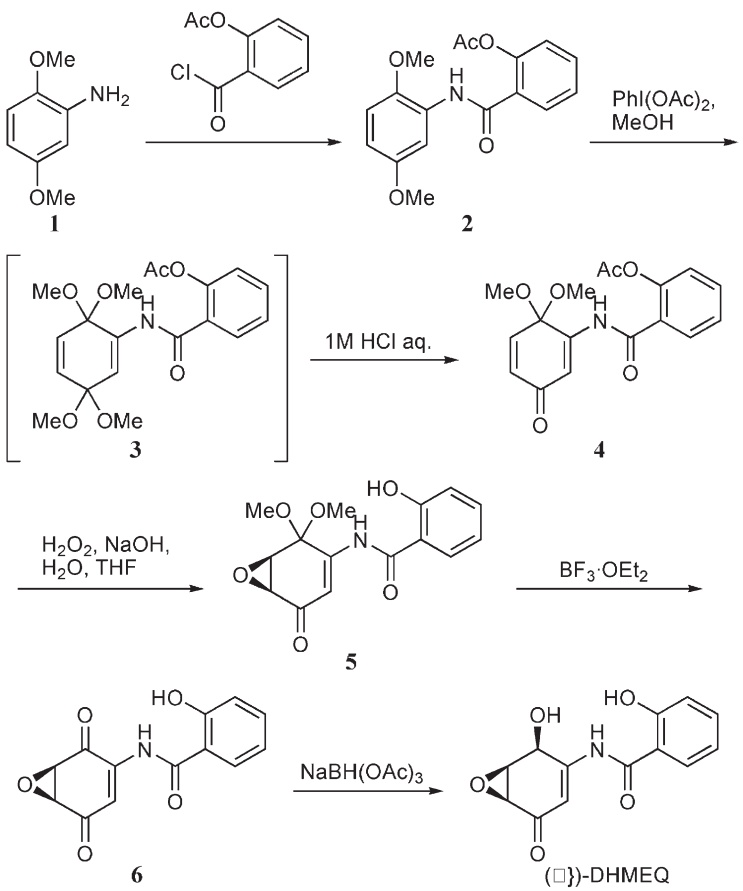

Scheme 1.

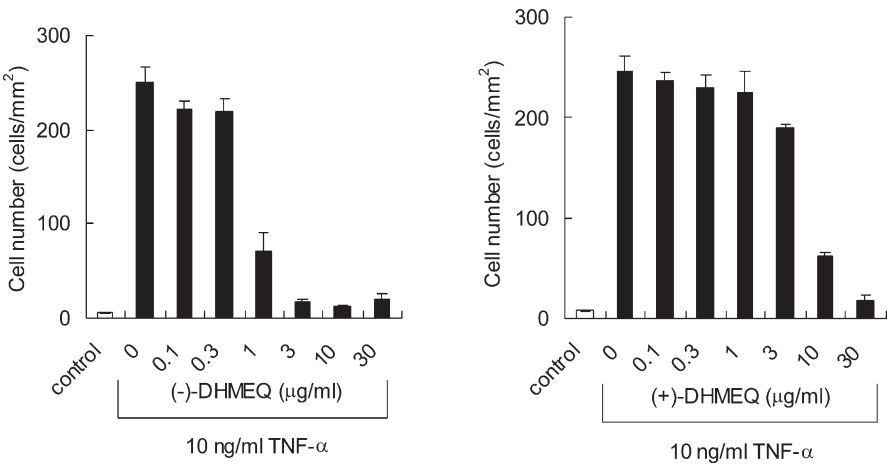

Figure 2. Inhibition of cellular adhesion activity by (−)- and (+)-DHMEQ in TNF-α-treated human umbilical vein endothelial cells (HUVEC). HUVEC were treated with TNF-α for 6 h in the presence or absence of DHMEQ enantiomer, then HUVEC were washed and added by HL-60 cells for 1 h.

gave epoxyquinone **6** in 70% yield. Furthermore, reduction of **6** with $NaBH(OAc)_3$ was found to occur regio- and stereo-selectively and afforded DHMEQ in high yield (88%). This procedure using $NaBH(OAc)_3$ did not yield epi-DHMEQ. The reduction of vinylogous amide group was not observed. Previously, we accomplished the optical resolution of DHMEQ as corresponding *tert*-butyldimethylsilylether derivative.[8] In the present research, we have developed more practical method to separate each enantiomer. We succeeded in direct enantiomeric separation of DHMEQ using Daicel Chiralpak AD. After the enantiomeric separation, each crude enantiomer was colored in dark blue. The crude compound (1.0 g) was dissolved in THF/EtOH/H_2O and the organic solvents were removed by evaporation. The residual slurry was filtered and washed with H_2O and THF to give about 800 mg each of purified (−) or (+)-DHMEQ.

2.2. Biological activities of (−)-DHMEQ

TNF-α induces NF-κB-mediated expression of adhesion molecules such as ICAM-1, VCAM-1, and E-selectin in human umbilical vein endothelial cells (HUVEC). The expression of these adhesion molecules can be detected by cell adhesion. TNF-α induced adhesion of human myelogenous leukemia HL-60 cells in HUVEC. The (−)-enantiomer was about 10 times more potent than the (+)-enantiomer in inhibition of NF-κB-mediated leukemic cell adhesion to the endothelial cells, as shown in Fig. 2.

Phorbol esters such as 12-*O*-tetradecanoylphorbol-13-acetate induces differentiation of human monocyte THP-1 cells into macrophages. It is not known whether NF-κB mediates this differentiation. Since (−)-DHMEQ was stronger than (+)-DHMEQ, we tested the effect of (−)-enantiomer on phorbol ester-induced differentiation of THP-1 cells. The differentiation can be assayed by production of reactive oxygen species and cellular adherence. As shown in Fig. 3A and B, (−)-DHMEQ inhibited TPA-induced activation of NF-κB and differentiation of THP-1 cells into macrophages, suggesting the involvement of NF-κB in the mechanism of differentiation.

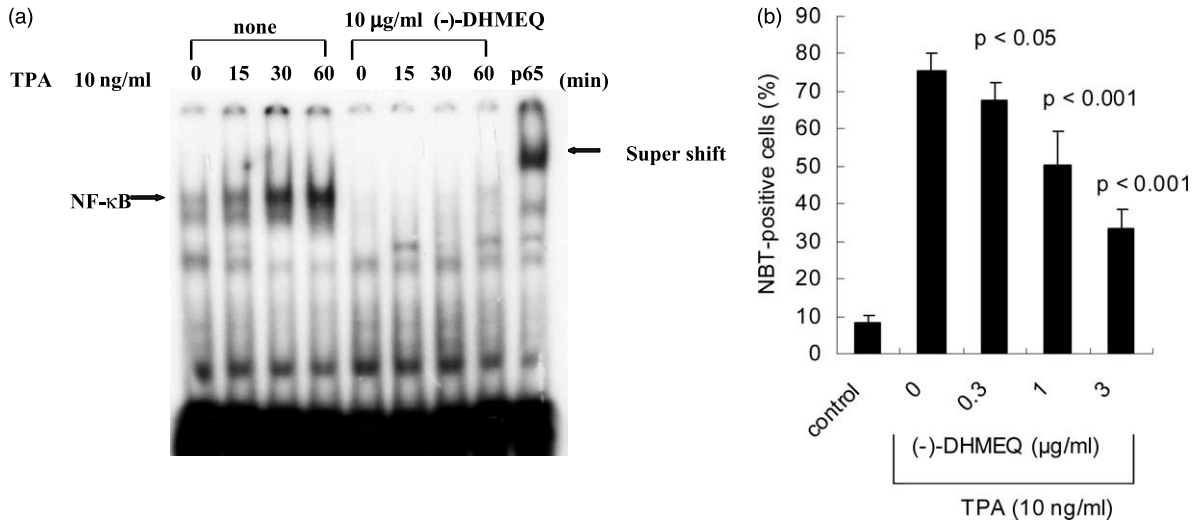

Figure 3. Inhibition of TPA-induced NF-κB activation and differentiation of THP cells into macrophages by (−)-DHMEQ. (A) Inhibition of NF-κB activation. (−)-DHMEQ with or without TPA were added to THP cells for the indicated periods. NF-κB activity was assayed by electrophoresis mobility shift assay (EMSA). B) Inhibition of differentiation. The cells were incubated for 24 h, and differentiation was assayed by NBT reduction. (−)-DHMEQ at 10 μg/mL weakly induced NBT-positive cells.

3. Conclusions

NF-κB is a transcription factor that induces inflammatory cytokines and anti-apoptotic proteins. We designed new NF-κB inhibitors based on the structure of the antibiotic epoxyquinomicin C. DHMEQ was synthesized in the racemic form. In the present research, we succeeded in direct chiral separation of DHMEQ. The (−)-enantiomer was 10 times more potent than the (+)-enantiomer. (−)-DHMEQ inhibited TPA-induced NF-κB activation and differentiation of mouse monocyte THP-1 cells into macrophages, suggesting the involvement of NF-κB in the mechanism of differentiation. Racemic DHMEQ was previously reported to show potent anti-inflammatory and anticancer activity in animals. Optically active agents rather than racemic compounds should be important for the clinical use. Thus, (−)-DHMEQ may be developed as a chemotherapeutic agent.

4. Experimental

4.1. Synthesis of racemic DHMEQ

General. ^{1}H NMR (300 MHz) and ^{13}C NMR (75.4 MHz) spectra were recorded with JEOL JNM Lambda-300 spectrometer. Chemical shifts (δ) are expressed in parts per million (ppm) from tetramethylsilane (TMS) as an internal standard. Mass spectra were recorded in the EI mode with JEOL JMS-GCmate mass spectrometer at the ionization energy of 70 eV. The melting points of solid substances were measured on Yanaco MP-S3 and uncorrected. Silica gel column chromatography was carried out using silica gel 60 particle size 0.063–0.200 mm (E. Merck, Darmstadt). Thin-layer chromatography (TLC) was carried out on 0.25 mm precoated plates of silica gel 60 F_{254} (E. Merck, Darmstadt). Reaction progress was monitored by either UV light (254 nm) or sprayed with 5% phosphomolybdic acid in ethanol as visualizing agent, followed in the latter case by heating on an electric plate. Preparative-thin layer chromatography (prep-TLC) was performed on 0.5 mm×20 cm×20 cm precoated silica gel-60 ($60F_{254}$) (E. Merck, Darmstadt) plates. Reactions involving air or moisture sensitive reagents were carried out in thoroughly dried conventional glass apparatus and solvents. Reactions were carried out under an argon atmosphere unless otherwise stated. All evaporations were carried out on a rotary evaporator under reduced pressure. Reaction temperatures were measured externally. Yields refer to chromatographically and spectroscopically pure compounds.

4.1.1. Acetic acid 2-(2,5-dimethoxy-phenylcarbamoyl)-phenyl ester (2). To a solution of 2,5-dimethoxyaniline (**1**) (1.22 g, 7.96 mmol) and acetylsalicyoyl chloride (1.90 g, 9.57 mmol) in dry THF (40 mL) was added dropwise pyridine (1.29 mL, 15.92 mmol) at 0 °C. The reaction mixture was stirred for 15 min and then allowed to warm to room temperature for 2 h. The reaction mixture was quenched with aqueous 1 N HCl, and extracted with ethyl acetate (20 mL×3), and the organic layers were washed with brine, dried over anhydrous sodium sulfate, and evaporated to yield a brown oily residue. Purification of this residue by using column chromatography over silica gel with ethyl acetate/*n*-hexane (1:5, v/v) as eluent yielded the benzamide **2** as a colourless oil 2.48 g (99%). R_f=0.31 (EtOAc/*n*-hexane, 1:2); ^{1}H NMR ($CDCl_3$) δ 2.34 (s, 3H), 3.80 (s, 3H), 3.85 (s, 3H), 6.59 (dd, 1H, *J*=9.0, 3.3 Hz), 6.80 (d, 1H, *J*=9.0 Hz), 7.14 (dd, 1H, *J*=8.1, 2.1 Hz), 7.35 (td, 1H, *J*=7.8, 1.2 Hz), 7.50 (td, 1H, *J*=8.1, 2.1 Hz), 7.96 (dd, 1H, *J*=7.8, 1.8 Hz), 8.28 (d, 1H, *J*=3.3 Hz), 8.93 (br s, 1H); ^{13}C NMR ($CDCl_3$) δ 21.0, 55.8, 106.2, 108.8, 110.7, 123.3, 126.4, 130.6, 132.2, 142.1, 147.8, 153.9, 162.9, 168.8; HRMS (EI) *m*/*z* calc for $C_{17}H_{17}NO_5$, 315.1107; found, 317.1111.

4.1.2. Acetic acid 2-(6,6-dimethoxy-3-oxo-cyclohexa-1,4-dienylcarbamoyl)phenyl ester (4). To a cold (0 °C) solution of **2** (12.1 g, 40.5 mmol) in MeOH (240 mL) was added $PhI(OAc)_2$ (19.6 g, 60.9 mmol). After stirred at rt for 3 h, the mixture was diluted with EtOAc (1 L) and washed with 1.0 M aqueous HCl (500 mL), saturated aqueous $NaHCO_3$ (500 mL), and brine (500 mL). The organic layer was dried and concentrated. The residue was purified by column chromatography on silica gel (EtOAc/hexane, 1:2) to provide 8.03 g (63%) of **4** as a white solid 8.03 g (63%). Mp 150–152 °C; R_f=0.48 (EtOAc/*n*-hexane, 1:1); ^{1}H NMR ($CDCl_3$) δ 2.33 (s, 3H), 3.18 (s, 6H), 6.32 (dd, 1H, *J*=10.2, 1.8 Hz), 6.59 (d, 1H, *J*=10.2 Hz), 7.06 (d, 1H, *J*=8.1 Hz), 7.26 (t, 1H, *J*=7.8 Hz), 7.43 (m, 2H), 7.90 (dd, 1H, *J*=7.8, 1.5 Hz), 8.81 (br s, 1H); ^{13}C NMR ($CDCl_3$) δ 20.8, 51.3, 94.1, 114.2, 123.3, 125.5, 126.2, 130.9, 133.0, 138.2, 147.1, 147.9, 163.6, 168.4, 185.7; HRMS (EI) *m*/*z* calc for $C_{16}H_{17}NO_6$, 331.1056; found, 331.1063.

4.1.3. *N*-(2,2-Dimethoxy-5-oxo-7-oxa-bicyclo[4.1.0]hept-3-en-3-yl)-2-hydroxy-benzamide (5). To a solution of **4** (779.0 mg, 2.35 mmol) in THF (20 mL) was added dropwise 30% aqueous hydrogen peroxide (4.3 mL) and aqueous 1 N sodium hydroxide (12 mL) at 0 °C. The mixture was stirred for 30 min and then allowed to warm to room temperature over a period of 2 h. The mixture was quenched with saturated aqueous sodium thiosulfate (5 mL) and extracted with ethyl acetate (10 mL×3). The organic layers were washed with brine, dried over anhydrous sodium sulfate, and evaporated to yield a residue. Purification of this residue by using column chromatography over silica gel with ethyl acetate/*n*-hexane/ (3:2, v/v) as eluent yielded the benzamide **5** (573.4 mg) as a white solid (80%). Mp 147–149 °C; R_f=0.59 (MeOH/$CHCl_3$, 1:10); ^{1}H NMR ($CDCl_3$) δ 3.32 (s, 3H), 3.56 (dd, 1H, *J*=3.9, 1.8 Hz), 3.72 (s, 3H), 3.87 (d, 1H, *J*=3.9 Hz), 6.94 (t, 1H, *J*=6.9 Hz), 7.00 (d, 1H, *J*=8.4 Hz), 7.20 (d, 1H, *J*=2.4 Hz), 7.35 (dd, 1H, *J*=1.2, 8.1 Hz), 7.46 (td, 1H, *J*=1.5, 6.9 Hz), 8.65 (br s, 1H), 11.35 (br s, 1H); ^{13}C NMR ($CDCl_3$) δ 50.9, 51.3, 51.4, 52.1, 95.7, 109.6, 119.1, 119.5, 125.8, 135.5, 144.7, 161.5, 168.7, 192.8; HRMS (EI) *m*/*z* calc for $C_{15}H_{15}NO_6$, 305.0899; found, 305.0892.

4.1.4. *N*-(2,5-Dioxo-7-oxa-bicyclo[4.1.0]hept-3-en-3-yl)-2-hydroxy-benzamide (6). To a stirred solution of **5** (555.5 mg, 1.82 mmol) in CH_2Cl_2 (20 mL) was added boron trifluoride etherate (571.9 μL, 4.55 mmol) at −20 °C. The reaction mixture was stirred for 30 min and then warmed up to room temperature for 2 h. On completion the reaction mixture was extracted with chloroform (10 mL×3),

and the organic layers were washed with brine, dried over anhydrous sodium sulfate, and evaporated to yield a brown residue, which upon purification by column chromatography over silica gel using ethyl acetate/*n*-hexane/ (1:2, v/v) as eluent yielded the epoxyquinone **6** 329.9 mg (70%) as a pale solid. Mp 210 °C (dec.); R_f=0.46 (acetone/*n*-hexane, 1:10); ^{1}H NMR ($CDCl_3$) δ 3.88 (dd, 1H, *J*=3.6, 2.1 Hz), 3.98 (d, 1H, *J*=3.6 Hz), 6.96 (t, 1H, *J*=7.8 Hz), 7.02 (d, 1H, *J*=7.8 Hz), 7.50 (d, 2H, *J*=7.5 Hz), 7.62 (d, 1H, *J*=2.1 Hz), 8.85 (br s, 1H), 11.16 (br s, 1H); ^{13}C NMR ($CDCl_3$) δ 53.8, 54.8, 115.5, 118.0, 118.9, 121.4, 132.1, 135.6, 141.0, 157.3, 166.1, 189.3, 192.6; HRMS (EI) *m*/*z* calc for $C_{13}H_9NO_5$, 259.0481; found, 259.0493.

4.1.5. 2-Hydroxy-*N*-(2-hydroxy-5-oxo-7-oxa-bicyclo-[4.1.0]hept-3-en-3-yl)benzamide (DHMEQ). To a stirred solution of **6** (24.3 mg, 0.09 mmol) in methanol (2 mL) was added sodium triacetoxyborohydride (19.9 mg, 0.09 mmol) at 0 °C. The reaction mixture was stirred for 15 min and then warmed up to room temperature for 30 min. The reaction mixture was quenched by adding water (0.5 mL), and extracted with ethyl acetate (10 mL×3), and the organic layers were washed with brine, dried over anhydrous sodium sulfate, and concentrated under reduced pressure. The residue was purified by prep-TLC using MeOH:$CHCl_3$ (1:10, v/v) as eluent to yield DHMEQ 21.5 mg (88%) as a white solid. Mp 185 °C (dec.); R_f=0.45 (MeOH/$CHCl_3$, 1:10); ^{1}H NMR (DMSO-d_6) δ 3.43 (dd, 1H, *J*=4.4, 2.2 Hz), 3.85 (dd, 1H, *J*=4.4, 2.6 Hz), 4.82 (d, 1H, *J*=8.1 Hz), 6.70 (d, 1H, *J*=7.7 Hz), 6.98 (t, 1H, *J*=7.7 Hz), 7.00 (d, 1H, *J*=8.4 Hz), 7.45 (td, 1H, *J*=8.6, 1.8 Hz), 7.92 (dd, 1H, *J*=8.1, 1.8 Hz), 11.06 (br s, 1H), 11.82 (br s, 1H); ^{13}C NMR (DMSO-d_6) δ 52.9, 53.5, 64.3, 105.4, 117.0, 118.2, 119.9, 131.1, 134.4, 151.4, 156.2, 164.8, 194.0; HRMS (EI) *m*/*z* calc for $C_{13}H_{11}NO_5$, 261.0637; found, 261.0629.

4.2. Preparation of optically active DHMEQ

Daicel Chiralpak AD (10 mm i.d. ×250 mm) was used for the optical resolution with MeOH containing 0.1–0.9% v/v AcOH as an effluent. Racemic DHMEQ (40 g) gave each crude enantiomer of about 12 g. After the separation the crude compound (1.0 g) was dissolved in THF/EtOH/H_2O (6:1:1, 400 mL) and the organic solvents were removed by evaporation. The residual slurry was filtered and washed with H_2O and THF to give about 800 mg each of purified (−) or (+)-DHMEQ. After the separation, (+)-DHMEQ and (−)-DHMEQ were obtained with optical rotation of $[\alpha]_D^{24}$ +225°(*c* 0.1 methanol) and $[\alpha]_D^{24}$ −241°(*c* 0.1 methanol), respectively.

4.3. Adhesion assay for HL-60 cells on HUVEC

HUVEC (4×10^4 cells/48-well) were incubated with DHMEQ for 2 h at 37 °C and then further incubated for 6 h in the absence or presence of 10 ng/mL TNF-α, and the medium was changed to the DHMEQ-free medium. Then, HL-60 cells were added to HUVEC at 6×10^4 cells/well. After 1 h incubation, nonadherent cells were removed by 3 washes with phosphate-buffered saline (PBS). The number of adherent HL-60 cells was counted under the phase-contrast microscope.

4.4. Electrophoresis mobility shift assay

For the preparation of nuclear extracts, the adherent cells were washed with Ca^{2+}, Mg^{2+}-free PBS (PBS^-) and then scraped off. The cells were suspended in 400 μL of a cold buffer consisting of 10 mM HEPES (pH 7.9), 1.5 mM DTT, and 0.2 mM PMSF. The suspension was then centrifuged, and the pellet was resuspended in 40 μL of a buffer consisting of 20 mM HEPES-KOH, (pH 7.9), 25% glycerol, 420 mM NaCl, 1.5 mM $MgCl_2$, 0.2 mM EDTA, 0.5 mM DTT, and 0.2 mM PMSF and left for 20 min on ice. The mixture was centrifuged at 15,000*g* for 5 min, and the supernatant was recovered as the nuclear extract. The protein content was assayed by using Coomassie Protein Assay Reagent (Pierce Endogen, Rockford, IL). Then, 4 μL of 5×binding buffer (75 mM Tris-HCl, pH 7.0, containing 375 mM NaCl, 7.5 mM EDTA, 7.5 mM DTT, 37.5% glycerol, 1.5% NP-40, and 1.25 mg/mL BSA) and 1 μL poly dI-dC (1 μg/mL) were added to 5 μg of a nuclear extract, and the whole volume adjusted to 12 μL with water. After the addition of 3 μL of the radioactive DNA probe (GGGGACTTTCC; Promega), the mixture was incubated at 25 °C for 20 min. Each extract was electrophoresed on a 20 mL, 4% polyacrylamide gel. After electrophoresis, the gel was dried, and the reactivity was visualized on an X-ray film at −80 °C.

4.5. Nitroblue tetrazolium reduction assay

Production of reactive oxygen species can be detected by nitroblue tetrazolium (NBT). THP-1 cell suspension (5×10^5 cells/mL, 500 μL) were incubated in 24 well plates. The cells were incubated with (−)-DHMEQ for 2 h, added with 10 ng/mL TPA (Sigma: St Louis, MO) and incubation for 24 h. After the incubation each cell suspension was mixed with the same volume of NBT solution containing 1.25 mg/mL NBT (Wako: Osaka, Japan) and 200 ng/mL TPA for 30 min at 37 °C. The cells were washed with PBS twice and added with trypsin buffer (0.5 g/L trypsin, 8.0 g/L NaCl, 0.2 g/L KCl, 0.0475 g/L Na_2PO_4, 0.06 g/L KH_2PO_4, 1.0 g/L glucose, 0.02 g/L phenol red, 0.35 g/L $NaHCO_3$, 0.2 g/L EDTA) to strip off the adherent cells. The cell suspension was collected and centrifuged at 3500 rpm for 5 min, washed with PBS and finally suspended in 40 μL PBS. The percentage of NBT-positive cells was evaluated by counting 400 cells under the microscope.

Acknowledgements

This work was financially supported in part by grants from the Grants-in-Aid for Scientific Research on Priority Areas (A) of the Ministry of Education, Science, Culture, and Sports of Japan, and the Keio University Special Grants-in-Aid for Innovative Collaborative Research Projects.

References and notes

1. Sen, R.; Baltimore, D. *Cell* **1986**, *46*, 705–716.
2. (a) Baeuerle, P. A.; Baltimore, D. *Cell* **1996**, *87*, 13–20.

(b) Baeuerle, P. A.; Henkel, T. *Annu. Rev. Immunol.* **1994**, *12*, 141–179.
3. (a) Antwerp, D. J. V.; Martin, S. J.; Kafri, T.; Green, D. R.; Verma, I. M. *Science* **1996**, *274*, 787–789. (b) Beg, A. A.; Baltimore, D. *Science* **1996**, *274*, 782–784. (c) Wang, C. Y.; Mayo, M. W.; Baldwin, Jr. A. S. *Science* **1996**, *274*, 784–787.
4. Baldwin, Jr. A. S. *Annu. Rev. Immunol.* **1996**, *14*, 649–683.
5. Erkel, G.; Anke, T.; Sterner, O. *Biochem. Biophys. Res. Commun.* **1996**, *226*, 214–221.
6. Gehrt, A.; Erkel, G.; Anke, T.; Sterner, O. *J. Antibiot.* **1998**, *51*, 455–463.
7. Matsumoto, N.; Tsuchida, T.; Umekita, M.; Kinoshita, N.; Iimuma, H.; Sawa, T.; Hamada, M.; Takeuchi, T. *J. Antibiot.* **1997**, *50*, 900–905.
8. Matsumoto, N.; Ariga, A.; To-e, S.; Nakamura, H.; Agata, N.; Hirano, S.; Inoue, J.; Umezawa, K. *Bioorg. Med. Chem. Lett.* **2000**, *10*, 865–869.
9. (a) Wipf, P.; Kim, Y. *J. Org. Chem.* **1994**, *59*, 3518–3519. (b) Wipf, P.; Kim, Y.; Jahn, H. *Synthesis* **1995**, 1549–1561.

Available online at www.sciencedirect.com
SCIENCE DIRECT®
Tetrahedron 60 (2004) 7067–7075
Tetrahedron

Jolkinolide D pharmacophore: synthesis and reaction with biomolecules

Akira Sakakura, Yui Takayanagi, Hiroki Shimogawa and Hideo Kigoshi*

Department of Chemistry, University of Tsukuba, Tsukuba, Ibaraki 305-8571, Japan

Received 22 May 2003; revised 11 August 2003; accepted 11 August 2003

Available online 25 June 2004

Abstract—To obtain information on the chemical modification of biomolecules with jolkinolide D, a bioactive diterpenoid of plant origin, jolkinolide D pharmacophore was synthesized, and its reactivity toward amino acids, nucleosides, and DNA was investigated.

1. Introduction

Jolkinolide D (**1**) is a diterpenoid isolated from *Euphorbia jolkini* Boiss in 1974,[1] and its stereostructure was recently determined by X-ray crystallographic analysis.[2] It exhibited cytotoxicity, inhibited tumor invasion into the basement membrane, and induced apoptosis in tumor cells.[2]

Jolkinolide D (**1**) has a γ,δ-unsaturated-β-hydroxy-α-methylene lactone unit as the pharmacophore structure, which suggests that jolkinolide D (**1**) might irreversibly alkylate biomolecules such as proteins and DNA in contrast to popular α-methylene lactones such as in germacranolides, eudesmanolides, guaianolides, and pseudoguaianolides[3] that would reversibly alkylate biomolecules (Scheme 1). Because there are no other compounds that have the pharmacophore, reactivities of the unit toward nucleophiles have not hitherto been investigated. Generally, cytotoxic compounds interact with biomolecules, such as enzymes/proteins and DNA, so we chose amino acids, a peptide, nucleosides, and DNA as nucleophiles and studied the reactivities of **1**.[4] We describe herein the synthesis of jolkinolide D pharmacophore (**2**) of racemic and optically active forms and their updated reactivities toward biological nucleophiles including histidine as an imidazole-containing amino acid and glutathione as a peptide.

2. Results and discussion

2.1. Synthesis of jolkinolide D pharmacophore (2)

Racemic jolkinolide D pharmacophore (**2**) was synthesized from (±)-6-(*tert*-butyldimethylsilyloxy)-3-methyl-2-cyclohexenone (**3**)[5] and 2-iodoallylalcohol (**4**)[6] (Scheme 2). Addition of the vinyllithium reagent, generated from iodide **4** and *t*-BuLi, to (±)-ketone **3** afforded diastereomeric diols (±)-**5** (56%) and (±)-**6** (33%). (±)-Diol **5** could be transformed into (±)-jolkinolide D pharmacophore (**2**). The TBS group of (±)-**5** was removed with Bu_4NF to give

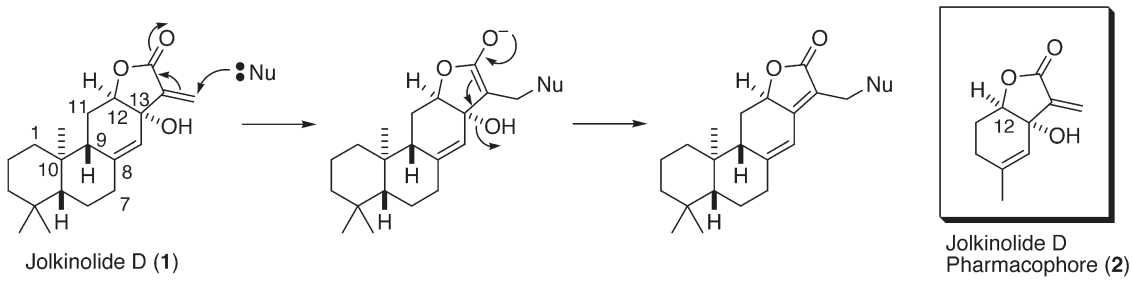

Scheme 1. Jolkinolide D (**1**) and its pharmacophore (**2**).

Keywords: Jolkinolide D; Pharmacophore; Diterpenoid; Synthesis; Reactivity; Alkylation.
* Corresponding author. Fax: +81-298-53-4313; e-mail address: kigoshi@chem.tsukuba.ac.jp

0040–4020/$ - see front matter © 2004 Elsevier Ltd. All rights reserved.
doi:10.1016/j.tet.2003.08.080

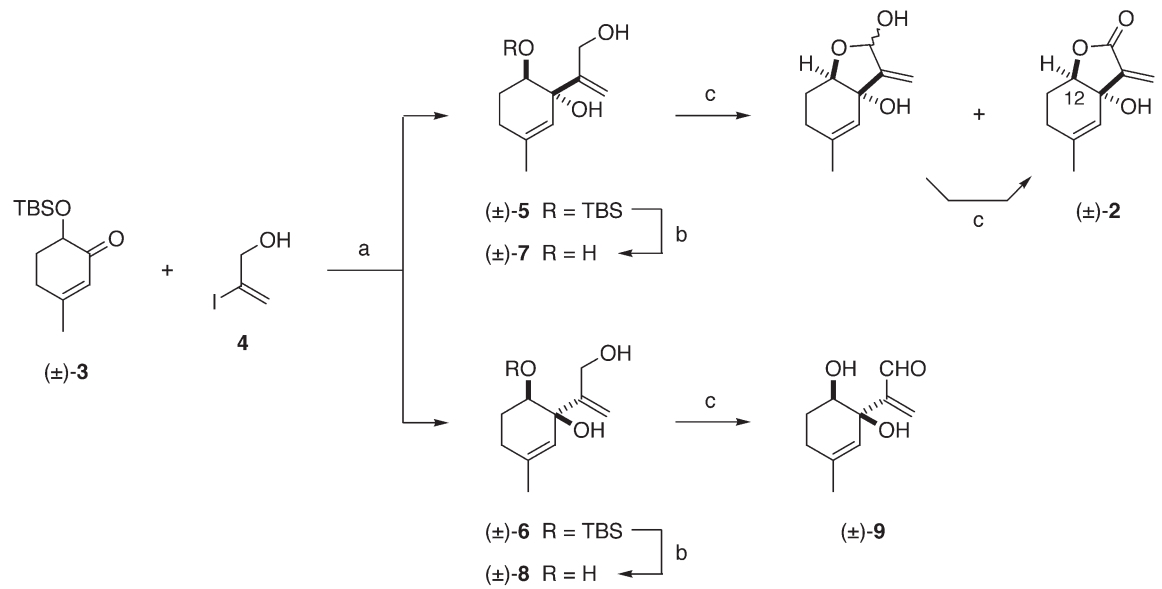

Scheme 2. Synthesis of (±)-jolkinolide D pharmacophore (**2**). Reagents and conditions: (a) *t*-BuLi, Et_2O, 0 °C; (b) Bu_4NF, THF, 0 °C; (c) MnO_2, $CHCl_3$, rt.

(±)-triol **7** (79%), whose oxidation with MnO_2 gave (±)-**2** (43%). On the other hand, (±)-diol **6** was converted into aldehyde **9** by the same procedure (24%). The stereochemistry of the ring juncture in (±)-**2** was established by the small coupling constants of H-12 (ddd, J=1.3, 3.0, 4.0 Hz).[7]

To investigate the difference in reactivities between racemic and optically active jolkinolide D pharmacophore (**2**), we then planned to synthesize (−)-**2**, which has the same absolute configuration as natural jolkinolide D (**1**). (−)-Jolkinolide D pharmacophore (**2**) was synthesized from (−)-acetoxyketone **10**, which was prepared by a reported procedure[8] with optimization to obtain the optically pure sample (34%, >99% ee)[9] (Scheme 3). Hydrolysis of the acetoxy group in (−)-**10** with $Sc(OTf)_3$[10] followed by protection of the hydroxyl group with *tert*-butyldimethylsilyl chloride (TBSCl) and Et_3N afforded (−)-ketone **3** (55%). (−)-Ketone **3** was transformed into (−)-jolkinolide D pharmacophore (**2**) by the same procedure as used for the synthesis of (±)-**2**.

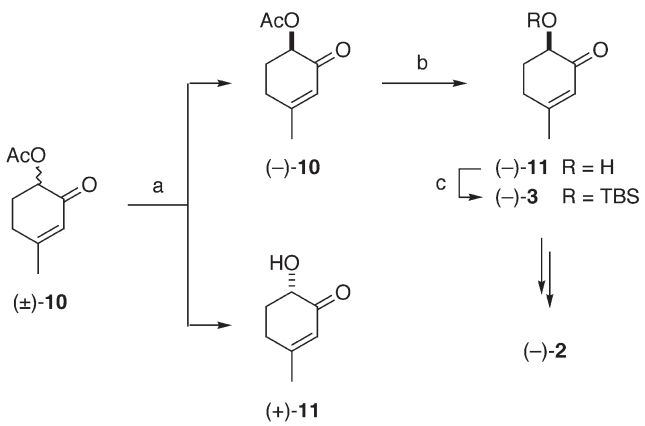

Scheme 3. Synthesis of (−)-jolkinolide D pharmacophore (**2**). Reagents and conditions: (a) pig liver esterase, 0.1 M phosphate buffer (pH 7.0), 15 °C; (b) $Sc(OTf)_3$, MeOH–H_2O (4:1), rt; (c) TBSCl, Et_3N, DMF, rt.

2.2. Reactions of jolkinolide D pharmacophore (2) with amino acids and glutathione

The reactivities of jolkinolide D pharmacophore (**2**) toward biomolecules have been investigated to obtain the basic information on the chemical modification of proteins and DNA with jolkinolide D (**1**).

Initially, the reactions of (±)-**2** with three amino acids and a peptide were examined. A typical amino acid L-alanine, sulfur-containing L-cysteine and glutathione, and an imidazole-containing L-histidine were reacted with an equal amount of (±)-**2** in aqueous THF (pH 7.5). The products were separated and purified by chromatography (ODS), and their structures were established by the spectroscopic method (UV, IR, NMR, 2D NMR, and MS spectra). The results are summarized in Table 1. (±)-**2** reacted with all amino acids employed here and glutathione to give alkylated products. The thiol groups in L-cysteine and glutathione were rapidly alkylated with (±)-**2** in high yield (64% in L-cysteine and 81% in glutathione). In the alkylation of glutathione, adduct **22**, an intermediate to **21**, was obtained as a diastereomeric mixture at the 15 position, which supported the alkylation mechanism shown in Scheme 1. In the case of L-alanine, which has no nucleophilic functional group in the amino acid residue, alkylation occurred only at the amino group to afford the monoalkylated product **14** (53%) and the dialkylated product **15** (4.3%). L-Histidine afforded three monoalkylated products, **16** (19%), **17** (26%), and **18** (17%), along with two dialkylated products **19** (3.8%) and **20** (8.5%). The product **16** was proved to be alkylated at the amino group, while the products **17** and **18** were alkylated at the imidazolyl group. These results indicate that the thiol group is the most reactive toward (±)-**2** among the nucleophilic groups in L-cysteine and glutathione, and that the amino group and the imidazolyl group in L-histidine have similar reactivity toward (±)-**2** at pH 7.5. The alkylated products were obtained as a diastereomeric mixture because racemic jolkinolide D pharmacophore

Table 1. Alkylation of amino acids and glutathione with jolkinolide D pharmacophore (**2**)[a]

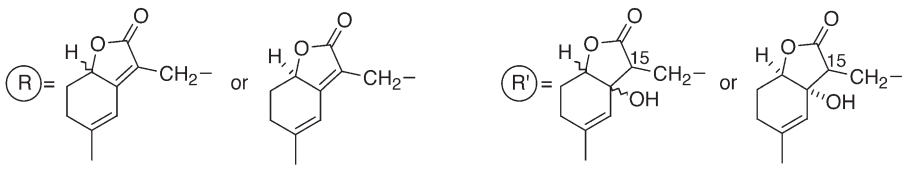

	Products (yields)	
L-Cysteine	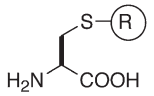 **12** (64%)[b] **12a** (38%)[c]	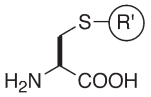 **13** (0%)[b] **13a** (23%)[c]
L-Alanine	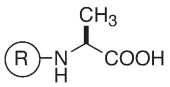 **14** (53%)[b] **14a** (20%)[c]	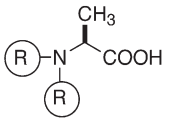 **15** (4.3%)[b] **15a** (0%)[c]
L-Histidine[d]	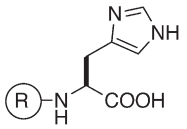 **16** (19%)[b] **16a** (34%)[c]	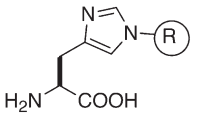 **17** (26%)[b] **17a** (29%)[c]
	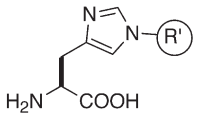 **18** (17%)[b] **18a** (15%)[c]	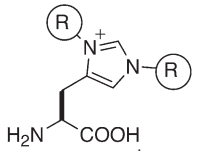 **19** (3.8%)[b] **19a** (5.4%)[c]
	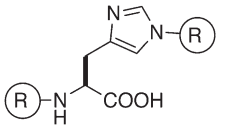 **20** (8.5%)[b] **20a** (5.0%)[c]	
Glutathione	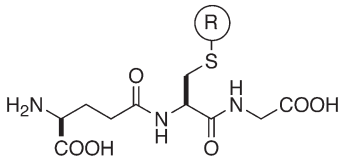 **21** (52%)[b] **21a** (37%)[c]	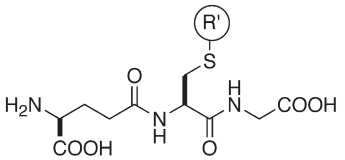 **22** (19%)[b] **22a** (60%)[c]
	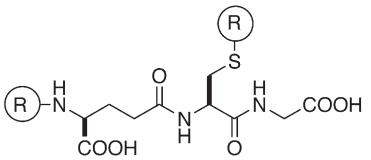 **23** (10%)[b] **23a** (0%)[c]	

[a] Reaction conditions: 0.2 M jolkinolide D pharmacophore (**2**) and amino acid (peptide) in aqueous THF, pH 7.5, ambient temperature, and 16 h.
[b] Yields of the products of the reaction with (±)-**2**.
[c] Yields of the products of the reaction with (−)-**2**.
[d] Owing to the low solubility of L-histidine to the solvent system, the alkylation experiment was executed in an aqueous THF solution of 0.1 M each of **2** and L-histidine.

(±)-**2** was employed. The diastereomeric ratios of **12**, **14**, **16**, **17**, and **21** were ca. 1:1, which were determined by the ^{1}H NMR analysis using **12a**, **14a**, **16a**, **17a**, and **21a**, obtained below, as the authentic samples. The yields of the alkylated products show some difference between the racemic and optically active **2**, however, the 1:1 ratio of products indicated that the chirality of **2** had essentially no effect on the alkylation. The differences in yields may be due to the experimental error in adjusting pH of the reaction media.

The alkylation of L-cysteine, L-alanine, L-histidine, and glutathione by (−)-**2** was next investigated. The alkylation conditions were the same as those employed for (±)-**2**. The results are shown in Table 1. (−)-**2** showed the same reactivity toward amino acids and glutathione as (±)-**2**. The alkylated products **12a**, **14a**, **16a**, **17a**, and **21a** could be obtained as a single isomer.

2.3. Reactions of jolkinolide D pharmacophore (2) with nucleosides and DNA

Four nucleosides, 2′-deoxyadenosine, 2′-deoxyguanosine, 2′-deoxycytidine, and thymidine were reacted with an equal amount of (±)-jolkinolide D pharmacophore (**2**) under the same conditions as those employed for amino acids. The results are listed in Table 2. The sites of alkylation in the purine and pyrimidine bases of the nucleosides were determined by comparison of the difference UV spectra between alkylated nucleosides and the reference compound **14** with the UV spectra of the known ethylated nucleosides in acidic, neutral, and basic solutions (Table 3).[11,12] Only in the case of 2′-deoxyguanosine, the alkylation reaction occurred to afford the product alkylated at the $N-1$ position of guanine, **24**. When alkylation of thymidine was executed under basic conditions (pH 8.7), the product **25**, formed by alkylation at the $N-3$ position of thymine, was obtained in 22% yield.

Table 2. Alkylation of nucleosides with jolkinolide D pharmacophore (**2**)[a]

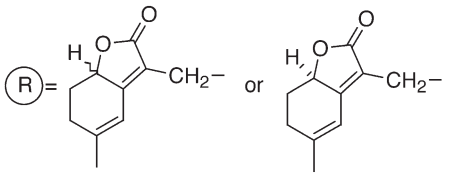

	Product (yield)
2′-Deoxyguanosine	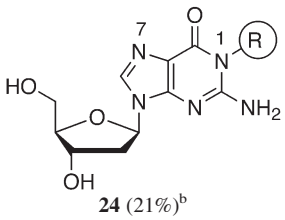 **24** (21%)[b] **24a** (5%, pH 7.5; 52%, pH 8.9)[c]
Thymidine	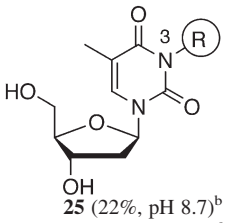 **25** (22%, pH 8.7)[b] **25a** (18%, pH8.7)[c]
2′-Deoxyadenosine	No reaction
2′-Deoxycytidine	No reaction

[a] Reaction conditions: 0.1 M for 2′-deoxyadenosine and 2′-deoxycytidine, 0.02 M for 2′-deoxyguanosine, 0.2 M for thymidine in aqueous THF, pH 7.5, ambient temperature, and 16 h.
[b] Yields of the products of the reaction with (±)-**2**.
[c] Yields of the products of the reaction with (−)-**2**.

Next, the alkylation of 2′-deoxyadenosine, 2′-deoxyguanosine, 2′-deoxycytidine, and thymidine by (−)-**2** was investigated. The results are shown in Table 2, which are essentially the same as those of the reactions of (±)-**2**. Under neutral conditions (pH 7.5), only 2′-deoxyguanosine was alkylated to give **24a** (5%). Under basic conditions, **24a** was obtained in a higher yield (pH 8.9, 52%), and thymidine was alkylated to give **25a** (pH 8.7, 18%). 2′-Deoxyadenosine and 2′-deoxycytidine were not alkylated under either neutral or basic conditions. The *N*−1 of deoxyguanosine as well as the *N*−7 is one of the active sites toward alkylating agents. The well-known alkylating agent, dimethyl sulfate, alkylates guanosine at the *N*−7 position[14] and thymidine at the *N*−3 position[15] under neutral and aqueous conditions. *N*−1 Alkylation of 2′-deoxyguanosine was found on treatment with methyl iodide in dimethyl sulfoxide under basic conditions.[16] In the present study, only the stable product might be isolated, because the alkylated deoxyguanosines at the *N*−7 position are unstable. To the best of our knowledge, Michael acceptors are well known to react with amino acid nucleophiles, however, there is little information so far about the reactions between Michael acceptors and nucleoside nucleophiles. To clarify the details of the alkylating profile of **2**, the further careful studies are needed.

DNA from salmon spermary was reacted with (±)-jolkinolide D pharmacophore (**2**) in aqueous methanol (pH 7.5) at 37 °C for a week. After the enzymatic hydrolysis,[13] the alkylated nucleosides were isolated and characterized as previously described. Two products **24** (0.48%) and **25** (0.26%) were obtained, which were the same products as in the reaction of nucleosides with (±)-**2**, but the yields were very low.

2.4. Biological activities of jolkinolide D pharmacophore

The preliminary biological tests of (±)-jolkinolide D pharmacophore (**2**) indicated that the artificial analog **2** exhibited weaker activities than jolkinolide D (**1**), concerning to the inhibitory activity against tumor invasion into the basement membrane and the induction of apoptosis in tumor cells. These results suggested that the A and B rings in **1** are important to the biological activities in cells somehow, maybe because of membrane permeability.

3. Conclusions

We have synthesized jolkinolide D pharmacophore (**2**) in the racemic form (19%, three steps) and the optically pure form (3.6%, six steps) and have investigated the reactivities of **2** toward amino acids, nucleosides, and DNA. The order of reactivity of **2** toward nucleophiles in amino acids at pH 7.5 is the thiol group in L-cysteine and glutathione>the imidazolyl group in L-histidine, the α-amino groups in amino acids>the carboxyl groups in amino acids. We also

Table 3. Difference UV spectra of jolkinolide D pharmacophore-nucleoside adducts and UV spectra of ethylated nucleosides

	pH 1[a]		pH 7[b]		pH 13[c]	
Alkylated nucleoside	λ_{max} (nm)	λ_{min} (nm)	λ_{max} (nm)	λ_{min} (nm)	λ_{max} (nm)	λ_{min} (nm)
24	262, 277	229	257, 272	227	258, 272 (sh)	226
Guanosine[d]	256, 277	228	253, 273 (sh)	226	258–266	232
N-1-Ethyl-2′-deoxyguanosine[d]	261, 272 (sh)	240	257, 270 (sh)	237	258, 270 (sh)	239
N-7-Ethyl-2′-deoxyguanosine[d]	257, 275 (sh)	229	257, 278	234	267[e]	249[e]
25	271	239	272	237	272	238
Thymidine[d]	267	234	267	234	267	245
N-3-Ethylthymidine[d]	269	240	269	240	270	240

[a] 0.1 M HCl/H_2O–MeOH (9:1).
[b] H_2O–MeOH (9:1).
[c] 0.1 M KOH/H_2O–MeOH (9:1).
[d] See Ref. 12.
[e] Imodazole ring-opened 7-ethyl-2′-deoxyguanosine.

demonstrated that **2** alkylated 2′-deoxyguanosine at the $N-1$ position and thymidine at the $N-3$ position and modified DNA at the same sites in lower yields. The further studies of biological activities of jolkinolide D pharmacophore are in progress.

4. Experimental

4.1. General

Unless otherwise noted, materials were obtained from commercial suppliers and used without further purification. Pig liver esterase (PLE) was purchased from SIGMA as a lyophilized powder. All reactions involving organometallic reagents were conducted under a nitrogen atmosphere. Fuji silysia silica gel BW-820 MH and Nacalai tesque Cosmosil 75C_{18}-OPN were used for column chromatography. NMR spectra were measured at 270 or 500 MHz for ^{1}H and 67.8 MHz for ^{13}C. Chemical shifts are described as δ values in ppm relative to TMS. J values are given in Hz.

4.1.1. (±)-Diols 5 and 6. To a stirred solution of 2-iodoallylalcohol (250 mg, 1.4 mmol) in Et_2O was added a 1.5 M solution of *t*-BuLi in pentane (2.3 mL, 3.4 mmol) at −78 °C. The mixture was stirred at 0 °C for 2.5 h, and then a solution of (±)-ketone **3** (100 mg, 0.45 mmol) in Et_2O (1 mL) was added dropwise. The resulting mixture was stirred at 0 °C for 1 h. After the addition of methanol (0.8 mL) and H_2O (5 mL), the reaction mixture was extracted with Et_2O (3×5 mL). The combined extracts were washed with brine (5 mL), dried (Na_2SO_4), and concentrated. The residue was purified by column chromatography on silica gel (4 g, hexane–Et_2O 2:1→1:1→1:2) to give (±)-**5** (76 mg, 56%) and (±)-**6** (44 mg, 33%). (±)-**5**: colorless oil; IR (neat) 3410, 1470, 1090, 1060, 890, 840 cm^{-1}; ^{1}H NMR (270 MHz, $CDCl_3$) δ 5.33 (s, 1H), 5.30 (d, J=1.7 Hz, 1H), 5.08 (d, J=1.7 Hz, 1H), 4.38 (d, J=12.2 Hz, 1H), 4.27 (d, J=12.2 Hz, 1H), 3.95 (t, J=6.9 Hz, 1H), 3.25 (br s, 1H), 3.04 (br s, 1H), 2.14–1.82 (m, 4H), 1.78 (s, 3H), 0.96 (s, 9H), 0.17 (s, 3H), 0.15 (s, 3H); ^{13}C NMR ($CDCl_3$) δ 149.0, 136.5, 125.9, 117.7, 78.0, 65.1, 28.9, 27.5, 25.9, 23.0, 18.2, −4.5, −4.5. A signal of one of quaternary carbons was not detected; MS (FAB) *m/z* 321 (M+Na)$^+$; HRMS (FAB) calcd for $C_{16}H_{30}NaO_3Si$ [(M+Na)$^+$] 321.1862, found 321.1878. (±)-**6**: colorless oil; IR (neat) 3390, 1470, 1100, 1010, 900, 840 cm^{-1}; ^{1}H NMR (270 MHz, $CDCl_3$) δ 5.25 (d, J=1.3 Hz, 1H), 5.21 (s, 1H), 5.10 (d, J=1.3 Hz, 1H), 4.29 (dd, J=4.3, 13.2 Hz, 1H), 4.09 (dd, J=7.9, 13.2 Hz, 1H), 3.86 (dd, J=4.0, 6.9 Hz, 1H), 2.62 (dd, J=4.3, 7.9 Hz, 1H), 2.14–1.75 (m, 4H), 1.73 (s, 3H), 0.90 (s, 9H), 0.11 (s, 3H), 0.09 (s, 3H). A signal of a hydroxyl proton was not detected; ^{13}C NMR ($CDCl_3$) δ 151.2, 137.1, 124.6, 115.0, 75.5, 71.8, 64.4, 27.7, 26.8, 25.8, 23.3, 18.1, −4.1, −4.5; MS (FAB) *m/z* 321 (M+Na)$^+$; HRMS (FAB) calcd for $C_{16}H_{30}NaO_3Si$ [(M+Na)$^+$] 321.1862, found 321.1886.

4.1.2. (±)-Triol 7. To a stirred solution of (±)-**5** (323 mg, 1.09 mmol) in THF (12 mL) was added a 1.0 M solution of Bu_4NF in THF (2.18 mL, 2.18 mmol) at 0 °C. The mixture was stirred at 0 °C for 30 min, diluted with saturated aqueous NH_4Cl (10 mL), and extracted with EtOAc (5×25 mL). The combined extracts were washed with brine (25 mL), dried (Na_2SO_4), and concentrated. The residue was purified by column chromatography on silica gel (20 g, hexane–acetone 3:1→2:1→1:1→1:2) to give (±)-**7** (158 mg, 79%): colorless solid; IR (neat) 3350, 1640, 1440, 1170, 1070, 1010, 920 cm^{-1}; ^{1}H NMR (270 MHz, $CDCl_3$) δ 5.36 (d, J=1.3 Hz, 1H), 5.30 (q, J=1.3 Hz, 1H), 5.10 (d, J=1.3 Hz, 1H), 4.32 (s, 2H), 3.85 (dd, J=3.3, 7.9 Hz, 1H), 2.77 (br s, 2H), 2.17–1.79 (m, 4H), 1.75 (s, 3H). A signal of a hydroxyl proton was not detected; ^{13}C NMR ($CDCl_3$) δ 151.8, 137.4, 126.8, 115.3, 77.6, 74.4, 63.7, 28.9, 27.5, 23.4; MS (FAB) *m/z* 207 (M+Na)$^+$; HRMS (FAB) calcd for $C_{10}H_{16}NaO_3$ [(M+Na)$^+$] 207.0997, found 207.0996.

4.1.3. (±)-Triol 8. (±)-Diol **6** (189 mg, 0.630 mmol) was transformed into (±)-triol **8** (91.4 mg, 80%) by the same procedure as described for (±)-**7**. (±)-**8**: colorless solid; IR (neat) 3370, 1670, 1440, 1380, 1050, 1020, 960 cm^{-1}; ^{1}H NMR (270 MHz, $CDCl_3$) δ 5.30 (d, J=1.0 Hz, 1H), 5.26 (s, 1H), 5.20 (d, J=1.0 Hz, 1H), 4.27 (d, J=12.5 Hz, 1H), 4.19 (d, J=12.5 Hz, 1H), 3.79 (t, J=7.3 Hz, 1H), 3.04 (br s, 2H), 2.29–1.79 (m, 4H), 1.74 (s, 3H). A signal of a hydroxyl proton was not detected; ^{13}C NMR ($CDCl_3$) δ 151.7, 138.6, 124.8, 114.9, 74.7, 72.0, 63.5, 28.6, 25.8, 23.3; MS (FAB) *m/z* 207 (M+Na)$^+$; HRMS (FAB) calcd for $C_{10}H_{16}NaO_3$ [(M+Na)$^+$] 207.0997, found 207.1013.

4.1.4. (±)-Jolkinolide D pharmacophore (2). To a stirred solution of (±)-**7** (50 mg, 0.27 mmol) in $CHCl_3$ (5 mL) was added MnO_2 (0.12 g, 1.37 mmol) at ambient temperature. The mixture was stirred at ambient temperature for 1 h. To the mixture was added MnO_2 (0.12 g, 1.37 mmol), and the mixture was stirred at ambient temperature for 1 h. Further, MnO_2 (0.12 g, 1.37 mmol) was added, and the mixture was stirred at ambient temperature for 1 h. The reaction mixture was filtered through a pad of Celite, and the residue was washed with $CHCl_3$. The filtrate and washings were combined and concentrated. The residue was purified by column chromatography on silica gel (9 g, hexane–EtOAc 2:1→1:1) to give (±)-**2** (4.4 mg) and a diastereomeric mixture of hemiacetals (27.8 mg). To a stirred solution of the diastereomeric mixture of hemiacetals (27.8 mg) in $CHCl_3$ (5 mL) was added MnO_2 (0.13 g, 1.53 mmol) at ambient temperature. The mixture was stirred at ambient temperature for 3 h. The reaction mixture was filtered through a pad of Celite, and the residue was washed with $CHCl_3$. The filtrate and washings were combined and concentrated. The residue was purified by column chromatography on silica gel (0.5 g, hexane–EtOAc 2:1→1:1) to give (±)-**2** (22.9 mg). Total yield: 27.3 mg (56%). (±)-**2**: colorless solid; UV (CH_3CN) λ_{max} 223 nm (ε 5500); IR (neat) 3400, 1760, 1670, 1270, 1150, 1010, 950 cm^{-1}; ^{1}H NMR (270 MHz, $CDCl_3$) δ 6.27 (s, 1H), 5.85 (s, 1H), 5.24 (m, 1H), 4.49 (ddd, J=1.3, 3.0, 4.0 Hz, 1H), 2.22–2.07 (m, 2H), 1.98–1.84 (m, 2H), 1.74 (s, 3H), a signal of a hydroxyl proton was not detected; ^{13}C NMR ($CDCl_3$) δ 168.8, 142.1, 140.0, 121.9, 121.1, 81.1, 72.8, 23.8, 23.7, 22.4; MS (FAB) *m/z* 203 (M+Na)$^+$, 181 (M+H)$^+$; HRMS (FAB) calcd for $C_{10}H_{12}NaO_3$ [(M+Na)$^+$] 203.0684, found 203.0685.

4.1.5. (±)-Aldehyde 9. To a stirred solution of (±)-**8**

(6.2 mg, 0.030 mmol) in $CHCl_3$ (5 mL) was added MnO_2 (61.2 mg, 0.70 mmol) at ambient temperature. The mixture was stirred at ambient temperature for 16 h. The reaction mixture was filtered through a pad of Celite, and the residue was washed with $CHCl_3$. The filtrate and washings were combined and concentrated. The residue was purified by column chromatography on silica gel (2 g, hexane–EtOAc 2:1→1:1) to give (±)-**9** (1.5 mg, 24%): colorless oil; UV (CH_3CN) λ_{max} 209 nm (sh, ε 4800); IR (neat) 3410, 2840, 1690, 1620, 1390, 1060 cm^{-1}; ^1H NMR (270 MHz, $CDCl_3$) δ 9.60 (s, 1H), 6.59 (s, 1H), 6.22 (s, 1H), 5.24 (s, 1H), 3.90 (m, 1H), 2.52 (d, J=5.9 Hz, 1H), 2.18–1.81 (m, 4H), 1.76 (s, 3H); ^{13}C NMR ($CDCl_3$) δ 197.5, 140.5, 124.4, 72.3, 29.9, 28.0, 25.5, three signals of quaternary carbons were not detected; MS (FAB) m/z 205 $(M+Na)^+$; HRMS (FAB) calcd for $C_{10}H_{14}NaO_3$ $[(M+Na)^+]$ 205.0841, found 205.0820.

4.1.6. (−)-6-Acetoxy-3-methyl-2-cyclohexenone (10). To a stirred solution of (±)-6-acetoxy-3-methyl-2-cyclohexenone (**10**) (2.4 g, 14.3 mmol) in DMSO (10 mL) was added 0.1 M phosphate buffer (pH 7.0, 250 mL) at 15 °C, and the mixture was stirred for 30 min. After PLE (50 mg) was added, the resulting mixture was stirred at 15 °C for 5 h. The reaction mixture was extracted with Et_2O (3×200 mL). The combined extracts were washed with brine, dried (Na_2SO_4), and concentrated. The residual oil was purified by column chromatography on silica gel (50 g, hexane–Et_2O 1:2) to give (−)-**10** (620 mg, 34%) along with (+)-6-hydroxy-3-methyl-2-cyclohexenone (**11**) (372 mg, 16%). (−)-**10**: colorless oil; $[\alpha]_D^{20}$=−163 (c 1.0, $CHCl_3$).

4.1.7. (−)-6-(*tert*-Butyldimethylsilyloxy)-3-methyl-2-cyclohexenone (3). To a stirred solution of (−)-**10** (1.58 g, 9.40 mmol) in a 1:4 mixture of MeOH and H_2O (10 mL) was added scandium triflate (920 mg, 1.86 mmol) at ambient temperature. The mixture was stirred at ambient temperature for 66 h, diluted with H_2O (20 mL), and extracted with EtOAc (3×25 mL). The combined extracts were washed with brine (10 mL), dried (Na_2SO_4), and concentrated to give the crude hydroxyketone (−)-**11** (1.58 g). The product was used for the next reaction without purification. The analytical sample of (−)-**11** was prepared by column chromatography on silica gel (hexane–Et_2O 1:1): colorless oil; $[\alpha]_D^{25}$=−164 (c 1.08, $CHCl_3$). To a solution of the crude (−)-**11** (1.58 g) in DMF (11 mL) was added Et_3N (2.2 mL, 16 mmol) and TBSCl (2.1 g, 14 mmol) at ambient temperature. The mixture was stirred at ambient temperature for 1 h, diluted with H_2O (14 mL), and extracted with Et_2O (3×14 mL). The combined extracts were washed with brine (14 mL), dried (Na_2SO_4), and concentrated. The residual oil was purified by column chromatography on silica gel (60 g, hexane–Et_2O 15:1→10:1) to give (−)-**3** (1.22 g, 55% from (−)-**10**): colorless oil; $[\alpha]_D^{21}$=−89.3 (c 1.0, $CHCl_3$).

4.1.8. (−)-Diol 5. The experimental procedure followed was as described for compound (±)-**5**. (−)-**5**: colorless oil; $[\alpha]_D^{22}$=−2.5 (c 0.10, $CHCl_3$).

4.1.9. (−)-Triol 7. The experimental procedure followed was as described for compound (±)-**7**. (−)-**7**: colorless solid; $[\alpha]_D^{22}$=14 (c 0.10, $CHCl_3$).

4.1.10. (−)-Jolkinolide D pharmacophore (2). The experimental procedure followed was as described for compound (±)-**2**. (−)-**2**: colorless solid; $[\alpha]_D^{22}$=−181 (c 0.10, $CHCl_3$).

Reaction of (±)-**2** with L-cysteine. L-Cysteine (3.8 mg, 31 μmol) was dissolved in H_2O (0.10 mL), and the pH was adjusted to 7.5 by adding a trace amount of 1 M NaOH. To the aqueous solution was added a solution of (±)-**2** (5.6 mg, 31 μmol) in THF (0.03 mL). The mixture was stirred at ambient temperature for 16 h and then concentrated. The residue was purified by column chromatography on ODS silica gel (0.5 g, MeOH–H_2O 1:10→1:4) to give **12** (5.6 mg, 64%): colorless solid; UV (H_2O–MeOH 9:1) λ_{max} 283 nm (ε 11,000); IR (neat) 3450, 1740, 1650, 1495, 1390, 1340, 1040 cm^{-1}; ^1H NMR (500 MHz, CD_3OD) δ 6.56 (s, 0.5H), 6.54 (s, 0.5H), 4.94 (dd, J=5.1, 13.2 Hz, 1H), 3.74 (m, 1H), 3.54 (d, J=13.5 Hz, 0.5H), 3.53 (d, J=13.5 Hz, 0.5H), 3.46 (d, J=13.5 Hz, 1H), 3.18 (dd, J=4.0, 14.7 Hz, 0.5H), 3.16 (dd, J=3.8, 14.4 Hz, 0.5H), 2.90 (dd, J=8.2, 14.7 Hz, 0.5H), 2.89 (dd, J=9.4, 14.4 Hz, 0.5H), 2.55–2.36 (m, 3H), 1.96 (s, 3H), 1.67–1.53 (m, 1H); MS (FAB) m/z 284 $(M+H)^+$; HRMS (FAB) calcd for $C_{13}H_{17}NNaO_4S$ $[(M+Na)^+]$ 306.0776, found 306.0784.

4.1.11. Reaction of (−)-2 with L-cysteine. (−)-**2** (5.1 mg, 28 μmol) and L-cysteine (3.4 mg, 28 μmol) were reacted at pH 7.5 for 16 h, to give **12a** (3.0 mg, 34%) and **13a** (1.9 mg, 22%). **12a**: ^1H NMR (270 MHz, CD_3OD) δ 6.55 (s, 1H), 4.94 (dd, J=5.1, 14.9 Hz, 1H), 3.77 (dd, J=3.8, 8.6 Hz, 1H), 3.55 (d, J=13.5 Hz, 1H), 3.46 (d, J=13.5 Hz, 1H), 3.18 (dd, J=4.3, 14.9 Hz, 1H), 2.91 (dd, J=8.4, 14.9 Hz, 1H), 2.52–2.36 (m, 3H), 1.96 (s, 3H), 1.63 (m, 1H). **13a**: UV (H_2O–MeOH 9:1) λ_{max} 282 nm (ε 7400); IR (neat) 3440, 1760, 1630, 1390, 1100, 1010 cm^{-1}; ^1H NMR (500 MHz, CD_3OD) δ 5.59 (s, 0.4H), 5.43 (s, 0.6H), 4.45 (s, 1H), 3.83–3.60 (m, 1H), 3.17 (m, 1H), 2.97 (m, 2H), 2.88–2.73 (m, 1H), 2.58–2.35 (m, 1H), 2.20–1.78 (m, 4H), 1.75 (s, 1.8H), 1.74 (s, 1.2H); MS (FAB) m/z 302 $(M+H)^+$; HRMS (FAB) calcd for $C_{13}H_{20}NO_5S$ $[(M+H)^+]$ 302.1062, found 302.1056.

4.1.12. Reaction of (±)-2 with L-alanine. L-Alanine (2.5 mg, 28 μmol) was dissolved in H_2O (0.10 mL), and the pH was adjusted to 7.5 by adding a trace amount of 1 M NaOH. To the aqueous solution was added a solution of (±)-**2** (5.0 mg, 28 μmol) in THF (0.03 mL) at ambient temperature. After stirring for 16 h, the reaction mixture was diluted with H_2O (3 mL) and extracted with $CHCl_3$ (3×3 mL). The aqueous layer was concentrated to give a solid, which was purified by column chromatography on ODS silica gel (0.5 g, MeOH–H_2O 1:20→1:10→1:4→1:1) and preparative HPLC (Develosil ODS-HG-5, 20×250 mm, CH_3CN–0.02 M aqueous NH_4OAc, 8.0 mL/min) to give **14** (3.7 mg, 53%). The combined $CHCl_3$ extracts were dried (Na_2SO_4) and concentrated to give a solid, which was purified by column chromatography on silica gel (0.5 g, hexane–acetone 3:1→2:1→1:1) to give **15** (0.5 mg, 4%) along with recovered (±)-**2** (0.1 mg, 2%). **14**: colorless solid; UV (H_2O–MeOH 9:1) λ_{max} 279 nm (ε 16,000); IR (KBr) 3510, 3360, 1760, 1665, 1590, 1400, 1365, 1335 cm^{-1}; ^1H NMR (270 MHz, CD_3OD) δ 6.61 (s, 0.5H), 6.57 (s, 0.5H), 5.05 (dd, J=5.3, 13.9 Hz, 1H),

4.03–3.73 (m, 2H), 3.54 (m, 1H), 2.55–2.43 (m, 3H), 2.00 (s, 3H), 1.95–1.65 (m, 1H), 1.48 (d, *J*=6.6 Hz, 3H); MS (FAB) *m/z* 252 $(M+H)^+$; HRMS (FAB) calcd for $C_{13}H_{18}NO_4$ $[(M+H)^+]$ 252.1236, found 252.1240. **15**: colorless solid; UV (H_2O–MeOH 9:1) λ_{max} 281 nm (ε 12,000); IR (neat) 1745, 1650, 1460, 1395, 1340, 1035 cm^{-1}; ^1H NMR (500 MHz, $CDCl_3$) δ 6.38 (s, 1H), 6.37 (s, 1H), 4.80–4.76 (m, 2H), 3.59–3.51 (m, 1H), 3.44–3.26 (m, 4H), 2.50–2.38 (m, 6H), 1.96 (s, 6H), 1.75–1.53 (m, 2H), 1.38 (d, *J*=7.0 Hz, 1.5H), 1.36 (d, *J*=7.0 Hz, 1.5H); MS (FAB) *m/z* 414 $(M+H)^+$; HRMS (FAB) calcd for $C_{23}H_{28}NO_6$ $[(M+H)^+]$ 414.1917, found 414.1889.

4.1.13. Reaction of (−)-2 with L-alanine. (−)-**2** (5.1 mg, 28 μmol) and L-alanine (2.5 mg, 28 μmol) were reacted at pH 7.5 for 16 h, to give **14a** (1.4 mg, 20%) along with recovered (−)-**2** (3.5 mg, 69%): **14a**: ^1H NMR (270 MHz, CD_3OD) δ 6.60 (s, 1H), 5.04 (dd, *J*=4.9, 13.0 Hz, 1H), 4.00–3.78 (m, 2H), 3.55 (m, 1H), 2.55–2.43 (m, 3H), 2.00 (s, 3H), 1.70 (m, 1H), 1.49 (d, *J*=6.5 Hz, 3H).

4.1.14. Reaction of (±)-2 with L-histidine. L-Histidine (9.0 mg, 58 μmol) was dissolved in H_2O (0.50 mL), and the pH was adjusted to 7.5 by adding a trace amount of 1 M NaOH. To the aqueous solution was added a solution of (±)-**2** (11 mg, 58 μmol) in THF (0.08 mL). The mixture was stirred at ambient temperature for 16 h and concentrated. The residue was purified by column chromatography on silica gel (ODS 0.8 g, MeOH–0.1 M aqueous TFA 1:20→1:5→1:1) and preparative HPLC (Develosil ODS-HG-5, 20×250 mm, CH_3CN–0.2 M aqueous TFA 15:85, 8.0 mL/min) to give **16** (3.6 mg, 19%), **17** (4.9 mg, 26%), **18** (3.2 mg, 17%), **19** (1.1 mg, 3.8%), and **20** (2.5 mg, 8.5%). **16**: colorless oil; UV (H_2O–MeOH 9:1) λ_{max} 280 (ε 7100); IR (neat) 1730, 1720, 1670, 1650, 1200, 1140 cm^{-1}; ^1H NMR (500 MHz, CD_3OD) δ 8.89 (s, 1H), 7.51 (s, 1H), 6.54 (s, 1H), 5.06 (dd, *J*=5.1, 13.7 Hz, 1H), 4.40 (m, 1H), 4.09 (s, 2H), 3.57 (dd, *J*=5.1, 15.5 Hz, 0.5H) 3.53 (dd, *J*=4.8, 16.9 Hz, 0.5H), 3.45 (m, 1H), 2.61–2.44 (m, 3H), 2.00 (s, 3H), 1.75–1.64 (m, 1H); MS (FAB) *m/z* 318 $(M+H)^+$; HRMS (FAB) calcd for $C_{16}H_{20}N_3O_4$ $[(M+H)^+]$ 318.1454, found 318.1467. **17**: colorless oil; UV (H_2O–MeOH 9:1) λ_{max} 279 (ε 5900); IR (neat) 3450, 1730, 1680, 1440, 1200, 1140 cm^{-1}; ^1H NMR (500 MHz, CD_3OD) δ 8.98 (s, 1H), 7.52 (s, 1H), 6.60 (s, 1H), 5.04 (dd, *J*=5.1, 13.6 Hz, 1H), 5.12 (s, 2H), 4.31 (t, *J*=6.7 Hz, 1H), 3.40 (dd, *J*=6.7, 15.9 Hz, 1H), 2.61–2.43 (m, 3H), 2.01 (s, 3H), 1.73–1.62 (m, 1H). A signal of a proton (β-position of histidine) was overlapped with the solvent signals; MS (FAB) *m/z* 318 $(M+H)^+$; HRMS (FAB) calcd for $C_{16}H_{20}N_3O_4$ $[(M+H)^+]$ 318.1454, found 318.1478. **18**: colorless solid; UV (H_2O–MeOH 9:1) λ_{max} 267 (ε 2100); IR (neat) 3440, 1770, 1680, 1640, 1430, 1200, 1140, 1000 cm^{-1}; ^1H NMR (500 MHz, CD_3OD) δ 8.75 (s, 1H), 7.54 (s, 1H), 5.39 (s, 1H), 4.51 (m, 2H), 4.43 (dd, *J*=8.2, 14.3 Hz, 1H), 4.16 (m, 1H), 3.41 (dd, *J*=5.2, 8.2 Hz, 1H), 3.30–3.24 (m, 2H), 2.17–2.07 (m, 2H), 1.99–1.88 (m, 2H), 1.81 (s, 3H); MS (FAB) *m/z* 336 $(M+H)^+$; HRMS (FAB) calcd for $C_{16}H_{22}N_3O_5$ $[(M+H)^+]$ 336.1559, found 336.1568. **19**: colorless solid; UV (H_2O–MeOH 9:1) λ_{max} 280 (ε 18,000); IR (KBr) 3450, 1750, 1680, 1440, 1210, 1040 cm^{-1}; ^1H NMR (500 MHz, CD_3OD) δ 9.19 (s, 1H), 7.61 (s, 1H), 6.58 (m, 1H), 6.56 (s, 1H), 5.15 (s, 2H), 5.12 (s, 2H), 5.08–4.95 (m, 2H), 4.46 (t, *J*=7.0 Hz, 0.5H), 4.45 (t, *J*=7.0 Hz, 0.5H), 3.60–3.38 (m, 2H), 2.63–2.41 (m, 6H), 2.02 (s, 3H), 2.01 (s, 3H), 1.75–1.60 (m, 2H); MS (FAB) *m/z* 480 (M^+); HRMS (FAB) calcd for $C_{26}H_{30}N_3O_6$ $[(M+H)^+]$ 480.2135, found 480.2138. **20**: colorless solid; UV (H_2O–MeOH 9:1) λ_{max} 280 (ε 17,000); IR (neat) 3480, 1740, 1660, 1430, 1340, 1200, 1140, 1040 cm^{-1}; ^1H NMR (500 MHz, CD_3OD) δ 9.02 (s, 1H), 7.57 (s, 1H), 6.61 (s, 1H), 6.53 (s, 1H), 5.13 (s, 2H), 5.06 (dd, *J*=5.2, 13.0 Hz, 1H), 5.05 (dd, *J*=5.2, 13.0 Hz, 1H), 4.42–4.34 (m, 1H), 4.08 (d, *J*=12.7 Hz, 1H), 4.04 (d, *J*=12.7 Hz, 1H), 3.56–3.38 (m, 2H), 2.61–2.43 (m, 6H), 2.01 (s, 3H), 2.00 (s, 3H), 1.74–1.63 (m, 2H); MS (FAB) *m/z* 480 $(M+H)^+$; HRMS (FAB) calcd for $C_{26}H_{30}N_3O_6$ $[(M+H)^+]$ 480.2135, found 480.2138.

4.1.15. Reaction of (−)-2 with L-histidine. (−)-**2** (10.5 mg, 58 μmol) and L-histidine (9.0 mg, 58 μmol) were reacted at pH 7.5 for 16 h to give **16a** (6.3 mg, 34%), **17a** (5.3 mg, 29%), **18a** (2.7 mg, 15%), **19a** (1.5 mg, 5.4%), and **20a** (1.4 mg, 5.0%). **16a**: ^1H NMR (270 MHz, CD_3OD) δ 8.85 (s, 1H), 7.49 (s, 1H), 6.54 (s, 1H), 5.05 (dd, *J*=5.1, 13.2 Hz, 1H), 4.30 (dd, *J*=6.2, 6.8 Hz, 1H), 4.04 (s, 2H), 3.50 (dd, *J*=6.2, 14.9 Hz, 1H), 3.42 (dd, *J*=6.8, 14.9 Hz, 1H), 2.60–2.40 (m, 3H), 1.99 (s, 3H), 1.71 (m, 1H). **17a**: ^1H NMR (270 MHz, CD_3OD) δ 8.93 (s, 1H), 7.50 (s, 1H), 6.60 (s, 1H), 5.11 (s, 2H), 5.04 (dd, *J*=5.7, 13.8 Hz, 1H), 4.29 (t, *J*=6.8 Hz, 1H), 3.39 (dd, *J*=6.8, 14.9 Hz, 1H), 2.58–2.41 (m, 3H), 2.01 (s, 3H), 1.68 (m, 1H). A signal of a proton (β-position of L-histidine) was overlapped with the solvent signals. **18a**: ^1H NMR (270 MHz, CD_3OD) δ 8.91 (s, 1H), 7.61 (s, 1H), 5.20 (s, 1H), 4.61 (dd, *J*=6.5, 14.0 Hz, 1H), 4.52 (dd, *J*=7.6, 14.0 Hz, 1H), 4.50 (dd, *J*=4.6, 11.3 Hz, 1H), 4.27 (t, *J*=7.0 Hz, 1H), 2.29–1.98 (m, 3H), 1.89–1.74 (m, 1H), 1.72 (s, 3H). Signals of three protons (H-14 of jolkinolide D pharmacophore and β-position of L-histidine) were overlapped with the solvent signals. **19a**: ^1H NMR (270 MHz, CD_3OD) δ 9.16 (s, 1H), 7.58 (s, 1H), 6.59 (s, 1H), 6.56 (s, 1H), 5.15 (s, 2H), 5.12 (s, 2H), 5.10–4.97 (m, 2H), 4.29 (m, 1H), 2.63–2.39 (m, 6H), 2.02 (s, 3H), 2.01 (s, 3H), 1.83–1.55 (m, 2H). Signals of two protons (β-position of L-histidine) were overlapped with the solvent signals. **20a**: ^1H NMR (270 MHz, CD_3OD) δ 8.76 (s, 1H), 7.45 (s, 1H), 6.58 (s, 1H), 6.52 (s, 1H), 5.07 (s, 2H), 5.03 (dd, *J*=4.6, 13.0 Hz, 2H), 4.10 (m, 1H), 4.01 (d, *J*=13.5 Hz, 1H), 3.93 (d, *J*=13.5 Hz, 1H), 2.61–2.43 (m, 6H), 2.01 (s, 3H), 1.99 (s, 3H), 1.74–1.63 (m, 1H). Signals of two protons (β-position of L-histidine) were overlapped with the solvent signals.

4.1.16. Reaction of (±)-2 with glutathione. Glutathione (17 mg, 55 μmol) was dissolved in H_2O (0.20 mL), and the pH was adjusted to 7.5 by adding a trace amount of 1 M NaOH. To the aqueous solution was added a solution of (±)-**2** (10 mg, 55 μmol) in THF (0.06 mL). The mixture was stirred at ambient temperature for 16 h and concentrated. The residue was purified by column chromatography on silica gel (ODS 0.6 g, MeOH–0.1 M aqueous TFA 1:10→1:9→1:8→1:7→1:3→1:1) and preparative HPLC (Develosil ODS-HG-5, 20×250 mm, CH_3CN–0.2 M aqueous TFA 82:18, 8.0 mL/min) to give **21** (17 mg, 52%), **22** (6.3 mg, 19%), **23** (4.2 mg, 10%) as the TFA salt. **21**: colorless oil; UV (H_2O–MeOH 9:1) λ_{max} 283 (ε 16,000); IR (neat) 3380, 1730, 1660, 1650, 1540, 1430, 1200,

1140 cm^{-1}; ^1H NMR (270 MHz, CD_3OD) δ 6.49 (s, 1H), 4.65 (dd, J=5.1, 9.0 Hz, 0.5H), 4.63 (dd, J=5.1, 9.0 Hz, 0.5H), 4.04 (t, J=5.1 Hz, 1H), 3.92 (s, 2H), 3.45 (br s, 2H), 3.03 (dd, J=5.1, 14.0 Hz, 0.5H), 3.02 (dd, J=5.1, 14.0 Hz, 0.5H), 2.77 (dd, J=9.0, 14.0 Hz, 0.5H), 2.76 (dd, J=9.0, 14.0 Hz, 0.5 Hz), 2.57 (t, J=6.9 Hz, 2H), 2.53–2.36 (m, 3H), 2.36–2.08 (m, 2H), 1.95 (s, 3H), 1.80–1.45 (m, 1H), A signal of a proton (H-12) was overlapped with the solvent signals; MS (FAB) m/z 470 $(M+H)^+$; HRMS (FAB) calcd for $C_{20}H_{28}N_3O_8S$ $[(M+H)^+]$ 470.1597, found 470.1598. **22**: colorless solid; IR (neat) 3320, 1740, 1670 1540, 1430, 1200, 1140, 1050, 1010 cm^{-1}; ^1H NMR (270 MHz, CD_3OD) δ 5.58 (s, 0.3H), 5.42 (s, 0.7H), 4.73–4.58 (m, 1H), 4.46–4.31 (m, 1H), 4.03–3.85 (m, 3H), 3.20–3.02 (m, 2H), 2.98–2.66 (m, 3H), 2.58 (m, 2H), 2.36–2.02 (m, 5H), 2.02–1.80 (m, 1H), 1.77 (s, 2.1H), 1.74 (s, 0.9H); MS (FAB) m/z 488 $(M+H)^+$; HRMS (FAB) calcd for $C_{20}H_{30}N_3O_9S$ $[(M+H)^+]$ 488.1703, found 488.1715. **23**: colorless solid; UV (H_2O–MeOH 9:1) λ_{max} 281 (ε 17,000); IR (neat) 3340, 1740, 1660, 1200, 1030 cm^{-1}; ^1H NMR (270 MHz, CD_3OD) δ 6.54 (br s, 1H), 6.49 (s, 1H), 5.06 (dd, J=5.3, 13.4 Hz, 1H), 4.98–4.91 (m, 1H), 4.63 (dd, J=5.1, 9.2 Hz, 0.5H), 4.62 (dd, J=5.1, 9.2 Hz, 0.5H), 4.08 (dd, J=5.4, 6.3 Hz, 1H), 4.02 (s, 2H), 3.93 (s, 2H), 3.45 (s, 2H), 3.04 (dd, J=5.1, 14.0 Hz, 0.5H), 3.03 (dd, J=5.1, 14.0 Hz, 0.5H), 2.77 (dd, J=9.2, 14.0 Hz, 0.5H), 2.76 (dd, J=9.2, 14.0 Hz, 0.5H), 2.66 (t, J=6.5 Hz, 2H), 2.62–2.37 (m, 6H), 2.32–2.18 (m, 2H), 2.00 (s, 3H), 1.95 (s, 3H), 1.83–1.55 (m, 2H); MS (FAB) m/z 632 $(M+H)^+$; HRMS (FAB) calcd for $C_{30}H_{38}N_3O_{10}S$ $[(M+H)^+]$ 632.2278, found 632.2274.

4.1.17. Reaction of (−)-2 with glutathione. (−)-**2** (10 mg, 55 μmol) and glutathione (17 mg, 55 μmol) were reacted at pH 7.5 for 16 h to give **21a** (20 mg, 60%) and **22a** (12 mg, 37%) as the TFA salt, respectively. **21a**: ^1H NMR (270 MHz, CD_3OD) δ 6.47 (s, 1H), 4.64 (dd, J=5.4, 8.9 Hz, 1H), 4.04 (t, J=5.9 Hz, 1H), 3.91 (s, 2H), 3.51 (d, J=13.5 Hz, 1H), 3.40 (d, J=13.5 Hz, 1H), 3.02 (dd, J=5.4, 14.3 Hz, 1H), 2.71 (dd, J=8.9, 14.3 Hz, 1H), 2.54 (t, J=6.8 Hz, 2H), 2.53–2.36 (m, 3H), 2.20 (m, 2H), 1.93 (s, 3H), 1.60 (m, 1H). A signal of a proton (H-12 of jolkinolide D pharmacophore) was overlapped with the solvent signals. **22a**: ^1H NMR (270 MHz, CD_3OD) δ 5.58 (s, 0.33H), 5.42 (s, 0.67H), 4.71–4.58 (m, 1H), 4.48–4.31 (m, 1H), 4.10–3.99 (m, 1H), 3.93 (s, 2H), 3.20–3.02 (m, 2H), 2.97–2.68 (m, 3H), 2.68–2.50 (m, 2H), 2.33–2.01 (m, 5H), 2.01–1.80 (m, 1H), 1.77 (s, 2H), 1.73 (s, 1H).

4.1.18. Reaction of (±)-2 with 2′-deoxyguanosine. 2′-Deoxyguanosine (7.9 mg, 28 μmol) was dissolved in H_2O (1.25 mL), and the pH was adjusted to 7.5 by adding a trace amount of 1 M NaOH. To the aqueous solution was added a solution of (±)-**2** (5.0 mg, 28 μmol) in THF (0.03 mL) at ambient temperature. After stirring for 16 h, the reaction mixture was diluted with H_2O (3 mL) and extracted with a 2:1 mixture of hexane and Et_2O (3×3 mL). The aqueous layer was concentrated to give a solid, which was purified by column chromatography on ODS silica gel (0.5 g, MeOH–H_2O 1:4→1:3→1:2→1:1→2:1) to give **24** (2.5 mg, 21%). The combined organic extracts were dried and concentrated to give a solid, which was purified by column chromatography on silica gel (0.5 g, $CHCl_3$–acetone–MeOH 10:1:0→5:5:1→3:3:1→2:2:1) to recover (±)-**2** (1.8 mg, 36%). **24**: colorless solid; UV (H_2O–MeOH 9:1) λ_{max} 257 (ε 10,000), 272 nm (ε 11,900); IR (neat) 3330, 1730, 1640, 1580, 1540, 1440, 1100 cm^{-1}; ^1H NMR (270 MHz, CD_3OD) δ 7.96 (s, 1H), 6.77 (s, 1H), 6.25 (dd, J=6.2, 7.3 Hz, 1H), 5.12 (d, J=15.1 Hz, 1H), 4.99 (dd, J=5.1, 14.0 Hz, 1H), 4.69 (d, J=15.1 Hz, 1H), 4.51 (ddd, J=3.1, 3.5, 6.2 Hz, 1H), 3.97 (ddd, J=3.5, 3.5, 4.1 Hz, 1H), 3.76 (dd, J=3.5, 12.2 Hz, 1H), 3.72 (dd, J=4.1, 12.2 Hz, 1H), 2.68 (ddd, J=6.2, 7.3, 13.5 Hz, 1H), 2.47–2.39 (m, 3H), 2.33 (ddd, J=3.1, 6.2, 13.5 Hz, 1H), 1.94 (s, 3H), 1.71–1.60 (m, 1H); MS (FAB) m/z 430 $(M+H)^+$; HRMS (FAB) calcd for $C_{20}H_{24}N_5O_6$ $[(M+H)^+]$ 430.1727, found 430.1708.

4.1.19. Reaction of (−)-2 with 2′-deoxyguanosine (pH 7.5). (−)-**2** (5.0 mg, 28 μmol) and 2′-deoxyguanosine (7.9 mg, 28 μmol) were reacted at pH 7.5 for 16 h to give **24a** (0.6 mg, 5%) along with recovered (−)-**2** (4.1 mg, 81%). **24a**: ^1H NMR (270 MHz, CD_3OD) δ 7.95 (s, 1H), 6.76 (s, 1H), 6.25 (dd, J=6.2, 7.6 Hz, 1H), 5.12 (d, J=15.9 Hz, 1H), 4.99 (dd, J=5.1, 14.0 Hz, 1H), 4.69 (d, J=15.9 Hz, 1H), 4.51 (ddd, J=3.0, 3.0, 6.2 Hz, 1H), 3.98 (ddd, J=3.0, 3.5, 4.1 Hz, 1H), 3.78 (dd, J=3.5, 12.2 Hz, 1H), 3.70 (dd, J=4.1, 12.2 Hz, 1H), 2.69 (ddd, J=6.2, 7.6, 13.5 Hz, 1H), 2.52–2.40 (m, 3H), 2.34 (ddd, J=3.0, 6.2, 13.5 Hz, 1H), 1.93 (s, 3H), 1.64 (m, 1H).

4.1.20. Reaction of (−)-2 with 2′-deoxyguanosine (pH 8.9). (−)-**2** (5.0 mg, 28 μmol) and 2′-deoxyguanosine (7.9 mg, 28 μmol) were reacted at pH 8.9 for 16 h to give **24a** (7.1 mg, 52%) along with recovered (−)-**2** (2.1 mg, 42%).

4.1.21. Reaction of (±)-2 with thymidine (pH 8.7). Thymidine (5.9 mg, 24 μmol) was dissolved in H_2O (0.1 mL), and the pH was adjusted to 8.7 by adding a trace amount of 1 M NaOH. To the aqueous solution was added a solution of (±)-**2** (4.4 mg, 24 μmol) in THF (0.03 mL) at ambient temperature. After stirring for 16 h, the reaction mixture was diluted with H_2O (3 mL) and extracted with EtOAc (3×3 mL). The aqueous layer was concentrated to give a solid, which was purified by column chromatography on silica gel (ODS, 0.5 g, MeOH-H_2O 1:10→1:3→1:2→1:1) to give impure **25** (1.9 mg). The combined organic extracts were dried and concentrated to give a solid, which was purified by column chromatography on silica gel (ODS, 0.5 g, MeOH–H_2O 1:10→1:3→1:2→1:1) to give impure **25** (4.7 mg) along with recovered (±)-**2** (1.7 mg, 39%). Further purification of the combined impure **25** by preparative HPLC (Develosil ODS-HG-5, 20×250 mm, MeOH–H_2O 40:60→45:55, linear gradient, 50 min, 5.0 mL/min) gave **25** (2.1 mg, 22%). **25**: colorless solid; UV (H_2O–MeOH 9:1) λ_{max} 274 nm (ε 18,000); IR (neat) 3430, 1740, 1700, 1650, 1340, 1050 cm^{-1}; ^1H NMR (500 MHz, $CDCl_3$) δ 7.40 (q, J=1.2 Hz, 1H), 6.38 (s, 0.5H), 6.37 (s, 0.5H), 6.18 (t, J=6.5 Hz, 0.5H), 6.17 (t, J=6.5 Hz, 0.5H), 4.93 (d, J=14.7 Hz, 0.5H), 4.91 (d, J=14.7 Hz, 0.5H), 4.79 (d, J=14.7 Hz, 0.5H), 4.77 (d, J=14.7 Hz, 0.5H), 4.74 (dd, J=4.9, 13.5 Hz, 1H), 4.60 (m, 1H), 4.01 (ddd, J=3.3, 3.3, 3.3 Hz, 1H), 3.94 (br d, J=12.4 Hz, 1H), 3.86 (br d, J=12.4 Hz, 1H), 2.56 (br s, 1H), 2.44–2.33 (m, 5H), 1.93 (s, 3H), 1.91 (s, 3H), 1.63–1.58 (m, 1H), 1.57 (br s, 1H); MS (FAB) m/z 405

$(M+H)^+$; HRMS (FAB) calcd for $C_{20}H_{25}N_2O_7$ [$(M+H)^+$] 405.1662, found 405.1667.

4.1.22. Reaction of (−)-2 with thymidine (pH 8.7). (−)-**2** (4.1 mg, 23 μmol) and thymidine (5.5 mg, 23 μmol) were reacted at pH 8.7 for 16 h to give **25a** (1.0 mg, 18%) along with recovered (−)-**2** (3.5 mg, 84%). **25a**: ^{1}H NMR (500 MHz, $CDCl_3$) δ 7.35 (q, *J*=0.9 Hz, 1H), 6.38 (s, 1H), 6.17 (t, *J*=6.7 Hz, 1H), 4.92 (d, *J*=14.9 Hz, 1H), 4.76 (d, *J*=14.9 Hz, 1H), 4.74 (dd, *J*=5.3, 13.7 Hz, 1H), 4.60 (m, 1H), 3.98 (ddd, *J*=3.2, 3.5, 3.5 Hz, 1H), 3.92 (br d, *J*=12.2 Hz, 1H), 3.81 (br d, *J*=12.2 Hz, 1H), 2.51–2.27 (m, 5H), 1.93 (s, 3H), 1.91 (s, 3H), 1.73–1.44 (m, 1H).

4.1.23. Reaction of (±)-2 with DNA. DNA from salmon spermary (30 mg, 0.10 mmol in nucleotide) was dissolved in H_2O (1.5 mL), and the pH was adjusted to 7.5 by adding a trace amount of 1 M NaOH. To the aqueous solution was added a solution of (±)-**2** (17.4 mg, 0.10 mmol) in MeOH (0.15 mL) at 37 °C. After stirring at 37 °C for a week, the reaction mixture was diluted with H_2O (3 mL) and extracted with EtOAc (3×3 mL). The aqueous layer was concentrated to give a solid, which was hydrolyzed with deoxyribonuclease I (Takara, 1830 unit) in an aqueous buffer [3.6 mL, 50 mM Tris–HCl (pH 9.0), 5 mM $MgCl_2$, 10 mM 2-mercaptoethanol] at 37 °C overnight. To the reaction mixture were added snake venom phosphodiesterase (Worthington Biochemical Corporation, 63.5 unit) and bacterial alkaline phosphatase (Takara, 30.5 unit), and the mixture was incubated at 37 °C for 24 h. The hydrolysate was separated by preparative HPLC (Develosil ODS-HG-5, 20×250 mm, MeOH–H_2O 40:60→45:55, linear gradient, 50 min, 5.0 mL/min) to give **24** (0.2 mg, 0.48%) and **25** (0.1 mg, 0.26%) along with 2′-deoxyadenosine, 2′-deoxyguanosine, 2′-deoxycytidine, and thymidine. The combined organic extracts were dried and concentrated to recover (±)-**2** (16.3 mg, 94%).

Acknowledgements

This work was supported in part by a Grant-in-Aid for Priority Area from the Ministry of Education, Culture, Sports, Science, and Technology of Japan, Suntory Institute for Bioorganic Research, Shorai Foundation for Science and Technology, Yamada Science Foundation, the Fujisawa Foundation, University of Tsukuba Research Projects, and Wako Pure Chemical Industries, Ltd. The IR and NMR spectra were recorded at the Chemical Analysis Center, University of Tsukuba.

References and notes

1. Uemura, D.; Hirata, Y. *Chem. Lett.* **1974**, 819–822.
2. Kigoshi, H.; Ichino, T.; Yamada, K.; Ijuin, Y.; Makita, S. F.; Uemura, D. *Chem. Lett.* **2001**, 518–519.
3. Fischer, N. H.; Oliver, E. J.; Fisher, H. D. *Fortschr. Chem. Org. Naturst.* **1979**, *38*, 47–390.
4. Part of this work has been published: see Sakakura, A.; Takayanagi, Y.; Kigoshi, H. *Tetrahedron Lett.* **2002**, *43*, 6055–6058.
5. Lin, J.; Nikaido, M. M.; Clark, G. *J. Org. Chem.* **1987**, *52*, 3745–3752.
6. Irifune, S.; Kibayashi, T.; Ishii, Y.; Ogawa, M. *Synthesis* **1988**, 366–369.
7. The numbering adopted in this paper corresponds to that of jolkinolide D (**1**).
8. (a) Tanyeli, C.; Demir, A. S.; Dikici, E. *Tetrahedron: Asymmetry* **1996**, *7*, 2399–2402. (b) Tanyeli, C.; Sezen, B.; Dikici, E.; Fleischhauer, J.; Repges, C.; Wang, Y.; Gawronski, J.; Kacprzak, K. *Enantiomer* **2001**, *6*, 219–227.
9. Enantiomeric excess value was determined by the comparison of the $[\alpha]_D$ value of (−)-**11** ($[\alpha]_D^{25}$ −164 (*c* 1.08, $CHCl_3$)), obtained by hydrolysis of (−)-**10** with $Sc(OTf)_3$, with the literature value of its enantiomer of 95.6% ee ($[\alpha]_D^{25}$ +156.6)[8].
10. Demir, A. S.; Sesenoglu, O. *Org. Lett.* **2002**, *4*, 2021–2023.
11. Singer, B. *Biochemistry* **1972**, *11*, 3939–3947.
12. Singer, B.; Grunberger, D. *Molecular Biology of Mutagens and Carcinogens*; Plenum: New York, 1983; pp 328–329.
13. Wu, R.; Kaiser, A. D. *Proc. Natl. Acad. Sci. U.S.A.* **1967**, *57*, 170–177.
14. Haines, J. A.; Reese, C. B.; Todd, L. *J. Chem. Soc.* **1962**, 5281–5288.
15. Singer, B. *Biochemistry* **1975**, *14*, 4353–4357.
16. Broom, A. D.; Townsend, L. B.; Jones, J. W.; Robins, R. K. *Biochemistry* **1964**, *3*, 494–500.

Available online at www.sciencedirect.com
SCIENCE DIRECT®
Tetrahedron 60 (2004) 7077–7084
Tetrahedron

Synthesis, conformation and PKC isozyme surrogate binding of indolinelactam-Vs, new conformationally restricted analogues of (−)-indolactam-V

Yu Nakagawa,[a] Kazuhiro Irie,[a,*] Yusuke Komiya,[a] Hajime Ohigashi[a] and Ken-ichiro Tsuda[b]

[a]*Division of Food Science and Biotechnology, Graduate School of Agriculture, Kyoto University, Kyoto 606-8502, Japan*
[b]*Fundamental Research Laboratories NEC Corporation, 34 Miyukigaoka, Tsukuba 305-8501, Japan*

Received 29 May 2003; revised 19 August 2003; accepted 19 August 2003

Available online 24 June 2004

Abstract—New conformationally restricted analogues of tumor promoter (−)-indolactam-V (**1**), indolinelactam-Vs (**8**, **11**) and their hexyl derivatives at position 1 or 7 (**9**, **10**, **12**, **13**), were synthesized from **1**. (3*R*)-Indolinelactam-V (**8**) adopted a conformation similar to the twist form of **1** with a *cis* amide, while the conformation of (3*S*)-indolinelactam-V (**11**) was close to that of the sofa form of **1** with a *trans* amide. 7-Hexyl derivatives of **8** and **11** (**10**, **13**) showed binding affinities for C1 domains of protein kinase C (PKC) isozymes compared to **1**, but exhibited little selectivity among these PKC isozymes. However, introduction of the hexyl group at position 1 of **8** and **11** significantly enhanced their binding selectivity for novel PKC isozymes. The best selectivity for novel PKC isozymes was observed in (3*S*)-1-hexylindolinelactam-V (**12**) with a sofa-like conformation. These results suggest that a sofa-restricted analogue of **1** with a hydrophobic chain at an appropriate position would be a promising lead for designing agents with a high selectivity for novel PKC isozymes.

1. Introduction

Protein kinase C (PKC) isozymes are serine/threonine-specific protein kinases involved in a variety of cellular functions such as gene expression, growth, differentiation and apoptosis.[1] PKC isozymes are subdivided into three groups; conventional PKCs (α, βI, βII, γ), novel PKCs (δ, ϵ, η, θ) and atypical PKCs (ζ, ι/λ) (Fig. 1).[2,3] Conventional and novel PKCs contain two cysteine-rich C1 domains (C1A, C1B), both of which bind tumor promoters such as 12-*O*-tetradecanoylphorbol 13-acetate (TPA)[4] and teleocidin B-4.[5] Recent investigations have suggested that novel PKCs (δ, ϵ, η) are involved in mouse skin tumor promotion[6–9] and that the C1B domains of these PKC isozymes are the main targets of tumor promoters.[10,11] Design of new agents with high selectivity for C1B domains of novel PKCs is thus indispensable in elucidating the precise mechanism of skin-tumor promotion.

The naturally occurring tumor promoter (−)-indolactam-V (**1**)[12,13] is a promising lead compound for such agents since it has a simple structure and shows a binding preference for C1B domains over C1A domains of novel PKCs (Fig. 2).[14] (−)-Indolactam-V (**1**) exists as two stable conformers in solution at room temperature; the twist form with a *cis* amide geometry and the sofa form with a *trans* amide geometry.[15] We have recently found that the sofa-restricted analogue of **1** (**5**), not the twist-restricted analogue (**4**),[16] shows significant selectivity for novel PKCs.[14] These results suggest that the conformation of **1** plays a crucial role in its binding selectivity for PKC isozymes.

(3*R*)- and (3*S*)-2-Oxyindolactam-V (**6**, **7**),[17,18] isolated from the culture broth of *Streptomyces blastmyceticum* NA34-17 adopted slightly different conformations from both the twist and the sofa forms of **1**. However, these compounds were inactive in several in vitro bioassays that correlate with in vivo tumor promotion probably due to the steric hindrance between the carbonyl group at position 2 and receptors such as PKC isozymes.[19,20] (3*R*)- and (3*S*)-Indolinelactam-Vs (**8**, **11**), which lack a carbonyl group at position 2, might be new conformationally restricted analogues of **1** and may exhibit different binding selectivity for PKC isozymes from that of **1**, **4** and **5**. We report here the synthesis, conformation and PKC isozyme surrogate binding of indolinelactam-Vs (**8**, **11**) and their hexyl derivatives at positions 1 and 7 (**9**, **10**, **12**, **13**) (Fig. 3).

Keywords: (−)-Indolactam-V; Indolinelactam-V; Phorbol ester; Protein kinase C; Tumor promoter.
* Corresponding author. Tel.: +81-75-753-6282; fax: +81-75-753-6284; e-mail address: irie@kais.kyoto-u.ac.jp

0040–4020/$ - see front matter © 2004 Elsevier Ltd. All rights reserved.
doi:10.1016/j.tet.2003.08.081

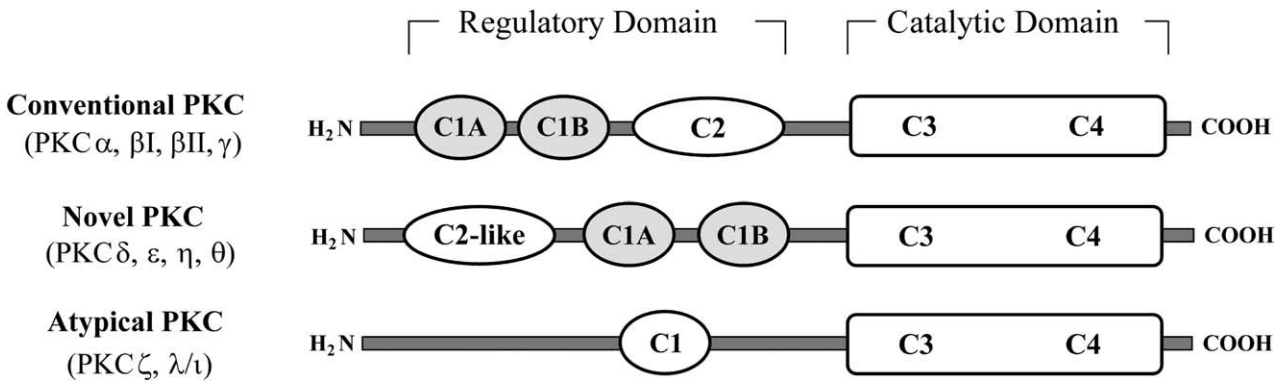

Figure 1. Structures of PKC isozymes.

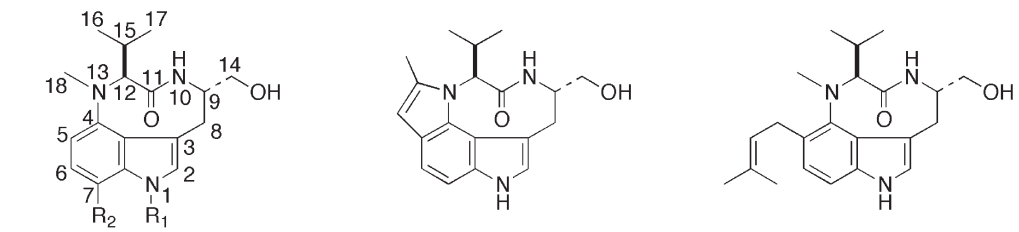

$R_1 = R_2 = H$; (-)-Indolactam-V (**1**)
$R_1 = n\text{-}C_6H_{13}$, $R_2 = H$;
(-)-1-Hexylindolactam-V (**2**)
$R_1 = H$, $R_2 = n\text{-}C_6H_{13}$;
(-)-7-Hexylindolactam-V (**3**)

Twist-restricted analogue (**4**)

Sofa-restricted analogue (**5**)

Figure 2. Structures of indolactam forms.

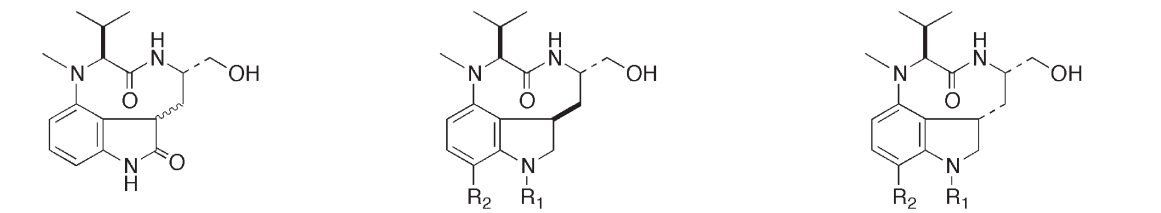

(3*R*)-2-Oxyindolactam-V (**6**)
(3*S*)-2-Oxyindolactam-V (**7**)

$R_1 = R_2 = H$; (3*R*)-Indolinelactam-V (**8**)
$R_1 = n\text{-}C_6H_{13}$, $R_2 = H$;
(3*R*)-1-Hexylindolinelactam-V (**9**)
$R_1 = H$, $R_2 = n\text{-}C_6H_{13}$;
(3*R*)-7-Hexylindolinelactam-V (**10**)

$R_1 = R_2 = H$; (3*S*)-Indolinelactam-V (**11**)
$R_1 = n\text{-}C_6H_{13}$, $R_2 = H$;
(3*S*)-1-Hexylindolinelactam-V (**12**)
$R_1 = H$, $R_2 = n\text{-}C_6H_{13}$;
(3*S*)-7-Hexylindolinelactam-V (**13**)

Figure 3. Structures of 2-oxyindolactam-Vs (**6**,**7**) and indolinelactam-Vs (**8**–**13**).

2. Results and discussion

(3*R*)- and (3*S*)-Indolinelactam-Vs (**8**, **11**) were synthesized from (−)-indolactam-V (**1**). Reduction of the indole ring of **1** proceeded easily with sodium cyanoborohydride in acetic acid[21] to give two diastereomers **8** and **11** (31 and 20%, respectively). The ^{1}H NMR spectra of **8** and **11** in $CDCl_3$ showed that each compound existed as a single conformer at room temperature and at −40 °C (Table 1). A significant NOE interaction between H-3 (δ 3.84) and H-12 (δ 4.37) was observed in **8**, suggesting that **8** is the (3*R*) isomer. The downfield shift of the ^{1}H NMR signals H-10 (δ 7.31) and H-12 (δ 4.37), and the lack of an NOE interaction between these protons, are characteristic of the twist form of **1**[15] and indicate that **8** adopts the twist-like conformation with a *cis* amide. On the other hand, **11** was the (3*S*) isomer because of a significant NOE interaction between H-3 (δ 3.17) and H-9 (δ 4.25) protons. As observed in the sofa form of **1**,[15] the ^{1}H NMR signals for H-10 (δ 4.92) and H-12 (δ 3.08) in **11** shifted upfield and an NOE interaction was observed between them. These results indicate that the conformation of **11** is close to the sofa form of **1** with a *trans* amide.

To determine the conformations of **8** and **11** precisely, we performed conformational studies using molecular mechanics and quantum mechanics calculations. The initial structure of **8** was calculated by MM2 with the distances between H-3 and H-12, and between H-9 and H-18 fixed at 2 Å in accordance with the NOE data. The resultant structure was optimized by PM3. The initial structure of **11** was similarly determined with the three NOE interactions between H-3 and H-9, H-3 and H-18, and H-10 and

Table 1. ^{1}H NMR data of (−)-indolactam-V (**1**) and (3*R*)- and (3*S*)-indolinelactam-Vs (**8**, **11**) in $CDCl_3$ (500 MHz, 300 K)

No.	δ (multiplicity, *J* in Hz)			
	(−)-Indolactam-V (**1**)		(3*R*)-Indolinelactam-V (**8**)	(3*S*)-Indolinelactam-V (**11**)
	Twist[a]	Sofa[a]	Twist-like[b]	Sofa-like[c]
1	7.99 (br. s)	8.27 (br. s)	3.75 (br. s)	3.73 (br. s)
2	6.89 (s)	7.06 (s)	3.18 (dd, *J*=8.9, 0.9)	3.21 (d, *J*=8.4)
			3.77 (t, *J*=8.9)	3.52 (dd, *J*=8.4, 6.6)
3			3.84 (m)	3.17 (m)
5	6.51 (d, *J*=7.5)	7.06 (d, *J*=8.2)	6.23 (d, *J*=7.9)	6.52 (d, *J*=7.8)
6	7.06 (t, *J*=7.5)	7.17 (t, *J*=8.2)	6.98 (t, *J*=7.9)	7.02 (t, *J*=7.8)
7	6.91 (d, *J*=7.5)	7.28 (d, *J*=8.2)	6.21 (d, *J*=7.9)	6.48 (d, *J*=7.8)
8	3.00 (dd, *J*=17.4, 3.8)	2.83 (d, *J*=14.0)	1.70 (dt, *J*=12.6, 2.0)	1.87 (dt, *J*=12.2, 1.8)
	3.20 (d, *J*=17.4)	3.11 (dd, *J*=14.0, 4.8)	1.92 (dt, *J*=12.6, 4.6)	2.06 (q, *J*=12.2)
9	4.30 (m)	4.46 (m)	4.01 (m)	4.25 (m)
10	6.59 (br. s)	4.72 (d, *J*=10.8)	7.31 (d, *J*=6.2)	4.92 (br.s)
12	4.39 (d, *J*=10.2)	2.99 (d, *J*=10.8)	4.37 (d, *J*=8.6)	3.08 (d, *J*=10.7)
14	3.54 (m)	3.44 (m)	3.43 (m)	3.37 (m)
	3.74 (m)	3.44 (m)	3.64 (m)	3.56 (m)
15	2.62 (m)	2.40 (m)	2.43 (m)	2.26 (m)
16	0.93 (d, *J*=6.4)	1.25 (d, *J*=7.1)	1.10 (d, *J*=6.4)	1.14 (d, *J*=6.7)
17	0.63 (d, *J*=6.8)	0.94 (d, *J*=7.1)	0.90 (d, *J*=6.8)	0.94 (d, *J*=6.5)
18	2.92 (s)	2.75 (s)	2.84 (s)	2.62 (s)

[a] Twist: Sofa=1.0: 0.4 (0.004 M).
[b] 0.079 M.
[c] 0.046 M.

H-12 used to restrict the distance between these proton pairs to 2 Å. Further optimization of these initial structures was carried out by a Hartree–Fock calculation with the 6-31G* basis set to give the optimized structures of **8** and **11** as shown in Figure 4. The conformations of **8** and **11** resembled the twist and the sofa forms of **1**, respectively. However, the spatial arrangement of the methylene group at position 8 in **8** and **11** was quite different from that of the twist and the

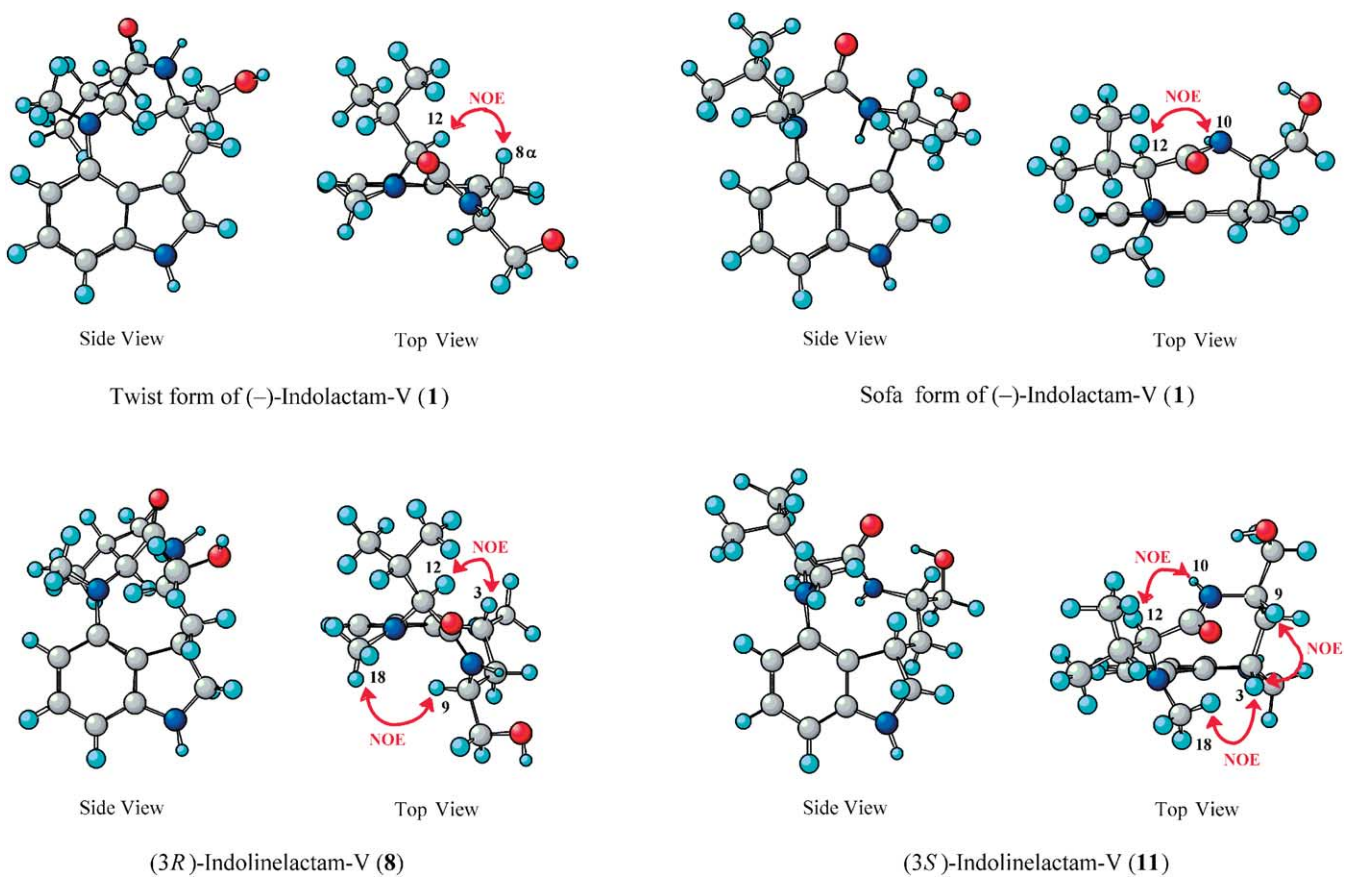

Figure 4. Stable conformations of twist (upper left) and sofa (upper right) form of (-)-indolactam-V (**1**), (3*R*)-indolinelactam-V (**8**, lower left) and (3*S*)-indolinelactam-V (**11**, lower right). The initial structures were determined by MM2 and PM3 calculations based on the indicated NOE interactions. Optimization was carried out by a Hartree-Fock calculation with the 6-31G* basis set.

Table 2. K_i Values for inhibition of the specific binding of [^{3}H]PDBu by (−)-indolactam-V (**1**), the twist- and sofa-restricted analogues of **1** (**4**, **5**), and (3*R*)- and (3*S*)-indolinelactam-Vs (**8**, **11**)

PKC C1 peptide	K_i (nM)				
	1[a]	**4**[a]	**5**[a]	**8**	**11**
Conventional PKC					
α-C1A (72-mer)[b]	21 (1.0)[c]	39 (3.9)	6000 (730)	13,000 (2500)	ND[d]
α-C1B	4000 (870)	4500 (1200)	11,000 (900)	>10,000	ND
β-C1A (72-mer)	19 (4.5)	25 (2.6)	8200 (830)	8900 (1800)	ND
β-C1B	140 (4.4)	330 (21)	321 (25)	16,000 (2500)	ND
γ-C1A	140 (14)	110 (8.0)	12,000 (2400)	>10,000	ND
γ-C1B	210 (5.0)	270 (26)	790 (140)	17,000 (3800)	ND
Novel PKC					
δ-C1A	1900 (190)	2900 (570)	23,000 (4300)	>10,000	ND
δ-C1B	8.3 (1.1)	31 (6.6)	21 (4.4)	660 (45)	5000 (960)
ϵ-C1A	4100 (50)	2500 (850)	15,000 (3100)	8200 (2100)	ND
ϵ-C1B	7.7 (1.2)	29 (4.1)	12 (2.4)	920 (190)	7700 (2200)
η-C1A	3800 (480)	1300 (2.0)	8600 (1400)	11,000 (730)	ND
η-C1B	5.5 (0.6)	14 (3.2)	6.2 (0.4)	310 (42)	2200 (400)
θ-C1A	NT[e]	NT	NT	NT	NT
θ-C1B	8.7 (1.2)	43 (6.8)	26 (2.2)	400 (52)	7700 (600)

[a] These data are cited from Ref. 14.
[b] Ten residues from both N and C-termini of the previous α-C1A and β-C1A were elongated as the solubility of the original 52-mer peptides was extremely low.
[c] Standard deviation of at least two separate experiments.
[d] Not detected.
[e] Not tested. The K_d value of [^{3}H]PDBu to θ-C1A could not be measured because of its very weak binding affinity.

sofa forms of **1**, respectively. These results indicate that **8** and **11** are new conformationally restricted analogues of **1**.

Binding affinities of **8** and **11** for PKC isozyme C1 domains were evaluated by inhibition of the specific binding of [^{3}H]phorbol 12,13-dibutyrate (PDBu) to the synthetic C1 peptides (about 50–70 amino acids) of all PKC isozymes as reported previously.[11,22,23] PKC C1 peptides exhibit PDBu binding affinities comparable to the whole PKC isozymes enabling evaluation of PKC isozyme selectivity, as well as C1 domain selectivity of PKC C1 domain-binding compounds. Using the PKC C1 peptides, the concentration required to cause 50% inhibition of the [^{3}H]PDBu binding (IC_{50}) was measured. The binding affinities of **8** and **11** for each PKC C1 peptide were expressed as K_i values calculated from the IC_{50} and the K_d value of [^{3}H]PDBu as reported by Sharkey and Blumberg.[23] Table 2 summarizes the K_i values of **8** and **11** along with those of (−)-indolactam-V (**1**) and its conformationally restricted analogues (**4**, **5**).

(3*R*)- and (3*S*)-Indolinelactam-Vs (**8**, **11**) showed quite low binding affinities for all PKC C1 peptides compared with those of **1**, **4** and **5**. The binding affinities of **8** for almost all PKC C1 peptides were more than 50-fold lower than those of **1**, and **11** exhibited little binding affinity for all PKC C1 peptides. Since introduction of a substituent at position 2 in **1** abolished the tumor-promoting activity due to steric hindrance,[24] the quite low PKC binding affinities of **8** and **11** might be due to the steric hindrance between the two hydrogen atoms at position 2 and the C1 peptides of PKC isozymes. Interestingly, the selectivity of **8** for the C1B peptides of novel PKCs (δ, ϵ, η, θ), relative to both C1

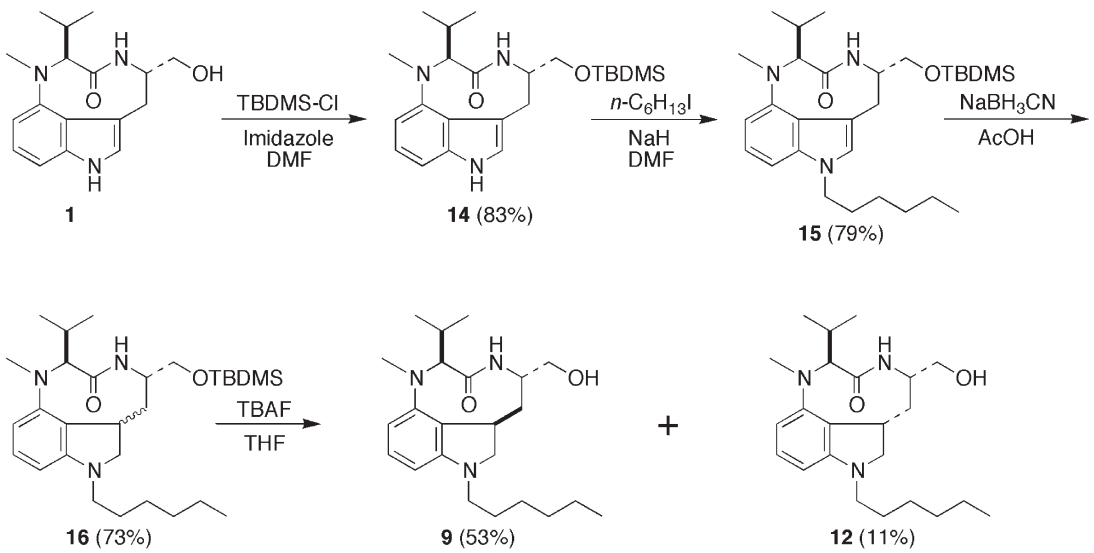

1 **14** (83%) **15** (79%) **16** (73%) **9** (53%) **12** (11%)

Scheme 1. Synthesis of 1-hexylindolinelactam-Vs (**9**,**12**).

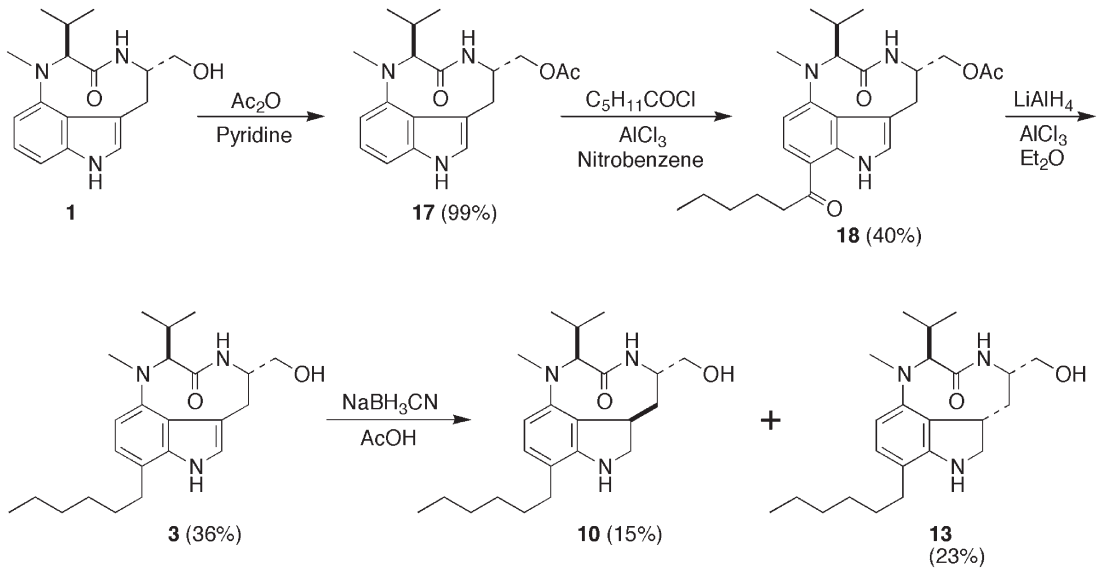

Scheme 2. Synthesis of 7-hexylindolinelactam-Vs (**10**,**13**).

peptides of conventional PKCs (α, β, γ), was considerably higher than that of **1** and **4**. This result was unexpected since the conformation of **8** has many points of similarity to that of **4**, which showed low selectivity for the C1B peptides of novel PKCs relative to the C1A peptides of conventional PKCs. It is not clear whether the conformational difference between **4** and **8**, such as the spatial arrangement of the methylene group at position 8, or the possible steric hindrance of hydrogen atoms at position 2, produces the binding selectivity of **8**. However, **8** could be a lead compound for a new agent that selectively binds to the C1B domains of novel PKCs.

Since introduction of a hydrophobic alkyl chain at position 1 or 7 in **1** dramatically increases its binding affinity for phorbol ester receptors such as PKC isozymes,[24] we attempted to enhance the PKC binding ability of **8** and **11** by introducing a hexyl group at position 1 or 7. The 1-hexyl derivatives of **8** and **11** (**9**, **12**) were synthesized from (−)-indolactam-V (**1**) in four steps as shown in Scheme 1. After protection of the hydroxyl group of **1** with a *tert*-butyldimethylsilyl (TBDMS) group (83%), a hexyl group was introduced at position 1 by S_N2 reaction of **14** with 1-iodohexane (79%). The indole ring of **15** was reduced with sodium cyanoborohydride followed by removal of the TBDMS group with tetrabutylammonium fluoride (TBAF) to give (3*R*)-1-hexylindolinelactam-V (**9**, 57%) and its (3*S*)-isomer (**12**, 11%). Synthesis of the 7-hexyl derivatives (**10**, **13**) is shown in Scheme 2. 7-Hexylindolactam-V (**3**)[25] was synthesized in three steps (14% from **1**) according to our previously reported method.[24] Hydride reduction of **3** was then carried out to give the desired two diastereomers (15% for **10**, 23% for **13**). Proton NMR spectroscopy showed that each of the 1- and 7-hexyl derivatives of **8** and **11** existed as a single conformer in $CDCl_3$ at room temperature and at −40 °C. Conformer analysis similar to that mentioned above indicated that the conformations of **9** and **10** were almost the same as the twist-like form of **8**. On the other hand, the calculated conformation of **12** and **13** was the sofa-like form similar to that of **11**. These results indicate that introduction of the hexyl group at position 1 or 7 does not influence the conformations of **8** and **11**.

Recent investigations suggest that the C1A domain of conventional PKCs (α, β, γ) is mainly involved in phorbol ester binding and translocation from the cytosol to plasma membrane,[26,27] whereas the C1B domain of novel PKCs (δ, ϵ, η, θ) plays a predominant role in translocation in response to TPA.[28] Our binding study using PKC C1 peptides also supports these results; the major binding site

Table 3. K_i Values for inhibition of the specific binding of [^{3}H]PDBu by 1-hexyl derivatives

PKC C1 peptide	K_i (nM)		
	(−)-1-Hexylindolactam-V (**2**)	(3*R*)-1-Hexylindolinelactam-V (**9**)	(3*S*)-1-Hexylindolinelactam-V (**12**)
Conventional PKC			
α-C1A (72-mer)	5.8 (1.1)[a]	170 (25)	550 (44)
α-C1A (72-mer)	9.8 (1.6)	240 (14)	1200 (27)
γ-C1A	18 (2.4)	570 (90)	1800 (290)
Novel PKC			
δ-C1B	0.22 (0.04)	4.7 (0.5)	16 (1.5)
ϵ-C1B	0.47 (0.12)	7.0 (0.8)	14 (0.9)
η-C1B	0.34 (0.11)	4.9 (0.8)	12 (2.0)
θ-C1B	1.41 (0.03)	7.0 (0.6)	12 (1.3)

[a] Standard deviation of at least two separate experiments.

Table 4. K_i Values for inhibition of the specific binding of [^{3}H]PDBu by 7-hexyl derivatives

PKC C1 peptide	K_i (nM)		
	(−)-7-Hexylindolactam-V (**3**)	(3*R*)-7-Hexylindolinelactam-V (**10**)	(3*S*)-7-Hexylindolinelactam-V (**13**)
Conventional PKC			
α-C1A (72-mer)	1.2 (0.1)[a]	15 (1.2)	65 (14)
β-C1A (72-mer)	2.5 (0.1)	35 (5.4)	91 (17)
γ-C1A	2.6 (0.2)	89 (12)	136 (29)
Novel PKC			
δ-C1B	0.21 (0.02)	4.7 (0.2)	12 (0.5)
ϵ-C1B	0.36 (0.07)	7.0 (0.8)	13 (1.3)
η-C1B	0.18 (0.05)	2.9 (0.3)	13 (3.1)
θ-C1B	0.59 (0.05)	6.1 (0.9)	13 (1.4)

[a] Standard deviation of at least two separate experiments.

of (−)-indolactam-V (**1**) is the C1A domain for conventional PKCs and the C1B domain for novel PKCs.[14] Thus, binding affinities of **9**, **10**, **12** and **13**, along with (−)-1- and (−)-7-hexylindolactam-Vs (**2**, **3**), were evaluated for C1A peptides of conventional PKCs and C1B peptides of novel PKCs (Tables 3 and 4). The binding affinities of 7-hexyl derivatives (**3**, **10**, **13**) for all PKC C1 peptides dramatically increased compared with those of the corresponding core compounds (**1**, **8**, **11**). Unexpectedly, the selectivity of **10** for novel PKCs was lower than that of **8**, and **13** did not show significant selectivity, regardless of its sofa-like conformation. This conformation is similar to **5**, which showed increased selectivity for novel PKCs. In contrast to the 7-hexyl derivatives, the selectivity for novel PKCs was improved in the 1-hexyl derivatives. These derivatives (**2**, **9**, **12**) showed lower binding affinities for conventional PKCs compared with the corresponding 7-hexyl derivatives (**3**, **10**, **13**), but similar binding affinities for novel PKCs. These results suggest that for indolactam derivatives the position of the hydrophobic chain is more important than the conformation for exhibiting novel PKC selectivity. However, **12**, which has a sofa-like conformation, showed the highest selectivity for novel PKC C1B peptides; the binding affinities of **12** for PKCη- and θ-C1B peptides were approximately 50-fold and more than 100-fold higher than those for C1A peptides of PKCα, β and γ, respectively. Since the sofa-restricted form of **1** (**5**) bound selectively to novel PKCs, sofa analogues of **1** with a hydrophobic chain at an appropriate position may be promising agents that exhibit high selectivity not only for novel PKCs but also among novel PKCs.

3. Conclusions

We have synthesized (3*R*)- and (3*S*)-indolinelactam-Vs (**8**, **11**) along with their hexyl derivatives (**9**, **10**, **12**, **13**) as new conformationally restricted analogues of (−)-indolactam-V (**1**) in order to find new lead compounds with a high selectivity for novel PKC isozymes. (3*R*)-Indolinelactam-Vs (**8**–**10**) adopted a conformation similar to the twist form of **1** with a *cis* amide, and the conformation of the (3*S*)-isomers (**11**–**13**) was close to that of the sofa form with a *trans* amide. Although the binding affinities of **8** and **11** to PKC C1 peptides were far less than those of **1**, the introduction of a hexyl group at position 1 or 7 resulted in PKC binding affinities comparable to those of **1**. Corresponding to the structure–activity studies of **1**,[24] 7-hexyl derivatives (**10**, **13**) bound to conventional PKCs (α, β, γ) more strongly than 1-hexyl derivatives (**9**, **12**) probably due to steric hindrance between the hexyl group at position 1 and conventional PKCs. However, a similar effect was not observed in novel PKCs (δ, ϵ, η, θ); the binding affinities of 1- and 7-hexyl derivatives of **8** and **11** for novel PKC C1B peptides were similar to each other. (3*S*)-1-Hexylindolinelactam-V (**12**), with a sofa-like conformation, exhibited about 50–300 fold greater selectivity for C1B domains of novel PKCs than for C1A domains of conventional PKCs, indicating that sofa-restricted analogues of **1** with a hydrophobic chain at an appropriate position, such as **5** and **12**, would be likely lead compounds for the rational design of novel PKC selective modulators. The present results provide a basis for the synthesis and exploitation of such compounds as medicinal agents.

4. Experimental

4.1. General remarks

The following spectroscopic and analytical instruments were used: UV, Shimadzu UV-2200A; Digital Polarimeter, Jasco DIP-1000; ^{1}H NMR, Bruker ARX500 (ref. TMS); HPLC, Waters Model 600E with Model 2487 UV detector; (HR) EI-MS, JOEL JMS-600H. HPLC was carried out on a YMC packed SH-342-5 (ODS, 20 mm i.d. ×250 mm) column (Yamamura Chemical Laboratory). Wako C-200 gel (silica gel, Wako Pure Chemical Industries) and YMC A60-350/250 gel (ODS, Yamamura Chemical Laboratory) were used for column chromatography. [^{3}H]PDBu (17.0 Ci/mol) was purchased from PerkinElmer Life Sciences Research Products. All other chemicals and reagents were purchased from chemical companies and used without further purification.

4.1.1. Synthesis of (3*R*)- and (3*S*)-indolinelactam-Vs (8, 11). To a solution of (−)-indolactam-V (**1**, 48.8 mg, 162 μmol) in acetic acid (1 ml) was added $NaCNBH_3$ (25 mg, 397 μmol) at room temperature. After stirring for 1.5 h, another $NaCNBH_3$ (25 mg, 397 μmol) was added and the reaction mixture was stirred for another 2.5 h. The reaction was quenched by the addition of H_2O (1 ml) and the mixture was poured into saturated $NaHCO_3$ aq (20 ml), followed by extraction with EtOAc. The EtOAc layer was

washed with brine, dried over Na_2SO_4 and concentrated. The residue was purified by HPLC on YMC SH-342-5 using 25% CH_3CN to give **8** (15.1 mg, 50 μmol, 31%) and **11** (9.6 mg, 32 μmol, 20%). Compound **8**: $[\alpha]_D$ −478.0° (*c*=0.700, MeOH, 302.5 K); UV λ_{max} (MeOH) nm (ϵ): 303 (2000), 238 (24,000); ^{13}C NMR δ ($CDCl_3$, 0.079 M, 500 MHz, 300 K) ppm: 19.65, 21.85, 30.50, 34.87, 39.30, 40.12, 52.87, 53.95, 66.25, 68.16, 102.02, 107.87, 117.97, 129.23, 150.85, 152.83, 175.70; HR-EI-MS *m*/*z*: 303.1937 (M^+, calcd for $C_{17}H_{25}N_3O_2$, 303.1947). Compound **11**: $[\alpha]_D$ +146.0° (*c*=0.477, MeOH, 300.2 K); UV λ_{max} (MeOH) nm (ϵ): 298 (2600), 244 (9500); ^{13}C NMR δ ($CDCl_3$, 0.046 M, 500 MHz, 300 K) ppm: 19.06, 19.87, 24.11, 34.77, 40.29, 40.58, 54.43, 57.22, 66.11, 76.10, 106.68, 119.35, 129.04, 130.39, 150.87, 152.46, 170.88; HR-EI-MS *m*/*z*: 303.1918 (M^+, calcd for $C_{17}H_{25}N_3O_2$, 303.1947).

4.1.2. Synthesis of (3*R*)- and (3*S*)-1-hexylindolinelactam-Vs (9, 12). To a mixture of (−)-indolactam-V (**1**, 44.0 mg, 146 μmol) and imidazole (30.0 mg, 441 μmol) in dry DMF (0.5 ml) was added TBDMS-Cl (24.1 mg, 160 μmol) at 0 °C. After stirring for 1 h at 0 °C, the reaction mixture was poured into H_2O and extracted with EtOAc. The EtOAc layer was washed with brine, dried over Na_2SO_4 and concentrated. The residue was purified by column chromatography on Wako gel C-200 using hexane and increasing amounts of EtOAc to give **14** (50.3 mg, 121 μmol, 83%).

NaH in oil (11.6 mg, 290 μmol) was washed with hexane and suspended in dry DMF (0.5 ml) under an Ar atmosphere To this suspension was added **14** (50.3 mg, 121 μmol) in dry DMF (0.5 ml) at 0 °C. After stirring for 10 min, 1-iodohexane (21.4 μl, 145 μmol) was added dropwise and the reaction mixture was stirred for 1 h at 0 °C. The mixture was poured into H_2O (20 ml) and extracted with EtOAc. The EtOAc layer was washed with brine, dried over Na_2SO_4 and concentrated. The residue was purified by column chromatography on Wako gel C-200 using hexane and increasing amounts of EtOAc to give **15** (47.4 mg, 95 μmol, 79%). Compound **15**: $[\alpha]_D$ −107.0° (*c*=0.188, MeOH, 298.3 K); UV λ_{max} (MeOH) nm (ϵ): 307 (8200), 230 (25,000); ^1H NMR δ ($CDCl_3$, 0.068 M, 500 MHz, 300 K, twist:sofa=3.3:1) ppm for twist conformer: 0.03 (3H, s), 0.05 (3H, s), 0.63 (3H, d, *J*=6.8 Hz), 0.87 (9H, s), 0.88 (3H, t, *J*=7.0 Hz), 0.92 (3H, d, *J*=6.4 Hz), 1.30–1.36 (6H, m), 1.81 (2H, m), 2.61 (1H, m), 2.87 (1H, dd, *J*=17.4, 3.5 Hz), 2.91 (3H, s), 3.14 (1H, d, *J*=17.4 Hz), 3.45 (1H, dd, *J*=10.1, 9.8 Hz), 3.63 (1H, dd, *J*=10.1, 4.3 Hz), 3.98 (2H, t, *J*=7.4 Hz), 4.21 (1H, m), 4.38 (1H, d, *J*=10.2 Hz), 6.16 (1H, br.s), 6.49 (1H, d, *J*=7.9 Hz), 6.76 (1H, s), 6.84 (1H, *J*=7.9 Hz), 7.07 (1H, t, *J*=7.1 Hz); HR-EI-MS *m*/*z*: 499.3574 (M^+, calcd for $C_{29}H_{49}N_3O_2Si$, 499.3594).

To a solution of **15** (39.1 mg, 78 μmol) in acetic acid (0.5 ml) was added $NaCNBH_3$ (9.0 mg, 140 μmol) at room temperature. After stirring for 1.5 h additional $NaCNBH_3$ (9.0 mg, 140 μmol) was added and the reaction mixture was stirred for another 2.5 h. The reaction was quenched by the addition of H_2O (1 ml) and the mixture was poured into saturated $NaHCO_3$ aq (20 ml) and extracted with EtOAc. The EtOAc layer was washed with brine, dried over Na_2SO_4 and concentrated. The residue was purified by column chromatography on Wako gel C-200 using hexane and increasing amounts of EtOAc to give **16** (28.5 mg, 56.9 μmol, 73%) as a mixture of two diastereomers.

TBAF·$5H_2O$ (108 mg, 338 μmol) was added to **16** (28.5 mg, 56.9 μmol) in THF (1.4 ml) at 0 °C. After stirring for 40 min at 0 °C, the reaction mixture was poured into 5% $KHSO_4$ aq and extracted with EtOAc. The EtOAc layer was washed with brine, dried over Na_2SO_4 and concentrated. The residue was purified by HPLC on YMC SH-342-5 using 80% MeOH to give **9** (11.7 mg, 30.2 μmol, 53%) and **12** (2.5 mg, 6.5 μmol, 11%). Compound **9**: $[\alpha]_D$ −435.0° (*c*=0.435, MeOH, 301.2 K); UV λ_{max} (MeOH) nm (ϵ): 310 (2500), 246 (30,000); ^1H NMR δ ($CDCl_3$, 0.060 M, 500 MHz, 300 K) ppm: 0.90 (3H, t, *J*=6.8 Hz), 0.91 (3H, d, *J*=6.8 Hz), 1.10 (3H, d, *J*=6.4 Hz), 1.34–1.37 (6H, m), 1.55 (2H, m), 1.63 (1H, t, *J*=12.2 Hz), 1.92 (1H, dt, *J*=12.2, 4.6 Hz), 2.43 (1H, m), 2.83 (3H, s), 2.88 (1H, m), 3.13 (1H, d, *J*=8.6 Hz), 3.23 (1H, m), 3.43 (1H, t, *J*=8.6 Hz), 3.44 (1H, m), 3.50 (1H, t, *J*=6.0 Hz), 3.65 (1H, m), 3.73 (1H, m), 4.02 (1H, m), 4.36 (1H, d, *J*=8.4 Hz), 6.05 (1H, d, *J*=8.0 Hz), 6.17 (1H, d, *J*=8.0 Hz), 7.02 (1H, t, *J*=8.0 Hz), 7.41 (1H, d, *J*=6.4 Hz); ^{13}C NMR δ ($CDCl_3$, 0.060 M, 125 MHz, 300 K) ppm: 14.07, 19.68, 21.84, 22.66, 26.85, 27.31, 30.60, 31.70, 35.03, 38.34, 39.52, 48.47, 54.00, 58.63, 66.25, 68.27, 99.45, 107.04, 118.06, 129.18, 150.64, 153.71, 175.92; HR-EI-MS *m*/*z*: 387.2884 (M^+, calcd for $C_{23}H_{37}N_3O_2$, 387.2886). Compound **12**: $[\alpha]_D$ +215.0° (*c*=0.052, MeOH, 300.8 K); UV λ_{max} (MeOH) nm (ϵ): 307 (2800), 259 (13,900); ^1H NMR δ ($CDCl_3$, 0.013 M, 500 MHz, 300 K) ppm: 0.90 (3H, t, *J*=6.6 Hz), 0.95 (3H, d, *J*=6.5 Hz), 1.14 (3H, d, *J*=6.7 Hz), 1.32–1.37 (6H, m), 1.56 (2H, m), 1.88 (1H, dd, *J*=14.1, 2.5 Hz), 2.03 (1H, q, *J*=13.2 Hz), 2.26 (1H, m), 2.62 (3H, s), 2.76 (1H, m), 3.11 (1H, d, *J*=10.7 Hz), 3.14 (3H, m), 3.22 (1H, m), 3.41 (1H, m), 3.58 (1H, m), 4.24 (1H, m), 4.85 (1H, br.s), 6.29 (1H, d, *J*=7.8 Hz), 6.44 (1H, d, *J*=7.8 Hz), 7.06 (1H, t, *J*=7.8 Hz); ^{13}C NMR δ ($CDCl_3$, 0.013 M, 125 MHz, 300 K) ppm: 14.06, 19.07, 19.85, 22.63, 24.15, 26.91, 27.16, 31.67, 34.88, 39.07, 41.05, 49.15, 54.83, 62.44, 66.30, 76.05, 104.25, 117.95, 129.13, 130.46, 150.51, 153.52, 171.33; HR-EI-MS *m*/*z*: 387.2868 (M^+, calcd for $C_{23}H_{37}N_3O_2$, 387.2886).

4.1.3. Synthesis of (3*R*)- and (3*S*)-7-hexylindolinelactam-Vs (10, 13). (−)-7-Hexylindolactam-V (**3**)[25] was treated in a manner similar to that described for the synthesis of **9** and **12** to give **10** (2.5 mg, 6.5 μmol, 15%) and **13** (3.8 mg, 9.8 μmol, 23%). Compound **10**: $[\alpha]_D$ −397.0° (*c*=0.165, MeOH, 299.4 K); UV λ_{max} (MeOH) nm (ϵ): 305 (3000), 237 (26,000); ^1H NMR δ ($CDCl_3$, 0.013 M, 500 MHz, 300 K) ppm: 0.89 (3H, t, *J*=6.8 Hz), 0.92 (3H, d, *J*=6.8 Hz), 1.10 (3H, d, *J*=6.4 Hz), 1.32 (4H, m), 1.37 (2H, m), 1.57 (2H, m), 1.70 (1H, t, *J*=12.2 Hz), 1.89 (1H, dt, *J*=12.2, 4.5 Hz), 2.36 (2H, t, *J*=7.8 Hz), 2.45 (1H, m), 2.84 (3H, s), 2.97 (1H, br.s), 3.22 (1H, d, *J*=8.9 Hz), 3.44 (1H, m), 3.58 (1H, br.s), 3.64 (1H, m), 3.78 (1H, t, *J*=8.9 Hz), 3.83 (1H, m), 4.04 (1H, m), 4.33 (1H, d, *J*=8.4 Hz), 6.22 (1H, d, *J*=8.2 Hz), 6.84 (1H, d, *J*=8.2 Hz), 6.97 (1H, d, *J*=6.5 Hz); ^{13}C NMR δ ($CDCl_3$, 0.013 M, 125 MHz, 300 K) ppm: 14.12, 19.72, 21.83, 22.67, 29.07, 29.46, 30.67, 30.81, 31.77, 35.07, 39.47, 40.14, 52.88, 53.81, 66.31, 68.26, 108.08, 116.07, 118.11, 128.58, 148.80, 150.55, 175.71; HR-EI-MS *m*/*z*: 387.2889 (M^+, calcd for $C_{23}H_{37}N_3O_2$,

387.2886). Compound **13**: $[\alpha]_D$ +114.0° (c=0.151, MeOH, 300.4 K); UV λ_{max} (MeOH) nm (ϵ): 298 (3300), 243 (9700); ^{1}H NMR δ ($CDCl_3$, 0.020 M, 500 MHz, 300 K) ppm: 0.89 (3H, t, J=6.8 Hz), 0.94 (3H, d, J=6.5 Hz), 1.14 (3H, d, J=6.7 Hz), 1.32 (4H, m), 1.36 (2H, m), 1.56 (2H, m), 1.89 (1H, dd, J=13.2, 2.2 Hz), 2.06 (1H, q, J=13.2 Hz), 2.24 (1H, m), 2.40 (2H, t, J=7.8 Hz), 2.62 (3H, s), 3.06 (1H, d, J=10.6 Hz), 3.18 (1H, m), 3.25 (1H, d, J=8.3 Hz), 3.42 (1H, m), 3.52 (1H, t, J=7.4 Hz), 3.58 (1H, m), 3.60 (1H, br.s), 4.25 (1H, m), 4.62 (1H, br.s), 6.49 (1H, d, J=8.0 Hz), 6.87 (1H, d, J=8.0 Hz); ^{13}C NMR δ ($CDCl_3$, 0.020 M, 125 MHz, 300 K) ppm: 14.11, 19.08, 19.85, 22.65, 24.16, 29.01, 29.36, 30.91, 31.74, 34.82, 40.59 (two carbon signals overlapped), 54.55, 57.17, 66.24, 76.25, 119.18, 120.89, 128.89, 129.81, 148.43, 150.04, 171.10; HR-EI-MS m/z: 387.2884 (M^+, calcd for $C_{23}H_{37}N_3O_2$, 387.2886).

4.2. Conformer analysis

The most stable conformations of indolinelactam-Vs (**8**–**13**) were estimated by the Chem 3D (Cambridge Soft) and AMOSS-H11 (NEC quantum chemistry group) programs. The initial structures were calculated by molecular mechanics calculation using MM2 theory with the distance between two protons (H-3 and H-12, and H-9 and H-18 for **8**–**10**, H-3 and H-9 protons, H-3 and H-18 protons and H-10 and H-12 protons for **11**–**13**) fixed at 2 Å congruent with NOE data. The resultant structures were optimized by a semiempirical quantum mechanics calculation using PM3 theory. Further optimization of these calculated structures was carried out by ab initio molecular orbital schemes using a Hartree–Fock theory with the 6-31G* basis set to give the most stable conformers.

4.3. Inhibition of specific [^{3}H]PDBu binding to PKC isozyme C1 peptides

The [^{3}H]PDBu binding to the PKC isozyme C1 peptides was evaluated using the procedure of Sharkey and Blumberg[23] with modifications as reported previously[11] under the following conditions: 50 mM Tris–maleate buffer (pH 7.4 at 4 °C), 5–20 nM a PKC isozyme C1 peptide, 20–40 nM [^{3}H]PDBu (17.0 Ci/mmol), 50 μg/ml 1,2-di(*cis*-9-octadecenoyl)-*sn*-glycero-3-phospho-L-serine, 3 mg/ml bovine γ-globulin, and various concentrations of an inhibitor. Binding affinity was evaluated by the concentration required to cause 50% inhibition of the specific [^{3}H]PDBu binding, IC_{50}, which was calculated by a computer program (SAS) with a probit procedure. The binding constant, K_i, was calculated using the method of Sharkey and Blumberg.[23]

Acknowledgements

This work was partly supported by a Grant-in-Aid for Scientific Research on Priority Areas (2) (No. 13024245) (for K.I.) and Scientific Research (A) (2) (No. 15208012) (for H.O. and K.I.) from the Ministry of Education, Culture, Sports, Science and Technology, the Japanese Government, and from the Japan Society for the Promotion of Science for Young Scientists (Y.N.).

References and notes

1. Nishizuka, Y. *FASEB J.* **1995**, *9*, 484–496.
2. Ron, D.; Kazanietz, M. G. *FASEB J.* **1999**, *13*, 1658–1676.
3. Newton, A. C. *Chem. Rev.* **2001**, *101*, 2353–2364.
4. Hoppe, W.; Brandel, F.; Strell, I.; Röhrl, M.; Grassmann, J.; Hecker, E.; Bartsch, H.; Kreibich, G.; Szczepanski, C. *Angew. Chem.* **1967**, *79*, 824.
5. Fujiki, H.; Sugimura, T. *Adv. Cancer Res.* **1987**, *49*, 223–264.
6. Lu, Z.; Hornia, A.; Jiang, Y. W.; Zang, Q.; Ohno, S.; Foster, D. A. *Mol. Cell Biol.* **1997**, *17*, 3418–3428.
7. Reddig, P. J.; Dreckschimdt, N. E.; Ahrens, H.; Simsiman, R.; Tseng, C. P.; Zou, J.; Oberley, T. D.; Verma, A. K. *Cancer Res.* **1999**, *59*, 5710–5718.
8. Reddig, P. J.; Dreckschmidt, N. E.; Bourguignon, S. E.; Oberley, T. D.; Verma, A. K. *Cancer Res.* **2000**, *60*, 595–602.
9. Chida, K.; Hara, T.; Hirai, T.; Konishi, C.; Nakamura, K.; Nakao, K.; Aiba, A.; Katsuki, M.; Kuroki, T. *Cancer Res.* **2003**, *63*, 2404–2408.
10. Hunn, M.; Quest, A. F. G. *FEBS Lett.* **1997**, *400*, 226–232.
11. Shindo, M.; Irie, K.; Nakahara, A.; Ohigashi, H.; Konishi, H.; Kikkawa, U.; Fukuda, H.; Wender, P. A. *Bioorg. Med. Chem.* **2001**, *9*, 2073–2081.
12. Endo, Y.; Shudo, K.; Okamoto, T. *Chem. Pharm. Bull.* **1982**, *30*, 3457–3462.
13. Irie, K.; Hirota, M.; Hagiwara, N.; Koshimizu, K.; Hayashi, H.; Marao, S.; Tokuda, H.; Ito, Y. *Agric. Biol. Chem.* **1984**, *48*, 1269–1274.
14. Masuda, A.; Irie, K.; Nakagawa, Y.; Ohigashi, H. *Biosci. Biotechnol. Biochem.* **2002**, *66*, 1615–1617.
15. Endo, Y.; Shudo, K.; Itai, A.; Hasegawa, M.; Sakai, S. *Tetrahedron* **1986**, *42*, 5905–5924.
16. Irie, K.; Isaka, T.; Iwata, Y.; Yanai, Y.; Nakamura, Y.; Koizumi, F.; Ohigashi, H.; Wender, P. A.; Satomi, Y.; Nishino, H. *J. Am. Chem. Soc.* **1996**, *118*, 10733–10743.
17. Hagiwara, N.; Irie, K.; Koshimizu, K.; Hayashi, H.; Murao, S.; Tokuda, H.; Ito, Y. *Agric. Biol. Chem.* **1985**, *49*, 2529–2530.
18. Hagiwara, N.; Irie, K.; Funaki, A.; Hayashi, H.; Arai, M.; Koshimizu, K. *Agric. Biol. Chem.* **1988**, *52*, 641–648.
19. Hagiwara, N.; Irie, K.; Tokuda, H.; Koshimizu, K. *Carcinogenesis* **1987**, *8*, 963–965.
20. Irie, K.; Hagiwara, N.; Tokuda, H.; Koshimizu, K. *Carcinogenesis* **1987**, *8*, 547–552.
21. Gribble, G. W.; Lord, P. D.; Skotnick, J.; Dietz, S. E.; Eaton, J. T.; Johnson, J. L. *J. Am. Chem. Soc.* **1974**, *96*, 7812–7814.
22. Irie, K.; Oie, K.; Nakahara, A.; Yanai, Y.; Ohigashi, H.; Wender, P. A.; Fukuda, H.; Konishi, H.; Kikkawa, U. *J. Am. Chem. Soc.* **1998**, *120*, 9159–9167.
23. Sharkey, N. A.; Blumberg, P. M. *Cancer Res.* **1985**, *45*, 19–24.
24. Irie, K.; Koshimizu, K. *Memb. Colloid Agric. Kyoto Univ.* **1988**, *132*, 1–59.
25. Kozikowski, A. P.; Ma, D.; Du, L.; Lewin, N. E.; Blumberg, P. M. *J. Am. Chem. Soc.* **1995**, *117*, 6666–6672.
26. Raghunath, A.; Ling, M.; Larsson, C. *Biochem. J.* **2003**, *370*, 901–912.
27. Quest, A. F. G.; Bell, R. M. *J. Biol. Chem.* **2000**, *269*, 20000–20012.
28. Szallasi, Z.; Bögi, K.; Gohari, S.; Biro, T.; Acs, P.; Blumberg, P. M. *J. Biol. Chem.* **1996**, *271*, 18299–18301.

Available online at www.sciencedirect.com
SCIENCE DIRECT®
Tetrahedron 60 (2004) 7085–7091
Tetrahedron

RK-805, an endothelial-cell-growth inhibitor produced by *Neosartorya* sp., and a docking model with methionine aminopeptidase-2

Yukihiro Asami,[a,b] Hideaki Kakeya,[a,*] Rie Onose,[a] Yie-Hwa Chang,[c] Masakazu Toi[d] and Hiroyuki Osada[a,b,*]

[a]*Antibiotics Laboratory, Discovery Research Institute, RIKEN, 2-1 Hirosawa, Wako, Saitama 351-0198, Japan*
[b]*Graduate School of Science and Engineering, Saitama University, 255 Shimo-Okubo, Saitama, Saitama 338-8570, Japan*
[c]*Health Sciences Center, St. Louis University School of Medicine, 1402 S. Grand Blvd., St. Louis, MO 63104, USA*
[d]*Tokyo Metropolitan Komagome Hospital, 3-18-22 Honkomagome, Bunkyo-ku, Tokyo 113-8677, Japan*

Received 19 June 2003; revised 5 September 2003; accepted 5 September 2003

Available online 19 June 2004

Abstract—We found that a fungus *Neosartorya* sp. produced an angiogenesis inhibitor, RK-805. By spectroscopic analyses and semi-synthetic methods from fumagillin, the structure of RK-805 was identified as 6-oxo-6-deoxyfumagillol, which has not been reported as a natural product. RK-805 preferentially inhibited the growth of human umbilical vein endothelial cells (HUVECs) rather than that of human normal fibroblast in cell proliferation assays and blocked endothelial cell migration induced by vascular endothelial growth factor (VEGF). Moreover, RK-805 selectively inhibited methionine aminopeptidase-2 (MetAP2), but not methionine aminopeptidase-1 (MetAP1). The docked structure of RK-805 complexed with human MetAP2 indicated that not only a covalent bond between a nucleophilic imidazole nitrogen atom of His231 and the carbon of the reactive spirocyclic epoxide of RK-805, but also a hydrogen bond between NH (Asn329) and the carbonyl group of RK-805 at C-6 promote close contact in the binding pocket of the enzyme. Taken together, these results suggest that structure activity relationships of RK-805 derivatives at both C-4 and C-6, in comparison with ovalicin and TNP-470, would be useful for development of new angiogenesis inhibitors.

1. Introduction

Angiogenesis, the formation and growth of new blood capillaries from pre-existing vessels, is a vital function for the growth of normal tissues during embryogenesis, as well as for the malignant growth of solid tumors. The process of angiogenesis in endothelial cells consists of several distinct and sequential steps such as degradation of the basement membrane by proteolytic enzymes, migration (chemotaxis) toward the stimulus, proliferation, formation of vascular loops, maturation of neovessels, and neosynthesis of basement membrane constituents. Under pathological conditions, such as tumor progression, diabetic retinopathy, and rheumatoid arthritis, the control mechanisms can be disordered primarily by a number of angiogenic factors, and this process can lead to abnormal angiogenesis. The inhibition of angiogenesis is therefore emerging as a promising strategy to cure angiogenesis-related diseases.[1–4]

In this regard, several angiogenesis inhibitors derived both from natural products and by chemical synthesis have been studied. These include peptide inhibitors angiostatin,[5] endostatin,[6] and NK4,[7] as well as thalidomide,[8] TNP-470,[9] marimastat,[10] and SU6668,[11] which are small molecules. We have also established cell-based screening systems for identifying novel angiogenesis inhibitors blocking signaling pathway induced by vascular endothelial growth factor (VEGF) or exhibiting selective growth inhibitory activity in endothelial cells. Recently, we reported the identification of novel angiogenesis inhibitors, i.e. the highly functionalized pentaketide dimers epoxyquinols A and B,[12–15] and azaspirene[16,17] with a 1-oxa-7-azaspiro[4.4]non-2-ene-4,6-dione skeleton from fungal metabolites (Fig. 1).

In the course of our research to discover angiogenesis inhibitors among the secondary metabolites of microorganisms, RK-805 was discovered from the fermentation broth of a fungus, *Neosartorya* sp. The structure was elucidated as 6-oxo-6-deoxyfumagillol by spectroscopic analyses and chemical modifications of fumagillin. It is noted that RK-805 might be a precursor metabolite or be a shunt

Keywords: Angiogenesis inhibitor; Microbial metabolites; Endothelial cells; Methionine aminopeptidase-2; docking model.
* Corresponding authors. Tel.: +81-48-467-9542; fax: +81-48-462-4669; e-mail address: hkakeya@riken.jp

0040–4020/$ - see front matter © 2004 Elsevier Ltd. All rights reserved.
doi:10.1016/j.tet.2003.09.104

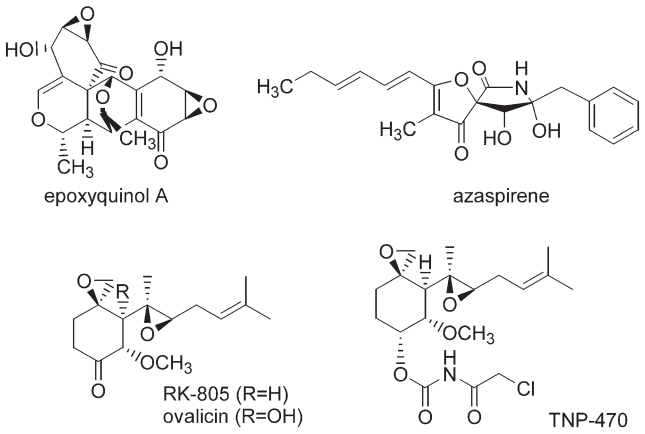

Figure 1. Structures of epoxyquinol A, azaspirene, RK-805, ovalicin, and TNP-470.

metabolite in fumagillin-biosynthesis. We describe in this paper the fermentation, isolation, structure elucidation, and the specificity and effects of RK-805 toward methionine aminopeptidase-2 (MetAP2) as well as growth and migration of endothelial cells.

2. Results and discussion

The producing strain, *Neosartorya* sp. was cultured in the fermantation medium (15 l) at 28 °C for 3 days, and the ethyl acetate extract of the whole broth was obtained. Then, the successive purification procedures by a silica gel column chromatography, a preparative reverse-phase HPLC, and a preparative TLC afforded 5.0 mg of RK-805 as a colorless oil. The molecular formula of RK-805 was determined to be $C_{16}H_{24}O_4$, based on the HREI-MS data (*m/z*: 280.1723); this formula was supported by ^{1}H and ^{13}C NMR spectrum data. The UV spectrum had an end absorption and an absorption maximum of the IR spectrum at 1730 cm^{-1} suggested the presence of a carbonyl group.

All single-bond connections between ^{1}H and ^{13}C in RK-805 were elucidated by PFG-HMQC and DEPT experiments. The NMR data and the molecular formula indicated the presence of one methoxy, three methyls, four methylenes, three sp^3 methines and one sp^2 methine, and four quaternary carbons, including a carbonyl carbon. As regards the ^{1}H–^{1}H correlations in PFG-DQFCOSY, H-11 through H-13 indicated the presence of olefinic protons and an epoxide methine (Fig. 2(A)). In addition, long range couplings from H-11 and H-15 to C-10 and from H-16 and H-17 to C-13 and C-14 were observed in an HMBC experiment (Fig. 2(A)). The cyclohexanone skeleton was confirmed by ^{1}H–^{1}H correlations on PFG-DQFCOSY: from H-4 to H-5 and H_2-7 to H_2-8, as well as by ^{1}H–^{13}C correlations in the PFG-HMBC spectra: the strong two-and three-bond ^{1}H–^{13}C correlations from H-4 and H-8 to C-3, from H-18 of the methoxy proton signal to C-5, and the correlations of the carbonyl carbon at C-6 with the protons on C-4, C-5, C-7, and C-8. The exocyclic epoxide ring on cyclohexanone was confirmed by the chemical shifts, coupling constants, and two-bond correlations from H-2 to C-3 in the PFG-HMBC spectrum. The relative configuration of RK-805 was elucidated by NOE experiments. Significant NOEs between

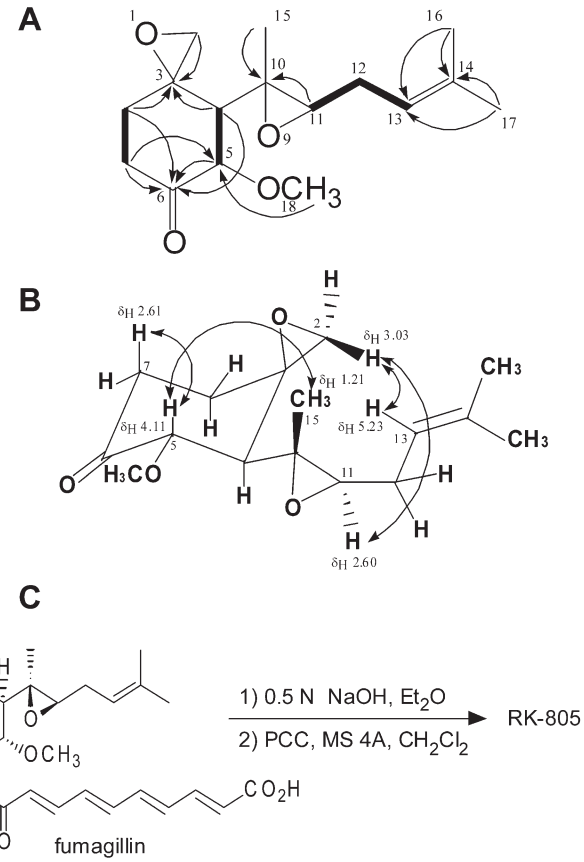

Figure 2. Structure determination of RK-805. (A) Key correlations in PFG-DQFCOSY and PFG-HMBC spectra in RK-805. The bold lines show the proton spin networks, and the arrows show the ^{1}H–^{13}C long-range correlations. (B) Summary of the NOE spectra. The arrows point to significant NOEs.

H-15 (δ_H 1.21) and H-5 (δ_H 4.11), H-13 (δ_H 5.23) and H-2 (δ_H 3.03), and H-11 (δ_H 2.60) and H-2 (δ_H 3.03) indicated a *trans* configuration for the epoxide on the side chain at C-4. The experimental results showed that no NOE was observed between H-15 (δ_H 1.21) and H-11 (δ_H 2.60), thereby also supporting this configuration. The NOE between H-5 (δ_H 4.11) and H-7 (δ_H 2.61) indicated a diaxial conformation for these protons (Fig. 2(B)). Moreover, the deduced structure was confirmed by chemical modifications from fumagillin: Hydolysis of fumagillin in the alkali condition, followed by oxidation with PCC to give synthetic RK-805 in 82% yield over two steps (Fig. 2(C)). The physico-chemical properties of natural RK-805 were identical with those of synthetic RK-805. Thus, the structure of RK-805 including its absolute configuration was determined to be 6-oxo-6-deoxyfumagillol, which has reported as a synthetic analogue of fumagillin and ovalicin.[18,19] The ^{1}H and ^{13}C NMR assignments for RK-805 are summarized in Section 4. It is possible that RK-805 is a precursor metabolite or is a shunt metabolite in fumagillin-biosynthesis, as fumagillin possesses a long aliphatic side chain at C-6 via an ester bond.

The core structure of RK-805 was similar to that of fumagillin and other fumagillin analogues, e.g. ovalicin[20] isolated from marine fungal metabolites and its synthetic analogue TNP-470 (*O*-(chloroacetylcarbamoyl)fumagillol, AGM-1470).[21] The structure of RK-805 is different from the structure of ovalicin and TNP-470 as regards the C-4 and

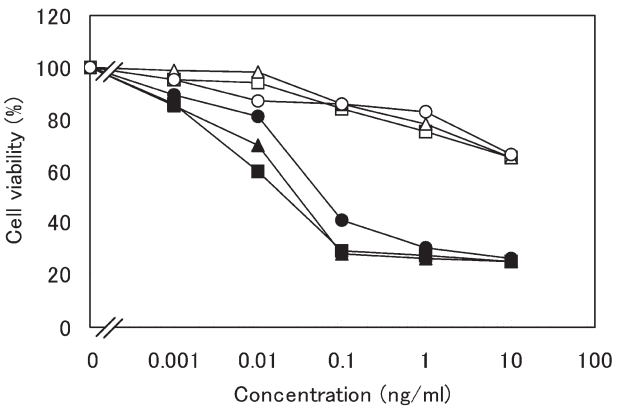

Figure 3. RK-805 effectively inhibits the growth of HUVECs. The growth of HUVECs: ■, Ovalicin (IC_{50}=0.02 ng/ml); ▲, RK-805 (IC_{50}=0.03 ng/ml); ●, TNP-470 (IC_{50}=0.06 ng/ml). The growth of WI-38 cells: □, Ovalicin ($IC_{50}\geq$10 ng/ml); △, RK-805 ($IC_{50}\geq$10 ng/ml); ○, TNP-470 ($IC_{50}\geq$10 ng/ml).

C-6 positions, respectively. Although the growth inhibitory activity by fumagillin-related compounds against human endothelial cells has been reported, little is known about their effects on the growth of human normal fibroblast. We therefore tested the inhibitory activity of RK-805 in both human umbilical vein endothelial cells (HUVECs) and normal human lung fibroblast WI-38 cells. RK-805, ovalicin, and TNP-470 did not exhibit remarkable inhibitory activity, even at 10 ng/ml, in WI-38 cells, whereas they did inhibit the cell growth of HUVECs in a dose-dependent manner, as shown in Figure 3. The IC_{50} values of RK-805, ovalicin, and TNP-470 were 0.03, 0.02, and 0.06 ng/ml, respectively, indicating that RK-805 exhibited selective inhibitory activity in HUVECs, as did both ovalicin and TNP-470.

We performed a chemotaxicell chamber assay, as there has been no report on the effect of RK-805 on endothelial cell migration in three-dimensional-cultutres systems of HUVECs. In this assay, HUVECs in the top chamber migrated and penetrated the filters, entering the lower chamber supplemented with 12.5 ng/ml of an angiogenic factor, VEGF-containing medium, as determined by counting the number of cells attached to the lower side of the filter after 18 h of incubation. VEGF significantly induced cell migration, whereas 10 μM of SU5614, an inhibitor of VEGF receptor tyrosine kinase,[22] inhibited the VEGF-induced cell migration. RK-805 also inhibited the cell migration induced by VEGF in a dose-dependent manner, without showing significant cell toxicity; this results was estimated by a trypan blue dye exclusion assay. The ED_{50} value of RK-805 was ca. 10 ng/ml, as shown in Figure 4. Ovalicin and TNP-470 exhibited almost the same inhibitory activity in this assay. These results suggest that RK-805 blocks the function of endothelial cell migration activated by VEGF.

Methionine aminopeptidase-2 (MetAP2) has been identified as the molecular target for the fumagillin family.[23–25] However, the selectivity of RK-805 against MetAP2 has been unclear. We therefore investigated the selective inhibitory effect of RK-805 on MetAP2 activity on agar plates containing the *map1* null strain, *Saccharomyces cerevisiae* (*MAP1/map1::HIS3*). The map1 null strain and the map2 null strain (*MAP2/map2::URA3*) is viable with a slower growth rate, whereas the *map1* and *map2* double-null strain is nonviable.[26] Although wild-type and *map2* null mutant are resistant to RK-805, ovalicin, and TNP-470, the growth of the *map1* null mutant was completely inhibited by these three fumagillin-related molecules (Fig. 5(A)–(C)). The inhibitory activities of RK-805 and ovalicin on MetAP2 were more potent than that of TNP-470 (Fig. 5(D)). These results indicate that yeast MetAP2, but not MetAP1, is a common target for RK-805, ovalicin, and TNP-470.

MetAPs, cobalt-containing metalloproteases, which remove the NH_2-terminal methionine from proteins in a non-processive manner, are highly conserved in *Escherichia coli*, *Saccharomyces cerevisiae*, and humans.[27–29] In 1998, Clardy, J. et al. revealed a covalent bond between an epoxide group on the cyclohexane ring of fumagillin and a histidine residue (His-231) at the active site of the human

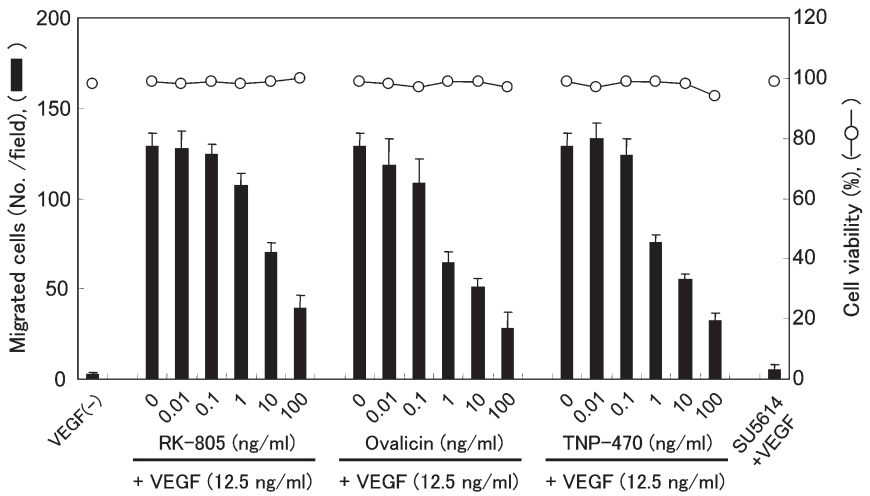

Figure 4. RK-805 blocks endothelial cell migration induced by VEGF. HUVECs stimulated upon VEGF-treatment were incubated with either various concentrations of RK-805, ovalicin, TNP-470, or 10 μM of SU5614 in the upper chamber for 18 h. Thereafter, the cells were fixed with MeOH and stained with Wright solution. The cells migrated to the lower surface, induced by VEGF, were counted manually under a microscope at a magnification of x100 (bold column). Values are the means±SD for triplicate samples. Cell viability was assessed by a trypan blue dye exclusion assay (bold line).

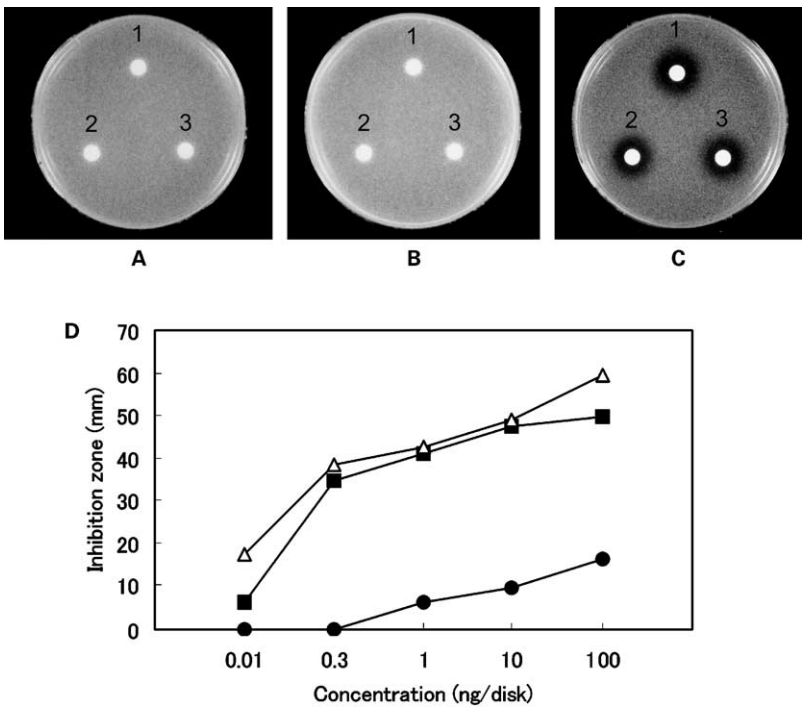

Figure 5. Selective MetAP2 inhibitory activity of RK-805. (A–C) Wild-type *Saccharomyces cerevisiae* W303 (A). *map2* null strain (*MAP2/map2::URA3*) (B). *map1* null strain (*MAP1/map1::HIS3*) (C). RK-805 (**1**, 0.3 ng/disk), Ovalicin (**2**, 0.3 ng/disk), and TNP-470 (**3**, 30 ng/disk). (D) Determination of respective MetAP2 inhibitory activities of the compounds using agar diffusion assays on the MetAP1 null strain (MAP1/map1::HIS3). △: RK-805, ■: ovalicin, ●: TNP-470.

MetAP2 crystal structure.[30] We investigated a three-dimensional model of human MetAP2 and RK-805 built from the known X-ray coordinates (PDB ID: 1B59) using a COMTEC 4D OCTANE 2, R12000A Workstation and Insight II. The predicted overall structure of RK-805 complexed with human MetAP2 is shown in Figure 6. The docked structure indicated that not only a covalent bond between an imidazole nitrogen atom of His231 and a carbon of the spirocyclic epoxide of RK-805, but also a hydrogen bond between NH (Asn329) and a carbonyl group of RK-805 promoted close contact to fit well in the binding pocket of the enzyme, even though RK-805 lacks the aliphatic side chain at C-6 of fumagillin and a hydroxyl group at the C-4 of ovalicin.

The development of angiogenesis inhibitors as novel anticancer agents has been one of the most challenging objectives of contemporary cancer research. Among several angiogenesis inhibitors characterized within the last decade, TNP-470, a synthetic analogue of fumagillin, is currently in clinical trials for the treatment of a variety of cancers, including solid tumors as well as Kaposi's sarcoma.[31,32] The fumagillin family has been shown to block endothelial cell proliferation and cell cycle progression of cells in the G1

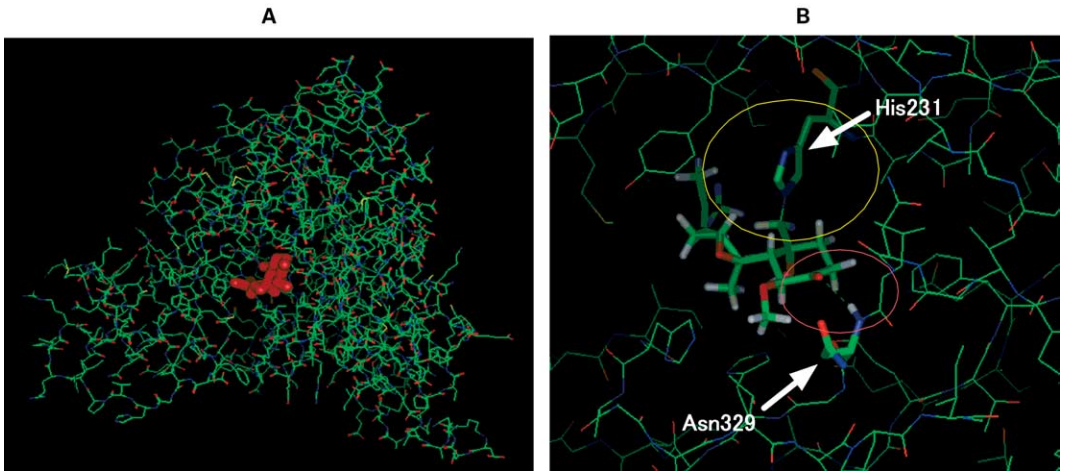

Figure 6. Proposed binding image of RK-805 complexed with human MetAP2. (A) Overall structure of the complex between MetAP-2 (PDB ID: 1B59) and RK-805. In the stick model, red indicates the atoms of RK-805 molecules in the active site. (B) A covalent bond is shown between an imidazole nitrogen atom of His231 and the carbon of the spirocyclic epoxide (yellow ring). The hydrogen bond between NH (Asn329) and the carbonyl group of RK-805 is shown (red ring). Carbon atoms are green, oxygen atoms are red, hydrogen atoms are white, and nitrogen atoms are blue.

phase.[9,33,34] Although MetAP2 has been identified as a molecular target of these compounds, it remains unclear how inhibition of this enzyme leads to cell cycle arrest, antiangiogenic activity, and in vivo antitumor effects. There could be a vital MetAP2-specific intracellular substrate that is sensitive to fumagillin-type drugs including RK-805. Turk, B. E. et al. reported that the in vitro inhibitory activity of RK-805 against MetAP2 activity was 15-fold and 6-fold less than that of ovalicin and TNP-470, respectively.[19] However, the potency of RK-805 and ovalicin in the endothelial assays (Figs. 3 and 4) and the yeast growth inhibition assay (Fig. 5) here is almost the same, suggesting that those compounds have different rates of cellular uptake and metabolism in intact cells. In addition, preliminary pharmacokinetic and metabolic experiments have indicated that TNP-470 was biotransformed in the primary cultures of human hepatocytes and in the microsomal fractions of various human tissues.[35] These finding have increased the hope of identifying a more stable analogue of fumagillin-type molecules. Therefore, structure activity relationships of analogues of RK-805 at both C-4 and C-6 would be useful for development of new MetAP2 inhibitors. Moreover, the potential therapeutic value of angiogenesis inhibitors has also been evaluated in combination with different anticancer modalities including chemotherapeutic agents, cytokines, and radiotherapy.[36] Thus, the identification of novel angiogenesis inhibitors would provide a range of tools that would be therapeutic in cases involving pathologic angiogenesis.

3. Conclusion

In conclusion, we identified RK-805, 6-oxo-6-deoxyfumagillol, as an angiogenesis inhibitor isolated from a fungus, *Neosartorya* sp., in an endothelial cell-based assay. RK-805 exhibited potent inhibitory activity not only as regards in endothelial cell growth, but also in VEGF-induced endothelial cell migration. In addition, RK-805 selectively inhibited MetAP2 activity, but not MetAP1 activity. The important aspect of the binding model of RK-805 with human MetAP2 was that a carbonyl group of RK-805 formed a hydrogen bond with NH (Asn329) at the active site of the enzyme, which was not seen in the case of fumagillin or TNP-470. RK-805 is a promising agent in this context; a structure-based drug design that would include a modification of this carbonyl group might shed light on the development of novel angiogenesis inhibitors. Further study of structure-activity relationships and novel bioactive natural products is currently underway.

4. Experimental

4.1. General

Optical rotation was recorded on a JASCO DIP-370 spectrometer and the IR spectra were obtained on a SHIMADZU FT-IR 8100M spectrophotometer. ^{1}H and ^{13}C NMR spectra were taken on a JEOL ECP-500 NMR spectrometer. The mass spectra were measured on a JEOL JMS-SX102. Chemical shifts are reported in parts per million relative to acetone (^{1}H, δ 2.04; ^{13}C, δ 29.8). Data for ^{1}H NMR are reported as follows: chemical shift, assignment, integration, multiplicity (s=singlet, d=doublet, t=triplet, q=quartet, m=multiplet), and coupling constants. Data for ^{13}C NMR are reported as follows: chemical shift, assignment, and multiplicity (s=singlet, d=doublet, t=triplet, q=quartet).

4.2. Fermentation and purification

The producing strain *Neosartorya* sp. was inoculated into two 500 ml Erlenmeyer flasks containing 75 ml of a sterile seed medium and was incubated on a rotary shaker at 28 °C for 3 days. The seed medium was composed of soluble starch 2%, glucose 1%, soybean meal 1.5%, malt extract 0.5%, potato dextrose 10%, vegetable extract 10%, $MgSO_4{\cdot}7H_2O$ 0.05%, and KH_2PO_4 0.05%. This seed medium (150 ml) was transferred to 15 l of the same production medium in a 30-L jar fermentor. The fermentation was carried out at 28 °C for 3 days with agitation at 350 rpm and an air flow of 15 l min^{-1}. The culture broth was centrifuged and the mycelial cake was extracted with acetone. The extract was concentrated in vacuo to an aqueous solution, which was extracted with an equal volume of ethyl acetate. The organic layer was concentrated in vacuo to dryness. The concentrate was applied to silica gel column chromatography. The materials were eluted with a stepwise gradient of $CHCl_3$–CH_3OH. The active fraction in $CHCl_3$–CH_3OH (50:1) was concentrated in vacuo to yield an oily material. Further purification of RK-805 was carried out by reverse-phase HPLC using a preparative ODS column (2 i.d.×25 cm, Senshu Scientific Co. Ltd., Tokyo, Japan). Finally, 5.0 mg of RK-805 was purified by preparative TLC with $CHCl_3$–CH_3OH (50:1).

4.3. Physico-chemical properties of RK-805

Colorless oil; HREI-MS *m/z*: 280.1723 (calcd for $C_{16}H_{24}O_4$: 280.1675); UV λ_{max} (MeOH) nm: End abs.; IR ν_{max} (neat) cm^{-1}: 2950, 1730, 1650, 1120; $[\alpha]_D^{20}=-61.3°$ (*c* 0.30, $CHCl_3$), lit.[18] $[\alpha]_D^{24}=-64.9°$ (*c* 0.21, $CHCl_3$); the R_f value in the solvent system of $CHCl_3$–MeOH (50:1) was 0.46 on a silica gel TLC (Merck 60 F_{254}). The *Rt* was 17.1 min in HPLC analysis: PEGASIL ODS (4.6 i.d. ×250 mm, Senshu Scientific Co. Ltd., Tokyo, Japan); flow rate, 1 ml/min; detection, 215 nm; mobile phase, a linear gradient solvent system CH_3CN–H_2O from 20:80 to 100:0 for 20 min. ^{1}H NMR (500 MHz, acetone-d_6) δ 1.21 (15-H, 3H, s), 1.64 (16-H, 3H, s), 1.66 (8-H_a, 1H, ddd, *J*=3.5, 5.3, 13.0 Hz), 1.72 (17-H, 3H, s), 1.88 (4-H, 1H, d, *J*=10.6 Hz), 2.08 (8-H_b, 1H, ddd, *J*=1.3, 5.3, 13.0 Hz), 2.23 (12-H, 2H, m), 2.36 (7-H_a, 1H, ddd, *J*=1.3, 5.3, 14.2 Hz), 2.60 (11-H, 1H, t, *J*=6.3 Hz), 2.61 (7-Hb, 1H, m), 2.72 (2-Ha, 1H, d, *J*=4.6 Hz), 3.03 (2-H_b, 1H, d, *J*=4.6 Hz), 3.38 (18-H, 3H, s), 4.11 (5-H, 1H, d, *J*=10.6 Hz), 5.23 (13-H, 1H, t, *J*=7.4 Hz); ^{13}C NMR (125 MHz, acetone-d_6) δ 14.35 (15-C, q), 17.98 (16-C, q), 25.80 (C-17, q), 28.14 (C-12, t), 33.58 (C-8, t), 37.39 (C-7, t), 52.35 (C-2, t), 53.89 (C-4, d), 57.89 (C-18, q), 59.19 (C-10, s), 59.29 (C-3, s), 60.60 (C-11, d), 83.84 (C-5, d), 120.10 (C-13, d), 134.79 (C-14, s), 207.28 (C-6, s).

4.4. Synthesis of RK-805

Fumagillin (0.9 mg, 0.0020 mmol) was added to a 0.5 N

NaOH–Et_2O solution (1 ml, v/v=1:1), and was stirred at room temperature for 2.5 h. Then, the reaction mixture was diluted with H_2O and Et_2O, and extracted with Et_2O. The resulting organic layer was washed with brine, dried over Na_2SO_4, and concentrated in vacuo to afford 0.54 mg (quant.) of fumagillol. To a suspension of PCC (1 mg, 0.0046 mmol) and powdered molecular sieves 4A (3.0 mg) in CH_2Cl_2 (1 ml) was added a solution of the above fumagillol solution in CH_2Cl_2 (0.5 ml) stirring in an ice-water bath. The mixture was stirred for 1 h at room temperature. Florisil and CH_2Cl_2 were added to the mixture, which was filtered through a pad of Celite and Florisil, and the filtrate was concentrated in vacuo. The residue was purified by preparative TLC with $CHCl_3$–CH_3OH (50:1) to give synthetic RK-805 (0.45 mg, 82.0% yield in two steps).

4.5. Endothelial cell proliferation assay

Human umbilical vein endothelial cells (HUVECs) were cultured in Humedia-EG2 medium (KURABO, Osaka, Japan) at 37 °C under a 5% CO_2 atmosphere. WI-38 cells (normal human lung fibroblast cells) were cultured in DMEM (Dulbecco's modified eagle medium) containing 10% fetal calf serum in a 5% CO_2 incubator at 37 °C. Sub-confluently growing (80%-90%) cells were trypsinized. HUVECs and WI-38 cells were seeded on 96-well microplates ($1.5–3.0\times10^3$ cells per well). Test compounds were added, and further incubated for 48 h (WI-38 cells) or 96 h (HUVECs). The cell number was evaluated by the subsequent color reaction. 2-(2-methoxy-4-nitrophenyl)-3-(4-nitrophenyl)-5-(2,4-disulfophenyl)-2*H*-tetrazolium, monosodium salt, WST-8™ (Nacalai Tesque, Kyoto, Japan) was added, and the cells were further incubated for 3–4 h at 37 °C. The absorbance (A_{450}) of each well was measured by a Wallac 1420 multilabel counter (Amersham Biosciences, Piscataway, NJ). Each result is the mean±S.D. (n=three experiments).

4.6. Endothelial cell migration assay

Human umbilical vein endothelial cells (HUVECs) (1×10^5 cells) suspended in Humedia-EG2 medium with various concentrations of test compounds were added to the upper compartment of a chemotaxicell chamber (KURABO, Osaka) and incubated with HuMedia-EG2 medium containing 12.5 ng/ml of VEGF in the lower compartment for 18 h at 37 °C in a 5% CO_2 atmosphere. The filter was fixed with MeOH and stained with Wright solution. The cells on the upper surface of the filter were removed by wiping the filter with cotton swabs. Cells that migrated through the filter to the lower surface were counted manually under a microscope at a magnification of ×100. Values are means±SD for triplicate samples. Cell viability was assessed by a trypan blue dye exclusion assay.

4.7. Yeast growth inhibition assay

Inhibition of MetAP2 activity was determined on an agar plate containing the *map1* null strain (*MAP1/map1::HIS3*), *Saccahromyces cerevisiae*.[25] Sterile filter disks impregnated with 10 μl of compounds were placed on the assay plate, and the plates were further incubated at 30 °C for 72 h. As references, wild-type strain *S. cerevisiae* W303 and the *map2* null strain (*MAP2/map2::URA3*) were also tested.[25]

4.8. Molecular modeling of RK-805 on MetAP2

The computer model of the binding image was constructed by means of a COMTEC 4D OCTANE 2, R12000A Workstation (Silicon Graphics, Inc., Mountain View, CA) and Insight II (Accelrys, Inc., San Diego, CA).

Acknowledgements

This work was supported in part by a Special Project Funding for Basic Science (Chemical Biology Research) from RIKEN, and a grant from the Ministry of Education, Culture, Sports, Science and Technology, Japan. We are grateful to Ishida, K. (RIKEN) for his valuable suggestions concerning the docking model.

References and notes

1. Kerbel, R.; Folkman, J. *Nat. Rev. Cancer* **2002**, *2*, 727–739.
2. Cristofanilli, M.; Charnsangavej, C.; Hortobagyi, G. N. *Nat. Rev. Drug Disc.* **2002**, *1*, 415–425.
3. Gasparini, G. *Drugs* **1998**, *58*, 17–38.
4. Shibuya, M. *Cell Struct. Funct.* **2001**, *26*, 25–35.
5. O'Reilly, M. S.; Holmgren, L.; Shing, U.; Chen, C.; Rosenthal, R. A.; Moses, M.; Lane, W. S.; Cao, Y.; Sage, E. H.; Folkman, J. *Cell* **1994**, *79*, 315–328.
6. O'Reilly, M. S.; Boehm, T.; Shing, Y.; Fukai, N.; Vasios, G.; Lane, W. S.; Flynn, E.; Birkhead, J. R.; Olsen, B. R.; Folkman, J. *Cell* **1997**, *88*, 277–285.
7. Nakabayashi, M.; Morishita, R.; Nakagami, H.; Kuba, K.; Matsumoto, K.; Nakamura, T.; Tano, Y.; Kaneda, Y. *Diabetologia* **2003**, *46*, 115–123.
8. D'Amato, R. J.; Loughnan, M. S.; Flynn, E.; Folkman, J. *Proc. Natl. Acad. Sci. U.S.A.* **1994**, *91*, 4082–4085.
9. Zhang, Y.; Griffith, E. C.; Sage, J.; Jacks, T.; Liu, J. O. *Proc. Natl. Acad. Sci. U.S.A.* **2000**, *97*, 6427–6432.
10. Jia, M. C.; Schwartz, M. A.; Sang, Q. A. *Adv. Exp. Med. Biol.* **2000**, *476*, 181–194.
11. Bergers, G.; Song, S.; Meyer-Morse, N.; Bergsland, E.; Hanahan, D. *J. Clin. Invest.* **2003**, *111*, 1287–1295.
12. Kakeya, H.; Onose, R.; Koshino, H.; Yoshida, A.; Kobayashi, K.; Kageyama, S.-I.; Osada, H. *J. Am. Chem. Soc.* **2002**, *124*, 3496–3497.
13. Kakeya, H.; Onose, R.; Yoshida, A.; Koshino, H.; Osada, H. *J. Antibiot.* **2002**, *55*, 829–831.
14. Shoji, M.; Yamaguchi, J.; Kakeya, H.; Osada, H.; Hayashi, Y. *Angew. Chem. Int. Ed.* **2002**, *41*, 3192–3194.
15. Shoji, M.; Kishida, S.; Takeda, M.; Kakeya, H.; Osada, H.; Hayashi, Y. *Tetrahedron Lett.* **2002**, *43*, 9155–9158.
16. Asami, Y.; Kakeya, H.; Onose, R.; Yoshida, A.; Matsuzaki, H.; Osada, H. *Org. Lett.* **2002**, *4*, 2845–2848.
17. Hayashi, Y.; Shoji, M.; Yamaguchi, J.; Sato, K.; Yamaguchi, S.; Mukaiyama, T.; Sakai, K.; Asami, Y.; Kakeya, H.; Osada, H. *J. Am. Chem. Soc.* **2002**, *124*, 12078–12079.
18. Marui, S.; Kishimoto, S. *Chem. Pharm. Bull.* **1992**, *40*, 575–579.

19. Turk, B. E.; Su, Z.; Liu, J. O. *Bioorg. Med. Chem.* **1998**, *6*, 1163–1169.
20. Bollinger, P.; Sigg, H. P.; Weber, H. P. *Helv. Chim. Acta* **1973**, *56*, 819–830.
21. Marui, S.; Itoh, F.; Kozai, Y.; Sudo, K.; Kishimoto, S. *Chem. Pharm. Bull.* **1992**, *40*, 96–101.
22. Sun, L.; Tran, N.; Tang, F.; App, H.; Hirth, P.; Mcmahon, G.; Tang, C. *J. Med. Chem.* **1998**, *41*, 2588–2603.
23. Griffith, E. C.; Su, Z.; Turk, B. E.; Chen, S.; Chang, Y.-H.; Wu, Z.; Biemann, K.; Liu, J. O. *Chem. Biol.* **1997**, *4*, 461–471.
24. Griffith, E. C.; Su, Z.; Niwayama, S.; Ramsay, C. A.; Chang, Y.-H.; Liu, J. O. *Proc. Natl. Acad. Sci. U.S.A.* **1998**, *95*, 15183–15188.
25. Sin, N.; Meng, L.; Wang, M. Q. W.; Wen, J. J.; Bornmann, W. G.; Crews, C. M. *Proc. Natl. Acad. Sci. U.S.A.* **1997**, *94*, 6099–6103.
26. Li, X.; Chang, Y.-H. *Proc. Natl. Acad. Sci. U.S.A.* **1995**, *92*, 12357–12361.
27. Ben-Bassat, A.; Bauer, K.; Chang, S.-Y.; Myambo, K.; Boosman, A.; Chang, S. *J. Bacteriol.* **1987**, *169*, 751–757.
28. Chang, Y.-H.; Teichert, U.; Smith, J. A. *J. Biol. Chem.* **1990**, *265*, 19892–19897.
29. Arfin, S. M.; Kendall, R. L.; Hall, L.; Weaver, L. H.; Stewart, A. E.; Matthews, B. W.; Bradshaw, R. A. *Proc. Natl. Acad. Sci. U.S.A.* **1995**, *92*, 7714–7718.
30. Liu, S.; Widom, J.; Kemp, C. W.; Crews, C. M.; Clardy, J. *Science* **1998**, *282*, 1324–1327.
31. Twardowski, P.; Gradishar, W. J. *Curr. Opin. Oncol.* **1997**, *9*, 584–589.
32. Figg, W. D.; Kruger, E. A.; Price, D. K.; Kim, S.; Dahut, W. D. *Invest. New Drugs* **2002**, *20*, 183–194.
33. Turk, B. E.; Griffith, E. C.; Wolf, S.; Biemann, K.; Chang, Y.-H.; Liu, J. O. *Chem. Biol.* **1999**, *6*, 823–833.
34. Yeh, J.-R. J.; Mohan, R.; Crews, C. M. *Proc. Natl. Acad. Sci. U.S.A.* **2000**, *97*, 12782–12787.
35. Placidi, L.; Cretton-Scott, E.; de Sousa, G.; Rahmani, R.; Placidi, M.; Sommadossi, J. P. *Cancer Res.* **1995**, *55*, 3036–3042.
36. Herbst, R. S.; Madden, T. L.; Tran, H. T.; Blumenschein, Jr. G. R.; Meyer, C. A.; Seabrooke, L. F.; Khuri, F. R.; Puduvalli, V. K.; Allgood, V.; Fritsche, Jr. H. A.; Hinton, L.; Newman, R. A.; Crane, E. A.; Fossella, F. V.; Dordal, M.; Goodin, T.; Hong, W. K. *J. Clin. Oncol.* **2002**, *20*, 4440–4447.

Available online at www.sciencedirect.com
SCIENCE DIRECT®
Tetrahedron
Tetrahedron 60 (2004) 7093–7098

A new cytotoxic polychlorinated sulfolipid from contaminated Adriatic mussels

Patrizia Ciminiello,[a,*] Carmela Dell'Aversano,[a] Ernesto Fattorusso,[a,*] Martino Forino,[a] Silvana Magno,[a] Paola Di Meglio,[b] Angela Ianaro[b] and Roberto Poletti[c]

[a]*Dipartimento di Chimica dellve Sostanze Naturali, Università degli studi di Napoli 'Federico II', via D. Montesano 49, Napoli 80131, Italy*
[b]*Dipartimento di Farmacologia Sperimentale, Università degli studi di Napoli 'Federico II', via D. Montesano 49, Napoli 80131, Italy*
[c]*Centro di Ricerche Marine, via A. Vespucci 2, Cesenatico 47042 (FC), Italy*

Received 1 October 2003; revised 12 December 2003; accepted 12 December 2003

Available online 26 June 2004

Abstract—A detailed analysis of toxic shellfish collected in the Adriatic sea in October 2000 allowed us to isolate a new cytotoxic chlorosulfolipid (**3**). Its gross structure has been elucidated through an extensive NMR analysis including various 2D techniques; the relative stereochemistry has been solved by applying the Murata's method. Compound **3** showed to posses cytotoxic activity against WEHI 164 and J774 cells. The presence of chlorosulfolipids in toxic mussels from the northern Adriatic sea has not to be considered incidental as we have been detecting these cytotoxic compounds since 1998. Their simultaneous and constant presence together with typical marine biotoxins represents a further risk both to consumers' health and aquacultures economic proceeds.

1. Introduction

Chlorosulfolipids are unusual naturally occurring compounds, which were first isolated at the end of the 1960s from some species of freshwater microalgae such as *Ochromonas danica* and *Ochromonas malhamensis*, where they constitute 15% of total lipids.[1] Successively they were detected also in three species of Xanthophyceae, *Tribonema aequale*,[2] *Botrydium granulatum* and *Monodus subterraneus* and in two species of Chlorophyta, *Elakatothrix viridis* and *Zygnema*.[3] In 1979 Mercer and Davies examined about 30 species chosen in a wide range of algal classes and orders for their chlorosulfolipid content; they found that, in marked contrast to the freshwater algae, in marine spp. chlorosulfolipids level was usually not detectable or at least an order of magnitude lower than that of the lowest freshwater species examined.[4] In spite of the quite large number of algae examined, just a few chlorosulfolipids were structurally characterized; anyway, the stereochemical details were never studied. On the basis of the available structural data, algal chlorosulfolipids were divided in two different series: polychlorodocosane 1,14-disulfates and polychlorotetracosane 1,15-disulfates, with a number of chlorine atoms that ranges from 1 to 6, in various combinations of positions on the aliphatic chain. In most cases, the exact location of the chlorine atoms could not be determined.[5] While the biological role of chlorosulfolipids is practically unknown, some quite interesting results have been obtained on the biogenetic origin of these compounds. Particularly, it has been shown that radioactively labelled acetate and malonate are readily incorporated into the chorosulfolipids of *O. danica*;[6] even-numbered, saturated fatty acids are also readily incorporated, but their efficiency of incorporation increases with increasing chain length.[7] On the contrary unsaturated fatty acids are poorly incorporated. Finally, evidence was provided to show that chlorination of the chlorosulfolipids is a sequential process.[8,9] In the frame of a research program on toxic Adriatic mussels we have carried on since the beginning of the 1990s, we recently found that these organisms contained additional cytotoxic material besides typical polyether biotoxins. Investigation aimed to the identification of these compounds succeeded in the isolation of several unknown molecules; among them we isolated two unique compounds, which can be included into the class of chlorosulfolipids, even if they are, structurally, quite different from the previously reported ones. The first compound is a hexachloromonosulfate,[10] **1**, while the second, **2**, very recently characterized, contains 11 chlorines, in addition to a fatty acid acyl moiety.[11] Probably, these cytotoxic compounds originate, just like typical biotoxins, from harmful microalgae which are accumulated by the continuous filter feeding process of mussels. Interestingly, presence of chlorosulfolipids in Adriatic

Keywords: Polychlorinated sulfolipid; Marine biotoxin; Toxic Adriatic mussels.
* Corresponding authors. Tel.: +39-81-678507; fax: +39-81-678552 (P.C.); tel.: +39-81-678503 (E.F.); e-mail addresses: ciminiel@unina.it; fattoru@unina.it

0040–4020/$ - see front matter © 2004 Elsevier Ltd. All rights reserved.
doi:10.1016/j.tet.2003.12.072

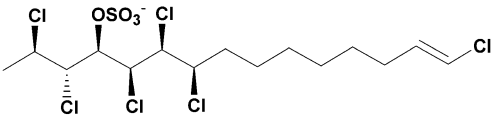

1

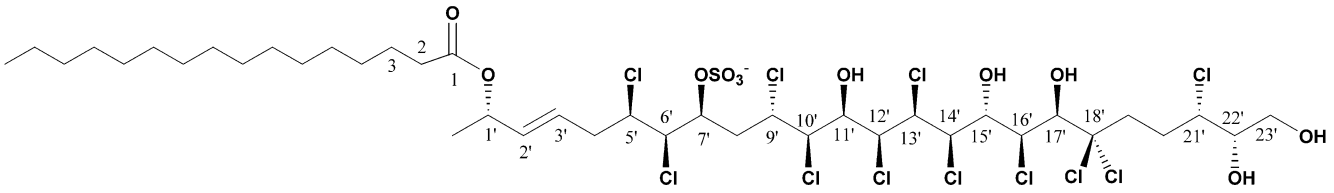

2

mussels has not to be considered accidental, as we have been reporting them since 1998. Unfortunately, the characterization of all the toxic compounds is not an easy task, considering that they are usually present in a very small amount. We succeeded now in the isolation, stereochemical elucidation and determination of cytotoxic activity of a new chlorosulfolipid from mussels of the Northern Adriatic sea (hexadecanoic acid 5′,6′,9′,10′,12′,13′,14′,16′,18′,21′-undecachloro-11′,15′,22′,23′-tetrahydroxy-1′-methyl-7′-sulfooxy-tricos-2′-enyl ester, **3**), strictly related to compound **2**. The finding of this novel compound further highlights unique structural features of marine chlorosulfolipids when compared to the freshwater ones. Undoubtedly, it would be very interesting to detect the producing organism. In this way, larger amounts of cytotoxic material could be recovered for toxicological studies, in order to shed some light on their potential risk to shellfish consumers' health.

2. Results and discussion

Toxic mussels *Mytilus galloprovincialis* were collected in October 2000 from one sampling site located along the Emilia Romagna coast in Italy during a period of high toxicity. Lethal potency of organic extracts was determined by the official mouse bioassay proposed by professor Yasumoto.[12] Isolation of **3** from toxic animals was first guided by the above-mentioned assay and, in the final purification steps, by the less material-consuming cytotoxicity tests (see Section 3). Chromatographic behavior and preliminary evaluation of NMR data of **3** allowed us to recognize its close relationship with compound **2** previously isolated from the same source. This was further supported by the negative ion HRESIMS spectrum, which provided an intense pseudomolecular ion cluster, characteristic of highly polychlorinated compounds; molecular formula, $C_{40}H_{66}O_{10}SCl_{11}$, determined on the peak at *m*/*z* 1127.0977, suggested **3** to be smaller than **2** by one oxygen atom. Consequently, the most obvious and immediate hypothesis was that **3** had the same structure of **2** apart from the lacking of just one among the five hydroxyl groups present in **2**. The number as well as the chemical shift values of methyls, methylenes, methines and unprotonated carbons, emerged from a combined analysis of ^{13}C NMR spectrum and DEPT experiment, were fully consistent with the above structural hypothesis. Unfortunately, a comparison of proton and carbon NMR spectra of the two compounds did not allow to verify our hypothesis and to unambiguously individuate the position where the OH group was missing. This was due to the complexity of the spectra showing many overlapping signals, which hampered an easy and unambiguous assignment of the resonances. Therefore, we needed to carry out structural analysis of **3** by individuating all the spin systems. This was performed on the peracetylated derivative (**4**), whose ^1H NMR spectrum, as for compound **2**, showed a much better dispersion of the signals, especially in the critical mid-field region. The first and important information gained by analysis of this derivative was the presence of the four hypothesized –OH groups in **3**, since as many ^1H NMR signals typical of acetylic methyls emerged both in ^1H and ^{13}C spectra of **4**. It was finally corroborated by a negative ion ESIMS spectrum, which showed a pseudomolecular ion cluster of peaks at *m*/*z* 1291, 1293, 1295, 1297, 1299, 1301 and 1303, corresponding to a tetra-acetylated derivative of **3**. As for compound **2**, a careful analysis of ^1H NMR, COSY and HOHAHA spectra led us to observe two spin systems in the functionalized part of the molecule, the first of which ranging from CH_3-1′ to C17′ and the second from C19′ to

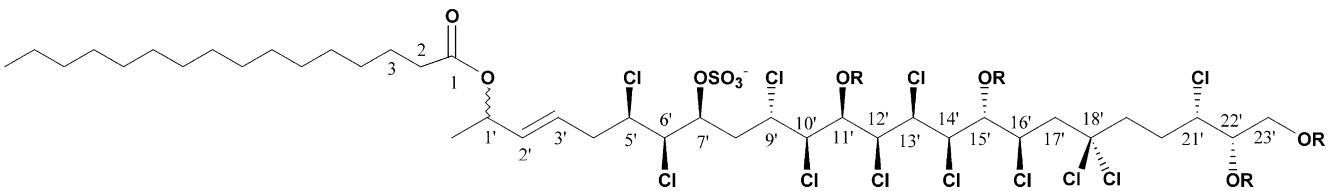

3 R = H

4 R = $COCH_3$

C23′, respectively. Acylic portion of our molecule was established to be an unbranched hexadecanoyl moiety spanning from C1 to C16, by individuating the protons located at the ends of the alkyl chains, whose signals parallel those of the corresponding protons of the acyl chain of **2** (H_2-2 δ 2.24; H_2-3 δ 1.53; H_2-15 δ 1.25; H_3-16 δ 0.89). The spin system was concluded through connection of the above portions with the unbranched C_{11} central chain, whose protons resonate as a broad band at δ 1.32. A diagnostic correlation in HMBC spectrum between triplet at δ 2.24 (H_2-2) and C1 (δ_c 173.0), as well as between the latter carbon and H1′ (δ_H 5.33) led us to individuate the exact location of the ester functionality. Final confirmation of the presence of an hexadecanoyl moiety in our compound was provided by a MS/MS ESI spectrum which revealed an intense fragmentation at *m/z* 255 $[C_{16}H_{31}O_2]^-$. The whole of the above evidence defined the total carbon sequence of **4**, considering that the only way to connect the two part structures CH_3-1′/C17′ and C19′/C23′ is through the only still unlocated carbon, namely the unprotonated one resonating at δ 92.7. Observed HMBC cross peaks between C-18′ and H_2-17′ as well as between C-18′ and H_2-19′ were

Table 1. $^3J_{H,H}$, $^2J_{C,H}$ and $^3J_{C,H}$ of C5′–C17′ and C21′–C22′ portions of compound **4**

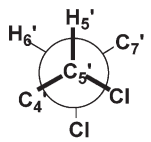

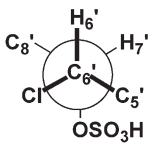

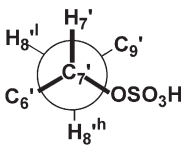

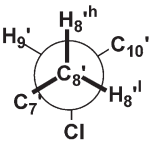

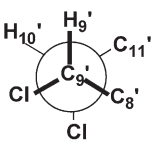

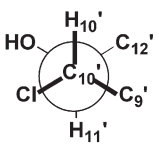

threo

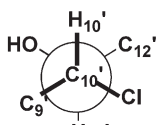

erythro

C5'-C6' axis	C6'-C7' axis	C7'-C8' axis	C8'-C9' axis	C9'-C10' axis	C10'-C11' axis
$^3J_{H5'-H6'}$ small	$^3J_{H6'-H7'}$ small	$^3J_{H7'-H8'^l}$ small	$^3J_{H8'^h-H9'}$ small	$^3J_{H9'-H10'}$ small	$^3J_{H10'-H11'}$ large
$^3J_{H5'-C7'}$ small	$^3J_{H6'-C8'}$ small	$^3J_{H7'-H8'^h}$ large	$^3J_{H8'^l-H9'}$ large	$^3J_{H9'-C11'}$ small	$^3J_{H10'-C12'}$ small
$^3J_{C4'-H6'}$ small	$^3J_{C5'-H7'}$ small	$^3J_{H7'-C9'}$ small	$^3J_{H8'^l-C10'}$ small	$^3J_{C8'H10'}$ large	$^3J_{C9'-H11'}$ small
$^2J_{C5'-H6'}$ small	$^2J_{C6'-H7'}$ small	$^3J_{C6'-H8'^h}$ small	$^3J_{H8'^h-C10'}$ small	$^2J_{C9'-H10'}$ large	$^2J_{C10'-H11'}$ large
$^2J_{C6'-H5'}$ small	$^2J_{C7'-H6'}$ small	$^3J_{C6'-H8'^l}$ small	$^3J_{C7'-H9'}$ small	$^2J_{C10'-H9'}$ small	$^2J_{C11'-H10'}$ large
		$^2J_{C7'-H8'^l}$ small	$^2J_{C9'-H8'^l}$ large		
		$^2J_{C7'-H8'^h}$ large	$^2J_{C9'-H8'^h}$ small		

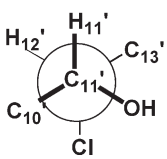

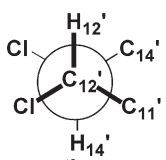

threo

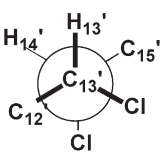

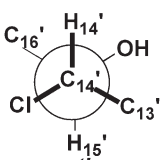

erythro

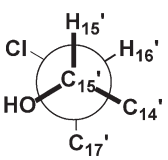

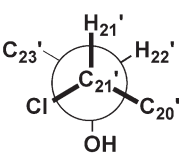

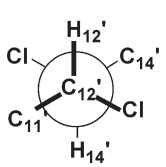

erythro

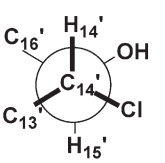

threo

C11'-C12'axis	C12'-C13' axis	C13'-C14'axis	C14'-C15' axis	C15'-C16' axis	C21'-C22' axis
$^3J_{H11'-H12'}$ small	$^3J_{H12'-H13'}$ large	$^3J_{H13'-H14'}$ small	$^3J_{H14'-H15'}$ large	$^3J_{H15'-H16'}$ small	$^3J_{H21'-H22'}$ small
$^3J_{H11'-C13'}$ small	$^3J_{H12'-C14'}$ small	$^3J_{H13'-C15'}$ small	$^3J_{H14'-C16'}$ small	$^3J_{H15'-C17'}$ large	$^3J_{H21'-C23'}$ small
$^3J_{C10'-H12'}$ small	$^3J_{C11'-H13'}$ small	$^3J_{C12'-H14'}$ small	$^3J_{C13'-H15'}$ small	$^3J_{C14'-H16'}$ small	$^3J_{C20'-H22'}$ small
$^2J_{C11'-H12'}$ small	$^2J_{C12'-H13'}$ large	$^2J_{C13'-H14'}$ small	$^2J_{C14'-H15'}$ large	$^2J_{C15'-H16'}$ small	$^2J_{C21'-H22'}$ small
$^2J_{C12'-H11'}$ small	$^2J_{C13'-H12'}$ large	$^2J_{C14'-H13'}$ small	$^2J_{C15'-H14'}$ large	$^2J_{C16'-H15'}$ large	$^2J_{C22'-H21'}$ small

All Coupling constants were measured by PS-HMBC.

fully consistent with this assumption. In order to fully determine planar structure of our compound it remained to assign the exact location of substituents on carbon chain, namely eleven chlorine atoms, four acetoxy groups and one sulfate. Evidence for the presence of this last group came from IR (ν_{max} 1240, 1220 and 820 cm^{-1}) and MS/MS spectra (fragment ions at *m/z* 97 $[HSO_4]^-$ and 80 $[SO_3]^-$). HMBC spectrum was again very helpful allowing to locate the four acetoxy groups thanks to intense correlations between carbonyl carbons (δ_C 171.9, 168.0, 169.5 and 171.3) with H-11′, H-15′, H-22′ and H_2-23′, respectively. Position of sulfate was the last problem to be solved, since the remaining substituents were all chlorine atoms. Sulfate group was located at C-7, on account of resonance of carbon atom at significantly lower field (δ_C 74.3) when compared with those of the remaining sp^3 methine carbons. Once described the planar structure of **4** we assigned values of all protons and carbons in not-acetylated compound **3** through a retrospective analysis of its NMR data. Bearing in mind structure of compound **2** previously isolated, it was immediate to observe that the difference between **3** and **2** was restricted to C-17′. In fact, in **2** C-17′ was a methine substituted with a −OH group, while in **3** the same carbon appeared to be a methylene correlated with two diastereotopic protons resonating at δ 2.79 and δ 3.29, respectively. At this point stereochemistry elucidation of our compound immediately appeared to be conveniently faced following the successful strategy employed for compound **2**. *E* configuration of the double bond was deduced from coupling constant between H-2′/H-3′ (16.0 Hz) and cross peaks in the ROESY spectrum between H-2′ and H-4′ as well as between H-3′ and H-1′. The relative configurations of the carbon atoms present in the part structures C-5′/C-16′ and C-21′/C-22′ were assigned through a wide application of the *J*-based method developed by Murata.[13,14] It is to be noted that the small amount of available material hampered a quantitative evaluation of $^2J_{C-H}$ and $^3J_{C-H}$ required for relative stereochemistry assignment. Anyway, the heteronuclear coupling constants were only qualitatively (small or large) determined simply by comparing intensities of the cross peaks in PS-HMBC spectrum. According to Murata, this qualitative elaboration is allowed taking into account the significant differences in $^2J_{C-H}$ and $^3J_{C-H}$ values between *anti* and *gauche* rotamers. As reported in Table 1 combination of $^3J_{H-H}$, $^2J_{C-H}$ and $^3J_{C-H}$ allowed us to unambiguously individuate the right stereochemical relationship for each pair of vicinal or alternate asymmetric carbons. Only for C-10′/C-11′, C-12′/C-13′ and C-14′/C-15′ axis, where a H/H *anti* arrangement occurs, $^3J_{H-H}$, $^2J_{C-H}$ and $^3J_{C-H}$ values did not support an unequivocal assignment of spatial disposition of the substituents. In these cases, as suggested by Murata, the relative configurations could be assigned through evaluation of ROE correlations. In particular ROESY spectrum evidenced an intense correlation between H-9′ and H-12′, as well as between H-11′ and H-14′, while no ROE emerged between H-13′ and H-16′, thus suggesting a *threo* dominant rotamer both for C-10′/C-11′ and C-12′/C-13′ axis, and an *erythro* one for C-14′/C-15′, respectively. In this way, we were able to solve the relative stereochemistry of the fragments C-5′/C-16′ and C-21′/C-22′ of the molecule, which resulted to be 5′*R*, 6′*R*, 7′*S*, 9′*S*, 10′*R*, 11′*R*, 12′*S*, 13′*S*, 14′*R*, 15′*R*, 16′*S* or its enantiomer, and 21′*S*, 22′*S* or its enantiomer, respectively (Table 1). To fully clarify the stereochemistry of our compound, it remained to individuate the configuration of the isolate stereogenic carbon in position 1′ and to upgrade the relative stereochemistry of the fragments C-5′/C-16′ and C-21′/ C-22′ to the absolute one. Unfortunately, paucity of **3** excluded any possibility of applying current methods of absolute stereochemistry elucidation, which involve reaction with chiral auxiliaries. Anyway, considering that the assigned relative configurations of the fragments C-5′/C-16′ and C-21′/C-22′ in **4** parallel those of the corresponding chiral carbon sequences in **2**, whose absolute configuration was determined, and on account of the very reasonable assumption that **2** and **3** are biogenetically related, we can assume that they share the same absolute stereochemistry, 5′*R*, 6′*R*, 7′*S*, 9′*S*, 10′*R*, 11′*R*, 12′*S*, 13′*S*, 14′*R*, 15′*R*, 16′*S*, 21′*S*, 22′*S*. Compound **3** was tested for its antiproliferative activity on WEHI 164 and J774, and it was found to inhibit the growth of all cell lines evaluated at 72 h with an IC_{50} of 10.4 and >20 μg/ml, respectively.

3. Experimental

3.1. General

^1H (500 MHz) and ^{13}C NMR (125 MHz) spectra were measured on a Bruker AMX-500 spectrometer; chemical shifts are referenced to the residual solvent signals (CD_3COCD_3: δ_H=2.05; δ_C=205.7 and 29.8; CD_3OD: δ_H=3.34). Methyl, methylene and methine carbons were distinguished by a DEPT experiment. Homonuclear ^1H connectivities were determined by using COSY experiment. One bond heteronuclear $^1H-^{13}C$ connectivities were determined with the Bax and Subramanian HMQC pulse sequence.[15] Two and three bond $^1H-^{13}C$ connectivities were determined by HMBC experiments optimized for a $^{2,3}J$ of 10 Hz. Low and high resolution ESIMS (negative ion mode) were performed by M-Scan S. A. (12, chemin des Aulx, 1228 Plan-les-Ouates, Switzerland) on a VG Analytical ZAB 2SE high field mass spectrometer. Negative ESI MSMS was carried out with a Thermofinnigan LCQ MAT (ion trap) mass spectrometer. Medium pressure liquid chromatographies (MPLC) were performed on a Büchi 861 apparatus using RP-18 (40–63 μm) stationary phase.

3.1.1. Isolation of 3. Chlorosulfolipid **3** was isolated from acetone extracts of contaminated shellfish (*Mytilus galloprovincialis*) digestive glands (total 1.8 kg dry weight) collected in October 2000 from one sampling site located along the Emilia Romagna coasts in Italy, following procedures closely parallel to those described previously. The digestive glands were found toxic by the mouse bioassay method for DSP. The digestive glands were extracted two times with acetone and after evaporation the residue was extracted thrice with EtOAc. The extracts obtained after removal of the solvent were dissolved in 80% MeOH and partitioned against *n*-hexane. Subsequently, the MeOH layer was diluted to 40% MeOH and further partitioned against CH_2Cl_2. The dichloromethane toxic residue was fractionated by repeated bioassay-guided column chromatography on ODS (aq. MeOH) and successively on TOYOPEARL (MeOH). The final HPLC

Table 2. ^{13}C and ^{1}H NMR spectroscopic data of compound **3** and **4** (CD_3COCD_3)[a]

3			**4**		
Position	δ_H, mult., *J* in Hz	δ_C, mult.	Position	δ_H, mult., *J* in Hz	δ_C, mult.
1	—	174.4	1	—	173.0
2	2.24 m	30.9	2	2.24 t 7.3	31.0
3	1.53 m, 7.3	25.4	3	1.53 q 7.3	25.0
4–14	1.32[b]	20.3	4–14	1.32[b]	20.3
15	1.25[b]	20.1	15	1.25[b]	20.1
16	0.89 t 7.4	14.1	16	0.89 t 7.4	14.1
1′	5.29 q 6.5	70.4	1′	5.33 quintet 6.5	70.6
2′	5.73 dd 6.5 – 15.3	134.3	2′	5.69 dd 6.5, 16.0	134.0
3′	5.79 dt 6.4 – 15.3	126.7	3′	5.75 dt 7.1, 7.1, 16.0	126.7
4′	2.82 m	39.0	4′	2.78 m	39.0
5′	4.52[b]	62.6	5′	4.56 dd 8.7, 1.8	61.0
6′	4.22 dd 1.2–2.8	60.0	6′	4.59 m	65.6
7′	4.84[b]	76.3	7′	4.75 dd 0, 2.0, 11.0	74.3
8′a	2.12 m	39.2	8′a	2.10 m	35.3
8′b	2.23 m	39.2	8′b	2.17 m	
9′	4.91[b]	66.0	9′	5.02 dd 0, 0.9, 10.3	58.6
10′	4.85[b]	58.9	10′	4.82 dd 0.9, 10.0	66.2
11′	4.38[b]	75.7	11′	5.22 dd 0.5, 11.2	70.8
12′	4.44[b]	67.0	12′	4.61 dd 0.5, 9.6	65.0
13′	4.83[b]	65.9	13′	4.81 dd 1.2, 9.6	60.7
14′	4.23[b]	60.8	14′	5.08 dd 1.2, 10.1	59.4
15′	4.57 dd 2.0–10.3	76.8	15′	5.52 dd 1.5, 10.1	77.3
16′	4.83[b]	57.9	16′	4. 81 dd 1.5, 9.2	56.7
17′a	2.81[b]	53.1	17′a	2.79[b]	52.5
17′b	3.22 d 17.2	53.1	17′b	3.29 d 17.2	52.5
18′	—	95.7	18′	—	92.7
19′	2.56 m	40.0	19′	2.55 m	40.8
20′a	2.30 m	38.5	20′a	2.18 m	39.8
20′b	2.52 m	38.5	20′b	2.35 m	39.8
21′	4.27[b]	65.4	21′	4.52 ddd 0.9, 7.7, 1.9	60.9
22′	4.19[b]	69.7	22′	5.40 ddd 0.9, 4.2, 5.5	72.9
23′a	4.24[b]	64.2	23′a	4.28 m	63.2
23′b	4.12[b]	64.2	23′b	4.32 m	
CH_3-1′	1.27[b]	20.8	CH_3-1′	1.25[b]	20.0
			CO-11′	—	171.9
			CO-15′	—	168.0
			CO-22′	—	169.5
			CO-23′	—	171.3

[a] Assignment based on DEPT, COSY, HMQC, HMBC and NOE-difference experiments.
[b] Overlapped with other signals.

purification was carried out on a RP 18 column with CH_3OH-H_2O 7:3 as eluent, thus obtaining 2.1 mg of pure compound **3**: $[\alpha]_D^{25}=+84.1$ (c=0.0013 g, MeOH); ^{1}H and ^{13}C NMR (CD_3COCD_3) data are reported in Table 2; IR (KBr) ν_{max} 1240, 1220 and 820 cm^{-1}; ESIMS (negative ion mode) *m/z* 1123, 1125, 1127, 1129, 1131, 1133, 1135; HRESIMS *m/z* 1127.0977 $C_{40}H_{66}O_{10}S\ ^{35}Cl_{10}\ ^{37}Cl$ requires 1127.0878.

3.1.2. Acetylation of 3. 1.5 mg of **3** were treated with Ac_2O in anhydrous pyridine for 12 h, thus obtaining 1.9 mg of peracetylated **4** ^{1}H and ^{13}C NMR (CD_3COCD_3) data are reported in Table 2; IR (KBr) ν_{max} 1240, 1220 and 820 cm^{-1}; ESIMS (negative ion mode) *m/z* 1291, 1293, 1295, 1297, 1299, 1301 and 1303.

3.2. Cytotoxicity assay

WEHI 164 cells (murine fibrosarcoma cell line) were maintained in adhesion with Dulbecco's Modified Eagle's Medium (DMEM) supplemented with 10% heat-inactivated fetal bovine serum (FBS), 25 mM HEPES, penicillin (100 U/ml), streptomycin (100 μg/ml) and 2 mM L-glutamine. J774 cells (murine monocyte/macrophage cell line) were grown in adhesion on Petri dishes with DMEM medium supplemented with 10% FBS, 25 mM Hepes, penicillin (100 U/ml), streptomycin (100 μg/ml) and 2 mM L-glutamine. All reagents for cell culture were from Biowhittaker. MTT [3-(4,5-dimethylthiazol-2-yl)-2,5-phenyl-2H-tetrazolium bromide] was from Sigma. WEHI 164 and J774 (1×10^4 cells) were plated on 96-well plates in 50 μl and allowed to adhere at 37 °C in 5% CO_2/95% air for 2 h. Thereafter the medium was replaced with 50 μl of fresh medium and 50 μl of 1:4 v/v serial dilution of the test compound **3** was added and then the cells were incubated for 72 h. The cells viability was assessed through an MTT conversion assay. Briefly, after 72 h of incubation, 25 μl of MTT (5 mg/ml) were added to each well and the cells were incubated for additional 3 h. Following this time, the cells were lysed and the dark blue crystal solubilized with 100 μl of a solution containing 50% (v:v) *N*,*N*-dimethylformamide, 20% (v:v) SDS with an adjusted pH of 4.5. The optical density (OD) of each well was measured with a microplate spectrophotometer equipped with a 620 nm filter. The viability of each cell line in response to treatment with compound **3** was calculated as: % dead cells=100−(OD

treated/OD control)×100. The results are expressed as IC_{50} (the concentration that inhibited the cell growth by 50%).

Acknowledgements

It is a result of a research supported by MURST PRIN, Rome, Italy. NMR and FABMS spectra were performed at 'Centro di Ricerca Interdipartimentale di Analisi strumentale', Università degli studi di Napoli 'Federico II'. The assistance of the staff is gratefully appreciated.

References and notes

1. Elovson, J.; Vagelos, P. R. *Biochemistry* **1970**, *9*, 3110.
2. Mercer, E. I.; Davies, C. L. *Phytochemistry* **1974**, *13*, 1607.
3. Mercer, E. I.; Davies, C. L. *Phytochemistry* **1975**, *14*, 1545.
4. Mercer, E. I.; Davies, C. L. *Phytochemistry* **1979**, *18*, 457.
5. Haines, T. H. *Ann. Rev. Microbiol.* **1973**, *27*, 403.
6. Elovson, J. *Biochemistry* **1974**, *13*, 2105.
7. Elovson, J. *Biochemistry* **1974**, *13*, 3483.
8. Mooney, L. C.; Haines, T. H. *Biochemistry* **1973**, *12*, 4469.
9. Thomas, G.; Mercer, E. I. *Phytochemistry* **1974**, *13*, 797.
10. Ciminiello, P.; Fattorusso, E.; Forino, M.; Di Rosa, M.; Ianaro, A.; Poletti, R. *J. Org. Chem.* **2001**, *66*, 578.
11. Ciminiello, P.; Dell'Aversano, C.; Fattorusso, E.; Forino, M.; Magno, S.; Di Rosa, M.; Ianaro, A.; Poletti, R. *J. Am. Chem. Soc.* **2002**, *124*, 13114.
12. Gazzetta Ufficiale della Repubblica Italiana 10 settembre 1990, n. 211; Decreti Ministeriali 1 agosto 1990, n. 256 e n. 257.
13. Matsumori, N.; Kaneno, D.; Murata, M.; Nakamura, H.; Tachibana, K. *J. Org. Chem.* **1999**, *64*, 866.
14. Murata, M.; Matsuoka, S.; Matsumori, N.; Kaneno, D.; Paul, G. K.; Tachibana, K. *J. Am. Chem. Soc.* **1999**, *121*, 870.
15. Bax, A.; Subramanian, S. *J. Mag. Reson.* **1986**, *67*, 565.